University of Southern Queensland

Faculty of Engineering and Surveying

AUSGeoid09 Performance in Mountainous Regions

by

Vittorio Sussanna

In fulfilment of the requirement of

Courses ENG4111 and ENG4112 Research Project

Towards the degree of

Bachelor of Spatial Science

October 2013

ABSTRACT

The Australian Height Datum 1971 (AHD71) is the current national vertical datum for Australia. AUSGeoid09 is the latest geoid model of an equipotential surface used to compute AHD71 heights (orthometric height) from ellipsoidal heights. This research reviews the theory of GNSS heightening to investigate the performance of AUSGeoid09 to derive AHD71 heights within the Snowy Mountains and Mid Hunter mountainous regions in NSW.

Absolute (i.e. single point) and relative (i.e. height difference between two points) sense comparisons were employed between geoid-derived heights and published AHD71. The improvement of AUSGeoid09 was evaluated as a function of difference between the AUSGeoid09 and AUSGeoid98. The result of both cases of study has confirmed an overall improvement in retrieving AUSGeoid09-derived AHD71 heights compared to AUSGeoid98 both in absolute and relative sense. However, the Snowy Mountains study area has outlined only a little improvement in absolute sense. Additionally, a possible slight slope within the AUSGeoid09 model was detected. This was evident when the residuals were plotted in their horizontal position; there was an improvement in the performance of the model in one particular direction indicating a possible slope in the AUSGeoid09 model in this specific region. This was not as evident in the Hunter region. The results have been positive in the last two decades where, GNSS technology has been used to carry vertical survey control. However, the continuous increase use of GNSS will eventually reach a stage where a new vertical datum will be necessary to create homogeneity.

University of Southern Queensland

Faculty of Health, Engineering and Sciences

ENG4111/ENG4112 Research Project

LIMITATIONS OF USE

The Council of the University of Southern Queensland, its Faculty of Health, Engineering & Sciences, and the staff of the University of Southern Queensland, do not accept any responsibility for the truth, accuracy or completeness of material contained within or associated with this dissertation.

Persons using all or any part of this material do so at their own risk, and not at the risk of the Council of the University of Southern Queensland, its Faculty of Health, Engineering & Sciences or the staff of the University of Southern Queensland.

This dissertation reports an educational exercise and has no purpose or validity beyond this exercise. The sole purpose of the course pair entitled "Research Project" is to contribute to the overall education within the student's chosen degree program. This document, the associated hardware, software, drawings, and other material set out in the associated appendices should not be used for any other purpose: if they are so used, it is entirely at the risk of the user.

CANDIDATE CERTIFICATION

I certify that the ideas, designs and experimental work, results, analyses and conclusions set out in this dissertation are entirely my own effort, except where otherwise indicated and acknowledged.

I further certify that the work is original and has not been previously submitted for assessment in any other course or institution, except where specifically stated.

Vittorio Sussanna

Student No: 0050092229

…….
(Signature)

…….
(Date)

ACKNOWLEDGMENTS

Acknowledgment goes to several people for the completion of this project. I will start by thanking both my supervisors Associate Professor Peter Gibbings and Dr. Volker Janssen, for their feedback and guidance which have been essential for the completion of this study.

I would like to thank Land and Property Information (LPI) for the opportunity to perform this study and for generously providing the necessary data.

I would also like to thank Robert Lock for his support, guidance and advice.

A special thank you also goes to Michael London, Greg Dickson, Tony Watson and Joel Haasdyk for sharing their extensive knowledge in least square adjustment and programs which have been fundamental for the completion of this research.

Finally I would love to thank my wife, son and new born daughter for their considerate patience and support. I have allocated quite a large amount of time to fulfil the requirement of this dissertation at the expenses of family time.

TABLE OF CONTENTS

ABSTRACT ..... **I**
LIMITATIONS OF USE ..... **II**
CANDIDATE CERTIFICATION ..... **III**
ACKNOWLEDGMENTS ..... **IV**
TABLE OF CONTENTS ..... **V**
LIST OF TABLES ..... **X**
LIST OF FIGURES ..... **XI**
NOMENCLATURE AND ACRONYMS ..... **XV**
CHAPTER 1 INTRODUCTION **1**
1.1 Overview **2**
1.2 The Problem **3**
1.3 Research Aim and Objectives **5**
1.4 Research Method **5**
1.5 Justification **6**
1.6 Scope and Limitation of the Research Project **7**
1.7 Summary **7**
CHAPTER 2 LITERATURE REVIEW **9**
2.1 Introduction **10**
2.2 Ellipsoidal Heights and the Vertical Datum **11**
2.3 Geoid Modelling **12**
2.3.1 Gravimetric Approach 13
2.3.2 Geometric Approach 13
2.3.3 Gravimetric and Geometric Combined Method 15
2.4 AHD71, the "Bumpy" Datum **15**
2.5 Sources of Errors Associated with Orthometric Heights **17**
2.6 AUSGeoid09, a Combined Quasigeoid Model Fitted to AHD71 ..... **18**
2.7 Online GPS Processing AUSPOS **20**
2.8 Method of Geoid Verification **20**
2.9 Computation with Microsearch GeoLab **23**
2.10 Current Standards for Vertical Control **24**
2.11 Previous Studies of Geoid Models **25**

2.11.1 Several Geoid Models over the Great Dividing Range Toowoomba 25
2.11.2 AUSGeoid98 in Costal and Mountainous Regions 26
2.11.3 AUSGeoid09 27
2.11.4 Performance of AUSGeoid09 in NSW 28
2.12 Conclusion 29
CHAPTER 3 RESEARCH METHOD 31
3.1 Introduction 32
3.2 Study Areas 32
3.2.1 Snowy Mountains 33
3.2.2 Mid Hunter 35
3.3 Checkpoints Network Marks 37
3.4 Data Evaluation 38
3.5 Data Computation 39
3.6 Validation Method 41
3.7 Conclusion 44
CHAPTER 4 COMPUTATION 45
4.1 Introduction 46
4.2 Control Marks 46
4.3 The Snowy Mountains GNSS Network 47
4.4 The Mid Hunter Network 49
4.5 The Adjustments 52
4.6 Adjustment Evaluation and Consideration 55
4.6.1 The Snowy Mountains Residuals 55
4.6.2 The Mid Hunter Residuals 56
4.7 Ellipsoidal Height Accuracy 57
4.7.1 The Snowy Mountains Ellipsoidal Height Accuracy 57
4.7.2 The Mid Hunter Ellipsoidal Heights Accuracy 58
4.8 Computation of N Values 58
4.9 Conclusion 59
CHAPTER 5 ABSOLUTE GEOID VERIFICATION 61
5.1 Introduction 62
5.2 Absolute Verification Test Structure 62
5.3 Comparison Over All Checkpoints 63

5.4 Comparison Every 100 m Increase of AHD71 64
5.5 The Absolute Comparison 64
5.5.1 The Snowy Mountains Comparison Over All Checkpoints 65
5.5.2 The Snowy Mountains Comparison Every 100 m Increase of AHD71 67
5.5.3 The Mid Hunter Comparison Over All checkpoints 68
5.5.4 The Mid Hunter Comparison Every 100 m Increase of AHD71 71
5.6 Results Discussion 72
5.6.1 The Snowy Mountains Absolute Result Discussion 72
5.6.2 The Snowy Mountain Graphical Representation Discussion 74
5.6.3 The Mid Hunter Result Discussion 76
5.6.4 The Mid Hunter Graphical Representation Discussion 78
5.7 Conclusion 78
CHAPTER 6 RELATIVE GEOID VERIFICATION 80
6.1 Introduction 81
6.2 Relative Verification Tests Structure 81
6.2.1 Comparison Over All Observed Baselines 83
6.2.2 Comparison Over All Possible Baselines 84
6.2.3 Comparison Within 100 km Baselines 84
6.2.4 Comparison Every 100 m Increase of Difference in Elevation 84
6.3 The Snowy Mountains Results 85
6.3.1 The Snowy Mountains Comparison Over All Observed Baselines 85
6.3.2 The Snowy Mountains Comparison Over All Possible Baselines 86
6.3.3 The Snowy Mountains Comparison Within 100 km Baselines 86
6.3.4 The Snowy Mountains Comparison every 100 m Increase of Difference in Elevation 87
6.3.5 The Snowy Mountains Graphical Representation 88
6.4 The Mid Hunter Results 91
6.4.1 The Mid Hunter Comparison Over All Observed Baselines 91
6.4.2 The Mid Hunter Comparison Over All Possible Baselines 91
6.4.3 The Mid Hunter Comparison Within 100 km Baselines 92
6.4.4 The Mid Hunter Comparison Every 100 m Increase of Difference in Elevation 93
6.4.5 The Mid Hunter Graphical Representation 94

6.5 Results Discussion 97
6.5.1 The Snowy Mountains Numerical Discussion 97
6.5.2 The Snowy Mountains Graphical Discussion 99
6.5.3 The Mid Hunter Numerical Discussion 100
6.5.4 The Mid Hunter Graphical Discussion 101
6.6 Conclusion 102
CHAPTER 7 CONCLUSION 104
7.1 Introduction 105
7.2 Absolute Verification Conclusion 105
7.3 Relative Verification Conclusion 107
7.4 Future Study 107
7.5 Project Conclusion 108
LIST OF REFERENCES 110
APPENDIX A
Project Specification……..……..……..A-115
APPENDIX B
Snowy Mountains and Mid Hunter Published AHD71 Heights and AUSPOS Solutions Report Summary……...…….B-117
APPENDIX C
Snowy Mountains and Mid Hunter Ellipsoidal Heights Relative to GRS80 Ellipsoid, Derived From GeoLab Constrained LSA and Estimate Accuracy at 95% Confidence Level…….….C-127
APPENDIX D
N Values Derived From AHD71, AUSGeoid09 and AUSGeoid98 and Subsequent Absolute Verification Residuals……...…….D-138
APPENDIX E
Descriptive Statistics of Absolute Verification Residuals, Between AHD71-Derived N Values and Geoid-Derived N Values with Bi-Linear, Bi-Quadratic, Bi-Cubic and Bi-Quartic Interpolation as a Function of 100 m Increases in AHD71……..……...E-158
APPENDIX F
Graphical Representation of the Absolute Verification……..……..F-177
APPENDIX G
Graphical Representation of the Relative Verification…….……...G-189

APPENDIX H

Descriptive Statistics of Relative Verification Residuals as a Function of Rise in Difference in Elevation……..……...H-195

LIST OF TABLES

CHAPTER 5

Table 5.1: Snowy Mountains descriptive statistics of absolute residuals, between AHD71-derived N values and geoid-derived N values with bi-linear, bi-quadratic, bi-cubic and bi-quartic interpolation over all checkpoints. 65
Table 5.2: Mid Hunter descriptive statistics of absolute verification residuals, between AHD71-derived N values and geoid-derived N values with bi-linear, bi-quadratic, bi-cubic and bi-quartic interpolation over all checkpoints. 69

CHAPTER 6

Table 6.1: Snowy Mountains descriptive statistics of relative verification residuals, between AHD71 differences and orthometric differences over 66 observed baselines using both AUSGeoid09 and AUSGeoid98 with bi-cubic interpolation 85
Table 6.2: Snowy Mountains descriptive statistics of relative verification residuals between AHD71 differences and orthometric differences over 5,356 possible baselines using both AUSGeoid09 and AUSGeoid98 with bi-cubic interpolation 86
Table 6.3: Snowy Mountains descriptive statistics of relative verification residuals between AHD71 differences and orthometric differences over 2,361 baselines within 100 km using both AUSGeoid09 and AUSGeoid98 with bi-cubic interpolation 87
Table 6.4: Mid Hunter descriptive statistics of relative verification residuals between AHD71 differences and orthometric differences over 104 observed baselines using both AUSGeoid09 and AUSGeoid98 with bi-cubic interpolation 91
Table 6.5: Mid Hunter descriptive statistics of relative verification residuals between AHD71 differences and orthometric differences over 3,320 possible baselines using both AUSGeoid09 and AUSGeoid98 with bi-cubic interpolation 92
Table 6.6: Mid Hunter descriptive statistics of relative verification residuals between AHD71 differences and orthometric differences over 2,526 possible baselines within 100 km using both AUSGeoid09 and AUSGeoid98 with bi-cubic interpolation 93

LIST OF FIGURES

CHAPTER 1

Figure 1.1: Relationship between ellipsoidal heights, AUSGeoid09 and AHD71. 2
Figure 1.2: Relationship between AHD71, AUSGeoid98 and ellipsoid.....4

CHAPTER 2

Figure 2.1: Relationships between ellipsoidal height (h), orthometric height (H) and geoid-ellipsoid separation (N) for (a) absolute, single-point and (b) relative heighting. 12
Figure 2.2: The 32 tide gauges used as zero height points for AHD71 and AHD83.....16
Figure 2.3: Deflection of the vertical. 22

CHAPTER 3

Figure 3.1: Location of the two study areas in NSW. 33
Figure 3.2: Snowy Mountains GNSS network and co-located AUSPOS solutions. 34
Figure 3.3: Typical terrain in the Snowy Mountains (Google Earth 2013a) 34
Figure 3.4: Mid Hunter GNSS network and co-located AUSPOS solutions.....36
Figure 3.5: Mid Hunter typical terrain (Google Earth 2013b).....37
Figure 3.6: Testing methodology process 43

CHAPTER 4

Figure 4.1: Snowy Mountains GNSS Baselines showing AUSPOS solutions, checkpoints and horizontal controls.....49
Figure 4.2: Mid Hunter GNSS Baselines showing AUSPOS solutions, checkpoints and horizontal controls.....51
Figure 4.3: Snowy Mountains final computed variance factor using Strangelove for both vertical and horizontal components and combined variance factor computed with *GeoLab* (constrained LSA) 54
Figure 4.4: Mid Hunter final computed variance factor using Strangelove for both vertical and horizontal components and combined variance factor computed with *GeoLab* (constrained LSA) 54

Figure 4.5: Loops composed by SS1521, PM111338, PM47640, SS5694 and COCP41N4 56

CHAPTER 5

Figure 5.1: Snowy Mountains absolute verification residuals between AHD71-derived N values and geoids-derived (AUSGeoid09 and AUSGeoid98) N values, with bi-linear interpolation plotted along increasing of longitudes 66
Figure 5.2: Snowy Mountains absolute verification residuals between AHD71-derived N values and geoids-derived (AUSGeoid09 and AUSGeoid98) N values, with bi-linear interpolation plotted along increasing of latitudes 66
Figure 5.3: Snowy Mountains graphical representation of the descriptive statistics of absolute verification residuals, between AHD71-derived N values and AUSGeoid09-derived N values, with bi-linear interpolation as a function of 100 m increases in AHD71 67
Figure 5.4: Snowy Mountains graphical representation of the descriptive statistics of absolute verification residuals, between AHD71-derived N values and AUSGeoid98-derived N values with bi-linear interpolation as a function of 100 m increases in AHD71 67
Figure 5.5: Snowy Mountains absolute verification residuals between AHD71-derived N values and geoids-derived (AUSGeoid09 and AUSGeoid98) N values with bi-linear interpolation plotted along increasing of AHD71 68
Figure 5.6: Mid Hunter absolute verification residuals between AHD71-derived N values and geoids-derived (AUSGeoid09 and AUSGeoid98) N values, with bi-linear interpolation plotted along increasing of longitudes 70
Figure 5.7: Mid Hunter absolute verification residuals between AHD71-derived N values and geoids-derived (AUSGeoid09 and AUSGeoid98) N values, with bi-linear interpolation plotted along increasing of latitudes 70
Figure 5.8: Mid Hunter graphical representation of the descriptive statistics of absolute verification residuals, between AHD71-derived N values and AUSGeoid09-derived N values with bi-linear interpolation as a function of 100 m increases in AHD71 71
Figure 5.9: Mid Hunter graphical representation of the descriptive statistics of absolute verification residuals, between AHD71-derived N values and AUSGeoid98-derived N values with bi-linear interpolation as a function of 100 m increases in AHD71 71

Figure 5.10: Mid Hunter absolute verification residuals between AHD71-derived N values and geoids-derived (AUSGeoid09 and AUSGeoid98) N values with bi-linear interpolation plotted along increasing of AHD71 72
Figure 5.11: Direction and magnitude of AUSGeoid09 residuals within the Snowy Mountains..... 76

CHAPTER 6

Figure 6.1: Snowy Mountains graphical representation of the descriptive statistics of relative verification residuals, between AHD71 differences and orthometric differences using AUSGeoid09 as a function of 100 m increase of difference in elevation 88
Figure 6.2: Snowy Mountains graphical representation of the descriptive statistics of relative verification residuals, between AHD71 differences and orthometric differences using AUSGeoid98 as a function of 100 m increase of difference in elevation 88
Figure 6.3: Snowy Mountains relative verification residuals between AHD71 and AUSGeoid09 (with bi-cubic interpolation) over 2,361 baselines shorter than 100 km, plotted together with current allowable 3rd order differential levelling miscloses 89
Figure 6.4: Snowy Mountains relative verification residuals between AHD71 and AUSGeoid98 (with bi-cubic interpolation) over 2,361 baselines shorter than 100 km, plotted together with current allowable 3rd order differential levelling miscloses 89
Figure 6.5: Snowy Mountains relative verification residuals between AHD71 and AUSGeoid09 (with bi-cubic interpolation) over 5,356 possible baselines as a function of difference in elevation 90
Figure 6.6: Snowy Mountains relative verification residuals between AHD71 and AUSGeoid98 (with bi-cubic interpolation) over 5,356 possible baselines as a function of difference in elevation 90
Figure 6.7: Mid Hunter graphical representation of the descriptive statistics of relative verification residuals, between AHD71 differences and orthometric differences using AUSGeoid09 as a function of 100 m increase of difference in elevation..... 94
Figure 6.8: Mid Hunter graphical representation of the descriptive statistics of relative verification residuals, between AHD71 differences and orthometric differences using AUSGeoid98 as a function of 100 m increase of difference in elevation..... 94

Figure 6.9: Mid Hunter relative verification residuals between AHD71 and AUSGeoid09 (with bi-cubic interpolation) over 2,526 baselines shorter than 100 km, plotted together with current allowable 3rd order differential levelling miscloses 95
Figure 6.10: Mid Hunter relative verification residuals between AHD71 and AUSGeoid98 (with bi-cubic interpolation) over 2,526 baselines shorter than 100 km, plotted together with current allowable 3rd order differential levelling miscloses 95
Figure 6.11: Mid Hunter relative verification residuals between AHD71 and AUSGeoid09 (with bi-cubic interpolation) over 3,320 possible baselines as a function of difference in elevation 96
Figure 6.12: Mid Hunter relative verification residuals between AHD71 and AUSGeoid09 (with bi-cubic interpolation) over 3,320 possible baselines as a function of difference in elevation 96

NOMENCLATURE AND ACRONYMS

AGQG2009	gravimetric component of AUSGeoid09
AHD71	Australian Height Datum 1971
ANLN	Australian National Levelling Network
AUSLIG	Australian Surveying and Land Information Group
AUSPOS	Online GPS processing service provided by Geoscience Australia
CORS	Continuously Operating Reference Station
CSRS	Canadian Spatial Reference System
EGM2008	Earth Gravitational Model 2008
GA	Geoscience Australia
GDA94	Geocentric Datum of Australia 1994
GNSS	Global Navigation Satellite System
GPS	Global Positioning System
GRS80	Geodetic Reference System 1980 ellipsoid
ICSM	Intergovernmental Committee on Surveying and Mapping
ITRF	International Terrestrial Reference Frame
LPI	Land and Property Information, a division of the NSW Department of Finance and Services
LSA	Least Squares Adjustment
LSC	Least Squares Collocation
MSL	Mean Sea Level
RMS	Root Mean Square
SCIMS	Survey Control Information Management System (NSW)
SMES	Survey Mark Enquiry Service (VIC)
WGS84	World Geodetic System 1984 ellipsoid

CHAPTER 1
INTRODUCTION

1.1 Overview

The Australian Height Datum 1971 (AHD71) is the current national vertical datum for Australia. It was computed by adjusting 97,230 km of 2-way levelling to the mean of 32 tide gauges around Australia observed in the 1960s in order to provide a surface that approximates Mean Sea Level (MSL) across the country (Roelse et al. 1971).

The introduction of Global Navigation Satellite System (GNSS) technologies has presented new means to compute position in more effective and efficient ways than ever before. However, GNSS observations refer to a mathematical representation of the earth known as the ellipsoid, which in general terms does not coincide with the AHD71. In this fashion, an equipotential surface known as geoid is used to convert between ellipsoidal heights and AHD71 heights (Janssen & Watson 2011).

AUSGeoid09 is the latest geoid model that best fits the AHD71. It was released in March 2011 by Geoscience Australia (GA) to replace the previous geoid model AUSGeoid98 (Featherstone et al. 2001). Both models are relative to the Geodetic Reference System 1980 (GRS80) ellipsoid and cover the area between 108ºE and 160ºE longitude and between 8ºS and 46ºS latitude. AUSGeoid09 N values are the common element between GNSS-derived ellipsoidal heights and AHD71 heights that allow the conversion from one to another (see Figure 1.1).

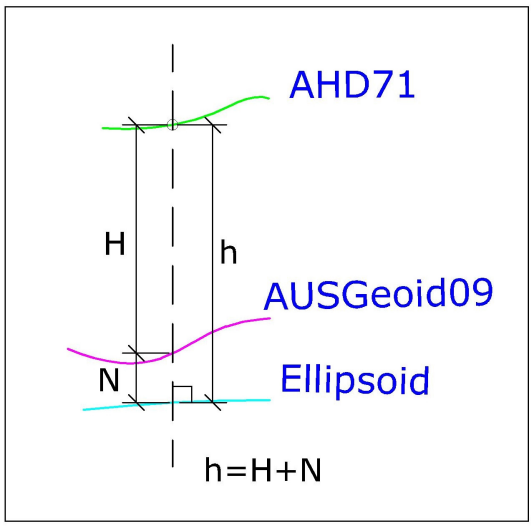

Figure 1.1: Relationship between ellipsoidal heights, AUSGeoid09 and AHD71.

Throughout the Australian terrain, AUSGeoid09 is expected to convert ellipsoidal heights to AHD71 heights with an accuracy of ±0.05 m (Brown 2010), with the exception of some pocket areas where the misfit can be greater than ±0.1 m, due to errors of other contributing elements such as levelling age, geoid anomalies or deficiency of data. On the other hand, AUSGeoid98 gives an absolute accuracy of ±0.4 m (Featherstone & Guo 2001; Janssen & Watson 2011).

The Snowy Mountains and the Mid Hunter GNSS network adjustments are two project areas located within mountainous regions in NSW with elevations that range from 5 to 2,200 metres. These two sites together encompass 186 Survey Control Information Management System (SCIMS) marks of accurately known AHD71 heights. SCIMS is a database of about 250,000 survey marks within NSW that contains coordinates, heights and other information (Kinlyside 2013). The GNSS networks are provided by Land and Property Information (LPI), a division of the NSW Department of Finance and Services responsible for providing geodetic control and related regulations for the state of NSW. This dissertation portrays the analysis of GNSS static networks approved by LPI to quantify the performance of AUSGeoid09 in mountainous regions and specify the expected improvement factor in the connection to AHD71 compared to its predecessor, AUSGeoid98.

1.2 The Problem

MSL is generally the surface of zero height that most countries have adopted as the base of their national vertical datum (Featherstone & Kuhn 2006; Janssen & Watson 2011). Heights above MSL are crucial information for various activities such as the flow of the water to identify flood areas. In Australia, MSL is defined by the AHD71. It was determined by setting to zero the average values of 32 tide gauges around Australia for a period of about 2 years that began in 1966. In reality, it is now known that the waters of the northern part of Australia are about 1 metre higher than the southern ones (Brown 2010). Therefore, the least squares adjustment (LSA) used to constrain the sprit levelling to the 32 tide gauges has introduced a large error causing a misfit between AHD71 and MSL. Additionally, a study conducted by Morgan (1992) has identified sources of errors mainly attributed to the third order spirit levelling employed.

Within the last two decades, GNSS technology has been the primary means for positioning, due to its accuracy, rapidity and accessibility. GNSS-based height observations are referenced to a mathematical representation of the earth known as the ellipsoid (Brown et al. 2011). Generally speaking, ellipsoidal heights are purely geometric values with no practical meaning. However, in most engineering projects, height must be directly correlated to gravity since gravity is the primary factor that rules the flow of water (Featherstone & Kuhn 2006). In this context the use of geoid models has helped GNSS users to compute AHD71 heights from ellipsoidal heights (Brown et al. 2011).

The geoid is a 3-dimensional surface with constant gravity that approximates the MSL. According to Featherstone et al. (2001), AUSGeoid98 is a gravimetric geoid computed using terrestrial and satellite gravity components. GNSS users have used this model to derive heights from the ellipsoid to the gravimetric surface. In reality, as it can be seen in Figure 1.2 AHD71, AUSGeoid98 and MSL are three different surfaces.

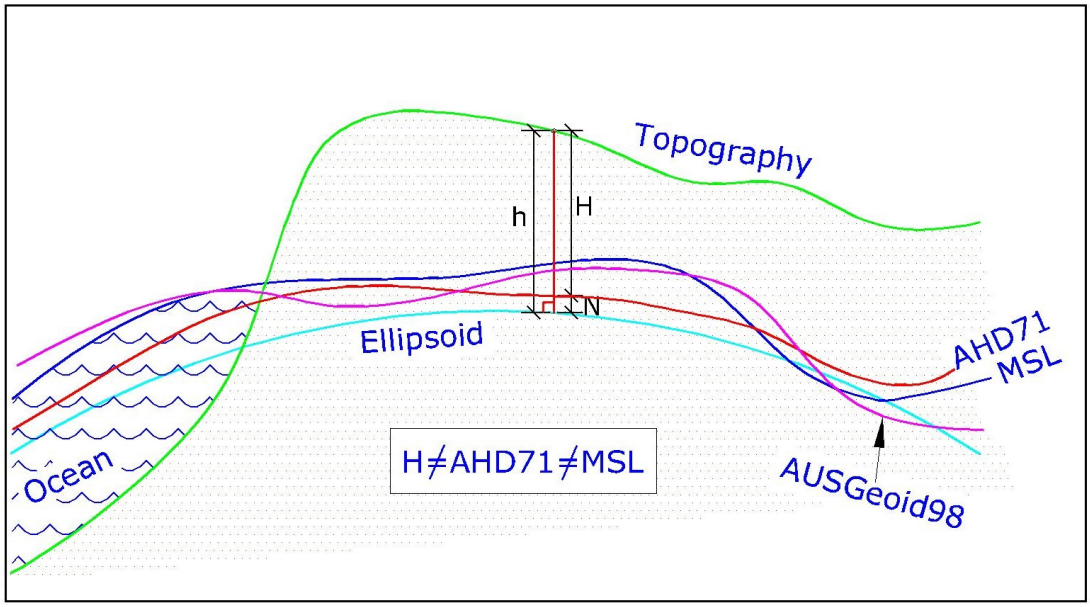

Figure 1.2: Relationship between AHD71, AUSGeoid98 and ellipsoid.

In particular AUSGeoi98 and AHD71 diverge by about 0.5 m (Brown 2010). On the other hand, AUSGeoid09 is a computed homogenous model which takes taking into account a geometric component retrieved from GNSS and AHD71 data and gravitational data. This includes mean gravity anomalies since gravity is collected

irregularly due to logistic access. This allows a conversion from GNSS heights to AHD71 heights with an accuracy of ±0.05 m (Brown 2010). However, a recent study conducted by Featherstone et al. (2010) on the computation of the AUSGeoid09 has demonstrated that the residual gravity anomalies are smaller than those evaluated in AUSGeoid98 with the biggest discrepancies in mountainous and coastal regions along the Great Diving Range (McDonald 2004) and Tasmania as a consequence of issues related to topography. In fact, based on Darbeheshti and Featherstone (2009), gravity in Australia can change dramatically within a few kilometres on the earth's surface. This implies the necessity to evaluate these areas in an objective sense using GNSS and levelling data. These findings form the basis of this dissertation to further investigate the nature and performance of the AUSGeoid09 model within mountainous regions using GNSS and published AHD71 heights.

1.3 Research Aim and Objectives

The aim of this research is to identify and clarify the accuracy of AUSGeoid09 in computing AHD71 heights from ellipsoidal heights within mountainous regions at 95% confidence level in the Snowy Mountains and Mid Hunter regions of NSW.

The objective is to help GNSS users to identify possible issues with the AUSGeoid09 geoid model that may occur in mountainous regions when retrieving AHD71 heights from GNSS observations.

1.4 Research Method

The nature of this research is to investigate the performance of AUSGeoid09 in mountainous regions. Present literature associated with the relationship between AHD71 and the geoid model is reviewed and substantiated. The first intent is to identify the method applied to convert ellipsoidal heights to AHD71 heights. The relationship between AHD71 and various methods of geoid computation will be investigated to clarify the reason for misfit. This is achieved through an analysis of the way in which AHD71 was established. Then the geoid model, the methodology and components used to design the current and previously used gravimetric model geoids will be revised.

Networks composed of GNSS observation will be subject to several adjustments performed using the *Microsearch GeoLab* (Microsearch 2013) least squares adjustment software. These adjustments will be constrained to the GRS80 ellipsoid holding accurate AUSPOS solutions (GA 2013) fixed, and AUSGeoid09 will be implemented to compute N Values. In this fashion, the AUSGeoid09-derived AHD71 heights are independent of published AHD71 heights. Precision is estimated at the 95% confidence level to obtain consistent statistical data.

Comparisons will be made between published AHD71 heights and those derived from AUSGeoid09. Furthermore, in order to quantify a rate of improvement for the new geoid model in computing AHD71 heights, results will be compared with its predecessor AUSGeoid98.

1.5 Justification

Over the last two decades, GNSS technology has been the most popular tool to derive position throughout the world in the fastest and most efficient manner (Brown 2010). Ellipsoidal heights derived from GNSS observations are in most circumstances converted to a local, national vertical height datum (Janssen 2009). This conversion includes the source of errors in the way AUSGeoid09 is defined and the deficient way of computation of the vertical datum such as AHD71 (Featherstone 2008).

In recent times, metadata is becoming more important since there are different sources of data, based on different surfaces. Modern systems such as Continuously Operating Reference Station (CORS) networks require data to be manipulated and transformed to a particular working surface. Within the Australian context, AUSGeoid09 is the model that allows this transformation from the ellipsoidal reference surface used by GNSS to AHD71 (Janssen & Watson 2010; Todd 2012).

The increasing use of GNSS technology will eventually reach a stage where a new vertical datum will be necessary to create homogeneity. However, at this point in time and from a practical point of view AHD71 is the current official national vertical datum. Research investigating AUSGeoid09 is fundamental to give GNSS users knowledge of potential anomalies and the possibility to generate correction surfaces.

1.6 Scope and Limitation of the Research Project

AUSGeoid09 will be tested within the Snowy Mountains and Mid Hunter regions, i.e. two mountainous regions of NSW. The datasets used are based entirely on authoritative GNSS network adjustments provided by LPI.

Accurate ellipsoidal heights derived from the AUSPOS online processing service provided by Geoscience Australia (GA 2013), are adopted to constrain the GNSS network adjustments to the GRS80 ellipsoid.

The check points of accurate AHD71 heights, where the AUSGeoid models are validated, will be SCIMS marks of class C order 3 or better (ICSM 2007).

GNSS static network observations will be weighted accordingly, based on an empirical method detailed in chapters 3 and 4. The quality of ellipsoidal heights, derived from the constrained adjustment to the ellipsoid, will be at 95% confidence level.

1.7 Summary

AUSGeoid09 is the latest geoid model used by GNSS users in Australia to convert ellipsoidal heights to AHD71 heights. Released in 2010 by Geoscience Australia, the model is expected to convert ellipsoidal heights to AHD71 heights and vice versa with an accuracy of ±0.05 m across most of the country (Brown et al. 2011). This was demonstrated by recent studies at the 95% confidence level. However, previous studies such as Brown et al. (2011) have also revealed that larger residuals occurred in coastal and mountainous regions.

This dissertation aims to examine the performance of AUSGeoid09 at the 95% confidence level within the Snowy Mountains and Mid Hunter mountainous regions in NSW. The project also aims to quantify the expected improvement in the connection to AHD71, limited to the study areas, by comparing both AUSGeoid98 and AUSGeoid09.

The outcomes of this project are expected to help GNSS users to identify the performance of AUSGeoid09 and its limitations in mountainous areas of NSW to derive AHD71 heights.

Having established the above, the next chapter will investigate the current theory related to geoid models, the relationship with the national vertical datum and methods and data used to verify a geoid model. Additionally, it will connect the problem outlined with real-world knowledge to better establish the basis of this research.

CHAPTER 2
LITERATURE REVIEW

2.1 Introduction

Chapter 1 has portrayed AUSGeoid09 as the current geoid model used by GNSS users to convert ellipsoidal heights to AHD71 heights and vice versa. This model is expected to carry out this conversion with an accuracy of ±0.05 m (Brown 2010) at the 95% confidence level. However, previous studies have also demonstrated that larger residuals occurred in coastal and mountainous regions due to difficulty in shaping the model in these sections (Featherstone et al. 2010). This suggests the necessity to further investigate mountainous and coastal regions. The method employed in this research will be fully detailed in Chapter 3.

The aim of this chapter is to provide information in regards to AHD71, the geoid model and their relationship. In addition, it will identify methods and data with their limitations used by previous researches to investigate geoid models. This is achieved by reviewing relevant available literature and case studies.

Initially, a review will be conducted of current practice with respect to GNSS heighting to provide theories and methods to obtain orthometric heights from GNSS-derived ellipsoidal heights via the implementation of a geoid model. The different approaches to compute the geoid model are explored and detailed information about AHD71 is investigated to understand the reason of misfit between the two. Additionally, current standards for vertical control and possible sources of error in the computation of geoid models, GNSS observations and conventional spirit levelling used to compute AHD71 are investigated to better establish the limitations of this study. A detailed analysis of AUSGeoid09 is provided to understand the method used to fit the model to AHD71. Absolute and relative methods of geoid verification are described as practical methods to check geoid performance. Additionally, AUSPOS online processing is evaluated as a practical and accurate method to determine ellipsoidal heights. Finally, previous case studies in the performance of several geoid models within mountainous regions and two case studies of AUSGeoid09 performance are explored to identify theories and methods of geoid validation relevant to this project.

2.2 Ellipsoidal Heights and the Vertical Datum

A practical utilisation of any geoid model is to convert GNSS-derived ellipsoidal heights into orthometric heights. In reality orthometric heights and AHD71 heights are not the same as it was shown in Figure 1.2. However, GNSS users have taken orthometric heights derived from previous models such as AUSGeoid98 to be an approximation of AHD71 heights (Brown et al. 2011), provided that both ellipsoidal heights and geoid model refer to the same ellipsoid. The aim is to compute geoid undulations (N), also kwon as N values or geoid-ellipsoid separation, in order to convert GNSS-derived ellipsoidal heights *h* into orthometric heights *H* (H≈AHD71). This conversion can be obtained in absolute or relative sense. The first method, also known as single point approach, is illustrated in Figure 2.1(a). It can be computed on a point P using the following algebraic relationship (Kearsley 1988):

$$H_p = h_p - N_p \tag{2.1}$$

(*Source:* Kearsley 1988, p. 11)

The second method illustrated in Figure 2.1(b) implies a calculation of the elevation of a point from another point with known accurate elevation. Put simply, the elevation of point B is computed by algebraically adding to the elevation of point A the difference in GPS-derived ellipsoidal heights and subtracting the difference in geoid separation with the following relationship (Kearsley 1988):

$$H_B = H_A + \Delta h_{BA} - \Delta N_{BA} \tag{2.2}$$

(*Source:* Kearsley 1988, p. 11)

which can be simplified to:

$$\Delta H_{AB} = \Delta h_{AB} - \Delta N_{AB} \tag{2.3}$$

(Source: Featherstone et al. 1998, p. 279)

where Δ denotes the difference in values from one point to another.

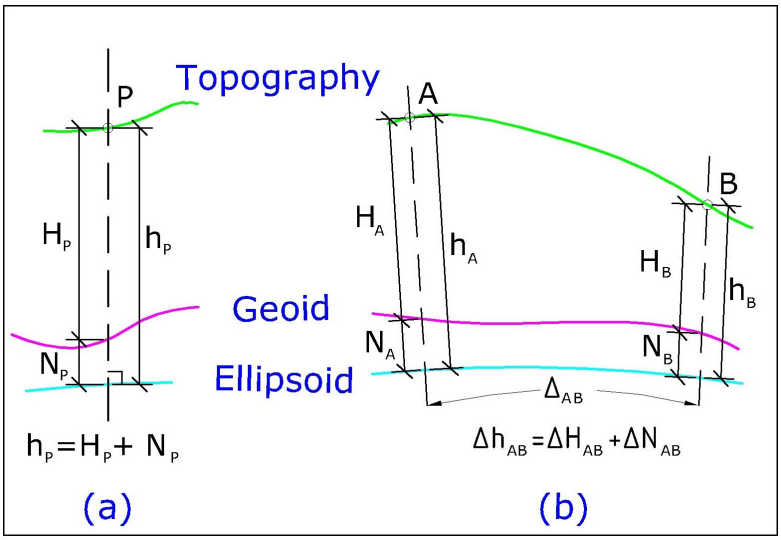

Figure 2.1: Relationships between ellipsoidal height (h), orthometric height (H) and geoid-ellipsoid separation (N) for (a) absolute, single-point and (b) relative heighting.

According to Kearsley (1988) and successively reinforced by Featherstone et al. (1998), the conversion from GNSS-derived heights to orthometric heights using the relative method is more accurate than the absolute one. Put simply, simultaneous observations in the relative method will minimise the almost coincident systematic errors by virtue of the difference. Baselines are observed between points to obtain the difference in ellipsoidal heights which will be converted into a difference of orthometric heights using the computed N values. However, the continuing expansion of CORS networks such as CORSnet-NSW (LPI 2013a) has increased the importance of computing N values in an absolute sense (Janssen & Watson 2011).

2.3 Geoid Modelling

A geoid is a surface where at any point the gravity is equal and perpendicular. As a matter of fact, gravity differs from one place to another in magnitude and direction due to the irregular shape of topography and underlying effects such as gravity anomalies due to large bodies of mass underground. It is referenced to the chosen ellipsoid with separations contained within ±100 m and direction slopes are less than 1 minute of arc. In this fashion, computations are made on the ellipsoid, which is a simpler mathematical shape where the geoid is fitted (Fryer 1972).

Modelling a geoid has been the crucial focus for most geodesists and several methods have been developed to construct a geoid model such as gravimetric interpolation, geometrical interpolation and a combination of the two (Featherstone et al. 1998).

2.3.1 Gravimetric Approach

Terrestrial gravity observation in conjunction with geopotential and digital terrain models can be used to retrieve geoid undulations. This approach makes it possible to compute a nationwide geoid model providing data is available. An example of this method is AUSGeoid93, evaluated by the Australian Surveying and Land Information Group (AUSLIG) (Featherstone et al. 1998) now known as GA. Furthermore, a review of this method was published by Kearsley (1988), affirming that an accuracy of 2 to 3 ppm can be achieved in the calculation of relative N values (ΔN). Comparisons were made to confirm the stated accuracy by rearranging equation 2.2 and retrieving ΔH through terrestrial levelling and Δh via GPS observations. The highest level reached was 7 ppm. However, errors exist within the levelling of the order of 1 ppm (Kearsley 1988).

2.3.2 Geometric Approach

Based on Featherstone et al. (1998) the same way that GNSS observations are used to compute orthometric heights using equation 2.1, GNSS-determined ellipsoidal heights on points of known orthometric heights can be used to determine N values for a particular point P by rearranging equation 2.1 into the following:

$$N_p = h_p - H_p \tag{2.4}$$

In an area of a few kilometres the geoid can be satisfactorily estimated as a flat surface (Featherstone et al. 1998). Hence, linear interpolation can be used to calculate the N values. Put simply, the orthometric height of a point X between two benchmarks observed by GNSS can be determined by the following equation:

$$H_X = H_A + \Delta h_{AX} - \frac{l_{AX}}{S_{AB}} \Delta N_{AB} \tag{2.5}$$

(Source: Featherstone et al. 1998, p. 281)

Where l_{AX} denotes the distance AX, and S_{AB} denotes the benchmarks separation between A and B.

However, this technique is rarely performed since there is a low possibility to carry out surveys along a line profile. Instead, GNSS occupation of three benchmarks, to create a plane, can be carried out to better match general survey procedures. At each of the three points, equation 2.6 is applied. The matrix calculation shown in equation 2.7 is used to solve for N_0 which defines the bias and N_1 and N_2 that denote the tilts of the geoid surface in regards to the ellipsoid of revolutions, while e and n are Easting and Northing in any plane coordinate system (Featherstone et al. 1998).

$$h - H = N = N_0 + N_1 e + N_2 n \tag{2.6}$$

$$\begin{pmatrix} N_0 \\ N_1 \\ N_2 \end{pmatrix} = \begin{pmatrix} 1 & e_A & n_A \\ 1 & e_B & n_B \\ 1 & e_C & n_C \end{pmatrix}^{-1} \begin{pmatrix} (h-H)_A \\ (h-H)_B \\ (h-H)_C \end{pmatrix} \tag{2.7}$$

(Source: Featherstone et al. 1998, pp. 281-2)

Once the coefficients N_0, N_1 and N_2 are solved, any point X within the plane defined by the three benchmarks A, B and C can be solved for *H* using the equation 2.8:

$$H_X = H_A + \Delta h_{AB} - N_A + N_0 + N_1 e_X + N_2 n_X \tag{2.8}$$

(Source: Featherstone et al. 1998, p. 282)

where e_X and n_X are known coordinates of a point X.

In addition, it is important to say that although this approach can be applied for general survey techniques, it is advisable to carry out a least squares method if more than three marks are observed. However, nowadays computer programs are used to compute geoid interpolation in the way detailed in section 2.9.

2.3.3 Gravimetric and Geometric Combined Method

A combination of the methods explained in sections 2.3.1 and 2.3.2 can deliver a geoid model of higher accuracy. It is important to note that this approach is a mixture of different sets of data. Therefore, it is assumed the orthometric heights are compatible with the marks that are part of the national vertical network. The addition of geometric components to the model gives detailed information between stations and consistency in the connection to the vertical datum, due to its derivations from GNSS observations on known benchmarks (Featherstone et al. 1998). AUSGeoid09 is an example of this method, and a detailed analysis is given in section 2.6.

2.4 AHD71, the "Bumpy" Datum

The AHD71 is the current national vertical datum that was primarily designed for meeting the mapping needs of the 1960s (Morgan 1992). It was established by a LSA of 97,230 km of 2-way levelling. MSL was set to zero at 30 tide gauges located around mainland Australia and 2 tide gauges in Tasmania (see Figure 2.2). Apart from this, the adjustment for the Tasmanian AHD was not carried out until 1983 (GA 2012a). Considering the technologies and techniques of that time, it was an extraordinary achievement to obtain the first national vertical datum of Australia. However, the AHD71 has been subject to criticism of homogeneity and accuracy since its creation. A study conducted by Morgan (1992) has identified sources of errors mainly attributed to the third order spirit levelling employed and the data modelling adopted. This was achieved through the analysis of the residuals of the original adjustment and the exclusive comparison of the re-levelling campaign accomplished between 1975 and 1976 from Coffs Harbour along the Queensland-New South Wales border to Cairns. The final consideration of this study has demonstrated that AHD71 is a the third order vertical datum, with most of the inconsistencies related to errors within the third order levelling and due to a substantial part of subsections not being fully constrained to control. Furthermore, AHD71 is not a fully physical datum. In fact, no gravity observations were made during the levelling campaign. Instead, a truncated normal-orthometric correction relative to the GRS27 ellipsoid was applied to the spirit levelling.

Even though this correction improved the loop closure, AHD71 still remained non-coincident with orthometric heights (Featherstone & Kuhn 2006).

The introduction of new technologies such as GNSS has provided different methods to carry out vertical control work and, as a consequence, unveiled AHD71 anomalies not referable to spirit levelling. In particular, AHD71 is distorted by about 1.5 m in the north-south direction caused by the LSA that held the 30 tide gauges to zero height without taking into account the sea-surface topography (Featherstone 1998, 2004, 2006; Featherstone & Kuhn 2006). In fact, cold and denser waters of southern Australia are about 1 metre lower than the warmer and less dense waters of northern Australia (Brown 2010).

It is clear from preceding discussions that AHD71 includes errors and does not match a gravimetric geoid model as well as desired. Since AHD71 is still the formal national vertical datum, it was necessary to develop a new geoid model that includes the anomalies within the vertical datum to improve the conversion from GNSS-derived ellipsoidal heights to AHD71 heights. Hence, the introduction of AUSGeoid09 described in section 2.6 was based on this concept.

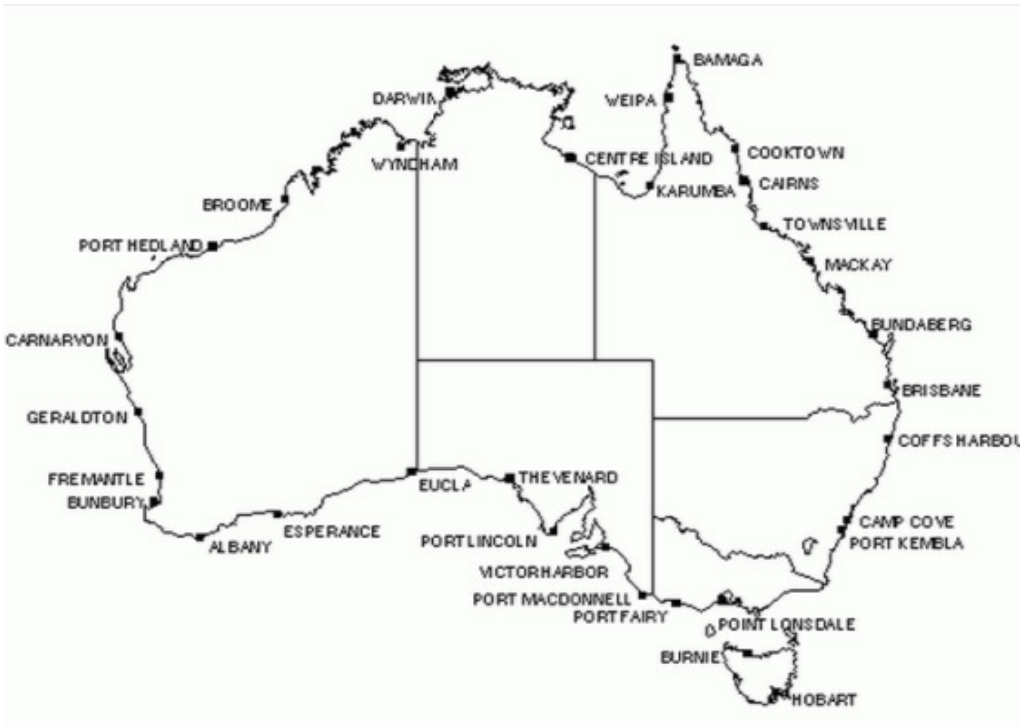

Figure 2.2: The 32 tide gauges used as zero height points for AHD71 and AHD83.

(Source: Geoscience Australia 2012b)

2.5 Sources of Errors Associated with Orthometric Heights

An orthometric height derived from GNSS or conventional levelling can be defined as accurate based on its closeness to a true value. Considering the study conducted by Higgins (1999), obtaining orthometric heights through GNSS observations is limited to measurements, the quality of the geoid model used and the distortions within the national vertical datum. In practice, in the last two decades orthometric heights derived from GNSS observations can be considered a suitable substitute to conventional terrestrial levelling in many applications (Meyer et al. 2006). However, in order to understand the sources of error present in GNSS heighting, it is crucial to minimise discrepancies and keep projects within error budget. Current literature has grouped errors associated with GNSS-derived heights mainly into three categories: satellite position and clock errors, signal propagation errors and receiver errors (Seeber 2003, p. 193), which mainly occur during data collection.

Geoid models include errors associated with the collection of gravimetric data. As mentioned in section 2.3, gravity differs in magnitude and direction from one location to another. In addition, it is difficult to collect gravity observations in locations with limited access. Therefore, it is challenging to estimate the accuracy achieved, and as such a geoid model may include anomalies within some regions and not in others. Moreover, existing benchmarks used in geometric geoid modelling include random and systematic errors. These errors are well known in regards to AHD71, due to the techniques and processing procedures used during the levelling campaign (Featherstone et al. 1998).

As it can be denoted from the above discussion, both the geoid model and the deduction of orthometric heights encompass errors that cannot be avoided and a ‘true’ value is subject to error itself. Hence, accuracy lies within an error range (McDonald 2004). However, according to Featherstone (2004), though GNSS and levelled data have several sources of error, they are the most suitable and practical methods to check a geoid model.

2.6 AUSGeoid09, a Combined Quasigeoid Model Fitted to AHD71

AUSGeoid09 is the first combined model that includes gravimetric and geometric data released in Australia to obtain AHD71 heights from GNSS observations. It refers to the GRS80 ellipsoid and covers the area encompassed between 108ºE and 160ºE longitude and between 8ºS and 46ºS latitude. The grids that compose the model are of 1' by 1' (approximately 1.8 by 1.8 km) which increases the density of about 4 times compared to AUSGeoid98. Previously geoid models such AUSGeoid98 have been computed taking into consideration only the gravimetric component. Consequently a rather low accuracy was achieved in retrieving orthometric heights and misfit issues were evident because it was assumed that AHD71 would be almost identical to the geoid surface. In reality, this is not the case and the inconsistency due to the anomalies within AHD71 illustrated in section 2.4 cannot be ignored. In order to help GNSS users to compute AHD71 heights effectively, it was necessary to add a geometric component to distort the gravimetric geoid model to AHD71 and thereby account for the misfit caused mainly by sea surface topography (Featherstone et al. 2010).

Before going any further, it is important to note that within the Australian context the concept of the quasigeoid is more appropriate than the geoid. By definition, a geoid is an equipotential surface at a right angle to the gravity vector that best approximates MSL, while the quasigeoid is a non-equipotential surface with no physical meaning relative to the earth's gravity field. The quasigeoid is almost coincident with the geoid, and quasigeoid heights are measured along the ellipsoidal normal (Featherstone & Kuhn 2006) . The AHD71 best describes those two surfaces since the spirit levelling observations have been corrected with normal gravity relative to the mean earth ellipsoid instead of gravity observations. However, in Australia the geoid-quasigeoid separation has been evaluated small enough to be ignored for practical purposes (Janssen & Watson 2010, 2011; Roelse et al. 1971) .

The gravimetric component of AUSGeoid09, known as AGQG2009, was achieved throughout the amalgamation of several gravimetric datasets. It was computed about 1 year before AUSGeoid09 using the best existing data for that particular point in time. First of all, the reference frame was based on the Earth Gravitational Model 2008 (EGM2008) and linked to the GRS80 ellipsoid for GDA94 compatibility. Gravimetric observations data is composed of 1.4 million observations of which half are new

gridded recordings. The grids to collect the gravimetric observations were established with GNSS of a general size of 2 to 4 km, but in some circumstances they were a lot smaller (up to 50 m) to avoid discrepancies due to large gravity differences. Furthermore, since Australia is an old continent, it unveils different mass densities where gravity is largely affected by even short distances. Therefore, in-land gravity anomalies were interpolated with a 9" x 9" grid GEO-DATA-DEM9S elevation model. The DNSC2008GRA marine gravity anomalies were implemented to normalise the coastal gravity anomalies. (Brown et al. 2011; Featherstone et al. 2010).

The geometric component can be defined as a model that represents the offset between the gravimetric model and AHD71. This geometric component was used to adjust and fit AGQG2009 to AHD71 with a least squares collocation (LSC) also known as cross validation approach. It was established with the combination of two different clusters of data. The first contains 2,638 marks observed with GNSS where accurate AHD71 was known and AHD71-ellipsoid separation was computed using the following equation (Brown et al. 2011):

$$N_{ahd} = h_{GDA94} - H_{ahd} \tag{2.9}$$

(*Source:* Brown et al. 2011, p. 29)

where

N_{ahd}	Denotes AHD71-ellipsoid separation
h_{GDA94}	Denotes ellipsoid height derived from GNSS observation
H_{ahd}	Denotes AHD71 elevation values provided by States and Territories of class LC or better

The second component comprises 4,233 levelling junction points obtained from the Australian National Levelling Network (ANLN). Since the ellipsoidal heights of the junction points were unknown, an adjustment was performed to obtain these heights. The 2,638 ellipsoidal heights were held fixed and, as a consequence, the junction points were distorted to the quasigeoid in order to gain the derived geoid undulations. Finally, the geoid separation can be deduced with equation 2.10 (Brown et al. 2011):

$$N_{ahd} = \left(dH_{ag} + N_{ag}\right) - H_{ahd} \tag{2.10}$$

(Source: Brown et al. 2011, p. 30)

Where dH_{ag} denotes orthometric height retrieved from adjustment and N_{ag} denotes N value retrieved from adjustment.

As it can be denoted from the above information, the geometric component implemented in AUSGeoid09 has distorted the gravimetric model to AHD71. In this fashion, AUSGeoid09 embraces almost the same anomalies of AHD71. In a similar way, this project will use published AHD71 heights to verify the performance of AUSGeoid09 within mountainous regions.

2.7 Online GPS Processing AUSPOS

In the last few years, dual frequency GNSS Receiver and CORS networks have been one of the central studies for geodesists. These studies have led organisations and government agencies to develop online services for post processing (Grinter & Roberts 2011). Geoscience Australia's Online GPS Processing Service (AUSPOS) is a free online GNSS data processing software developed by GA. It uses the IGS network and IGS product range to compute coordinates anywhere on the globe (GA 2013). The system uses the scientific Bernese software (Dach et al. 2007) and provides GDA94 as well as International Terrestrial Reference Frame 2008 (ITRF2008) coordinates (Altamimi et al. 2011). Ellipsoidal heights obtained from the AUSPOS online processing service are independent of AHD71 and AUSGeoid09. Therefore, this project will use ellipsoids heights obtained with AUSPOS to constrain the GNSS network to the GRS80 ellipsoid in the strategic method detailed in chapter 3.

2.8 Method of Geoid Verification

The two GNSS networks provided by LPI include benchmarks that form part of the AHD71 network, providing a geometric relationship where geoid undulation can be calculated (Featherstone et al. 2001). In this fashion, orthometric heights and GNSS data are used to verify the gravitational geoid model (Featherstone 2001). Even though

AUSGeoid09 is a combined model of gravimetric and geometric components, the above statement is considered valid since the primary use of a geoid model is to compute orthometric heights from ellipsoidal heights. Therefore, the combination of published AHD71 heights and GNSS data is a valuable real-world means to check a combined model.

In an absolute sense, the geoid model is verified in the connection to the reference ellipsoid. This method is based on spirit levelling data connected to the national vertical datum and GNSS data computed to an international reference frame. Put simply, the ellipsoidal heights can be retrieved by relating the GNSS observation to a geodetic datum such as the GDA94. Additionally, the absolute orthometric heights must be known, which is generally achieved by conventional spirit levelling. Then, the computed geoid heights can be retrieved using equation 2.1 (Featherstone 2001). This relationship is valid only if the N values and ellipsoidal heights refer to same ellipsoid or compatible ones (Moritz 1980). GPS-derived ellipsoidal heights nominally refer to the WGS84 ellipsoid, while AUSGeoid09 refers to the GRS80 ellipsoid. Even though these two ellipsoids differ slightly in the flattening, they are compatible at the 0.1 mm level (Featherstone & Kuhn 2006) and, as a consequence, equation 2.1 is valid. It is important to mention that this relationship ignores errors caused by the deflection of the vertical. As shown in Figure 2.3, orthometric heights follow the direction of the plumbline, while ellipsoidal heights follow the direction of the normal to the referenced ellipsoid. These two heights differ by a small angle known as the deflection of the vertical. In practice, the effect of this small difference can be assessed at any particular point by multiplying the deflection cosine by the orthometric height. Given that in Australia the deflection of the vertical is less than 30”, the consequent error is less than one millimetre (Featherstone 2006). Hence, it can be ignored and equation 2.1 is assumed to be valid to compute the geoid undulation and subject only to errors identified in section 2.5.

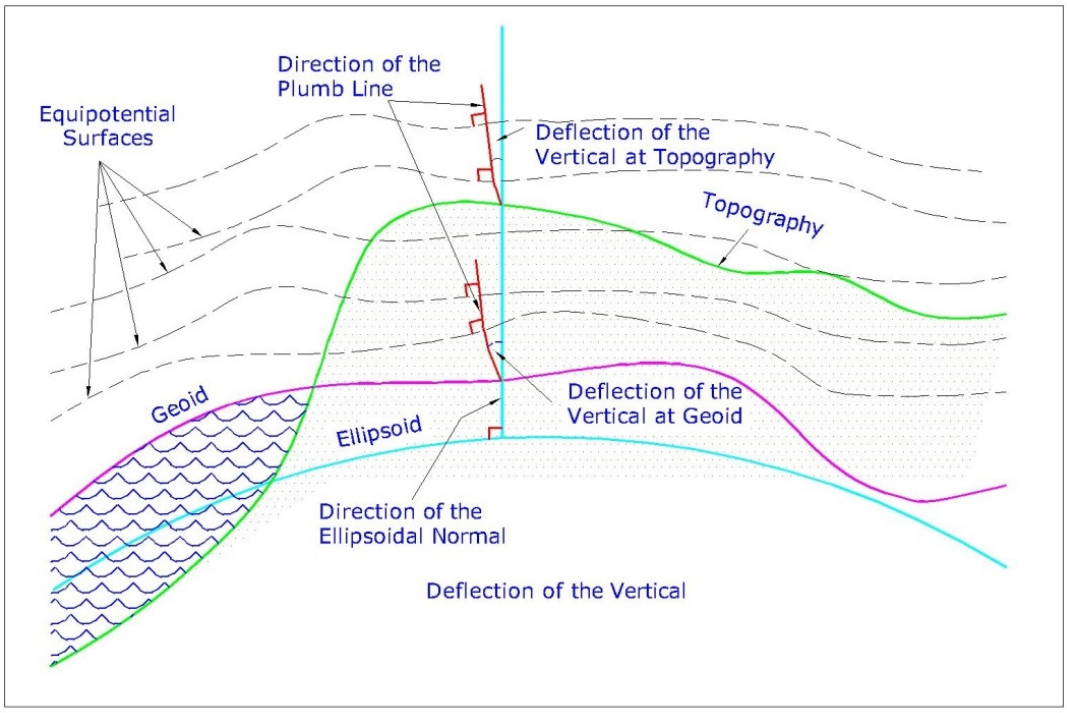

Figure 2.3: Deflection of the vertical.

On the other hand, the relative approach is probably more appropriate from a surveying point of view because it is based on the difference in heights over the same baseline (see 2.1(b)). Hence, systematic errors existing at each end of the baseline will be minimised due to the principle of differencing. Besides, the method is constrained to use the same ellipsoid referenced by the geoid model, and the model is verified using the following equation (Brown et al. 2011; Featherstone 2001):

$$N_A - N_B \approx (h_A - H_A) - (h_B - H_B) \tag{2.11}$$

(*Source:* Featherstone 2001, p. 810)

In this fashion, the above equality can be used to compute ΔN_{AB} over all possible baselines within a network of control points. However, a least squares adjustment needs to be accomplished to create a network with consistent ellipsoidal heights. The number of possible baselines over n control points is deduced using $n(n-1)$ while the distance between control marks is calculated using Vincenty's inverse formula (Brown et al. 2011; Featherstone 2001).

From a surveying point of view, the relative approach is more appropriate to validate the performance of a geoid model since it checks the performance to compute differences in height from one control point to another, which is the typical method to carry heights. However, this study aims to identify the accuracy in the connection to AHD71 using AUSGeoid09 in both the absolute and relative sense, as explained in Chapter 3.

2.9 Computation with Microsearch GeoLab

Microsearch GeoLab (Microsearch 2013) is a Windows-based program that uses the least squares method to calculate survey mark coordinates within geodetic networks. The program allows a variety of data sources such as directions, distances and GNSS observations. The program is structured to compute a least squares adjustment of survey measurements and provides detailed statistical analysis to further establish the quality achieved. This program supports the use of geoid models to compute geoid undulations and orthometric heights and any sort of coordinate transformation (BitWise Ideas Inc 2010). In addition, it supports GNSS baseline representations in the Conventional Terrestrial (CT) coordinate system format, which is a typical format used to symbolise baselines. This includes the Cartesian coordinates Northing-Easting-Up (N,E,U) of two points or their difference and the correlation matrix. Besides, the correlation matrix can be manipulated to have NE or NEU correlation (Dickson 2006).

The program includes four techniques to compute geoid interpolations: bi-linear, bi-quadratic, bi-cubic and bi-quartic. Each method interpolates the geoid model within the grid using polynomials of N values based on geographic coordinate increments. The only difference between the four methods is the number of points used during the interpolation process, i.e. 4 for bi-linear, 9 for bi-quadratic, 16 for bi-cubic and 25 for bi-quartic (Microsearch 2001, p. 143). There are other packages such as Leica Geo Office (LGO) (Leica Geosystems 2013), Trimble Geomatics Office (TGO) (Trimble 1999) and Trimble Business Centre (Trimble 2013) generally used to manipulate and manage GNSS observations. These computer programs support the use of geoid models and bi-linear and bi-quadratic interpolation only. However, bi-linear and bi-cubic

interpolations seem to be the two most popular techniques adopted by users (Featherstone 2001; Gibbings & McDonald 2005).

2.10 Current Standards for Vertical Control

As stated previously, the emphasis of this study is the comparison of AUSGeoid09-derived AHD71 heights and published AHD71 heights. However, it is important to understand the quality of the data in order to avoid overestimating the result of the adjustment that will be illustrated in Chapter 4. According to the *Standards and Practices for Control Surveys (SP1) Version 1.7* (ICSM 2007), errors propagate in different ways depending on the technique used to carry out height control. In this fashion, GNSS techniques include vertical error propagation proportional to the distance, while differential levelling propagates error to the square root of the distance.

In NSW, currently standard control survey work is guided by *the Surveyor General's Direction No. 12* (LPI 2012). This document emphasises that typical control surveys are achieved through precise measurements linked to the existing control network. The quality of the data is based on the concepts of class and order (Dickson 2012; LPI 2012). As defined by ICSM (2007), class is the precision achieved based on the equipment, technique, survey practice adopted, network design and method of reduction implemented. It is determined by a minimally constrained least squares adjustment and the semi-major axis ellipse error which is compared to the acceptable error using equation 2.12 for GNSS observations and equation 2.13 for differential levelling:

$$r = c(d + 0.2) \tag{2.12}$$

$$r = c\sqrt{d} \tag{2.13}$$

(ICSM 2007, pp. A-12)

where

r denotes the largest acceptable semi-major ellipse error
c is an empirically derived element that refers to a particular class
d is the distance between stations in km

The Surveyor General's Direction No. 12 identifies the order as the quality of the new coordinates based on how well they fit within the existing control network. Besides, LPI does not indicate any procedure to identify the order due to the assessment being subject to LPI's decision. However, *SP1 Version 1.7* bases the assessment of order on the technique adopted and it is evaluated from a constrained adjustment in conjunction with the class achieved, the order of the heights held fixed, the precision of height conversion and the accuracy of geoid undulation. The same equation used for class is used but with the difference that the *c* values are based on order.

2.11 Previous Studies of Geoid Models

Recent examinations of AUSGeoid09 and past investigations of preceding Australian gravimetric geoid models have emphasised different techniques to quantify the performance of these geoid models in the connection to AHD71. In reality, from these studies it appears that absolute and relative approaches are the two most practical ways to investigate the geoid model using GNSS and levelling data.

2.11.1 Several Geoid Models over the Great Dividing Range Toowoomba

One of the most interesting evaluations of geoid models was conducted by McDonald (2004) where 5 global and 2 Australian (AUSGeoid93, AUSGeoid98) geoid models were compared both in absolute and relative sense over 46.2 km along the Great Dividing Range escarpment of Toowoomba. The evaluation was established to compare geoid derived heights with a digital levelling traverse over 116 control points along the escarpment. Of all the models studied, this study found AUSGeoid98 (the most recent AUSGeoid at the time) to be the best of all models to derive AHD71 heights over the above site.

Particularly relevant to this research is the method of verification employed both in absolute and relative sense. Absolute verification was employed to compare N values derived by conventional digital levelling with geoid-derived ones over all of the 116 control points and as a function of 100 m rise in AHD71. The different geoids were also verified using the relative approach over all possible baselines between the 116 control

points where the baseline lengths between control points were computed using Vincenty's inverse formula. A part per million (ppm) was computed for each residual to further compare every model as a function of propagation of error proportional to baseline length. Finally to verify if any geoid model was a valid substitute to conventional levelling to derived AHD71 heights, a comparison was made between the relative residuals and standard accuracy for the 3rd order levelling based on the standard accuracy specified in ICSM (2004) (McDonald 2004).

A similar methodology will be employed for this project to verify the accuracy of AUSGeoid09 both in absolute and relative sense by comparing AUSGeoid09 and AUSGeoid98, which will be further detailed in Chapter 3.

2.11.2 AUSGeoid98 in Costal and Mountainous Regions

Probably one of the largest related studies focused on mountainous and coastal regions was conducted by Featherstone and Guo (2001). This study was aimed at investigating the improvement of AUSGeoid98 over AUSGeoid93 using map-based, graphical and descriptive statistical comparison of 1,013 GPS-AHD71 control points across the country. Additionally, the global OSU91A and EGM96 geoid models were compared to identify the best geoid model to obtain the conversion between GNSS-derived heights and AHD71 heights.

Map-based, graphical and descriptive statistical comparison is a method of comparing the geoid models in three steps. First, the map-based approach was used to identify spatial differences between the geoid and the control data. Then the graphical representation validates the performance of the model in a relative sense in terms of latitude, longitude and AHD71 values. Lastly, the statistical comparison gives a numerical representation of the connection to AHD71 with the assumption that differences between the control data and the gravitational model are equally distributed (Featherstone & Guo 2001).

The salient part of the study pertinent to this research is the statistical evaluation of 512,578 baselines between the 1,013 points used to quantify the connection of AUSGeoid93 and AUSGeoid98 to AHD71. Their study demonstrated that AUSGeoid98 better fits to AHD71 both in absolute and relative terms. In particular the

mountainous regions were evaluated as a function of 100 m increment in AHD71 heights and scatter plots were used to identify trends among different directions and elevations. However, it is important to note that the quality of the connection to AHD71 was based on the rate of improvement from AUSGeoid93 to AUSGeoid98 as the errors relating to data acquisition, control marks and incompatibility of AHD71 and the gravimetric model were not exactly quantifiable.

In a similar way, this project aims to represent the expected improvement of AUSGeoid09 to compute AHD71 heights based on a comparison between AUSGeoid98 and AUSGeoid09. Additionally, this project aims to verify AUSGeoid09 as a function of 100 m increment in AHD71 over all possible baselines between checkpoints.

2.11.3 AUSGeoid09

A nation-wide study to assess the quality of AUSGeoid09 was carried out by Brown et al. (2011). As described in section 2.6, AUSGeoid09 has been fitted to AHD71 through LSC. This method includes two constraints, i.e. correlation length and Root Mean Square (RMS). The correlation length was verified from 10 km to 500 km using an empirical approach in nine different tests. Instead of testing the RMS, AHD71 heights were assumed as true values and one sigma weights applied to all GNSS observations.

The relative approach was used to investigate the performance of AUSGeoid09 since GNSS surveys are generally carried out with the differential approach for the reasons explained in section 2.8. Brown et al. (2011) used 6,672 points to yield 22,254,456 baselines of different lengths. However, in order to give more significant evaluation for GNSS users and represent a realistic GNSS network, the total number of baselines was reduced to 622,928, which only represents baselines shorter than 100 km.

It was found that the RMS of the relative testing was approximately 0.03 m for all baselines. Only 2.9% of the 622,928 were above the tolerances of class LC specified in ICSM (2004), whereas the same test using AUSGeoid98 achieved just 51% of all the baselines below the same LC limits. Moreover, previous research of AUSGeoid models argued that gravimetric geoid models were not appropriate to obtain orthometric heights from GNSS observations in an absolute sense due to large residuals.

The introduction of AUSGeoid09 has improved this method exponentially (Janssen & Watson 2010). In fact, considering the cross validating testing, it is possible to covert GNSS-derived ellipsoidal heights into AHD71 height within ±0.03 m (1 sigma) uncertainty. However, some locations remain where the AUSGeoid09-dereived AHD71 heights and AHD71 heights differ in the order of a decimetre. In mountainous and coastal regions it is quite difficult to model a gravimetric geoid. Therefore, it is necessary to investigate these locations to identify anomalies and evaluate the geometric correctional surface to include within AUSGeoid09 in the near future (Brown et al. 2011). This study aims to investigate the performance of AUSGeoid09 to compute AHD71 heights within mountainous regions by implementing an objective research method explained in Chapter 3.

2.11.4 Performance of AUSGeoid09 in NSW

Janssen and Watson (2010, 2011) investigated the performance of AUSGeoid09 in NSW by quantifying the rate of improvement from AUSGeoid98. In order to achieve this, 513 AUSPOS solutions, 38 CORSnet-NSW stations and 7 GNSS networks were used in four different tests.

The first test was based on 513 AUSPOS solutions of 3 to 94 hours of GNSS data. These solutions were collected over several years prior to the research by LPI over marks with accurately known AHD71 values. Almost half of these were levelled marks with an accuracy classification of LCL3 or better and the remaining ones were C3 or better. Geoid undulations for both geoid models were calculated via interpolation at each of the AUSPOS solutions and comparisons were made with published AHD71 values in SCIMS. Instead of evaluating the residuals themselves, as they can be positive or negative, the RMS approach was adopted:

$$RMS = \sqrt{\frac{\sum_{i=1}^{n} x_i^2}{n}} \tag{2.14}$$

(Source: Janssen & Watson 2011, p. 31)

Where *n* denotes the number of residuals for x_1 to x_n.

It was found that the use of AUSGeoid09 decreased the RMS from 0.185 m to 0.069 m, revealing an improvement factor of 2.7 compared to AUSGeoid98. A similar test was performed using 38 CORSnet-NSW stations with GNSS data observed for seven days. Accurate AHD71 values were known as a part of the A1 network surveys used to tie these stations into the SCIMS network. In this instance, the use of AUSGeoid09 revealed an improvement factor of 4.1.

The last two tests performed in seven different locations were minimally constrained and fully constrained network adjustments, used to identify the rate of improvement. The sites were subject to a careful examination to incorporate different baseline lengths and changes in elevation as part of typical GNSS surveys. In particular, the constrained adjustment demonstrated a better overall fit with the use of AUSGeoid09, where in the majority of the cases the flagged residuals were removed compared with using AUSGeoid98. The minimally constrained adjustments were developed to hold fixed one accurate height only, located at the centre of each network. Again in these instances, the AUSGeoid09-derived AHD71 heights were achieved with an accuracy of within ±0.05 m as stated by GA. Two of the networks demonstrated accuracies outside the expected ±0.05 m. However, these GNSS networks contained baselines of 130 km in length, therefore it was expected to achieve a lower level of accuracy (Janssen & Watson 2010, 2011). Although their study investigated different elevations range, it did not include mountainous regions. Consequently, the aim of this research is to explore the performance of AUSGeoid09 within these regions.

2.12 Conclusion

This chapter has described and substantiated the theories and methods used to convert GNSS-derived ellipsoidal heights to (orthometric) AHD71 heights. Current literature specifying the techniques of geoid model verification, such as absolute and relative approaches, have been explored. It has been established that combining GNSS and levelling data is the best practical method to test a geoid model.

A review of AHD71-related literature has demonstrated that this national height datum is showing its age, containing distortions of about 1.5 m in the north-south direction. These distortions were mainly caused by ignoring sea-surface topography at the 30 tide

gauges used to define MSL during the definition of AHD71. In addition, the computation of orthometric heights with GNSS and levelling techniques includes errors that to some extent reduce accuracy of both the geoid model and AHD71. Therefore particular statistical analyses will be implemented to better establish the quality of the data.

The current standards for vertical control have been studied to identify the limitations of the data used in this research and to understand the quality of the class and order of the published SCIMS marks used as checkpoints.

Chapter 3 will explain and justify the methods employed to accomplish this research. This will include detailed information on the sites, control data, GNSS networks, software packages and techniques adopted.

CHAPTER 3
RESEARCH METHOD

3.1 Introduction

Chapter 2 reviewed the current methods used to convert GNSS-derived ellipsoidal heights to (orthometric) AHD71 heights through the implementation of a geoid model. The theories and methods used to test geoid models are considered crucial for a positive outcome of this project and set up the process to verify AUSGeoid09 as detailed in this chapter.

The aim of this chapter is to define the process employed to verify how well AUSGeoid09 converts GNSS-derived ellipsoidal heights into AHD71 heights in the Snowy Mountains and Mid Hunter mountainous regions of NSW.

A brief description of both study areas is given to contextualise the locations. Since control marks, GNSS networks and published SCIMS AHD71 heights are provided by LPI, a method of evaluation is defined in order to establish the correctness of data that will be used for the subsequent tests. The process implemented for data manipulation is presented with initial evaluation of precision based on LPI experience. The test approach is described and based on the current theories and methods defined in Chapter 2. Furthermore, an additional test aimed at comparing results in the connection to AHD71 using both AUSGeoid98 and AUSGeoid09 is briefly outlined in order to quantify a rate of improvement for the new geoid model in computing AHD71 heights.

3.2 Study Areas

This study includes two separate locations within mountainous regions in NSW, selected based on the availability of data and large differences in elevation. They are ideal locations to sample the performance AUSGeoid09, since they represent a typical mountainous elevation model within the Australian context. Two large GNSS networks are provided by LPI. GNSS observations and consequent adjustments were performed by LPI to bring survey control within the expectations of the network design based on *the Surveyor General's Direction No. 12* (LPI 2012). The GNSS observations will be fully analysed in Chapter 4, where a detailed metadata examination will be implemented to verify the data before any test is conducted. The first study area is located in the Snowy Mountains, while the second is located in the Mid Hunter region (Figure 3.1).

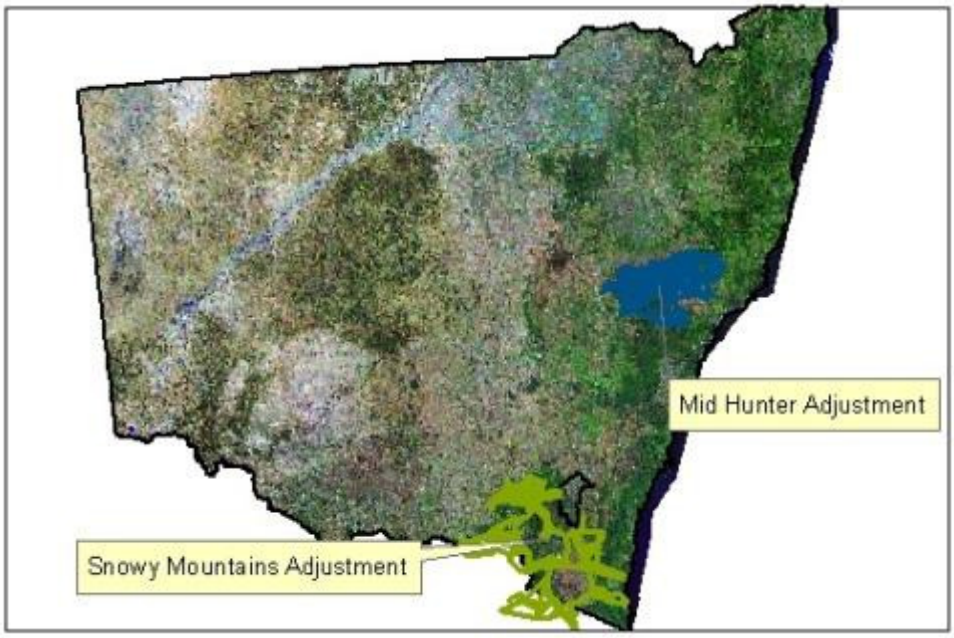

Figure 3.1: Location of the two study areas in NSW.

3.2.1 Snowy Mountains

The Snowy Mountains GNSS network adjustment illustrated in Figure 3.2 was a project undertaken by LPI to determine control for 50 cm and 10 cm pixel imagery requirements for several towns in the south-east of NSW. Additionally, the project was used to amalgamate previous adjustments to achieve both horizontal and vertical homogenous networks in SCIMS (Moss 2011). Over 1,300 independent baselines were observed between 429 marks. 105 marks were held fixed vertically, of which 94 were spirit levelled marks of accuracy LCL3 or better. The remaining 327 were left to float during the adjustment. The project covers an area between Albury, along the Victorian boundary to the coastal areas in the south, and between Tumut along the ACT boundary to Cooma in the north. The terrain encompasses an undulated topography composed of mountains reaching a peak of 2,200 m and low valleys with elevations of about 200 m (Moss 2011). A typical terrain model is shown in Figure 3.3.

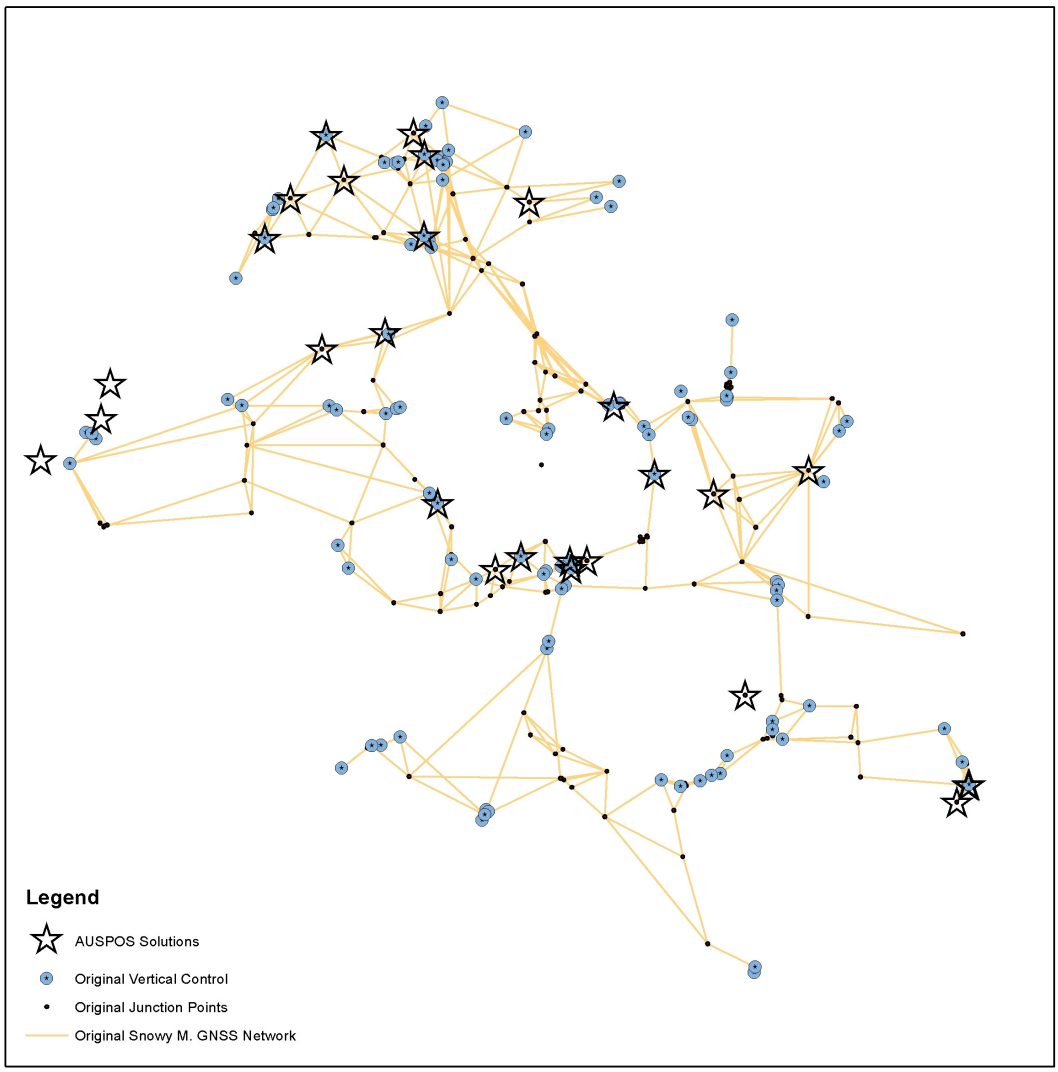

Figure 3.2: Snowy Mountains GNSS network and co-located AUSPOS solutions.

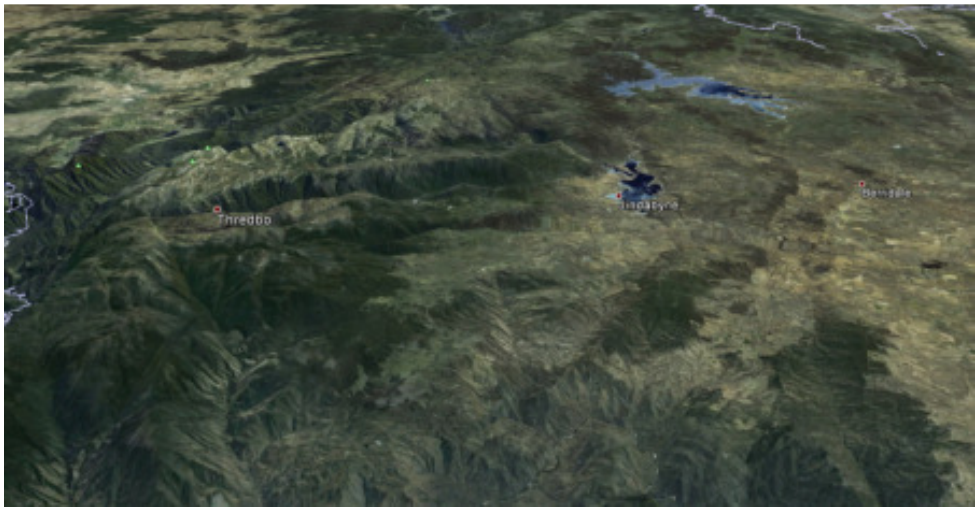

Figure 3.3: Typical terrain in the Snowy Mountains (Google Earth 2013a)

3.2.2 Mid Hunter

The Mid Hunter project was a GNSS network adjustment performed by LPI to determine survey control for general purposes in the Hunter region (Figure 3.4). It covers an area stretching from about 115 km south of Mount Royal National Park to 170 km east of Mudgee. The terrain is mainly composed of mountains and valleys with elevations ranging from 20 m to peaks that reach 1,400 m. Figure 3.5 illustrates the typical terrain formation. 154 marks were observed, of which 82 were held fixed vertically, while the remaining marks were left to float in the adjustment to bring in control where appropriate. Additionally, this project has amalgamated previous GNSS campaigns to create homogenous vertical and horizontal control marks within the SCIMS network (O'Kane 2011).

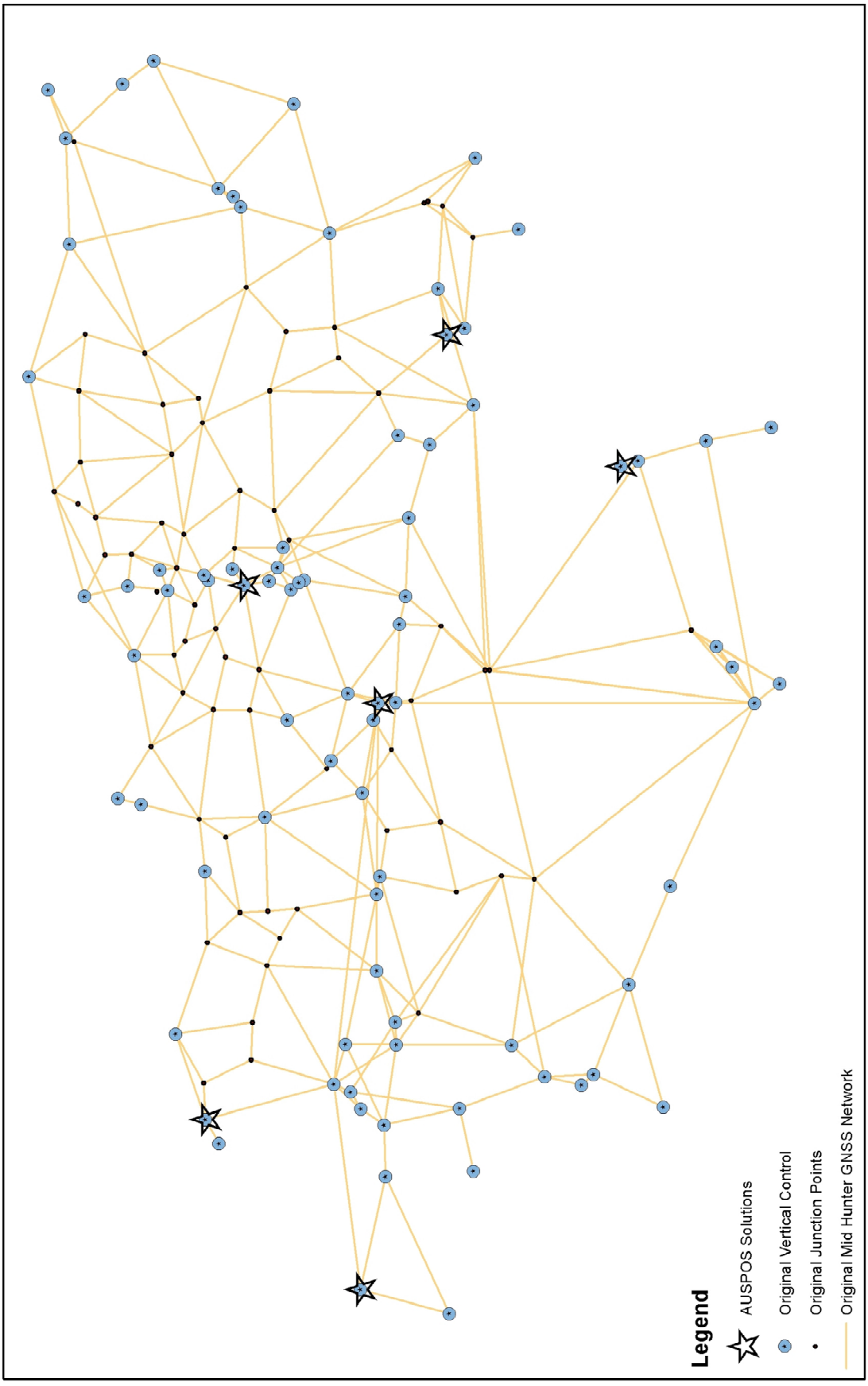

Figure 3.4: Mid Hunter GNSS network and co-located AUSPOS solutions

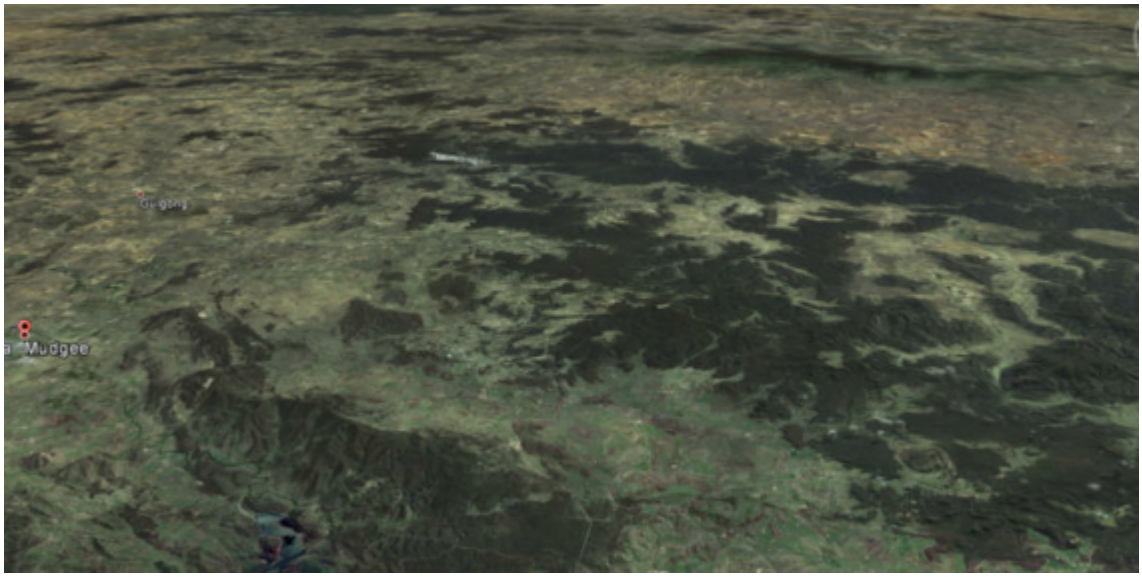

Figure 3.5: Mid Hunter typical terrain (Google Earth 2013b)

3.3 Checkpoints Network Marks

Both the Snowy Mountains and Mid Hunter GNSS networks were designed to achieve the most accurate outcomes horizontally and vertically. A Crucial part of the design was the strategic location and good quality of the SCIMS control marks that were held fixed within the constrained adjustments. As such, these control marks represent the checkpoints where this study will investigate the performance of AUSGeoid09 since they have not been floated by the LPI adjustments. Table B.1 and Table B.2 in Appendix B show the checkpoints for the Snowy Mountains and Mid Hunter networks respectively.

As this study is focused on the height component, there was more emphasis on the original source adjustments and methods used to hold “fixed” the AHD71 values in the Snowy Mountains and Mid Hunter adjustments, rather than concentrating on the horizontal components. Intrinsically, the research objective is to use marks that have been levelled with accurate LC class and L3 order or better. As previously stated, the Snowy Mountains GNSS network contains 105 such survey marks. On the other hand, the Mid Hunter GNSS network was fitted to AHD71 based on 82 SCIMS marks of which 50% are levelled with class LC order L3 or better and the remaining 40 marks

have obtained AHD71 values with different techniques of class C order 3 or better. Therefore both networks include 186 marks with medium to high accuracy AHD71 heights (Moss 2011; O'Kane 2011). The positions of the vertical control marks in the Snowy Mountains and Mid Hunter regions in relation to the original network adjustments performed by LPI are shown in Figure 3.2 and Figure 3.4 respectively.

3.4 Data Evaluation

SCIMS heights, AUSPOS solutions and GNSS observation data for this project were provided by LPI. At LPI, data collection manipulation and reduction is subject to rigid policies known as Surveyor General Directions to achieve the highest quality assurance (LPI 2013b). However, according to a study on the performance of AUSGeoid98 by Featherstone et al. (2001), the propagation of errors discussed within section 2.5 and the analysis of AHD71, it is clear that GNSS and spirit level data (and as consequence published AHD71 heights implemented for this project) are not ideal. Some errors do exist within data capture, manipulation and reduction. In this context, statistical analysis and thorough investigation of metadata prior to any computations are crucial to ascertain the correct estimation of precision to establish a realistic outcome of this research.

The majority of control marks within both study areas include benchmarks of class and order C3 or better. These marks are published AHD71 heights available in SCIMS. The campaign to establish these has been achieved at different times and from different sources. Therefore, it is expected to have some discrepancies in the accuracy stated (Featherstone 2001). It is important to note the possibility that marks have been disturbed over time. In reality, the investigation of this problem is beyond the scope of this research and SCIMS heights are assumed to be within the stated accuracy. However, where a mark is suspected to have moved or been disturbed, it will be disregarded from the comparison to the orthometric heights retrieved from AUSGeoid09 and AUSGeoid98.

The GNSS networks provided by LPI include different sources of data collected on different occasions. LPI has combined these sources to create these two large GNSS datasets (Moss 2011; O'Kane 2011). Before undertaking any test, it is crucial to verify

the quality of the data (Featherstone et al. 2001). Consequently, prior to any statistical computation, a thorough analysis of each adjustment's report will be undertaken. Particular attention will be given to the data collection campaign and reduction method implemented. The aim is to identify potential irregularities that may affect the estimation of precision. After evaluating the metadata to identify the strength and weakness of the two networks, a minimally constrained LSA will be performed with *Microsearch GeoLab* to further establish the accuracy quality of the networks. It should be noted that all baselines not applicable to this study will be removed, and new data available from the LPI database will be added if necessary.

The two GNSS network adjustments include several marks with accurate ellipsoidal heights previously obtained by LPI through the AUSPOS service. These AUSPOS solutions are based on observation sessions of 4 hours or more. Session details and accuracy achieved will be discussed and the AUSPOS report will be investigated.

3.5 Data Computation

A uniform network of ellipsoidal heights will be obtained through a LSA using *Microsearch GeoLab*. Available AUSPOS solutions from LPI will be used to constrain the network to the GRS80 ellipsoid. In addition, the same LSA will deliver N values with bi-linear, bi-quadratic, bi-cubic and bi-quartic interpolation using both the AUSGeoid09 and AUSGeoid98 models. Therefore, the retrieved N values at the 95% confidence level are independent of AHD71.

The input standard deviations of each GNSS baseline will be computed using Northing – Easting (NE) correlations, as opposed to Northing-Easting-Up (NEU) correlations. This ensures that the vertical component is left free to be adjusted onto the ellipsoid.

Put simply, at each instance the LSA will provide N values and a consistent network of ellipsoidal heights that will be used in the analysis outlined in the next section.

The initial quality of computed ellipsoidal heights will be based on the following considerations for the estimation of precision. Hence, GNSS static network observations will be weighted accordingly using the following criteria:

- **Horizontal**. 1.0 ppm + 0.0015 m constant and 0.0015 m centring.
- **Vertical**. 2.0 ppm + 0.015 m constant, 0.002 m height measurement and ±0.010 m input standard deviation.
- **Covariance matrix**. The correlation with the GNSS network will have NE correlation rather than NEU to leave the vertical component free in the connection to the GRS80 ellipsoid.

(Dickson 2006; London 2013)

These values are default values that LPI use as a starting point for all GNSS LSAs. These values have been determined not from any specific data but from 30 years of LSA experience by LPI staff. They provide a good starting point for identifying gross errors in the data. Once the data is cleaned from errors, these values are adjusted and the covariance matrices are recalculated to achieve a variance factor close to one in both the horizontal and vertical components and pass the Chi-square test. This is dependent, however, on having realistic input standard deviations. For example, where the initial variance factor is very low (for example 0.05), to achieve a variance factor close to one, the input standard deviations may need to be dropped to (say 1 mm + 0.2 ppm) or scaled down by a factor depending on the adjustment's performance. It is unlikely that this is what was actually measured and therefore the resultant error ellipses achieved are unrealistic. It would therefore be more desirable to leave the input standard deviations at more realistic values and have a low variance factor. That being said, a very low variance factor could be an indication of poor redundancy in the network.

LPI's policy is to separate the input standard deviations for the horizontal and vertical components. This allows for the fact that the vertical component of GNSS observations will in general be less accurate than the horizontal. In addition, at the analysis stage, the variance factors are looked at horizontally, vertically and combined. Using the separate standard deviations and variance factors ensures that neither component is skewing the resultant combined variance factor. LPI's in-house program *Strangelove* is used to modify the input standard deviations (and resultant covariance matrices) and for the analysis of the group variance factors and degrees of freedom (Dickson 2006, 2013; London 2013). Furthermore, the LSA residuals will be analysed in conjunction with redundancy values (ri) to identify gross errors. According to Harvey (1990), for each observed baseline it is possible to compute the *ri* value with the following equation:

$$ri = S_{vi}^2 / S_{li}^2 \tag{3.1}$$

(Source: Harvey 1990, p. 203)

where S_{vi}^2 denotes the variance of the residual and S_{li}^2 the variance of the observation. Generally speaking, the average *ri* values for a network is comprised from 0.5 to 0.8 (Harvey 1990, p. 204). It is important to note that the computation of *ri* values does not specifically detect a gross error but it helps to identify marginally detectable errors which are small errors within the observations. In fact, based on Caspary (1987, p. 89) the degree of which a residual is affected by a marginally detectable error is computed by multiplying the *ri* value times the gross error. In this fashion, as *ri* values approach 1, the greater is the influence of a gross error. Therefore, in a network where redundant measurements are available, if a particular baseline returns a flagged residual and a *ri* value is close to 1, there is a possibility that the baseline includes a marginally detectable error.

3.6 Validation Method

The performance of AUSGeoid09 in the two study areas will be verified using both the absolute and the relative approach. Several publications detailed in section 2.11 that are the base of this research have been considered in order to determine the most practical method to verify the geoid model.

In an absolute sense, AUSGeiod09 will be verified using equation 2.4 where AHD71-derived N values (N_{AHD}) are computed by subtracting the AHD71 height (H_{AHD}) at each checkpoint from the co-located ellipsoid height computed via the LSA (h). Finally, N_{AHD} will be compared with N values computed using AUSGeoid09 with bi-linear, bi-quadratic, bi-cubic and bi-quartic interpolation to define the residual R, i.e. $R = N_{AHD}$-N.

AUSGeoid09 will also be verified using the relative approach explained in section 2.8. This method will be applied to all possible baselines between checkpoints and where a direct observed baseline is available between two marks with accurately known AHD71 values. The model is verified by comparing the change in published AHD71 (ΔH_{AHD}) between two marks and the difference in GNSS-derived orthometric height (ΔH_{GNSS})

computed using equation 2.3. Then the residuals R will be computed using the following equations:

$$R = \Delta H_{AHD-AB} - \Delta H_{GNSS-AB} \tag{3.2}$$

A comparison of AUSGeoid09-derived AHD71 and levelled AHD71 will, to some extent, detect the closeness of the geoid model in the connection to the vertical datum. This approach is based on the assumption that AHD71 has no discrepancies. However, as explained in section 2.4, AHD71 is far from an ideal vertical datum. Additionally, the residuals will be compared with the 3rd order differential levelling misclose over the length of the baseline as it was implemented by Brown et al. (2011).

Featherstone and Guo (2001) quantified the quality of orthometric heights calculated with AUSGeoid98 by comparing the model with its predecessor AUSGeoid93. In this fashion, this study will compare the residuals in the connection to AHD71 using both AUSGeoid98 and AUSGeoid09. The comparison between these two models will quantify the expected improvement in the connection to AHD71. The entire testing methodology is summarised in Figure 3.6.

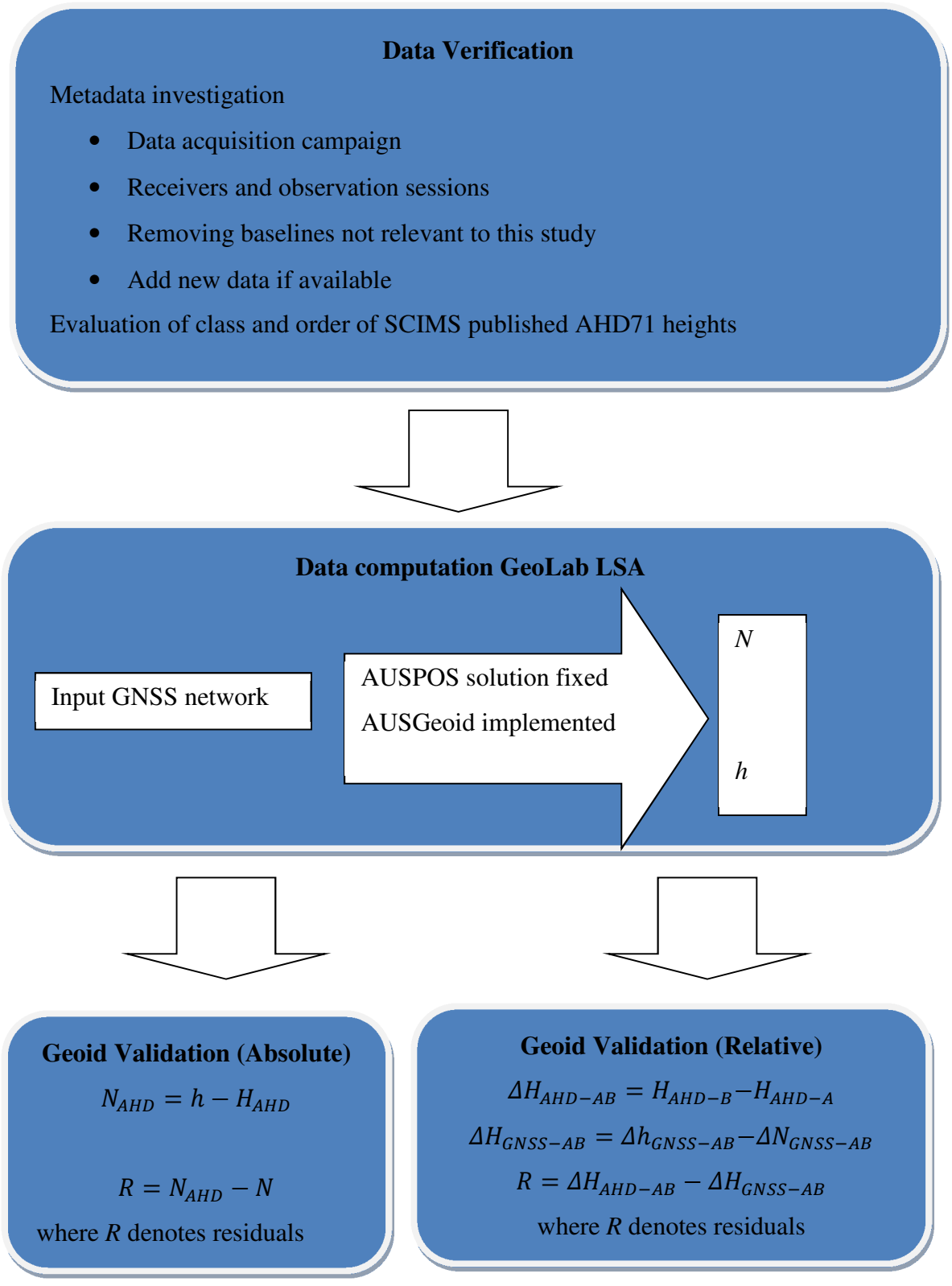

Figure 3.6: Testing methodology process

3.7 Conclusion

This chapter has outlined the location of the study areas and the methods employed to investigate AUSGeoid09 performance in two mountainous regions of NSW.

The study will be carried out in the Snowy Mountains and the Mid Hunter regions. These two areas include 186 published marks with accurate AHD71 heights that will represent the checkpoints for the project.

AUSPOS solutions, GNSS networks and SCIMS control marks provided by LPI are utilised for the purpose of this research. AUSPOS solutions will constitute the control marks that will constrain the networks to the GRS80 ellipsoid in order to obtain a consistent network of ellipsoidal heights. The same LSA will provide N values using both the AUSGeoid98 and AUSGeoid09 models via bi-linear, bi-quadratic, bi-cubic and bi-quartic interpolation methods. However, from Chapter 2 it has emerged that the data used for this project includes unavoidable sources of errors. Therefore, an investigation of the metadata and statistical analysis will be implemented to verify the data before any test is undertaken.

Initial estimation of precision is stated based on LPI past experiences. However, an empirical method to establish these values will be implemented to investigate possible errors within the dataset. Then the covariance matrix will be modified to obtain a variance factor of one and pass the Chi-square test.

Absolute and relative approaches will be adopted to verify AUSGeoid09 performance. These methods have been used in similar studies by other authors (see Chapter 2 for details). The absolute verification will be used to identify the accuracy of AUSGeoid09 considering a single point. The relative approach will investigate differential heighting, which is the familiar surveying technique generally used in practice.

Chapter 4 will outline the verification of the data prior to conducting any tests. This will include removing baselines not relevant to the tests, investigation of metadata and statistical analysis.

CHAPTER 4
COMPUTATION

4.1 Introduction

Chapter 3 detailed the method employed to guide this research and highlighted the tests that are implemented to verify the performance of AUSGeoid09 in the connection to AHD71 within two study areas, compared to the performance of AUSGeoid98. However, as it was acknowledged in section 3.4, it is imperative to evaluate the data used to verify any geoid model before performing any test.

Therefore, the aim of this chapter is to analyse the metadata and implement statistical measures to verify the accuracy of these datasets used for comparison within Chapters 5 and 6.

The AUSPOS solutions reports provided by LPI that will be used to fit the GNSS network to GRS80 will be investigated and a summary will be presented. Both GNSS networks will be evaluated in terms of their data collection, receivers used and the survey-processing techniques. The networks will be then assessed based on their design complexity and relevance to this research. This will unveil sections of the networks where additional baselines were added to improve the networks or where data was remove data due to its irrelevance to this project, without compromising any redundant measurements.

The two networks will be subject to several LSAs. Initially a minimally constrained LSA will be computed to verify the accuracy of the datasets as per relevant survey practice regulations. Then constrained LSAs will deliver ellipsoidal heights and N values using both AUSGeoid09 and AUSGeoid98 that will be used for testing in the following chapters. The result of the LSAs will be evaluated based on statistical measures that will identify the overall fit. Additionally, in order to identify the presence of gross errors, a systematic evaluation of standardised residuals in conjunction with redundancy values will be implemented. Finally the estimated average variance of the ellipsoidal heights of all checkpoints will be computed from the *GeoLab* output.

4.2 Control Marks

Ellipsoidal heights retrieved from AUSPOS solutions represent the control marks that are held fixed throughout both the Snowy Mountains and Mid Hunter networks. As

identified by Featherstone (2001) and explained in section 2.8, this constraint was necessary to connect the GNSS data to GDA94 and a have a homogenous network of ellipsoidal heights, relative to GRS80, for both networks. In this fashion, it was possible to compare the retrieved N values using both AUSGeoid09 and AUSGeoid98 with N_{AHD} values computed from the published AHD71 at the checkpoints. The campaigns to retrieve the AUSPOS solutions have been derived within several occasions, with different receivers and session lengths. Table B.3 and Table B.4 in Appendix B depict a summary from the AUSPOS solution reports that are used within the Snowy Mountains and Mid Hunter networks respectively.

Although the aim of this study is to verify the performance of AUSGeoid09 using the vertical component of the GNSS data, it was also important to evaluate the horizontal component. This is because *GeoLab* computes the variance factor as a result of a 3D adjustment. In this fashion, the marks that were held fixed horizontally within both original constrained adjustments performed by LPI were adopted within the constrained adjustments of this study. However, to further establish the accuracy of the vertical component, the variance factor was computed separately for both horizontal and vertical components using *Strangelove* and the input estimations of precision have been modified accordingly. In reality, the horizontal component did not affect the result of the ellipsoidal heights since the correlation was set to Northing-Easting only. However, the separation of the two was necessary to ensure that both components have variance factors close to 1.

4.3 The Snowy Mountains GNSS Network

The original network provided by LPI included a large dataset of GNSS observations combined in some pockets with a mean of 5 sets of conventional terrestrial direction and distance measurements. The overall network was designed with several small clusters of baselines joined together by long baselines. The majority of GNSS observations were collected during four campaigns from October 2010 to February 2011 with Trimble R7 and Trimble 4700 units. Other GNSS observations collected in 1997 and 2007 as part of former adjustments were added to create an output of coordinates consistent throughout SCIMS. All of the GNSS observations had different

session lengths based on the distance between marks and to achieve ambiguity resolution and recording rate (epoch) was set to 10 second interval. The data collected was then processed with Trimble Business Centre (TBC) version 2.3 or Trimble Geo Office (TGO) version 1.63. Finally, all the independent baselines were converted using the in-house program *Strangelove* in the NEU format with a covariance matrix and Northing-Easting correlation only (Moss 2011).

As this project is aimed to verify the performance of AUSGeoid09 and AUSGeoid98 using GNSS data and published AHD71 heights, it was necessary to remove all sets of conventional terrestrial distances and directions. Additionally, about 600 baselines were removed, firstly as they were irrelevant to this study, and secondly due to the fact that they were part of small clusters of networks that were tightening the network and negatively affecting the statistical analysis. Moreover, additional baselines available from LPI's database were added to the network to connect to TS632 and TS2880 to the west and PM28485 and TS7054 to the south-east of where AUSPOS solutions were available and include redundant measurements. However, no AUSPOS solutions were available within the south section of the network. As stated in section 3.3, the marks held fixed vertically within the original LSA performed by LPI represent the checkpoints of this study because their published heights in SCIMS were not altered by the original adjustment. However, 2 checkpoints are part of the Victorian Survey Mark Enquiry Service (SMES) of which the original AHD71 heights are known from the original LPI adjustment report (Moss 2011). Figure 4.1 illustrates the final network design showing checkpoints, fixed AUSPOS solutions and horizontal control marks. Although the network has been improved by adding extra redundant measurements, it was still far from an ideal design, as will be explained in section 4.6.

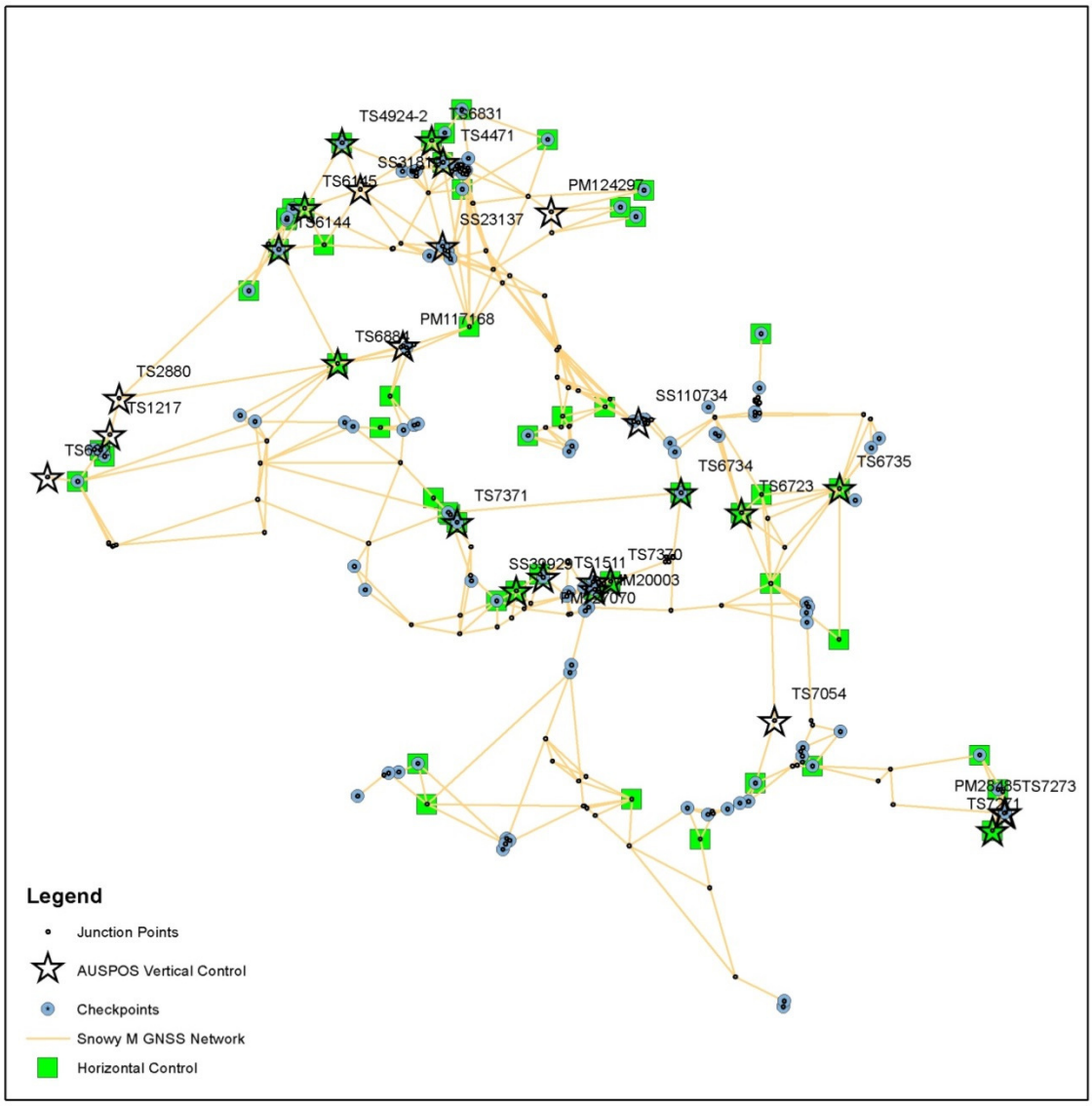

Figure 4.1: Snowy Mountains GNSS Baselines showing AUSPOS solutions, checkpoints and horizontal controls

4.4 The Mid Hunter Network

The Mid Hunter network is a more homogeneous network of baselines similar to a fish net, where marks are spread more evenly. In fact, almost all the baselines are about 15 to 20 km long. In spite of this, some shorter and longer baselines were included to add connectivity to particular control marks. The field observation campaign started in October 2010 and was completed December 2010. The data was collected using 2, 3 and in some cases 4 Leica Viva GNSS receivers in fast static mode at 10 second epoch. Session length varies from 20 minutes to several hours, according to the distance

between marks and to achieve ambiguity resolution. The collected raw data was processed with *Leica Geo Office* Version 7.0.1.0, and then the output file containing only of independent baselines was manipulated with *Strangelove* in the format NEU with covariance matrix and Northing-Easting correlation only (O'Kane 2011). In contrast to the Snowy Mountains, no data has been removed from this network as all of the observations are relevant for this study, and no redundant measurements were added. However, three baselines available from the LPI database were added to include TS6026 where an accurate AUSPOS solution was available. Figure 4.2 illustrates the final network design showing checkpoints, fixed AUSPOS solutions and horizontal control marks.

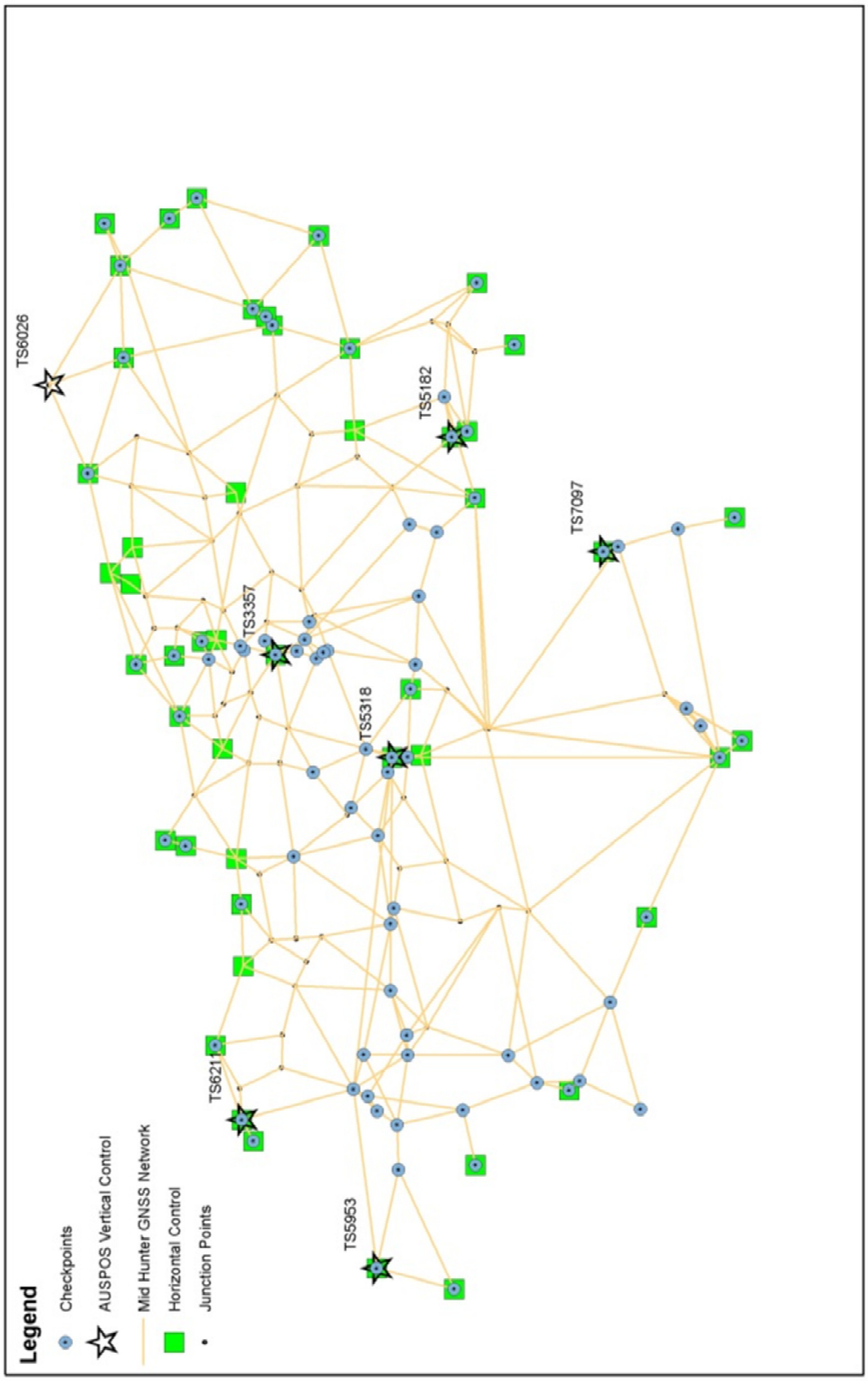

Figure 4.2: Mid Hunter GNSS Baselines showing AUSPOS solutions, checkpoints and horizontal controls

4.5 The Adjustments

The Snowy Mountains and Mid Hunter GNSS networks were subject to several adjustments computed using *GeoLab* to deliver a consistent network of ellipsoidal heights and N values using both AUSGeoid09 and AUSGeoid98. However, before computing any constrained adjustment it was necessary to perform a minimally constrained LSA as per Surveyor General's Direction No. 12 and SP1 to verify the quality of the data (ICSM 2007; LPI 2012).

Similarly to the research by Janssen and Watson (2011) detailed in section 2.11.4, a minimally constrained LSA was designed by holding fixed an AUSPOS solution vertically and one mark horizontally, both located approximately within the centre of the network. The estimations of precision listed in section 3.5 were used as input values to weight each baseline and the input standard deviation of ±0.010 m was assumed to compute ellipsoidal heights. These values were adopted as a starting point of an empirical method to identify gross errors and to modify the weighting of each baseline according to the network performance. In fact, it was necessary to run the minimally constrained LSA several times before reaching a stage where the variance factors for both networks was close to 1 and passed the Chi-square test.

The results of the first minimally constrained LSA did not depict any specific gross errors for both networks. However, the Snowy Mountains showed two baselines with the standard residual of the vertical component above the critical factor computed by *GeoLab* (see next section for residual consideration). Additionally, both networks returned a low combined variance factor of 0.3799 and 0.2719 for the Snowy Mountains and Mid Hunter networks respectively, and failing the Chi-square test. This denoted that, the initial estimations of precision were too optimistic and as consequence it was required to scale the GNSS observations to more realistic values. *Strangelove* was used to globally manipulate the input estimation of precision for both networks. In this fashion, both networks were weighted accordingly and several adjustment runs were performed until the variance factor for each network was close to 1 and passed the Chi-square test, with the following estimation of precision:

Snowy Mountains estimation of precision:

- **Horizontal**. 0.5 ppm + 0.004 m constant and 0.0015 m centring.

- **Vertical**. 1.0 ppm + 0.010 m constant, 0.003 m height measurement and ±0.010 m input standard deviation.

Mid Hunter estimation of precision:

- **Horizontal**. 0.7 ppm + 0.005 m constant and 0.0015 m centring.
- **Vertical**. 1.0 ppm + 0.015 m constant, 0.002 m height measurement and ±0.010 m input standard deviation.

The final positive outcome of the minimally constrained LSA established the method and path for the constrained LSA. In fact, the same empirical method adopted for the minimally constrained adjustment was implemented for the constrained one. However, since *GeoLab* used the combined variance factor as a result of a 3D LSA, it was imperative to compute variance factors for both horizontal and vertical components separately. This process was necessary to avoid unbalanced circumstance where a high vertical variance factor combined with a low horizontal one or vice versa results in a combined variance factor close to 1 and thus passes the Chi-square test. Therefore, once again the use of *Strangelove* was implemented to read *GeoLab* output files and compute each variance factor separately. In this fashion, vertical and horizontal elements of both networks were weighted accordingly and several attempts were necessary to reach a point where both variance factors were close to 1 and passed the Chi-square test. Additionally, the Mid Hunter network constrained LSA was required to increase the input standard deviation to ±0.012 m in order to reduce the amount of standardised residuals above the critical factor computed by *GeoLab*. The final estimation of precision implemented for both constrained LSAs is summarised below:

Snowy Mountains estimation of precision:

- **Horizontal**. 1.0 ppm + 0.005 m constant and 0.0015 m centring.
- **Vertical**. 1.0 ppm + 0.010 m constant, 0.002 m height measurement and ±0.010 m input standard deviation.

Mid Hunter estimation of precision:

- **Horizontal**. 1.8 ppm + 0.007 m constant and 0.0015 m centring.
- **Vertical**. 1.0 ppm + 0.005 m constant, 0.002 m height measurement and ±0.012 m input standard deviation.

The final computed variance factors for the Snowy Mountains constrained LSA are shown in Figure 4.3, while the results of the Mid Hunter constrained LSA are shown in Figure 4.4. The estimated accuracy of the derived ellipsoidal heights is discussed in section 4.7. (*GeoLab* output files for both constrained LSAs are included as a PDF format in the CD).

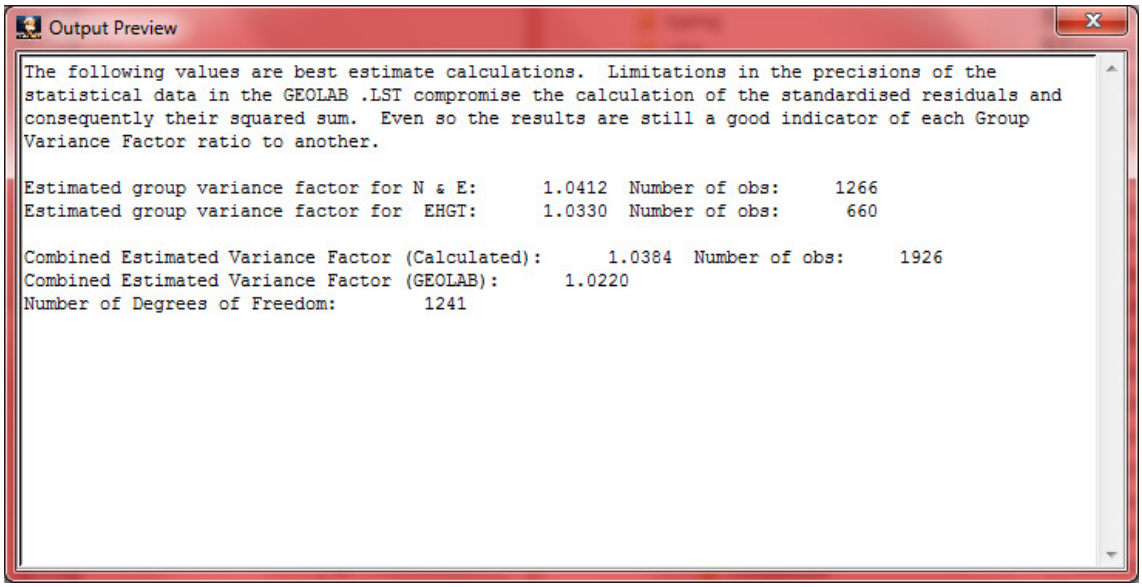

Figure 4.3: Snowy Mountains final computed variance factor using Strangelove for both vertical and horizontal components and combined variance factor computed with *GeoLab* (constrained LSA)

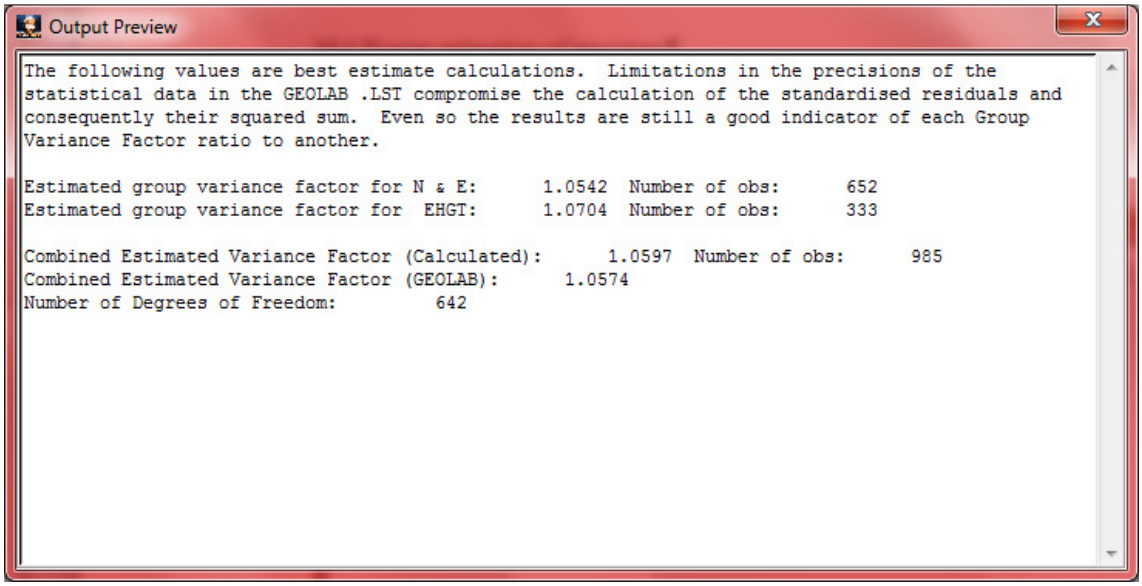

Figure 4.4: Mid Hunter final computed variance factor using Strangelove for both vertical and horizontal components and combined variance factor computed with *GeoLab* (constrained LSA)

4.6 Adjustment Evaluation and Consideration

As identified by Seeber (2003) and detailed in section 2.5, GNSS measurements are subject to several sources of error. In this fashion, a combination of measurements will give redundancy to further establish the confidence of the adjustment results. However, when a network is adjusted, there is not one true answer but a combination of possible solutions based on different combinations of the GNSS observations. This is a fundamental concept described by Harvey (1990). Additionally, Harvey (1990) stated that the Chi-square test is an excellent tool to identify the overall fit of the network, based on the input estimation of precision. However, the overall fit does not identify gross errors, which generally can be only identified by a thorough analysis of the standardised residuals and redundancy values. Hence, although both the Snowy Mountains and Mid Hunter LSAs pass the Chi-square test, it was fundamental to evaluate the redundancy and standardised residuals to identify any gross errors.

4.6.1 The Snowy Mountains Residuals

The constrained LSA identified 8 flagged residuals. However, within the vertical component only two baselines were above the critical value (4.206) computed by *GeoLab* as per the recommended program setting using the normal max distribution. In reality, the same flagged residuals were evident even in the minimally LSA. Therefore, this has identified the potential occurrence of a gross error within the following two baselines SS1521-PM111388 and PM47640-COCP41N4 or the loops composed by SS1521, PM111338, PM47640, SS5694 and COCP41N4 shown in Figure 4.5.

A redundancy analysis of each observed baseline part of the LSA has been computed using equation 3.1. According to Harvey (1990), the typical redundancy values for a network is comprised between 0.5 and 0.8. In this network, the majority of redundancy values fall within the expected values. Both of the above mentioned baselines fell within the expectations of a typical network. However, a few surrounding baselines revealed high redundancy values. Therefore, a method of exclusion was implemented to localise the gross error. Several LSAs were run and on each instance one baseline was removed. This test has detected that the largest residuals occurred at SS1521 and at COCP41N4. Therefore, these marks were removed from the adjustment. Since SS1521

was a mark of accurate AHD71, the total number of checkpoints was reduced to 104. As a matter of fact, questionable large redundancy values between 0.8 and 0.97 occurred throughout the network with standard residuals close to the critical factor computed by *GeoLab*. Therefore, it has been concluded that in part the statistical analysis is not a true representation of the survey due to constraints imposed by the network design. In fact, a major weakness of this network is the occurrence of several small patches of subordinate networks joined together. Even though this has limited the performances of the network, the dataset is still found to be a good practical method to verify AUSGeoid09 based on the accuracy of the ellipsoidal heights computed and detailed in section 4.7.1.

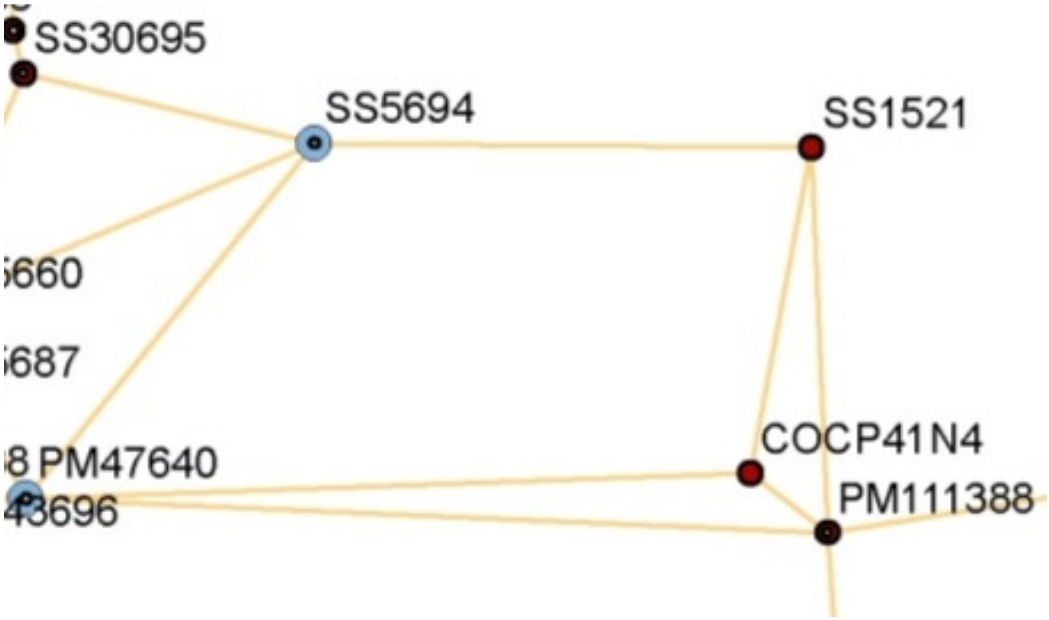

Figure 4.5: Loops composed by SS1521, PM111338, PM47640, SS5694 and COCP41N4

4.6.2 The Mid Hunter Residuals

The constrained LSA of the Mid Hunter, on the other hand, depicted no flagged residuals above the critical factor (4.052) computed by *GeoLab,* for both vertical and horizontal components. However, as it was previously stated, the input standard deviation had to be increased from ±0.010 m to ±0.012 m to avoid high standard residuals throughout the network. Even though there were no flagged residuals, the redundancy values were computed using equation 3.1 as implemented for the Snowy

Mountains LSA. In this case, the majority of redundancy values fell within the range denoted by Harvey (1990). However, about 33% of the observed baselines have redundancy values just above 0.8. In reality, there is no other evidence that denotes a potential gross error. Additionally, there were no flagged residuals and all standardised residuals of the vertical component were well below the critical factor computed by *Geolab2001*, resulting in confidence that this is a good set of data. Therefore, the whole network will be used for the purpose of this study.

4.7 Ellipsoidal Height Accuracy

The accuracy of the ellipsoidal heights for both study areas was evaluated as a result of minimally constrained LSAs. On the other hand, the average variance of the ellipsoidal heights was retrieved from the constrained LSA by squaring *GeoLab* computed standard deviations of each point. Then the 95% confidence level for both variance and standard deviation (sigma) was calculated by simply multiplying each value by 1.96.

4.7.1 The Snowy Mountains Ellipsoidal Height Accuracy

As previously stated, the statistical analysis of the Snowy Mountains dataset is not a true representation of the adjustment due to the network's design. In saying that, the overall network has generated a class A survey as per *SP1* (ICSM 2007). However, the class of survey has been evaluated by not taking into consideration some baselines where the vertical error has been slightly above the requirement. The ellipsoidal heights for the now 104 checkpoints have yielded an average variance of 0.0003 m (±0.016 m average sigma) and an average variance at 95% confidence level of 0.0006 m (±0.031 m average sigma) (see Table C.1 in Appendix C for ellipsoidal height variances and sigmas).

4.7.2 The Mid Hunter Ellipsoidal Heights Accuracy

The Mid Hunter has performed a little better than the Snowy Mountains LSA. The network has yielded a class A survey with minimal estimation of precisions (see previous section 4.5 for adjustment discussion).

The retrieved ellipsoidal heights for the 82 checkpoints have generated an average variance of 0.0002 m (±0.012 m average sigma) and an average variance at 95% confidence level of 0.0003 m (±0.024 m average sigma) (See Table C.2 in Appendix C for ellipsoidal height variances and sigmas).

4.8 Computation of N Values

The geoid validation both in absolute and relative sense, which will be detailed in Chapter 5 and Chapter 6, is based on the comparison of N values derived from both AUSGeoid09 and AUSGeoid98 models and N values derived from published AHD71 heights. At each checkpoint, the derived AHD71-N values (N_{AHD}) have been calculated by subtracting the AHD71 heights from the ellipsoidal heights computed from the constrained LSA using equation 2.4, i.e. $N_{AHD} = h - H_{AHD}$. The same network of ellipsoidal heights has been adopted to calculate N values with bi-linear, bi-quadratic, bi-cubic and bi-quartic interpolation methods. Hence, every computed N value has been retrieved from the same uniform network of ellipsoidal heights with the estimation of precision detailed within the previous sections. All LSAs used to compute the consistent network of ellipsoidal heights and derive N values have been computed using *GeoLab*. The computed N_{AHD} values and the N values from the geoid models for both networks are listed in Tables D.1, D.2, D.3, D.4 in Appendix D.

It is important to note that both AHD71 and geoid models include several sources of error as detailed in section 2.4 and section 2.5. Therefore, the following verification does not represent the true answer but the most practical method to verify the performance of AUSGeoid09 compared to AUSGeoid98 in the connection to AHD71. Additionally, Featherstone (2001) recognises that the error within AHD71 is difficult to quantify. However, since AUSGeoid09, as explained in section 2.6, is a result of a gravimetric model distorted to AHD71, it is assumed for the purposes of this research

that AHD71 has no error and any misfit may be associated with AUSGeoid09 anomalies.

4.9 Conclusion

This chapter has described the two GNSS networks based on the data collection campaign and processing, together with statistical measures to verify their accuracy. This is a fundamental concept since data collections include sources of errors. Therefore, the geoid validation is based on a datasets of known estimated precision to further establish error sources.

A consistent network of ellipsoidal heights has been computed throughout both the Snowy Mountains and the Mid Hunter GNSS networks. A thorough evaluation of the minimally constrained LSA has delivered for both datasets a class A survey. On the other hand, the estimated average variance of the ellipsoidal heights of the checkpoints was computed as a result of a constrained LSA. The Mid Hunter constrained LSA delivered a network of ellipsoidal heights with average variances of 0.0002 m (±0.012 m average sigma) and 0.0003 m (±0.024 m average sigma) evaluated at 95% confidence level, while the Snowy Mountains dataset delivered a network of ellipsoidal heights with average variances of 0.0003 m (±0.016 m average sigma) and 0.0006 m (±0.031 m average sigma) evaluated at 95% confidence level. However, the checkpoint SS1521 was removed from the Snowy Mountains network as the analysis of the standardised residuals in conjunction with redundancy values identified a potential gross error.

AUSPOS solutions were used to constrain both networks to the GRS80 ellipsoid. The reports of the AUSPOS solutions were summarised and presented to acknowledge their accuracy.

The uniform networks of ellipsoidal heights were used to compute N values with bi-linear, bi-quadratic, bi-cubic and bi-quartic interpolation methods using both AUSGeoid09 and AUSGeoid98. Additionally, the same ellipsoidal heights were used to derive N values from published AHD71 heights at each checkpoint. In this fashion, the comparison detailed within the next two chapters will be based on the same network of ellipsoidal heights and will be free of any connectivity to either AHD71 or

AUSGeoid98-09. Additionally, it is acknowledged that both AHD71 and AUSGeoid09 contain errors within their computation. However, since AUSGeoid09 has been fitted to AHD71, for the purpose of this study, it has been assumed that AHD71 is free of errors and the discrepancies that will emerge from the comparison are recognised to be attributed to anomalies within AUSGeoid09.

Chapter 5 will introduce the verification of AUSGeoid09 in an absolute sense within the Snowy Mountains and Mid Hunter regions.

CHAPTER 5
ABSOLUTE GEOID VERIFICATION

5.1 Introduction

Chapter 4 evaluated the two GNSS networks based on the data collection campaign and processing, together with statistical measures to verify the accuracy of these datasets. Furthermore, the computation of all ellipsoidal heights and N values used for the absolute and relative comparison were detailed in conjunction with the achieved accuracy.

This chapter will introduce the absolute verification of AUSGeoid09 in both study areas. N values derived from AHD71 heights will be compared with N values derived from both AUSGeoid09 and AUSGeoid98. The geoid-derived N values were computed with bi-linear, bi-quadratic, bi-cubic and bi-quartic interpolation methods. The method of comparison will be based on all checkpoints and a constant rise of elevation. Simple descriptive statistics will be used to verify the results by comparison. Additionally, the residuals will be verified graphically by plotting them according to their horizontal position and rise in elevation.

Finally, a discussion of the results of both study areas is offered to evaluate the performance of AUSGeoid09 and compare its results with its predecessor AUSGeoid98. In addition, this chapter will present the required knowledge to combine data presentations and discussions that will set the base of the final consideration in Chapter 7.

5.2 Absolute Verification Test Structure

The verification of AUSGeoid09 in absolute sense was based on the concept of absolute verification detailed within section 2.8 and previous studies detailed in section 2.11. In particular, this project aimed to represent the improvement of AUSGeoid09 to compute AHD71 heights based on a comparison of the results with AUSGeoid98. Therefore, N values computed from the published AHD71 heights at the checkpoints were compared with the N values computed from AUSGeoid09 and AUSGeoid98 with bi-linear, bi-quadratic, bi-cubic, bi-quartic interpolation methods by using the following two tests:

- Comparison over all checkpoints.
- Comparison every 100 m increase of AHD71.

Generally speaking, the primary expectation of these experiments is to quantify the precision of AUSGeoid09 to compute AHD71 heights on a single point basis and evaluate the four interpolation methods. Furthermore, the comparison between the two geoid models was employed to identify the expected rate of improvement and the magnitude of error relative to each interpolation method. Additionally, the evaluation of the accuracy of the computed N values will be the basis of the relative test detailed in Chapter 6.

5.3 Comparison Over All Checkpoints

This experiment will quantify the accuracy of AUSGeoid09 to derive AHD71 heights in an absolute sense for both study areas. In addition, a comparison between AUSGeoid09 and AUSGeoid98 will be carried out to investigate any improvement achieved by the use of the more recent model. The procedure outlined below has been employed for both the Snowy Mountains and Mid Hunter regions.

As illustrated in section 3.6, the derived AHD71 N values at each checkpoint have been calculated using equation 2.4 by subtracting from the ellipsoidal height retrieved from the LSA the published AHD71 height, i.e. $N_{AHD} = h - H_{AHD}$. Then at each checkpoint the residual R has been computed by subtracting from N_{AHD} the geoid-derived N value (N), i.e. $R = N_{AHD} - N$.

The residuals were then analysed using descriptive statistics tools of *Microsoft Excel 2010 (version 14.0.6129.5000)* (Microsoft 2013) including maximum, minimum, mean and standard deviation, which was also adopted by Brown et al. (2011) to have a simple method to compare samples. However, since it was necessary to deal with residuals of negative and positive signs, the Root Mean Square (RMS) was computed as Janssen and Watson (2011) adopted in their study reviewed in section 2.11.4.

The Z-statistics as adopted by McDonald (2004), detailed in section 2.11.1, were implemented to identify any outliers that were three times greater than the standard deviation. Additionally, to further establish the distribution of the residuals, the Kurtosis test was performed.

A graphical representation of the residuals, as employed by Featherstone and Guo (2001) and detailed in section 2.11.2, was generated for each interpolation method as a function of latitude and longitude to visualise the conclusion depicted from the numerical evaluation and to investigate any possible trend. Moreover, a combined graphical comparison for both AUSGeoid09 and AUSGeoid98 residuals is presented.

5.4 Comparison Every 100 m Increase of AHD71

This experiment will identify the accuracy of AUSGeoid09 to derive AHD71 heights in an absolute sense for both study areas over different elevation ranges. This test is based on the same approach used by Featherstone and Guo (2001), detailed in section 2.11.2, and adopted by McDonald (2004) as detailed in section 2.11.1. The same residuals used for the previous test (see section 5.3) were employed within this second test.

As in the previous test, the residuals were analysed using simple descriptive statistics including maximum, minimum, mean, standard deviation and RMS. Additionally, the Z-statistics were implemented to identify any outliers that were three times greater than the standard deviation of the residual sample. On the other hand, the distribution of the residuals using Kurtosis tests was not evaluated since the samples in some instances were too small.

A scatter plot based on the AHD71 increment is presented. This together with a subsequent trend line is employed to identify the possibility of slope or trend in the geoid model performance. This technique was also used by Featherstone and Guo (2001) in the evaluation of AUSGeoid98 residuals as detailed in section 2.11.2.

5.5 The Absolute Comparison

The outcomes of the absolute verification identified within the previous two sections for both study areas are detailed below. A comprehensive discussion is offered in section 5.6.

5.5.1 The Snowy Mountains Comparison Over All Checkpoints

The first test was employed to compare N values over all 104 checkpoints. A descriptive statistical analysis using both AUSGeoid09 and AUSGeoid98 is summarised in Table 5.1, while a discussion of the result is detailed in section 5.6.

Descriptive Statistics	AUSGeoid09			
	bi-linear	**bi-quadratic**	**bi-cubic**	**bi-quartic**
Count	104	104	104	104
RMS (m)	0.104	0.103	0.103	0.103
Range (m)	0.348	0.344	0.343	0.343
Mean (m)	0.076	0.076	0.076	0.076
Min (m)	-0.061	-0.059	-0.059	-0.059
Max (m)	0.287	0.285	0.284	0.284
Kurtosis	0.190	0.169	0.161	0.154
STD (m)	0.070	0.070	0.070	0.070
Outliers	0	0	0	0
	AUSGeoid98			
	bi-linear	**bi-quadratic**	**bi-cubic**	**bi-quartic**
Count	104	104	104	104
RMS	0.091	0.091	0.091	0.091
Range (m)	0.388	0.393	0.389	0.390
Mean (m)	0.022	0.019	0.020	0.019
Min (m)	-0.161	-0.165	-0.165	-0.165
Max (m)	0.227	0.227	0.224	0.224
Kurtosis	-0.320	-0.255	-0.278	-0.281
STD (m)	0.089	0.090	0.090	0.090
outliers	0	0	0	0

Table 5.1: Snowy Mountains descriptive statistics of absolute residuals, between AHD71-derived N values and geoid-derived N values with bi-linear, bi-quadratic, bi-cubic and bi-quartic interpolation over all checkpoints.

The residuals sources of the above descriptive analysis of AUSGeoid09 and AUSGeoid98 were plotted over the increasing GDA94 latitude and longitude for each of the four interpolation methods. Figure 5.1 and Figure 5.2 represent typical plots comparing AUSGeoid09 and AUSGeoid98 residuals with bi-linear interpolation as a function of GDA94 longitude and latitude respectively, while the comparison with the

bi-quadratic, bi-cubic and bi-quartic interpolation methods is presented from Figure F.1 to F.6 in Appendix F.

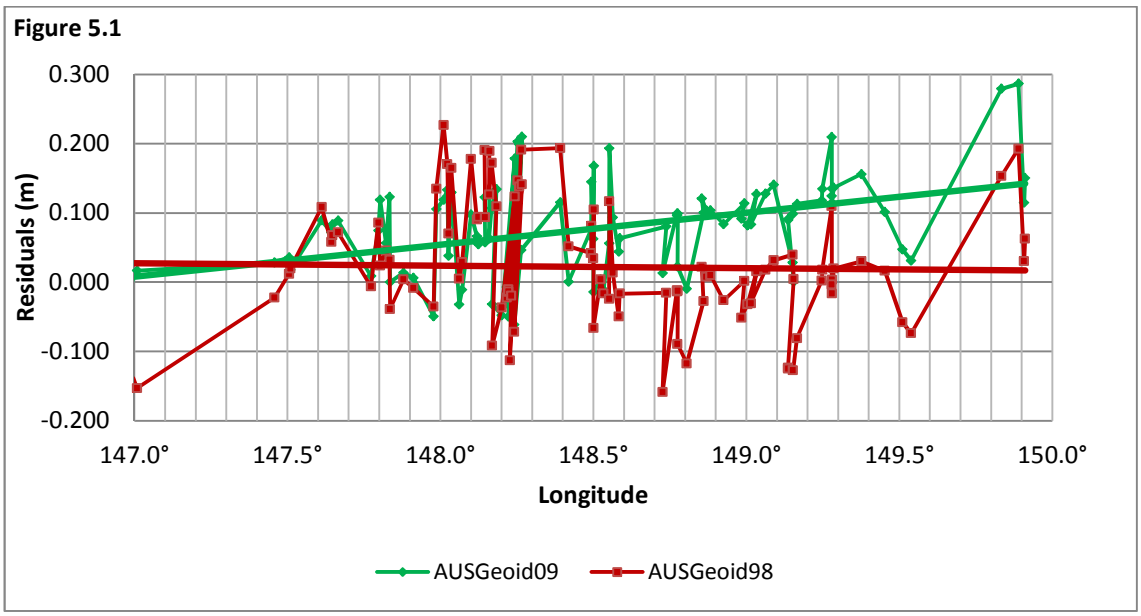

Figure 5.1: Snowy Mountains absolute verification residuals between AHD71-derived N values and geoids-derived (AUSGeoid09 and AUSGeoid98) N values, with bi-linear interpolation plotted along increasing of longitudes

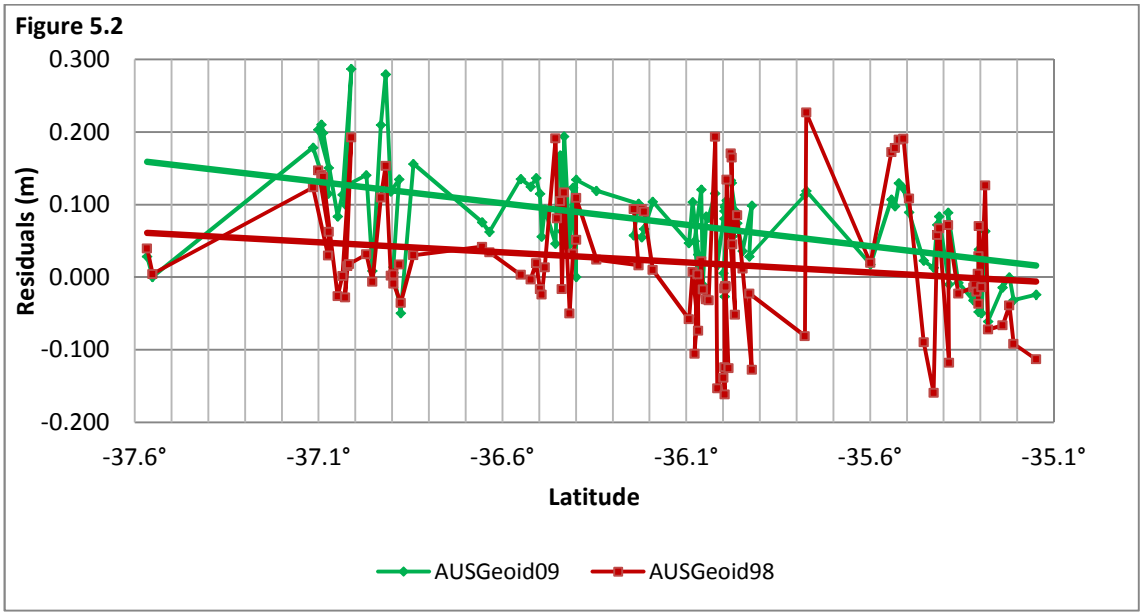

Figure 5.2: Snowy Mountains absolute verification residuals between AHD71-derived N values and geoids-derived (AUSGeoid09 and AUSGeoid98) N values, with bi-linear interpolation plotted along increasing of latitudes

5.5.2 The Snowy Mountains Comparison Every 100 m Increase of AHD71

Graphical representation of the descriptive statistical analysis of the absolute verification for AUSGeoid09 and AUSGeoid98, with bi-linear interpolation as a function of 100 m increase of AHD71 height is presented in Figure 5.3 and Figure 5.4, while the descriptive statistical analysis for all interpolation methods using both geoid models is summarised from Table E.1 to Table E.8 in Appendix E.

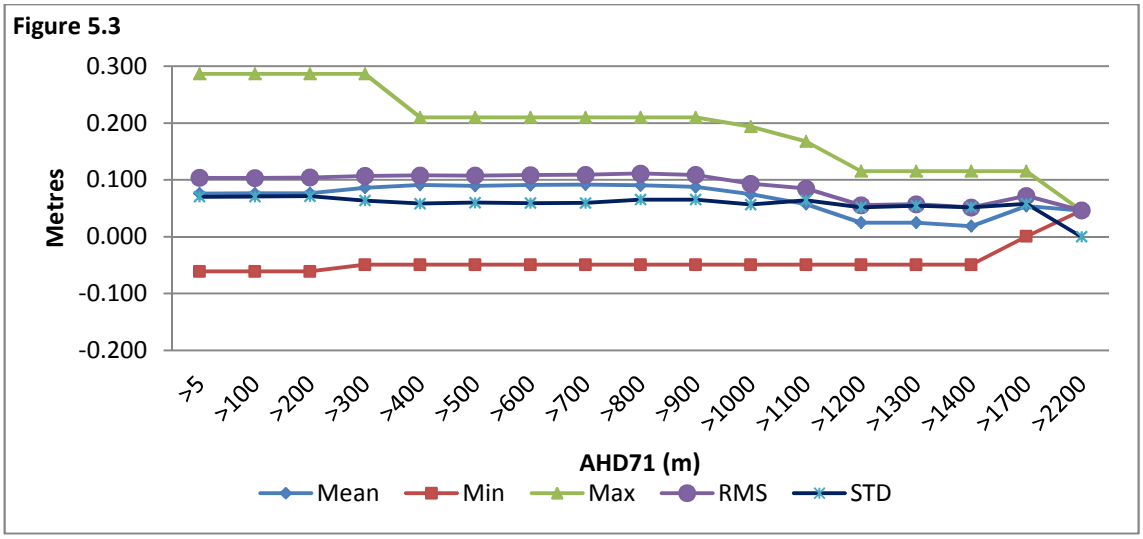

Figure 5.3: Snowy Mountains graphical representation of the descriptive statistics of absolute verification residuals, between AHD71-derived N values and AUSGeoid09-derived N values, with bi-linear interpolation as a function of 100 m increases in AHD71

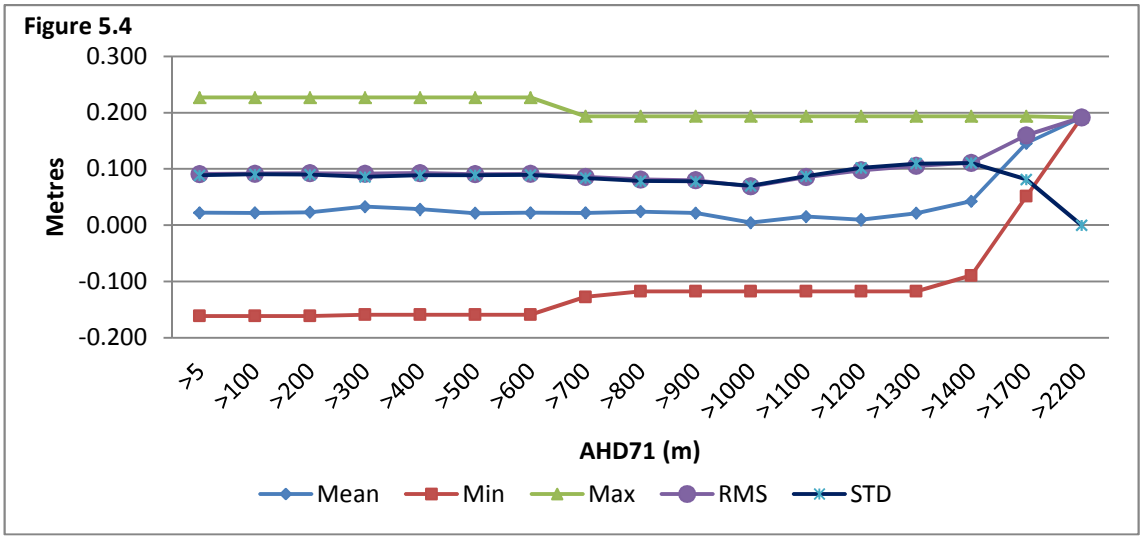

Figure 5.4: Snowy Mountains graphical representation of the descriptive statistics of absolute verification residuals, between AHD71-derived N values and AUSGeoid98-derived N values with bi-linear interpolation as a function of 100 m increases in AHD71

Figure 5.5 is a typical comparison for both geoid models as a function of increasing AHD71 elevation, using the bi-linear interpolation method. Figures F.7, F.8, F.9 in Appendix F compare the two models with bi-quadratic, bi-cubic and bi-quartic interpolation methods.

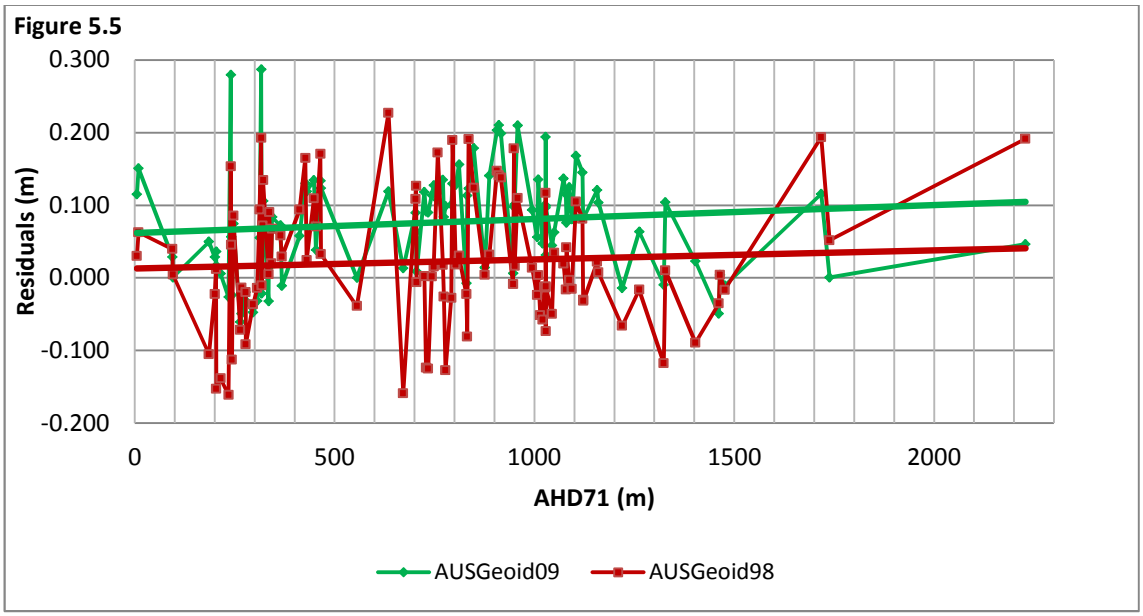

Figure 5.5: Snowy Mountains absolute verification residuals between AHD71-derived N values and geoids-derived (AUSGeoid09 and AUSGeoid98) N values with bi-linear interpolation plotted along increasing of AHD71

5.5.3 The Mid Hunter Comparison Over All checkpoints

A descriptive statistical analysis using both AUSGeoid09 and AUSGeoid98 is summarised in Table 5.2, while a discussion of the result is given in section 5.6.

Descriptive Statistics	AUSGeoid09			
	bi-linear	**bi-quadratic**	**bi-cubic**	**bi-quartic**
Count	82	82	82	82
RMS	0.041	0.042	0.042	0.042
Range (m)	0.239	0.242	0.243	0.243
Mean (m)	0.013	0.014	0.014	0.014
Min (m)	-0.105	-0.109	-0.109	-0.110
Max (m)	0.134	0.133	0.134	0.133
Kurtosis	0.730	0.828	0.836	0.866
STD (m)	0.040	0.040	0.040	0.040
outliers	0	0	0	0
	AUSGeoid98			
	bi-linear	**bi-quadratic**	**bi-cubic**	**bi-quartic**
Count	82	82	82	82
RMS	0.252	0.254	0.254	0.254
Range (m)	0.290	0.286	0.287	0.284
Mean (m)	-0.241	-0.243	-0.243	-0.243
Min (m)	-0.367	-0.360	-0.360	-0.360
Max (m)	-0.078	-0.074	-0.074	-0.076
Kurtosis	-0.907	-0.899	-0.897	-0.905
STD (m)	0.076	0.074	0.074	0.074
outliers	0	0	0	0

Table 5.2: Mid Hunter descriptive statistics of absolute verification residuals, between AHD71-derived N values and geoid-derived N values with bi-linear, bi-quadratic, bi-cubic and bi-quartic interpolation over all checkpoints.

The residuals sources of the above descriptive analysis of AUSGeoid09 and AUSGeoid98 were plotted over the increasing of GDA longitude and latitude for each of the four interpolation methods. Figure 5.6 and Figure 5.7 represent typical plots between AUSGeoid09 and AUSGeoid98 with bi-linear interpolation as a function of GDA longitude and latitude respectively, while the whole comparison with the remaining interpolation methods is presented from Figure F.10 to F.15 in Appendix F.

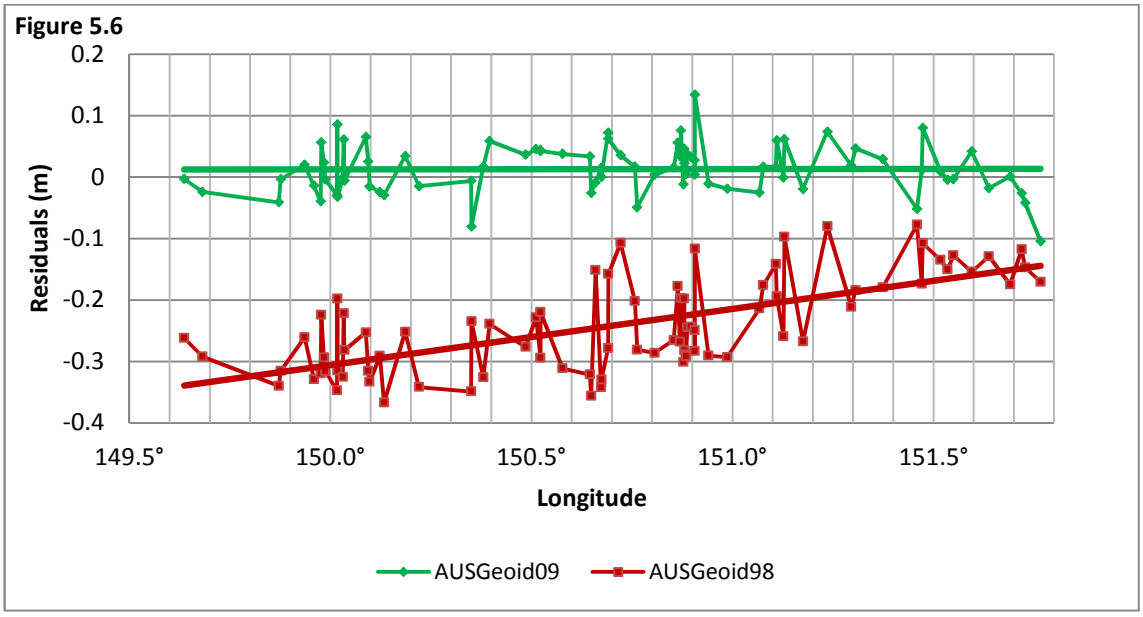

Figure 5.6: Mid Hunter absolute verification residuals between AHD71-derived N values and geoids-derived (AUSGeoid09 and AUSGeoid98) N values, with bi-linear interpolation plotted along increasing of longitudes

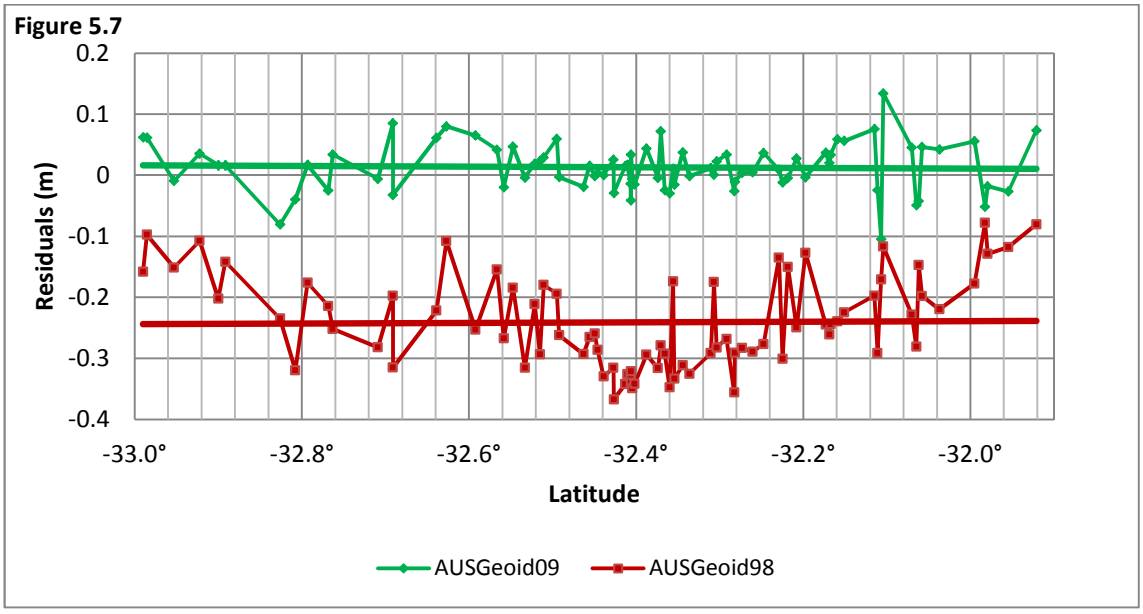

Figure 5.7: Mid Hunter absolute verification residuals between AHD71-derived N values and geoids-derived (AUSGeoid09 and AUSGeoid98) N values, with bi-linear interpolation plotted along increasing of latitudes

5.5.4 The Mid Hunter Comparison Every 100 m Increase of AHD71

Graphical representation of the descriptive statistical analysis of the absolute verification for AUSGeoid09 and AUSGeoid98, with bi-linear interpolation as a function of 100 m increase of AHD71, is presented in Figure 5.8 and Figure 5.9, while the descriptive statistical analysis for all interpolation methods for both geoid models are summarised in Table E.9 to Table E.16 in Appendix E.

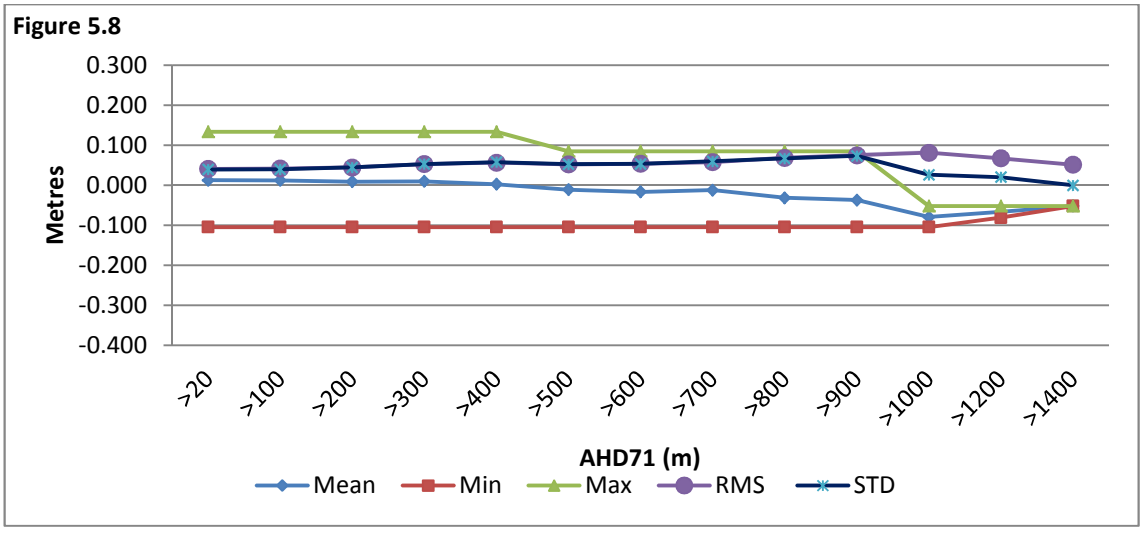

Figure 5.8: Mid Hunter graphical representation of the descriptive statistics of absolute verification residuals, between AHD71-derived N values and AUSGeoid09-derived N values with bi-linear interpolation as a function of 100 m increases in AHD71

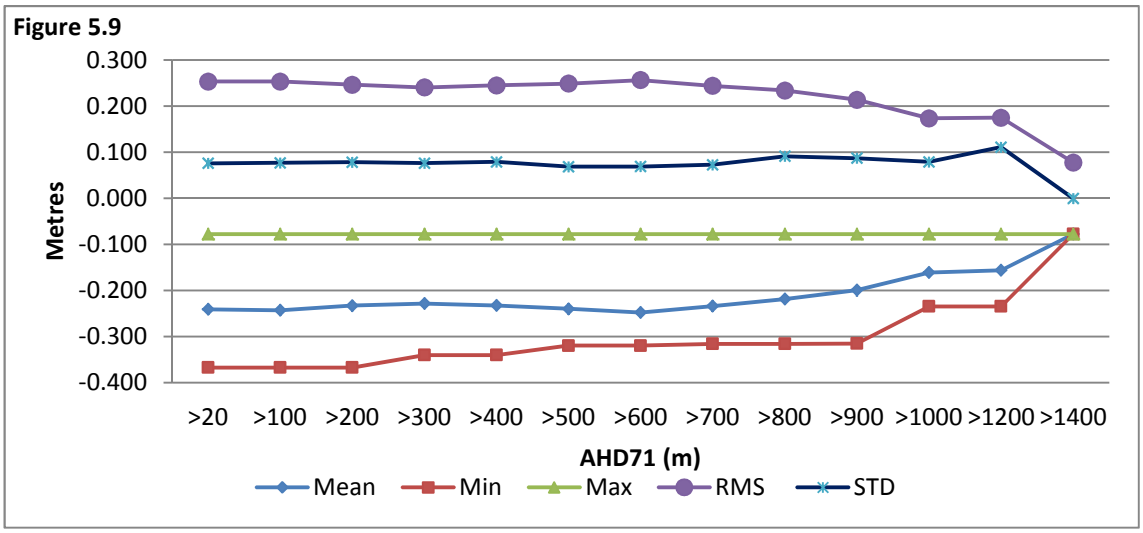

Figure 5.9: Mid Hunter graphical representation of the descriptive statistics of absolute verification residuals, between AHD71-derived N values and AUSGeoid98-derived N values with bi-linear interpolation as a function of 100 m increases in AHD71

Figure 5.10 below is a typical example for both geoid models compared as a function of increasing AHD71 elevation with bi-linear interpolation method, while Figures F.16, F.17, F.18 in Appendix F compared the two models with bi-quadratic, bi-cubic and bi-quartic interpolation methods.

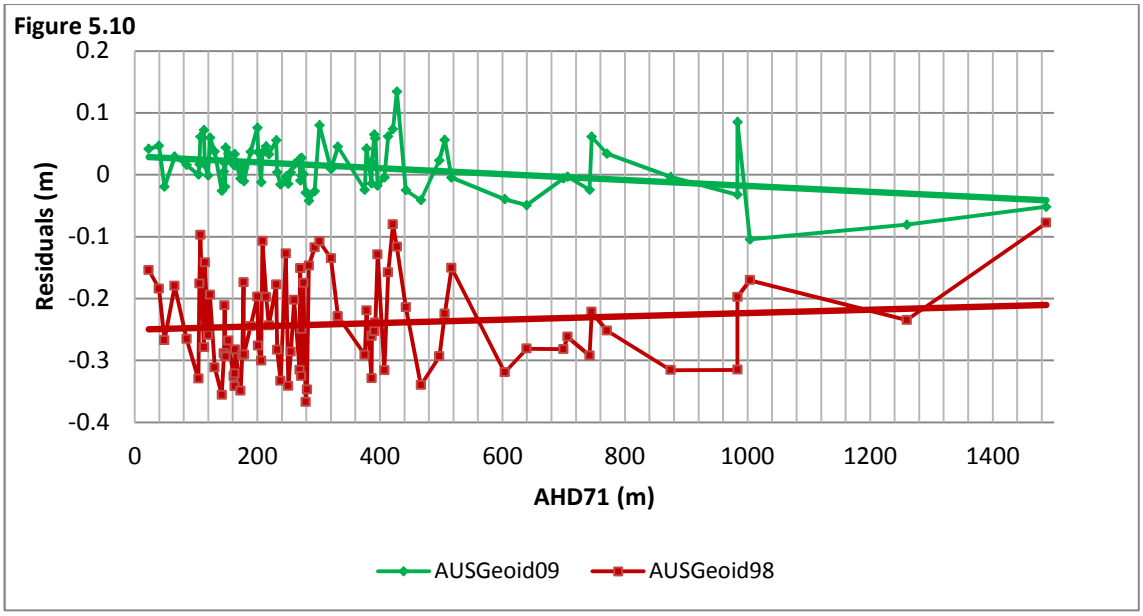

Figure 5.10: Mid Hunter absolute verification residuals between AHD71-derived N values and geoids-derived (AUSGeoid09 and AUSGeoid98) N values with bi-linear interpolation plotted along increasing of AHD71

5.6 Results Discussion

Section 5.5 has presented the results of the performance for both AUSGeoid09 and AUSGeoid98 within the two study areas in an absolute sense. This section will analyse the results achieved and a discussion is presented to establish the improvement in retrieving AHD71 heights with the use of AUSGeoid09, while, the overall result consideration is offered in Chapter 7.

5.6.1 The Snowy Mountains Absolute Result Discussion

Table 5.1 in section 5.5.1 presented the descriptive statistical analysis of the absolute verification for both AUSGeoid09 and AUSGeoid98 over all checkpoints. The N values at the 104 checkpoints were computed with bi-linear, bi-quadratic, bi-cubic and bi-

quartic interpolation and compared with N values derived from published AHD71 heights. Additionally, it is important to remember that N values and AHD71-derived N values were computed from the same homogenous network of ellipsoidal heights with average standard deviation of ±0.031 m at 95% confidence level (see section 4.7.1 for details).

Based on the descriptive statistical analysis of AUSGeoid09 detailed in Table 5.1, there is no significant difference in the use of different methods of interpolation. Additionally, the AUSGeoid09 N values listed Table D.1 in Appendix D differ from one interpolation method to another by only 1 or 2 mm. On the other hand, AUSGeoid98 seems to be consistent only with bi-quadratic, bi-cubic and bi-quartic interpolation, while bi-linear interpolation is slightly different in some instances, where the difference is about 7 mm. Most likely, the better consistency in different methods of interpolation is due to the AUSGeoid09 density being four times that of its predecessor. As detailed in section 2.6, AUSGeoid09 is composed of a grid of about 1.8 km by 1.8 km.

The comparison of the results of both geoid models denotes a moderate improvement of AUSGeoid09 with the standard deviation dropping form ±0.089 m to ±0.070 m. However, the RMS seems better with AUSGeoid98. Both models did not show any outliers greater than three times the standard deviations. However, the mean of the residuals is closer to zero in AUSGeoid98 than AUSGeoid09. This is because the AUSGeoid98 residuals are almost equally balanced between the positive and negative sign, with a range from -0.165 m to 0.224 m, while the majority of AUSGeoid09 residuals are positive within a range from -0.061 m to 0.285 m, which indicates a possible block shift within the AUSGeoid09 model. A closer evaluation of the residuals identifies that AUSGeoid98 residuals are of large magnitude and largely spread from the mean, while AUSGeoid09 includes only two checkpoints (TS5945 and TS5946) where the residuals seem to be very different from the sample. If those two residuals are removed, the range decreases by about 60 mm and 100% of the residuals are within ±0.130 m (2 sigma) of the mean. There is not enough evidence that highlights a gross error within those two checkpoints. Besides, this section of the network seemed to detect high positive residuals that will be further discussed within the graphical analysis.

To further establish the distribution of the residuals a Kurtosis test was performed. According to DeCarlo (1997), negative values of Kurtosis indicate flatness with a large number of residuals concentrated along the side of a normal distribution, while a positive value denotes a sample of a peak with the majority of the residuals concentrated within the proximity of the mean value. In this fashion, AUSGeoid09 residuals are more consistent with a normal distribution with a large amount of residuals close to the mean, while AUSGeoid98 residuals denoted flatness with a large amount of residuals along the side of the normal distribution.

Figure 5.3 and Figure 5.4 in section 5.5.2 and Tables E.1-E.8 in Appendix E show the performance of both geoid models as a function of 100 m increase in elevation. AUSGeoid98 does not indicate any major discrepancy or trend as a function of different elevation ranges. On the other hand, the same representation indicates that AUSGeoid09 improves the performance as elevation increases. In fact, the standard deviation and RMS decrease with increasing of elevation. However, these results are not a true representation of a continuous elevation model since this dataset does not include elevations between 1,400 m and 1,700 m and between 1,700 m and 2,200 m. Additionally, since the checkpoints are located within a large area, they do not represent a continuous elevation model. Hence, a graphical representation was introduced and a discussion is given in the following section.

5.6.2 The Snowy Mountain Graphical Representation Discussion

A graphical representation was employed as a function of the horizontal position of the checkpoints and as a function of the rise in AHD71 to identify anomalies or any possible trend. Recalling that all the compared N values were derived from the network of ellipsoidal heights with an average standard deviation of ±0.031 m at 95% confidence level (see section 4.7.1), the graphical representation discussion is presented below.

Figure 5.1 in section 5.5.1 and Figures F.1-F.3 in Appendix F illustrate the residuals of both models with bi-linear, bi-quadratic, bi-cubic and bi-quartic interpolation as a function of their longitudinal position. AUSGeoid98 residuals vary from positive to negative along the scatter plot. Therefore, they indicate no trend but it is possible to see how inconsistently the residuals are computed. AUSGeoid09 shows a trend where the

residuals seem to increase positively in the eastern direction. It appears that both models perform in a similar way, but AUSGeoid09 seems to include a slope from the middle of the subject network towards the coast.

The same residuals were then plotted as a function of their latitudinal position (see Figure 5.2 in section 5.5.1 and Figures F.4-F.6 in Appendix F). In these instances, both models seem to slope where the residuals decrease in the northern direction. Therefore, it was detected that the south-east side of this area may include an anomaly within the AUSGeoid09 model. A plan showing the direction and magnitude of the AUSGeoid09 residuals was plotted to further establish the overall behaviour of this model. As evident in Figure 5.11, it appears that the largest residuals occur around the south-east corner of the network.

Figure 5.5 in section 5.5.2 and Figures F.7-F.9 in Appendix F plot the residual of both models as a function of a 100 m increase of AHD71. Both modes did not identify any trend. However, AUSGeoid09 residuals show a shift of about 50 mm compared to the predecessor.

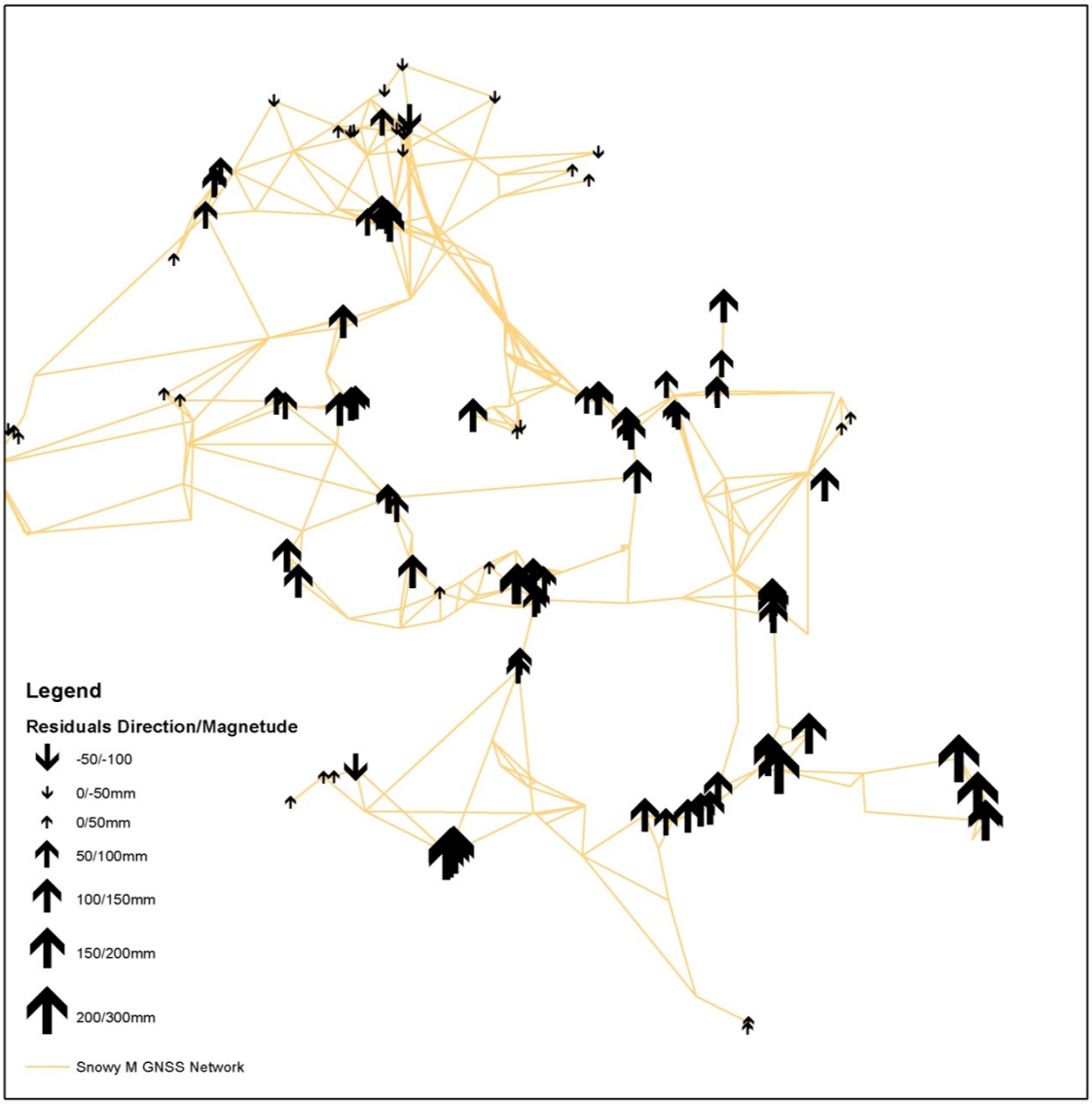

Figure 5.11: Direction and magnitude of AUSGeoid09 residuals within the Snowy Mountains

5.6.3 The Mid Hunter Result Discussion

Table 5.2 in section 5.5.3 presented the descriptive statistical analysis of the absolute verification for both AUSGeoid09 and AUSGeoid98 for all checkpoints. The N values at the 82 checkpoints were computed with bi-linear, bi-quadratic, bi-cubic and bi-quartic interpolation and compared with N values derived from published AHD71 heights. Recalling that all derived N values were computed from the same homogenous network of ellipsoidal heights with an average standard deviation of ±0.024 m at 95% confidence level (see section 4.7.2), a detailed discussion is presented below.

Again, the statistical analysis of AUSGeoid09, shown in Table 5.2, identifies no major differences in the use of the four methods of interpolation. As evident from Table D.3 in Appendix D, the derived N values differ from one interpolation method to another by only 1 or 2 mm with some sporadic cases where the difference is up to 4 mm. Once again, AUSGeoid98 shows consistency only between bi-quadratic, bi-cubic and bi-quartic interpolation methods. This confirms that the higher density of AUSGeoid09 has introduced better consistency when using different methods of interpolation.

The comparison of the statistical analysis of both models presented in Table 5.2 depicts a substantial improvement of AUSGeoid09 in retrieving AHD71 heights. The standard deviation dropped form ±0.074 m for AUSGeoid98 to ±0.040 m for AUSGeoid09. The RMS computed for AUSGeoid09 indicates an improvement factor of 6 compared to AUSGeoid98. None of the two models indicate any outliers of three times their standard deviation. However, AUSGeoid98 residuals are heavily negative, included in a range of about 300 mm for all interpolation methods. On the other hand, AUSGeoid09 residuals are well distributed between negative and positive values and 81 of 82 checkpoints are within ±0.080 m (2 sigma) of the mean.

The Kurtosis test was again implemented to verify the distribution of the residuals. It was found that AUSGeoid09 residuals are more consistent with a normal distribution with a large amount of residuals close to the mean, while AUSGeoid98 residuals denoted flatness and a large amount of residuals along the side of the normal distribution.

Figure 5.8 and Figure 5.9 in section 5.5.4 and Tables E.9-E.16 in Appendix E show the performance of both geoid models as a function of 100 m rises in AHD71. AUSGeoid09 seems to be consistent throughout the terrain model. However, RMS and standard deviation increased to almost double at around 1,000 m elevation. On the other hand, AUSGeoid98 shows the occurrence of large residuals at every elevation. The sample after 700 m elevation is too small to be adopted as true representation of the performance of both models. In addition, there are no checkpoints within 1,100 m and 1,300 m to detect and confirm any trend. Moreover, the elevation model is not part of a continuous terrain model due to marks being located in different sections of the network. Therefore, a graphical representation was introduced (see following section).

5.6.4 The Mid Hunter Graphical Representation Discussion

In order to further confirm descriptive statistics, a graphical representation was implemented based on the horizontal position of the checkpoints and as function of elevation rise in AHD71. Recalling that all the compared N values were computed using a homogenous network of ellipsoidal heights with an average standard deviation of ±0.024 m at 95% confidence level (see section 4.7.2), a detailed discussion of the graphical representation is presented below.

As seen from Figure 5.6, Figure 5.7 in section 5.5.3 and Figures F.10-F.15 in Appendix F, the residuals of both models were plotted as a function of their latitude and longitude position. AUSGeoid09 denotes an exceptional improvement 6 times better than AUSGeoid98 without any trend where the residuals are consistent, with some sporadic irregularities of 80 mm in magnitude. On the other hand, AUSGeoid98 residuals are heavily negative. Furthermore, the longitudinal graph shows a slope rising towards the east side, while the latitudinal graphs identified a dip in the middle of the study area.

The same residuals were plotted as a function of rises in AHD71 (see Figure 5.10 in section 5.5.4 and Figures F.16-F.18 in Appendix F). AUSGeoid09 denoted a trend where the residuals decrease as the elevation increases. However, as previously identified in section 5.6.3 only 10 test points were available above 700 m elevation. Therefore it is believed that this sample is not sufficiently large to denote any trend above this elevation.

5.7 Conclusion

This chapter has presented the absolute verification test results of AUSGeoid09 for both the Snowy Mountains and Mid Hunter regions. The testing was based on the comparison of AUSGeoid09 and AUSGeoid98 derived N values and N values computed from published AHD71 heights. The results were presented and evaluated using descriptive statistics. A graphical representation according to the horizontal position and as a function of 100 m rises in AHD71 elevation of the checkpoints was also presented.

Based on the Mid Hunter descriptive statistic and graphical representation of both AUSGeoid09 and AUSGeoid98, it was detected that AUSGeoid09 has achieved an extraordinary improvement with 70% of the residuals within ±0.040 m (1 sigma). RMS of both geoid models has delineated an improvement factor of 6 in favour of AUSGeoid09. Additionally, AUSGeoid09 residuals are consistent throughout the network, while AUSGeoid98 residuals are heavily negative with a slope to the eastern direction.

The Snowy Mountains network has not delineated an improvement of AUSGeoid09 compared to AUSGeoid98. Additionally, this dataset detected a slope within AUSGeoid09 from the north-west to south-east corner with the majority of the positive residuals at the south-east corner. However, the sample within this section of the network is too small to definitely point out any anomalies in AUSGeoid09. In fact, only two of the residuals are larger than the others. In saying that, 69% of AUSGeoid09 residuals are within ±70 mm (1 sigma) of the mean, while 69% of AUSGeoid98 residuals are within ±90 mm (1 sigma) of the mean.

Chapter 6 will introduce the verification of AUSGeoid09 in a relative sense for the Snowy Mountains and Mid Hunter study areas.

CHAPTER 6
RELATIVE GEOID VERIFICATION

6.1 Introduction

Chapter 5 has presented and discussed the performance of AUSGeoid09 from an absolute point of view. A descriptive statistical analysis and graphical representation was used to analyse the results and a comparison with the previous Australian geoid model was performed to estimate an improvement factor.

This chapter will introduce the verification of AUSGeoid09 and AUSGeoid98 in a relative sense, where the models will be verified as a result of the difference in height from one checkpoint to another. Additionally, this chapter will give the knowledge to combine data presentation and discussion that will set the base of the final consideration in chapter 7.

Both the Snowy Mountains and Mid Hunter networks will be investigated using all observed baselines, all possible baselines and all possible baselines shorter than 100 km between checkpoints. Then simple descriptive statistical analysis and graphical representation will be presented as a function of baseline length and as a rise of difference in elevation between checkpoints. In addition, the residuals will be compared with current standards for 3rd order differential levelling requirements to evaluate the possibility of AUSGeoid09 delivering a valid substitute to traditional levelling techniques. Furthermore, since GNSS heighting errors propagate proportional to the distance, each residual will be evaluated as a function of the baseline length to derive an average value expressed in parts per million (ppm).

A comprehensive discussion of the results for both study areas is offered to evaluate the performance of AUSGeoid09 and compare the results with its predecessor AUSGeoid98, while final considerations are presented in Chapter 7.

6.2 Relative Verification Tests Structure

From a surveying point of view, the relative verification is a more realistic approach than the absolute verification because it is based on the difference in heights over a baseline. Generally speaking, surveyors use this method to carry heights from established marks to new unestablished marks. This concept is less affected by errors

included within the absolute verification since common systematic errors are minimised by virtue of the difference (Brown et al. 2011; Featherstone 2001; McDonald 2004).

As shown in section 5.6, AUSGeoid09 has improved consistency to retrieve N values with the four interpolation methods within both study areas. The difference of N values computed using the four different methods of interpolation was shown to be of a magnitude of 1 or 2 mm. From previous studies of geoid validation it has emerged that bi-linear and bi-cubic are the two most popular techniques adopted by users (Featherstone 2001; Gibbings & McDonald 2005). Therefore, the relative tests were based only on N values computed with bi-cubic interpolation to keep consistency with previous studies and due to the minimal difference with the other methods of interpolation, which were considered irrelevant for the purposes of this study.

Based on the previous studies revised in section 2.11, the relative verification of AUSGeoid09 will be identified with the following comparison tests:

- Comparisons over all observed baselines
- Comparisons over all possible baselines
- Comparisons within 100 km baselines
- Comparisons every 100 m increase of difference in elevation

These four tests will verify the model by comparing the change in GNSS derived orthometric height (ΔH_{GNSS}) and the difference in published AHD71 (ΔH_{AHD}) over two marks using equation 3.2.

As in the absolute verification, a descriptive statistical analysis was performed using *Microsoft Excel 2010*. Maximum, minimum, mean and standard deviation, were computed to have a simple numerical representation of the population sample, which was also adopted by Brown et al. (2011). The Z-statistics were implemented to identify any outliers greater three times the standard deviation, while the Kurtosis test was employed to further establish the nature of the residuals in terms of normal distribution. However, since it was necessary to deal with residuals of different signs, the RMS was introduced as Janssen and Watson (2011) found it a useful tool in their study.

Comparison will be made between the two models to identify the rate of improvement of AUSGeoid09. Additionally, as implemented by Brown et al. (2011) and McDonald

(2004) in their studies, the residual absolute values were compared with the allowable miscloses of 3rd order differential levelling, as per *SP1* (ICSM 2007) where the maximum allowable error will be computed using equation 2.13 over each baseline length i.e. $12\sqrt{d}$. The shortest distance between checkpoints will be the GRS80 ellipsoidal distance derived using Vincenty's inverse formula (ICSM 2006). The latitude and longitude necessary to compute the distance were derived from the output file of *GeoLab*. The total number of residuals within the 3rd order differential levelling will be presented together with the descriptive statistical analysis. Considering *SP1* (ICSM 2007) as detailed in section 2.10, GNSS heighting errors propagate proportionally to distance, not to the square root of the distance as it is defined for differential levelling. Therefore, each baseline residual was expressed as ppm as it was employed by McDonald (2004) as detailed in section 2.11.1. Hence, it was possible to give evidence that matches the characteristics of the GNSS technique. The ppm values were computed by dividing the baseline's residual by the baseline length. The average ppm will be presented with the descriptive statistics.

Finally, a graphical representation as a function of baseline length and in relation to the 3rd order differential levelling will be presented to further establish the above numerical evaluation. Furthermore, the residuals will be plotted as a function of increment of difference in elevation.

From this verification it is expected to verify the accuracy of AUSGeiod09 in regards to GNSS levelling possibly being able to provide a valuable alternative to traditional differential levelling within mountainous regions.

6.2.1 Comparison Over All Observed Baselines

This comparison is expected to give specific verification over all observed baselines within the two study areas. In particular, this test is less susceptible to systematic errors that may occur with the absolute verification. According to Kearsley (1988) and Featherstone (2001), as detailed in sections 2.2 and 2.8, simultaneous observations will include, to some extent, the same magnitude of systematic errors that are minimised by virtue of differencing. However, the N values must be related to the same ellipsoid.

Therefore, AUSGeoid09 and AUSGeoid98 N values have been computed based on the GRS80 ellipsoid for both study areas (see Chapter 4).

6.2.2 Comparison Over All Possible Baselines

The subject areas will be extended to verify the geoid models using equation 3.2 over all possible baselines between the checkpoints. This test is expected to present the performance of AUSGeoid09 as a large scale network unit. As defined by Featherstone (2001) and acknowledged in section 2.8, the total number of baselines was computed using $n(n-1)$ where n is the number of checkpoints. Additionally, Featherstone (2001) states that this method requires all N values to be computed from the same network of ellipsoidal heights. In this fashion, both GNSS networks have been subject to LSAs to achieve a homogenous network of ellipsoidal heights fully detailed within Chapter 4.

6.2.3 Comparison Within 100 km Baselines

The comparison over all possible baselines between checkpoints includes long baselines, which are often well above 100 km in length. Generally speaking, it is unlikely that GNSS users perform network adjustments with baselines of this length, unless they contribute to state-wide or national control networks. Therefore, as employed by Brown et al. (2011) and described in depth in section 2.11.3, a third test to verify the performance of AUSGeoid09 will be based on all possible baselines up to 100 km in length. This test was aimed to offer substantial evaluation for GNSS users and represent a realistic GNSS network performance.

6.2.4 Comparison Every 100 m Increase of Difference in Elevation

Featherstone and Guo (2001) verified the performance of AUSGeoid98 as a function of 100 m increases in AHD71 elevation. Similarly, this test is aimed at verifying the performance of AUSGeoid09 as a function of 100 m increase of difference in elevation between checkpoints. This test used the total number of possible baselines computed

using the methodology detailed in section 6.2.2. This investigation is to verify if there is any particular tendency of AUSGeoid09 related to the differences in elevation.

6.3 The Snowy Mountains Results

The Snowy Mountains results of the four methods of relative verification described in section 6.2 are presented in the following subsections, while a discussion of the results is given in section 6.5.

6.3.1 The Snowy Mountains Comparison Over All Observed Baselines

The first test was employed to compare all observed baselines between checkpoints. The Snowy Mountains dataset includes 104 checkpoints of which 82 have been directly connected by simultaneous observations delivering only 66 baselines. A descriptive statistical analysis using both AUSGeoid09 and AUSGeoid98 is summarised Table 6.1.

Descriptive Statistics	AUSGeoid09	AUSGeoid98
Count	66	66
Range (m)	0.280	0.316
Mean (m)	0.010	0.011
Minimum (m)	-0.130	-0.111
Maximum (m)	0.150	0.204
Kurtosis	2.067	2.738
STD (m)	0.051	0.063
RMS (m)	0.051	0.064
ppm	7.866	8.129
Baseline within 3RD Order Differential Levelling	40 (61%)	37 (56%)
Mean Distance (m)	7527	7527
outliers	0	1

Table 6.1: Snowy Mountains descriptive statistics of relative verification residuals, between AHD71 differences and orthometric differences over 66 observed baselines using both AUSGeoid09 and AUSGeoid98 with bi-cubic interpolation

6.3.2 The Snowy Mountains Comparison Over All Possible Baselines

This test was aimed to verify and compare both geoid models at a large scale including the overall extension of the network. Since this study area comprises 104 checkpoints, the use of the equation $n(n-1)$ yields 5,356 possible baselines. Table 6.2 portrays the descriptive statistical analysis of these 5,356 baselines for both geoid models.

Descriptive Statistics	AUSGeoid09	AUSGeoid98
Count	5356	5356
Range (m)	0.625	0.769
Mean (m)	-0.012	-0.024
Minimum (m)	-0.343	-0.389
Maximum (m)	0.282	0.380
Kurtosis	-0.018	-0.157
STD (m)	0.099	0.124
RMS (m)	0.099	0.127
ppm	1.073	1.417
Baseline within 3RD Order Differential Levelling	4,149 (77%)	3,413 (64%)
Mean Distance (m)	113428	113428
outliers	15	15

Table 6.2: Snowy Mountains descriptive statistics of relative verification residuals between AHD71 differences and orthometric differences over 5,356 possible baselines using both AUSGeoid09 and AUSGeoid98 with bi-cubic interpolation

6.3.3 The Snowy Mountains Comparison Within 100 km Baselines

In order to evaluate the geoid models by a more realistic approach of common surveys, the number of all possible baselines was reduced to 2,361, which represents all possible baselines up to 100 km length. Table 6.3 presents the descriptive statistical analysis of these 2,361 baselines for both geoid models.

Descriptive Statistics	AUSGeoid09	AUSGeoid98
Count	2361	2361
Range (m)	0.531	0.769
Mean (m)	-0.008	-0.025
Minimum (m)	-0.249	-0.389
Maximum (m)	0.282	0.380
Kurtosis	-0.095	-0.036
STD (m)	0.081	0.120
RMS (m)	0.082	0.122
ppm	1.678	2.287
Baseline within 3RD Order Differential Levelling	1,676 (71%)	1,250 (53%)
Mean Distance (m)	60853	60853
outliers	7	6

Table 6.3: Snowy Mountains descriptive statistics of relative verification residuals between AHD71 differences and orthometric differences over 2,361 baselines within 100 km using both AUSGeoid09 and AUSGeoid98 with bi-cubic interpolation

6.3.4 The Snowy Mountains Comparison every 100 m Increase of Difference in Elevation

The 5,356 baselines were rearranged as a function of increment of difference in elevation. These baselines are located within different elevation ranges which, when combined together, deliver differences in elevation comprised from 0.05 m to 2,220 m. Figure 6.1 and Figure 6.2 show the descriptive statistical analysis for both geoid models as a function of difference in elevation, while a numerical representation is summarised in Table H.1 and Table H.2 in Appendix H.

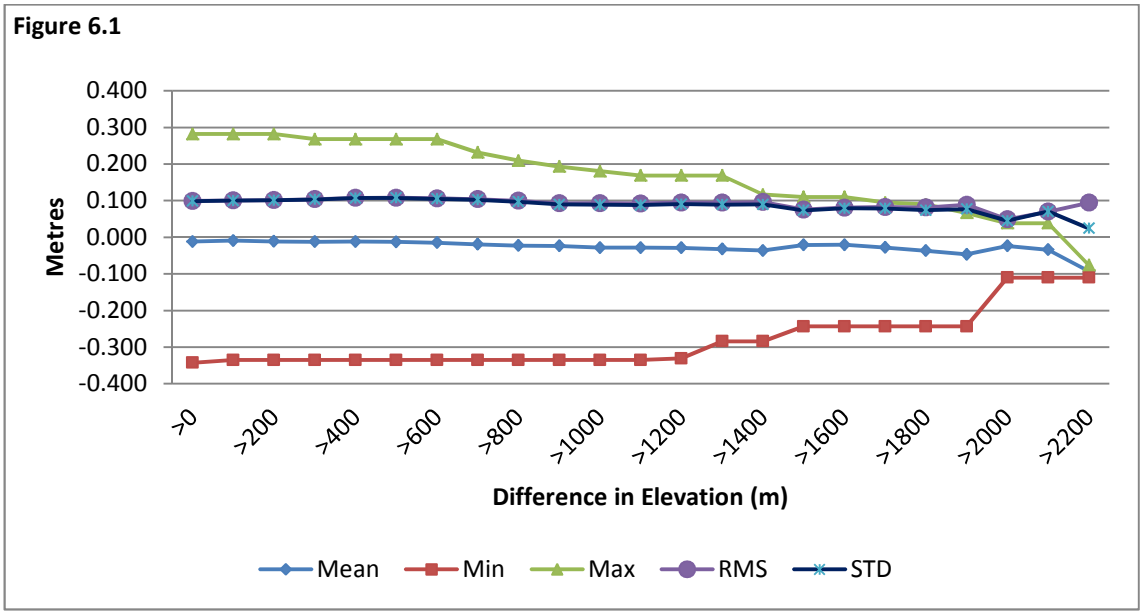

Figure 6.1: Snowy Mountains graphical representation of the descriptive statistics of relative verification residuals, between AHD71 differences and orthometric differences using AUSGeoid09 as a function of 100 m increase of difference in elevation

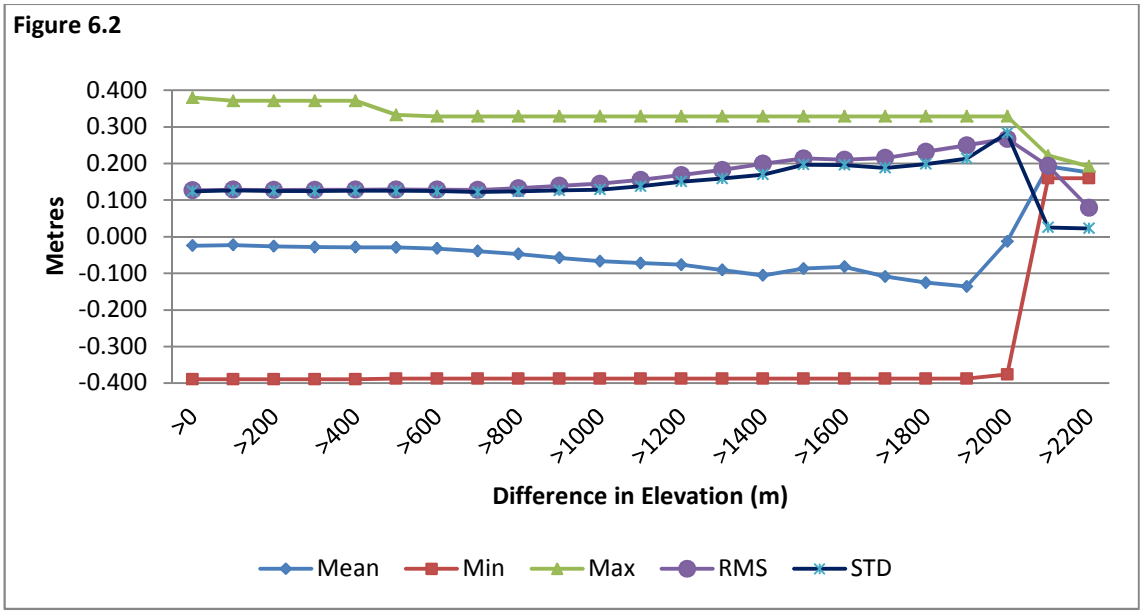

Figure 6.2: Snowy Mountains graphical representation of the descriptive statistics of relative verification residuals, between AHD71 differences and orthometric differences using AUSGeoid98 as a function of 100 m increase of difference in elevation

6.3.5 The Snowy Mountains Graphical Representation

The same residuals used for the above descriptive analysis were plotted as a function of the baseline lengths joined together with the allowable 3rd order differential levelling

miscloses and as function of difference in elevation. Figures 6.3 and 6.4 are typical scatter plots of AUSGeoid09 and AUSGeoid98 residuals as a function of baseline length (within 100 km). The remaining plots are shown in Figure G.1-G.4 in Appendix G.

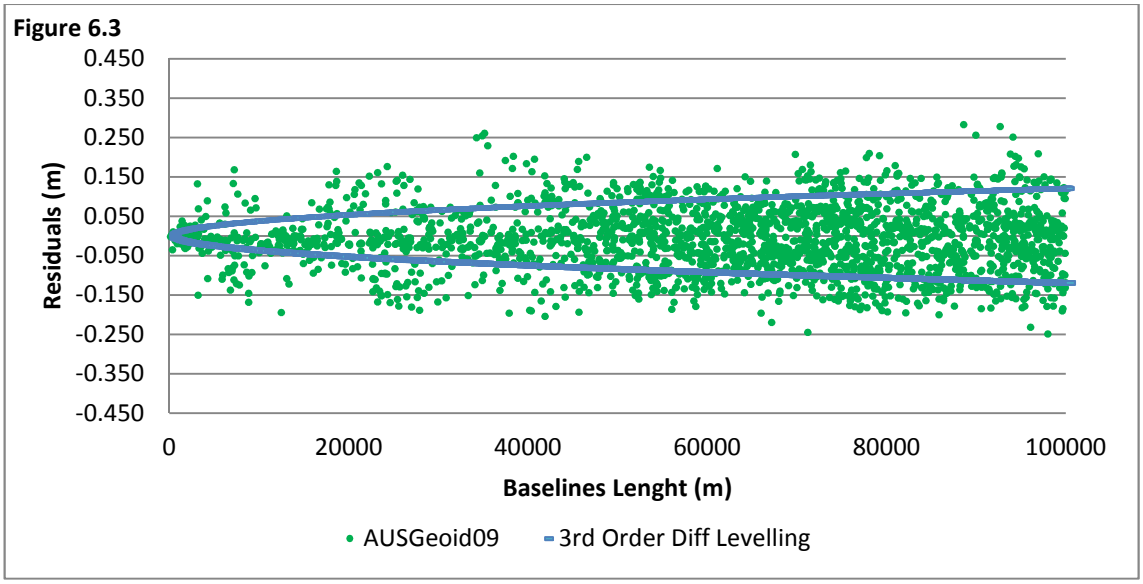

Figure 6.3: Snowy Mountains relative verification residuals between AHD71 and AUSGeoid09 (with bi-cubic interpolation) over 2,361 baselines shorter than 100 km, plotted together with current allowable 3rd order differential levelling miscloses

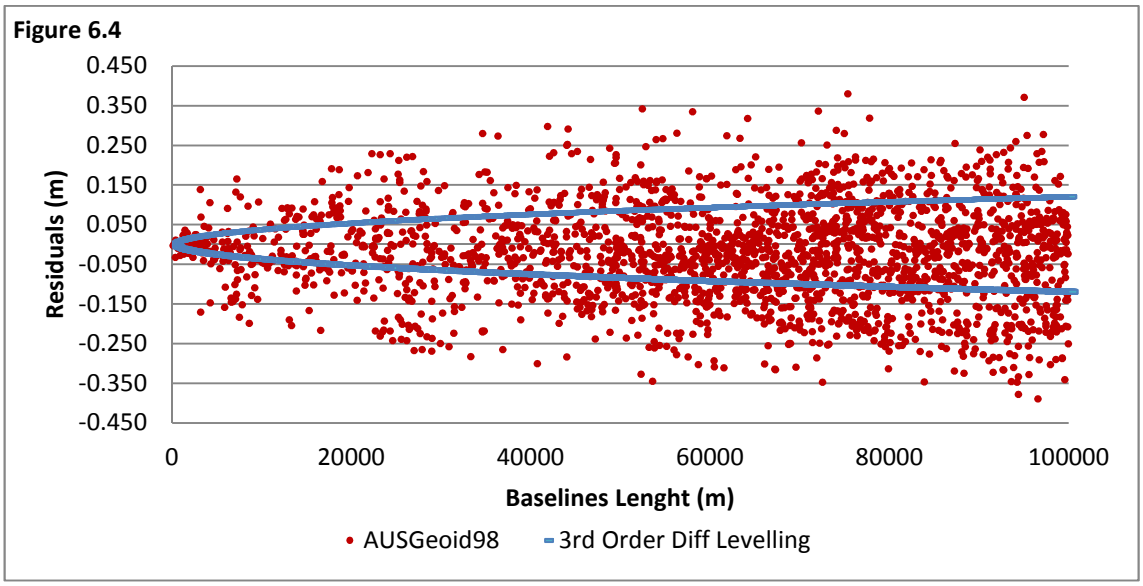

Figure 6.4: Snowy Mountains relative verification residuals between AHD71 and AUSGeoid98 (with bi-cubic interpolation) over 2,361 baselines shorter than 100 km, plotted together with current allowable 3rd order differential levelling miscloses

Figure 6.5 and Figure 6.6 show the residuals for AUSGeoid09 and AUSGeoid98 respectively as a function of difference in elevation.

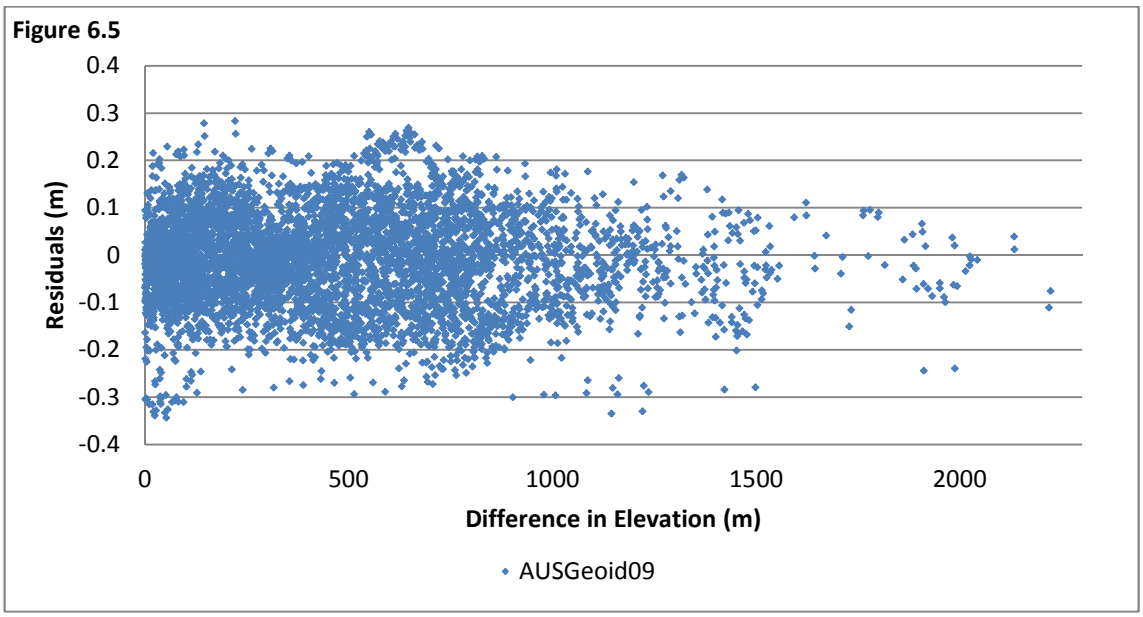

Figure 6.5: Snowy Mountains relative verification residuals between AHD71 and AUSGeoid09 (with bi-cubic interpolation) over 5,356 possible baselines as a function of difference in elevation

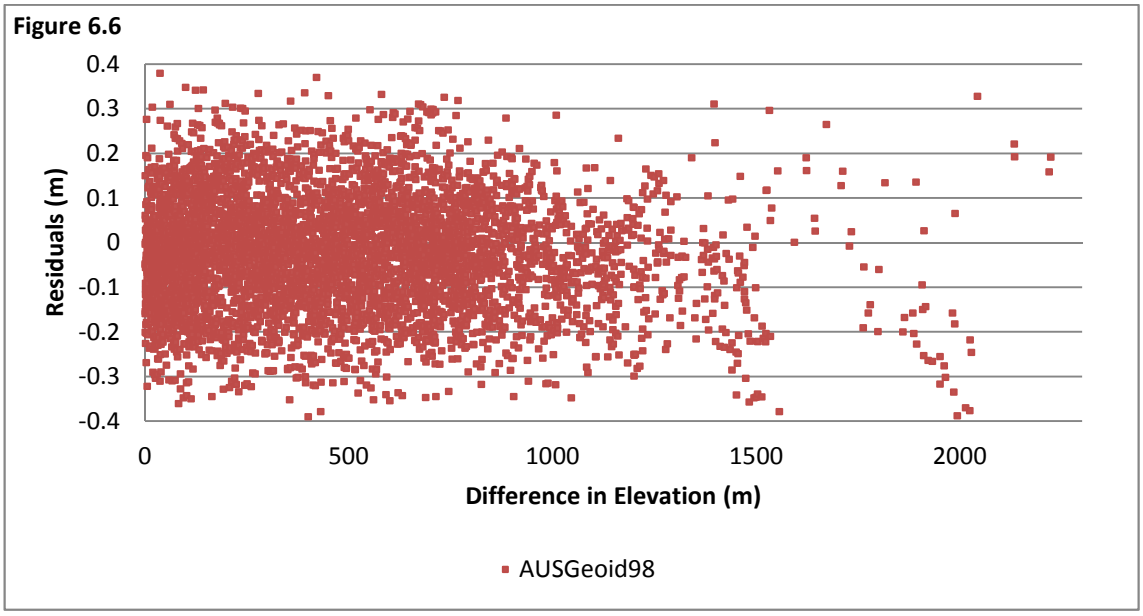

Figure 6.6: Snowy Mountains relative verification residuals between AHD71 and AUSGeoid98 (with bi-cubic interpolation) over 5,356 possible baselines as a function of difference in elevation

6.4 The Mid Hunter Results

The following subsections will present the Mid Hunter results of the four methods of relative verification described in section 6.2. A discussion of the results is given in section 6.5.

6.4.1 The Mid Hunter Comparison Over All Observed Baselines

The Mid Hunter includes 82 checkpoints of which 80 have been directly connected by simultaneous observations delivering only 104 baselines. A descriptive statistical analysis of these 104 baselines using both AUSGeoid09 and AUSGeoid98 is summarised in Table 6.4.

Descriptive Statistics	AUSGeoid09	AUSGeoid98
Count	104	104
Range (m)	0.252	0.272
Mean (m)	-0.006	0.002
Minimum (m)	-0.132	-0.104
Maximum (m)	0.120	0.168
Kurtosis	0.485	1.358
STD (m)	0.047	0.045
RMS (m)	0.047	0.045
ppm	4.008	3.669
Baseline within 3RD Order Differential Levelling	67 (64%)	70 (67%)
Mean Distance (m)	13114	13114
outliers	0	1

Table 6.4: Mid Hunter descriptive statistics of relative verification residuals between AHD71 differences and orthometric differences over 104 observed baselines using both AUSGeoid09 and AUSGeoid98 with bi-cubic interpolation

6.4.2 The Mid Hunter Comparison Over All Possible Baselines

The Mid Hunter network delivered 3,221 possible baselines between 82 checkpoints. Again, the total number of baselines was computed using the equation $n(n-1)$. However, the baseline between TS2672-1 and TS2672-2 was removed as it is only 5 m

long and not suited to be observed by GNSS. Additionally, this is also irrelevant in terms of geoid verification since the distance is much smaller than the geoid resolution. Table 6.5 presents the descriptive statistical analysis of the now 3,220 baselines for both geoid models.

Descriptive Statistics	AUSGeoid09	AUSGeoid98
Count	3320	3320
Range (m)	0.437	0.570
Mean (m)	0.001	-0.009
Minimum (m)	-0.243	-0.287
Maximum (m)	0.194	0.284
Kurtosis	0.325	-0.466
STD (m)	0.056	0.105
RMS (m)	0.056	0.105
ppm	0.944	1.464
Baseline within 3RD Order Differential Levelling	2,973 (90%)	2,035 (61%)
Mean Distance (m)	74930	74930
outliers	15	0

Table 6.5: Mid Hunter descriptive statistics of relative verification residuals between AHD71 differences and orthometric differences over 3,320 possible baselines using both AUSGeoid09 and AUSGeoid98 with bi-cubic interpolation

6.4.3 The Mid Hunter Comparison Within 100 km Baselines

The total number of all possible baselines was reduced to 2,526 that represent all possible baselines up to a length of 100 km. As discussed in the previous section, baseline TS2672-1 TS2672-2 was removed. Table 6.6 presents the descriptive statistical analysis of the 2,526 baselines for both geoid models.

Descriptive Statistics	AUSgeoi09	AUSgeoid98
Count	2526	2526
Range (m)	0.428	0.554
Mean (m)	0.003	-0.006
Minimum (m)	-0.243	-0.286
Maximum (m)	0.185	0.267
Kurtosis	0.431	-0.247
STD (m)	0.055	0.095
RMS (m)	0.055	0.095
ppm	1.119	1.645
Baseline within 3RD Order Differential Levelling	2,206 (87%)	1,547 (61%)
Mean Distance (m)	57380	57380
outliers	12	0

Table 6.6: Mid Hunter descriptive statistics of relative verification residuals between AHD71 differences and orthometric differences over 2,526 possible baselines within 100 km using both AUSGeoid09 and AUSGeoid98 with bi-cubic interpolation

6.4.4 The Mid Hunter Comparison Every 100 m Increase of Difference in Elevation

As per the Snowy Mountains network, the 3,320 baselines were reordered as a function of increment of difference in elevation. These baselines combined deliver differences in elevation comprising from 0.005 m to 1,480 m. Figure 6.7 and Figure 6.8 show the descriptive statistical analysis for both geoid models as a function of difference in elevation, while the numerical representation is summarised in Table H.3 and H.4 in Appendix H.

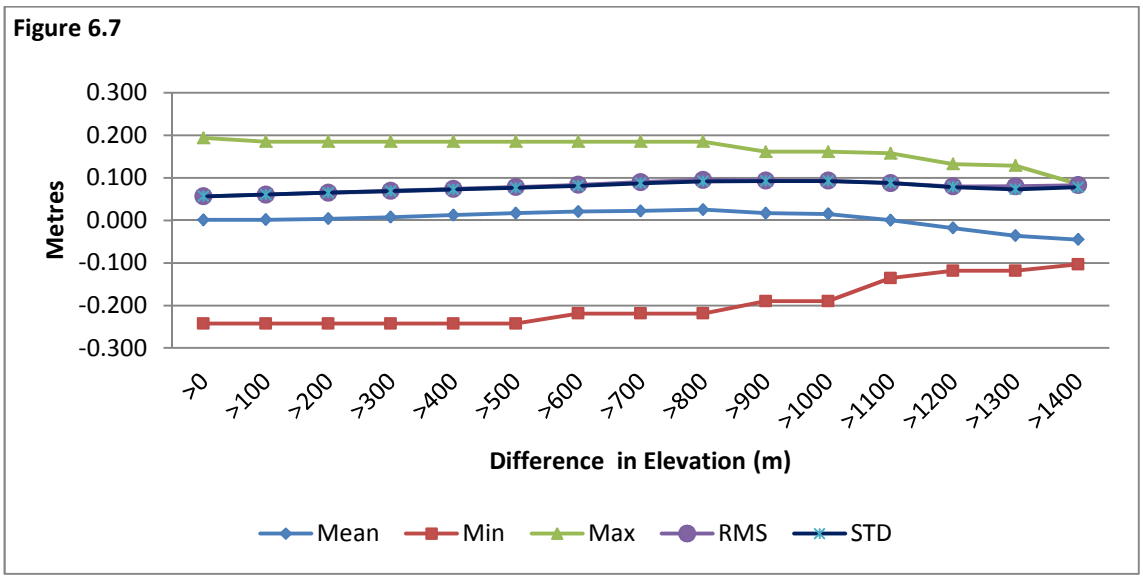

Figure 6.7: Mid Hunter graphical representation of the descriptive statistics of relative verification residuals, between AHD71 differences and orthometric differences using AUSGeoid09 as a function of 100 m increase of difference in elevation

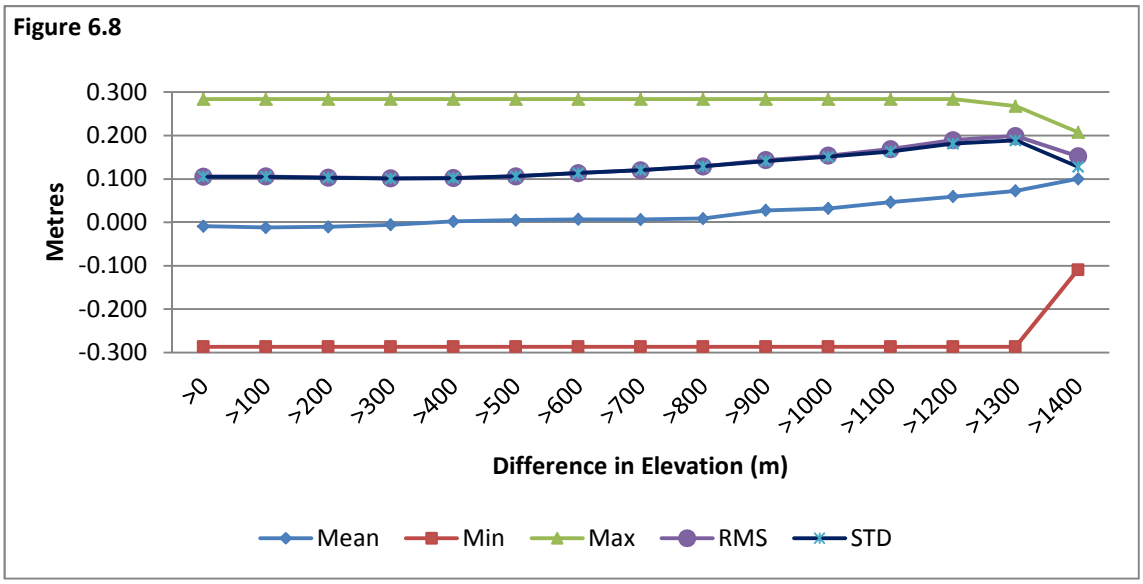

Figure 6.8: Mid Hunter graphical representation of the descriptive statistics of relative verification residuals, between AHD71 differences and orthometric differences using AUSGeoid98 as a function of 100 m increase of difference in elevation

6.4.5 The Mid Hunter Graphical Representation

Once again, a scatter plot was employed to visualise the residuals of both models, as a function of the baseline length joined together with the allowable 3rd order differential levelling misclose as per *SP1* and as a function of difference in elevation. Figure 6.9 and

Figure 6.10 show typical scatter plots of residuals as a function of baseline lengths for AUSGeoid09 and AUSGeoid98 (up to 100 km). The remaining plots are shown in Figures G.5-G.8 in Appendix G.

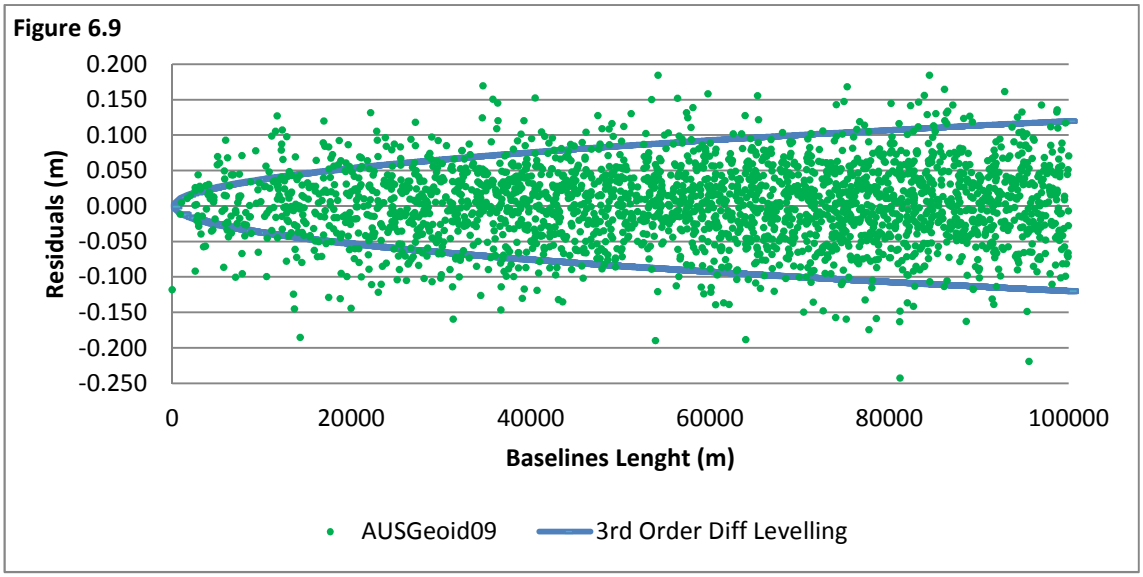

Figure 6.9: Mid Hunter relative verification residuals between AHD71 and AUSGeoid09 (with bi-cubic interpolation) over 2,526 baselines shorter than 100 km, plotted together with current allowable 3rd order differential levelling miscloses

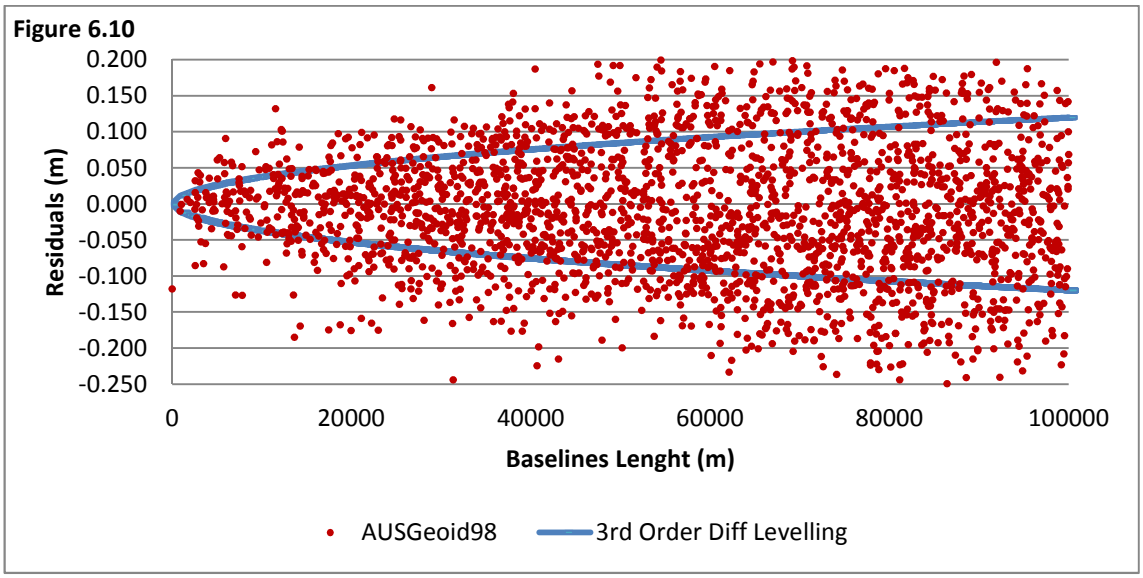

Figure 6.10: Mid Hunter relative verification residuals between AHD71 and AUSGeoid98 (with bi-cubic interpolation) over 2,526 baselines shorter than 100 km, plotted together with current allowable 3rd order differential levelling miscloses

Figure 6.11 and Figure 6.12 show the residuals for both AUSGeoid09 and AUSGeoid98 respectively as a function of difference in elevation.

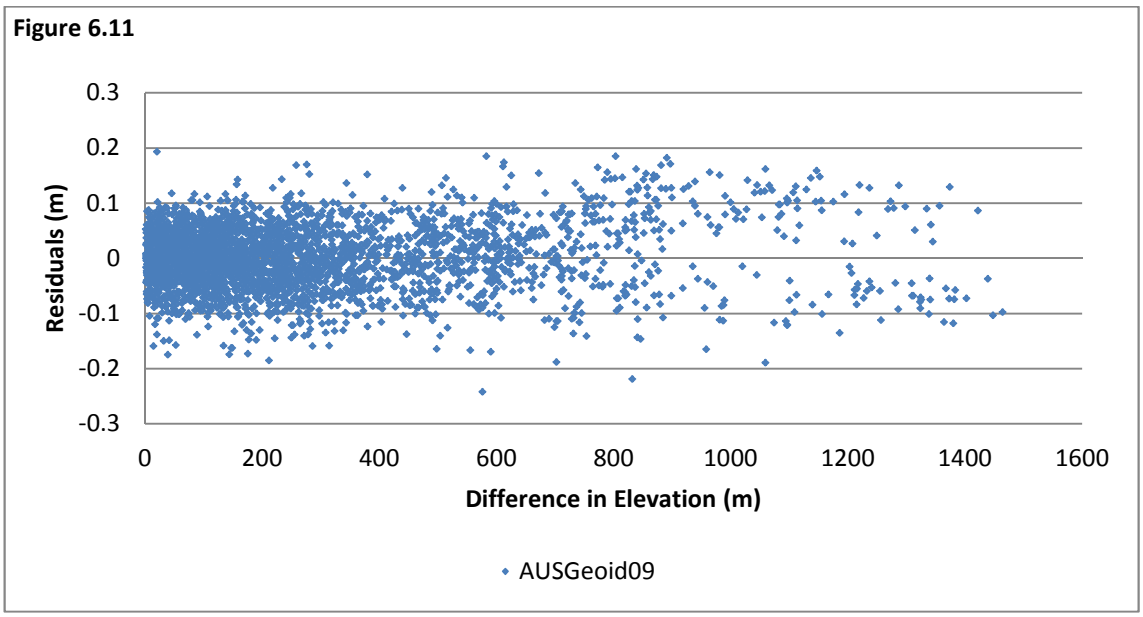

Figure 6.11: Mid Hunter relative verification residuals between AHD71 and AUSGeoid09 (with bi-cubic interpolation) over 3,320 possible baselines as a function of difference in elevation

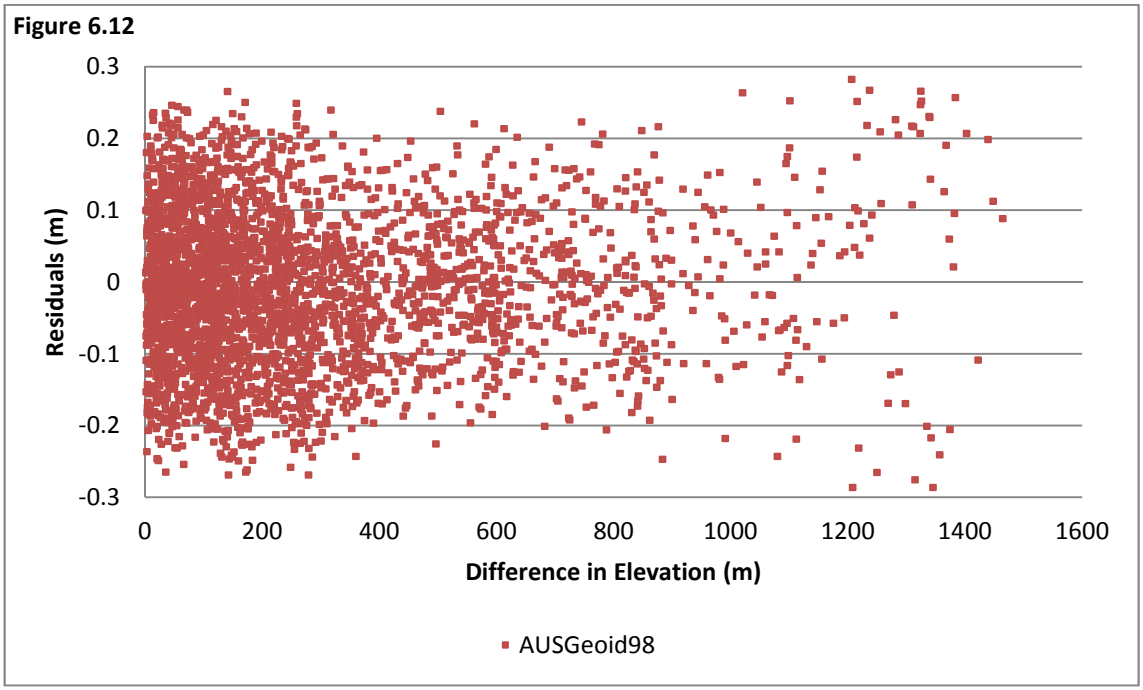

Figure 6.12: Mid Hunter relative verification residuals between AHD71 and AUSGeoid09 (with bi-cubic interpolation) over 3,320 possible baselines as a function of difference in elevation

6.5 Results Discussion

Section 6.3 and section 6.4 have presented the results of the performance testing for both AUSGeoid09 and AUSGeoid98 within the two study areas in a relative sense. This section will analyse the results achieved and a discussion is presented to establish the improvement in retrieving AHD71 heights with the use of AUSGeoid09. Final considerations will be offered in Chapter 7.

6.5.1 The Snowy Mountains Numerical Discussion

Section 6.3 presented the results of the four tests employed to verify the performance of AUSGeoid09 and AUSGeoid98 within the Snowy Mountains study area. The differences in elevation between published AHD71 heights were compared with the differences in orthometric heights derived from the homogeneous network of ellipsoidal heights with an average standard deviation of ±0.031 m at 95% confidence level (see section 4.7.1). Additionally, the orthometric heights were derived with bi-cubic interpolation. A discussion of the results for the relative verification is given below, while final considerations are offered in Chapter 7.

Table 6.1 in section 6.3.1 presented a descriptive statistical analysis of the residuals obtained from the 66 observed baselines available between checkpoints. Statistically, these samples have demonstrated that both geoid models perform in a similar way with a slight improvement of AUSGeoid09 over its predecessor. The RMS dropped from 0.064 m to 0.051 m, resulting in an improvement factor of 1.3. The two models differ in terms of an average ppm by 0.3 in favour of AUSGeoid09, which can be defined as 2 mm in elevation, if considering that the average baseline length is 7.5 km. There is no substantial difference when both models are compared with the 3rd order differential levelling allowable miscloses, as per the current standards of precision detailed in *SP1* (ICSM 2007). AUSGeoid09 showed that 40 of the 66 baselines are within 3rd order differential levelling specifications, i.e. only three more baselines than for AUSGeoid98.

Table 6.2 in section 6.3.2 shows the descriptive statistical analysis for 5,356 possible baselines between the 104 checkpoints. AUSGeoid09 residuals include 15 outliers

(greater 3 sigma) while AUSGeoid98 has not detected any outliers. Contrary to that, this test has demonstrated that AUSGeoid09 is a better model to derive AHD71 heights in a relative sense. The RMS dropped from 0.127 m to 0.099 m with the use of AUSGeoid09, again resulting in an improvement factor of 1.3. The average ppm is 1.1 ppm for AUSGeoid09 and 1.4 for AUSGeoid98. Even in this test, the average ppm differs from one model to another by about 0.3 ppm in favour of AUSGeoid09. However, in this test the average baseline length is 113 km. Therefore 0.3 ppm yields a difference of 33 mm over this baseline length. The most important result of this test is that 77% of 5,356 residuals computed using AUSGeoid09 fall within the estimation of precision for 3rd order differential levelling specified in *SP1*, while only 64% of AUSGeoid98 residuals achieved the same result.

Table 6.3 in section 6.3.3 shows the descriptive statistical analysis of 2,361 baselines between checkpoints shorter than 100 km. Both geoid models show almost the same number of outliers. However, AUSGeoid09 performed better than AUSGeoid98, with 71% of the residuals within 3rd order differential levelling specifications, while only 53% of AUSGeoid98 residuals fall within these expectations. The RMS dropped from 0.122 m to 0.082 m, which shows an improvement factor of 1.5. AUSGeoid09 residuals indicated a ppm of 1.7 which is 0.6 lower the AUSGeoid98. Considering the average baseline length is 61 km, 0.6 ppm yields a difference of 36 mm over this baseline length.

Figure 6.1 and 6.2 in section 6.3.4 and Table H.1 and Table H.2 in Appendix H presented the performance of AUSGeoid09 and AUSGeoid98 as a function of a 100 m rises of difference in elevation. The 5,356 possible baselines were employed to evaluate this test with differences in elevation between 0.05 m and 2,223 m. Based on the descriptive statistic in Table H.1 and Table H.2 there are no substantial discrepancies for both models. However, statistically there are more residual outliers in AUSGeoid09 than AUSGeoid98. In saying that, the magnitude of the residuals is smaller than AUSGeoid98 (see Figures 6.3, 6.4 in section 6.3.5 and Figures G.1-G.4 in Appendix G). The performance of AUSGeoid09 improves slightly as the difference in elevation increases. The RMS seems to be constant from 0 m to 1,500 m elevation, then decreases by about 0.030 m from 1,500 m to 2,200 m difference in elevation. On the other hand, AUSGeoid98 is performing worse with the increase of the difference in elevation,

showing a constant rise of RMS as the difference in elevation grows, reaching a peak of 0.169 m at 2,200 m from 0.092 m at 0.05 m difference in elevation.

6.5.2 The Snowy Mountains Graphical Discussion

The graphical representation was employed to visualise and further establish the above numerical representation as a function of the baseline length and difference in elevation. Recalling that the N values with bi-cubic interpolation were derived from the network of ellipsoidal heights, with average standard deviations of ±0.031 m at 95% confidence level (see section 4.7.1), the graphical representation discussion is presented below.

Figures G.1, G.2 in Appendix G show the numerical representation residuals derived from 66 observed baselines for both models. As evident from the above mentioned figures, both models showed large residuals within the 20 km baseline range, which confirms the numerical evaluation presented in section 6.2.1 and discussed in section 6.5.1. However, it is important to note that this test is not a true representation of the data, since the sample is quite small and the baselines are sporadically located in different sections of the network.

The graphical representation of the 6,356 residuals confirmed the numerical evaluation presented in section 6.2.2. Additionally, it appears by comparing Figure G.3 and Figure G.4 in Appendix G that the overall distribution of AUSGeoid09 residuals are closer to the 3rd order differential levelling specifications, indicating a better performance of AUSGeoid09.

Similarly, the 2,361 baselines up to 100 km were plotted and presented in Figure 6.3 and 6.4 in section 6.3.5 for both AUSGeoid09 and AUSGeoid98 respectively. This confirmed a better distribution for AUSGeoid09 residuals. 95% of the residuals are within ±0.160 m (2 sigma), while 95% of the AUSGeoid98 residuals are within ±0.240 m (2 sigma).

Finally, the 5,356 baselines were plotted as a function of difference in elevation. As seen from Figure 6.5 and Figure 6.6 in section 6.3.5, AUSGeoid09 performs better than its predecessor AUSGeoid98. AUSGeoid09 residuals are closer to zero and a better performance is visible throughout the elevation model scatter plot.

6.5.3 The Mid Hunter Numerical Discussion

Section 6.4 presented the results of four tests used to verify the performance of AUSGeoid09 and AUSGeoid98 within the Mid Hunter region. Recalling that the retrieved N values with bi-cubic interpolation used for the comparison were computed from the homogeneous network of ellipsoidal heights, with an average standard deviation of ±0.024 m at 95% confidence level (see section 4.7.2), a discussion of the result for the relative verification is given below, while final considerations are offered in Chapter 7.

Table 6.4 in section 6.4.1 presented a descriptive statistical analysis of 105 observed baselines available between checkpoints. AUSGeoid09 residuals did not include outliers, while AUSGeoid98 include one outlier. Statistically, these samples have demonstrated that both geoid models performed almost identically. In fact, the RMS differs only by 0.002 m and about 70% of the residuals for both models are within the 3rd order differential levelling specifications. Additionally, it is important to note that the highest AUSGeoid98 residuals occur in different elevation ranges without any particular pattern, while the highest AUSGeoid09 residuals occur in baselines with differences in height between 400 m and 750 m. However, it should be noted that only 6 baselines out of the 104 defined this trend. Moreover, this pattern was also identified in the comparison of all possible baselines over increases of difference in elevation that will be discussed later.

Table 6.5 in section 6.4.2 shows the descriptive statistical analysis for the 3,320 possible baselines between the 82 checkpoints. Even though AUSGeoid09 has denoted 14 outliers, this test has demonstrated an extraordinary improvement factor of 1.9 with the RMS of 0.105 m for AUSGeoid98 decreasing to 0.056 m in AUSGeoid09. The average ppm is 0.9 for AUSGeoid09 which is 0.6 lower than the one retrieved with AUSGeoid98. Considering that the average baseline length is 75 km, 0.6 ppm denotes a difference in elevation of 45 mm worse for AUSGeoid98. Additionally, 89% of the AUSGeoid09 residuals were well within the 3rd order differential levelling, while only 61% of AUSGeoid98 achieved this result.

Table 6.6 in section 6.4.3 shows a descriptive statistical analysis of 2,326 baselines between checkpoints shorter than 100 km. This test has, to some extent, confirmed the result of the previous test. In spite of the presence of 12 outliers (0.5%), AUSGeoid09

performs better than AUSGeoid98. An improvement factor of 1.7 is detected with the RMS dropping from 0.095 m for ASUGeoid98 to 0.055 m for AUSGeoid09. 87% of the residuals were within the 3rd order differential levelling, while only 61% of AUSGeoid98 fall within these expectations.

Figure 6.7 and figure 6.8 in section 6.4.4 and Table H.3 and Table H.4 in Appendix H presented the performance of AUSGeoid09 and AUSGeoid98 as a function of 100 m rise in difference in elevation, between the 82 checkpoints. The 3,320 possible baselines were employed to analyse this test. The elevation difference is comprised between 0.005 m and 1,450 m. Based on the descriptive statistics shown in Table H.3 and Table H.4, there are no substantial statistical discrepancies for both AUSGeoid09 and AUSGeoid98. Both models seem to perform poorer as the difference in elevation increases. However, AUSGeoid09 denotes consistency from 1,100 m up to 1,400 m elevation. In addition, the magnitude of AUSGeoid09 residuals is much smaller than those computed using AUSGeoid98 (see Figures 6.9, 6.10 in section 6.4.5 and Figures G.5-G.8 in Appendix G). Even though both models detected a similar trend, which shows large residuals as a function of the increase of difference in elevation, AUSGeoid09 once again performed better than AUSGeoid98 with the average RMS decreasing from 0.132 m for AUSGeoid98 to 0.079 m for AUSGeoid09.

6.5.4 The Mid Hunter Graphical Discussion

The graphical representation was employed to visualise and further establish the above numerical representation as a function of the baseline length and difference in elevation. Recalling that all the computed difference in orthometric heights with bi-cubic interpolation were derived from the network of ellipsoidal heights with average standard deviation of ±0.024 m at 95% confidence level (see section 4.7.2), the graphical representation discussion is presented below, while final considerations are offered in Chapter 7.

Figure G.5 and Figure G.6 in Appendix G show the numerical representation residual derived from 104 observed baselines for both models. As it can be seen, both models denoted large residuals within the 10 km range, and confirm the almost identical numerical evaluation detailed in section 6.4.1.

The graphical representation of the 3,320 residuals confirmed the numerical evaluation presented in section 6.4.2 (see Figure G.7 and Figure G.8 in Appendix G). Additionally, Figure G.7 shows the majority of AUSGeoid09 residuals within the 3rd order differential levelling specifications of *SP1*. Additionally, the range of residuals for AUSGeoid98 is larger than for AUSGoid09.

Similarly, the 2,326 baselines shorter than 100 km were plotted and presented in Figure 6.9 and Figure 6.10 in section 6.4.5 for both AUSGeoid09 and AUSGeoid98 respectively. This confirmed a better distribution for the AUSGeoid09 residuals. Once again AUSGeoid09 residuals are well within the 3rd order differential levelling specification as per *SP1*. Additionally, the overall plot of residuals is quite consistent with AUSGeoid09, while AUSgeoid98 residuals rise with the longer distances.

Finally, the 3,320 baselines were plotted as a function of increasing the difference in elevation between the above baselines. As it can be seen from Figure 6.11 and Figure 6.12 in section 6.4.5 both AUSGeoid09 and AUSGeoid98 denote large residuals with high differences in elevation. On the other hand, AUSGeoid09 is definitely more consistent within the first 600 m differences in elevation.

6.6 Conclusion

This chapter has presented the evaluation of AUSGeoid09 in a relative sense and has compared the results with its predecessor AUSGeoid98. This verification is based on the difference in heights over the same baseline, where the derived orthometric heights were computed with bi-cubic interpolation for both AUSGeoid09 and AUSGeoid98. The verification was implemented over all observed baselines, all possible baselines and all possible baselines shorter than 100 km between checkpoints. Descriptive statistics and scatter plots were employed as a function of baseline lengths and as a function of increments of difference in elevation. The shortest distance between two checkpoints was computed by Vincenty's inverse formula.

The discussion presented has demonstrated that AUSGeoid09 is the better model to derive AHD71 heights in a relative sense in both study areas compared to AUSGeoid98. In particular, it was detected that in all the performed tests the average ppm and RMS is

lower for AUSGeoid09. Moreover, the absolute residuals were compared with the current standard of 3rd order differential levelling. This comparison has demonstrated that in all the tests 70% or more of the AUSGeoid09 residuals are within this target, while only 60% or less of AUSGeoid98 residuals achieved the target.

The graphical representation has demonstrated that AUSGeoid09 residuals are well distributed and smaller than AUSGeoid98 residuals. However, the verification as a function of difference in elevation has detected the tendency of both models to produce large residuals in higher difference in elevation, which was also evident from the descriptive statistics. This phenomenon was only evident in the Mid Hunter region. However, even in this instance AUSGeoid09 performed better than AUSGeoid98.

Chapter 7 will deliver final considerations to draw conclusions in regards to the performance of AUSGeoid09, both in an absolute and relative sense within the Snowy Mountains and Mid Hunter regions.

CHAPTER 7
CONCLUSION

7.1 Introduction

Chapter 6 presented the results and a subsequent discussion of the relative verification of AUSGeoid09 and AUSGeoid98. As explained in Chapter 2, AUSGeoid09 is the current geoid model computed with both a gravimetric and a geometric component. The latter component was derived from AHD71 heights to adjust gravimetric one and deliver as a consequence a better fit to AHD71 datum. This adjustment was necessary due to AHD71 anomalies detailed in Chapter 2 which are the main reasons why previous AUSGeoid models and AHD71 do not coincide. The introduction of AUSGeoid09 to convert GNSS ellipsoidal heights into AHD71 heights and vice versa has introduced substantial improvement acknowledged by previous research. However, although the model has improved this conversion, large residuals were detected within coastal and mountainous regions.

Chapter 7 will provide a response to define the accuracy of AUSGeoid09 within the Snowy Mountains and Mid Hunter mountainous regions in NSW. The final consideration will be based on the results of the tests performed in the two large scale GNSS networks detailed in Chapter 5 and 6, both in an absolute and relative sense. In addition, the improvement of AUSGeoid09 will be based on the comparison with its predecessor AUSGeoid98.

7.2 Absolute Verification Conclusion

Appraisal of the test results and discussion offered in Chapter 5 reveal AUSGeoid09 has performed differently from the Snowy Mountains to the Mid Hunter regions in absolute sense. However, the model has demonstrated stability to derive N value with the four different interpolation methods. This has detected a better consistency than AUSGeoid98 since this model performs slightly different according to the interpolation method used. This was an expected result since the AUSGeoid09 resolution is 1’ (1.8 km by 1.8 km), which is four times denser than that of AUSGeoid98.

Based on the data representation of the Snowy Mountains area shown in section 5.5.1-5.5.2 and discussed in detail in section 5.6.1-5.62, AUSGeoid09 denotes no improvement in retrieving AHD71 heights in an absolute sense, compared to its

predecessor AUSGeoid98. Additionally, this dataset detected a slope within AUSGeoid09 from the north-west to south-east corner, with the majority of the positive residuals at the south-east corner. However, the sample within this part of the network is too small to definitely point out any anomalies in AUSGeoid09. In fact, only two of the residuals are larger than the others. Additionally, according to Featherstone et al. (2010) as detailed in section 2.6, only a predefined number of AHD71 marks were used to fit AUSGeoid09 to AHD71 across the country, and considering that AHD71 is defined by Morgan (1992) as a homogenous vertical datum of third order, it is possible that this section of the network contains an anomaly of AHD71 which is not included in the geometric component of AUSGeoid09. Therefore, future study should be implemented to find further evidence of any slope defects or improved performance with the use of AUSGeoid09. Even though this dataset identified the possibility of discrepancies with AUSGeoid09, statistically, it performed better than its predecessor AUSGeoid98. However, a block shift is required to deliver better accuracy than AUSGeoid98. This is due to the fact that the residuals of AUSGeiod09 are included in a smaller range and, if the two largest residuals are removed, 69% of the remaining ones are contained within ±0.070 m (1 sigma) of the mean, while 69% of the AUSGeoid98 residuals are within ±0.090 m (1 sigma) of the mean.

According to Mid Hunter data representation in section 5.5.3-5.5.4 and discussion in section 5.6.3-5.6.4, AUSGeoid09 has demonstrated an astonishing improvement in retrieving AHD71 heights in absolute sense compared with AUSGeoid98. A trend was not evident as a function of the horizontal position of the checkpoints or as a rise of elevation as it was detected in the Snowy Mountains network. However, descriptive statistics of elevations above 700 m were based on a small number of marks, which points out that further data would be required to confirm the improvement of AUSGeoid09 or define any trend. In saying that, the overall performance of AUSGeoid09 is extraordinary with 70% of the residuals were within ±0.040 m (1 sigma) of the mean, while only 61% of AUSGeoid98 residuals were within ±0.074 m (1 sigma) of the mean. Furthermore, AUSGeoid09 has demarcated a consistent performance throughout the network, and comparison of RMS values computed for both models indicates an improvement factor of 6 relative to AUSGeoid98.

7.3 Relative Verification Conclusion

Appraisal to the results shown in Chapter 6, AUSGeoid09 has demonstrated to be the better model to compute AHD71 heights from GNSS ellipsoidal heights from a relative point view, in both the Snowy Mountains and Mid Hunter study areas. It is important to note that the absolute verification has demonstrated consistency in the method of interpolation used, hence the relative verification was based on bi-cubic interpolation only, which was a method used by several users in previous studies detailed in Chapter 2.

The data representation for both the Snowy Mountains and Mid Hunter regions described in sections 6.3 and 6.4, and the discussion offered in section 6.5, have demonstrated an overall better performance of AUSGeoid09 in a relative sense compared to AUSGeoid98. In all the performed tests provided RMS and ppm values are smaller for AUSGeoid09. However, even if only in small percentages, AUSGeod09 has detected more outliers (greater than 3 sigma) than AUSGeoid98, which is quite acceptable, considering that in all cases AUSGeiod09 has detected standard deviations being almost half the size of AUSGeoid98.

The most relevant outcome of this study is that AUSGeoid09 has demonstrated the largest number of residuals in agreement with the current allowable standards of precision of 3rd order differential levelling as per *SP1*. This was detected in both study areas over all possible baselines and over all possible baselines shorter than 100 km.

Based on the verification as a function of rise in difference in elevation, it was detected the AUSGeoid09 is once again the better model in both study areas. A close evaluation of the Snowy Mountains residuals has indicated that AUSGeoid09 improved its performance as the difference in elevation increases. However, the Mid Hunter region has delivered the opposite results where the residuals seemed to increase as a function of increment in difference in elevation.

7.4 Future Study

This study has demonstrated that the AUSGeoid09 is a better model to derive AHD71 heights both in absolute and relative sense compared to its predecessor AUSGeoid98,

within the Snowy Mountains and Mid Hunter regions. However, the Snowy Mountains absolute verification has detected the possibility of an anomaly of AUSGeoid09 within the south-east corner section of the network. In addition, the relative verification of AUSGeoid09 in both study areas has shown discrepancies of performance in different elevation ranges.

Supplementary research should be implemented to further verify the occurrence of a slope in AUSGeoid09 within the Snowy Mountains region. Additionally, as the results of the two datasets are different, further research into other mountainous areas should be conducted to find further evidence of any slope defects or improved performance overall in the use of AUSGeoid09.

Finally, although AUSGeoid09 is a better model to retrieve AHD71 heights from ellipsoidal heights compared to its predecessor AUSGeoid98, discrepancies still do exist between AUSGeoid09 and AHD71 both in absolute and relative sense. However, the continuous increase use of GNSS technology such CORS stations will reach stages where homogeneity is required. In this fashion, the matter of future research is leading to investigate the feasibility of a new vertical datum to replace AHD71 using a combination of modern technology such as GNSS, including CORS stations, satellite and airborne gravity observation etc.

7.5 Project Conclusion

The aim of this project was to verify the performance accuracy of AUSGeoid09 to derive AHD71 from GNSS ellipsoidal heights within the Snowy Mountains and Mid Hunter mountainous regions in NSW. It has been found that AUSGeoid09 is the better model to derive AHD71 both in an absolute and relative sense compared to its predecessor AUSGeoid98.

The verification was based on the implementation of several tests where AUSGeoid09 and AUSGeoid98 accuracy was evaluated in the two mountainous regions both in absolute (i.e. single point) and relative (i.e. height difference between two points) sense. Comparison was employed between geoid-derived heights and published AHD71

heights. The improvement of AUSGeoid09 was evaluated as a function of difference between the two models.

It is very important to recall that this verification does not represent the indisputable verification of AUSGeoid09. Sources of error do exist within data and cannot be avoided. However, considering that the main use of AUSGeoid09 is to compute AHD71 heights from GNSS ellipsoidal heights, the data and method employed represent the most practical method of verification.

Finally, the positive results of AUSGeoid09 performance are encouraging, considering that within last two decades GNSS technology has been used to carry vertical control. However, inconsistency still remains between AUSGeoid09 and AHD71. Therefore, a new vertical datum could be the answer to eventually introduce consistency.

LIST OF REFERENCES

Altamimi, Z, Collilieux, X & Metivier, L 2011, 'ITRF2008: An improved solution of the international terrestrial reference frame', *Journal of Geodesy*, vol. 85, no. 8, pp. 457-73, viewed 24/05/2013.

BitWise Ideas Inc 2010, *What is Geolab?*, BitWise Ideas Inc, viewed 02/05/2013, <http://www.bitwiseideas.com/Products/GeoLab/WhatIsGeoLab.htm>.

Brown, N 2010, 'AUSGeoid09 Converting GPS heights to AHD heights', *AUSGEO news*, no. 97, pp. 1-3, viewed 20/03/2013, Geoscience Australia.

Brown, NJ, Featherstone, WE, Hu, G & Johnston, GM 2011, 'AUSGeoid09: A more direct and more accurate model for converting ellipsoidal heights to AHD heights', *Journal of Spatial Science*, vol. 56, no. 1, pp. 27-37, Taylor & Francis.

Caspary, WF 1987, *Concepts of network and deformation Analysis*, 3 edn, University of New South Wales, Sydney.

Dach, R, Hugentobler, U, Fridez, P & Meindl, M 2007, 'Bernese GPS software version 5.0', Astronomical Institute, University of Bern. .

Darbeheshti, N & Featherstone, WE 2009, 'Non-stationary covariance function modelling in 2D least-squares collocation', *J Geoid*, vol. 83, pp. 495-508, viewed 10/5/2013.

DeCarlo, LT 1997, 'On the meaning and use of Kurtosis ', *Psychological Method*, vol. 2, no. 3, pp. 292-307, viewed 10/08/2013, Fordham University.

Dickson, G 2006, Dr GEOLAB or how I learned to stop worrying and love 3D adjustments, LPI, viewed 02/05/2013.

Dickson, G 2012, 'Control Surveys: Why things are the way they are and not the way you think they should be!', in APAS 2012: *proceedings of theAPAS 2012* Wollongong, NSW.

Dickson, G 2013, Personal conversation about variance factor and correlation matrices.

Featherstone, WE 1998, 'Do we need a gravimetric geoid or a model of the Australian height datum to transform GPS heights in Australia?', *Australian Surveyor*, vol. 43, no. 4, pp. 273-80.

Featherstone, WE 2001, 'Absolute and relative testing of gravimetric geoid models using global positioning system and orthometric height data', *Computers and Geosciences*, vol. 27, no. 7, pp. 807-14, viewed 20/04/2013, The Western Australian Centre of Geodesy, The Western Australian Centre of Geodesy.

Featherstone, WE 2004, 'Evidence of a north-south trend between AUSGeoid98 and the Australian Height Datum in south-west Australia', *Survey Review*, vol. 37, no. 291, pp. 334-43, viewed 17/04/213, The Western Australian Centre for Geodesy.

Featherstone, WE 2006, 'Yet more evidence for a north-south slope in the Australian Height Datum', *Journal of Spatial Science*, vol. 51, no. 2, pp. 1-6.

Featherstone, WE 2008, 'GNSS-based heighting in Australia: Current, emerging and future issues', *Journal of Spatial Science*, vol. 53, no. 2, pp. 115-33.

Featherstone, WE & Guo, W 2001, 'Evaluations of the precision of AUSGeoid98 versus AUSGeoid93 using GPS and Australian Height Datum data', *Geomatics Research Australasia*, vol. 74, pp. 75-102, viewed 27/04/2013, The Western Australian Centre of Geodesy, The Western Australian Centre of Geodesy.

Featherstone, WE & Kuhn, M 2006, 'Height systems and vertical datums: A review in the Australian context', *Journal of Spatial Science*, vol. 51, no. 1, pp. 21-41.

Featherstone, WE, Dentith, MC & Kirby, JF 1998, 'Strategies for the accurate determination of orthometric heights from GPS', *Survey Review*, vol. 267, no. 34, pp. 278-96, viewed 12/04/2013, The Western Australia Centre of Geodesy.

Featherstone, WE, Kirby, JF, Kearsley, AHW, Gilliland, JR, Johnston, GM, Steed, J, Forberg, R & Sideris, MG 2001, 'The AUSGeoid98 geoid model of Australia data treatment, computations and comparisons with GPS-levelling data', *Journal of Geodesy*, vol. 75, pp. 313-30, viewed 01/03/2013, Taylor and Francis, Taylor and Francis.

Featherstone, WE, Kirby, JF, Hirt, C, Filmer, MS, Claessens, SJ, Brown, NJ, Hu, G & Johnston, GM 2010, 'The AUSGeoid09 model of the Australian Height Datum', *Journal of Geodesy*, vol. 85, no. 3, pp. 133-50.

Fryer, JC 1972, 'The Australian Geoid', *The Australian Surveyor*, vol. 24, no. 4, pp. 203-14, viewed 13/04/213, University of Southern Queensland.

Geoscience Australia (GA) 2012a, *Australia Height Datum*, Geoscience Australia, viewed 21/04/2013, <http://www.ga.gov.au/earth-monitoring/geodesy/geodetic-datums/australian-height-datum-ahd.html>.

Geoscience Australia (GA) 2012b, *Figure 2.2: The 32 tide gauges used as zero height points for AHD71 and AHD83*, 6 kb, Geoscience Australia, Australia, 2012, gif, <http://www.ga.gov.au/earth-monitoring/geodesy/geodetic-datums/australian-height-datum-ahd.html>.

Geoscience Australia (GA) 2013, *AUSPOS-Online GPS processing*, viewed 02/03/2013, <http://www.ga.gov.au/bin/gps.pl>.

Gibbings, P & McDonald, AJ 2005, 'An evaluation of geoid models on the Great Dividing Range escarpment ', *Spatial Science Queensland*, pp. 30-7, viewed 10/04/2013, University of Southern Queensland.

Google Earth 2013a, *Figure 3.3: Snowy Mountains typical terrain*, jpg.

Google Earth 2013b, *Figure 3.5: Mid Hunter typical terrain*, jpg.

Grinter, T & Roberts, C 2011, 'Precise Point Positioning: Where are we now? ', in International Global Navigation Satellite Systems Society IGNSS Symposium 2011 *proceedings of the International Global Navigation Satellite Systems Society IGNSS Symposium 2011* Sydney NSW, <http://www.lpi.nsw.gov.au/surveying/corsnet-nsw/gnss_publications/gnss_publications_list?id=164446>.

Harvey, BR 1990, *Practical least squares and statistics for surveyors*, 3 edn, University of New South Wales, Sydney.

Higgins, MB 1999, 'Heighting with GPS: possibilities and limitations', in Geodesy and Surveying in the Future: The Importance of Heights: *proceedings of theGeodesy and Surveying in the Future: The Importance of Heights* International Federation of Surveyors (FIG), Gavle, Sweden, <http://www.fig.net/comm/cvs/higgins.htm>.

Inter-Governmental Committee on Surveying and Mapping (ICSM) 2006, *Geocentric datum of Australia technical manual version 2.3(1)*, viewed 25/07/2013, <http://www.icsm.gov.au/gda/gdav2.3.pdf>.

Inter-Governmental Committee on Surveying and Mapping (ICSM) 2007, *Standards and practices for control surveys (SP1) version 1.7*, ICSM, viewed 20/03/2013, <http://www.icsm.gov.au/publications/sp1/sp1v1-7.pdf>.

Janssen, V 2009, 'Understanding coordinate systems, datums and transformations in Australia', in SSSI Biennial Inernational Conference: *proceedings of theSSSI Biennial Inernational Conference* Adelaide, pp. 697-715,

<http://www.lpi.nsw.gov.au/surveying/corsnet-nsw/gnss_publications/gnss_publications_list?id=164448>.

Janssen, V & Watson, T 2010, 'Improved AHD71 height determination from GNSS using AUSGeoid09 in New South Wales, Australia', *Journal of Global Positioning Systems*, vol. 9, no. 2, pp. 112-21, Land and Property Information NSW.

Janssen, V & Watson, T 2011, 'Performance of AUSGeoid09 in NSW ', in APAS2011: *proceedings of theAPAS2011* LPI, Bathurst, pp. 27-36.

Kearsley, AHW 1988, 'The determination of the geoid ellipsoid separation for GPS levelling', *The Australian Surveyor*, vol. 34, no. 1, pp. 11-8, viewed 21/03/213, University of Southern Queensland, Taylor & Francis.

Kinlyside, D 2013, 'SCIMS3: The next generation survey control information management system', in APAS 2013: *proceedings of theAPAS 2013* Canberra, ACT.

Land and Property Information (LPI) 2012, *Surveyor General"s Directions No. 12*, Land & Property Information (LPI), Sydney, viewed 25/04/2013, <http://www.lpi.nsw.gov.au/surveying/publications/surveyor_generals_directions>.

Land and Property Information (LPI) 2013a, *CORSnet-NSW*, viewed 2/5/2013, <http://corsnet.com.au/>.

Land and Property Information (LPI) 2013b, *Surveyor General's Directions*, viewed 02/05/2013, <http://www.lpi.nsw.gov.au/surveying/publications/surveyor_generals_directions>.

Leica Geosystems 2013, *Leica Geo Office V 8.2*, <http://www.leica-geosystems.com/en/Leica-Geo-Office_4611.htm>.

London, M 2013, Personal conversation about variance factor and correlation matrices, 2013.

McDonald, AJ 2004, 'Which geoid model should be used for GPS heighting on the toowoomba bypass project? ', undergraduate program thesis, University of Southern Queensland, Toowoomba QLD.

Meyer, TH, Roman, DR & Zilkoski, DB 2006, 'What does height really mean? Part IV: GPS orthometric heighting', *Surveying and Land Information Science*, vol. 66, no. 3, pp. 165-83, viewed 15/04/2013, University of Connecticut, DigitalCommons@UConn.

Microsearch 2001, *Microsearch GeoLab 2001 Field Manual*, viewed 02/03/2013, <http://www.bitwiseideas.com/Downloads/PDF/GeoLabFieldGuide.pdf>.

Microsearch 2013, *Microsearch GeoLab 2001*, 2001.9.20.0, <http://www.msearchcorp.com/>.

Microsoft 2013, *Microsoft EXCEL*, 14.0.6129.5000, <http://office.microsoft.com/en-au>.

Morgan, P 1992, 'An analysis of the Australian Height Datum 1971', *The Australian Surveyor*, vol. 37, no. 1, pp. 46-63, viewed 29/03/2012, University of Southern Queensland.

Moritz, H 1980, ' Geodetic Reference System 1980', *Bulletin Geodesique*, vol. 54, no. 4, pp. 395-405, viewed 23/05/2013.

Moss, O 2011, DIAS 2010 summer program - Snowy Mountains block, Land & Property Information, 13/10/2011, 234543, viewed 07/04/2013.

O'Kane, P 2011, Hunter Valley GNSS subspine, Land & Property Information, 4/2/2011, 234497, viewed 12/04/2012.

Roelse, A, Granger, HW & Graham, JW 1971, *The adjustment of the Australian levelling survey 1970-1971*, 12, Division of National Mapping, Canberra, Australia,<.

Seeber, G 2003, *Satellite Geodesy*, second edn, Walter de Gruyter, New York.

Todd, P 2012, 'Positioning future with AUSGeoid09', in Spatial Sciences Symposium 2012: *proceedings of theSpatial Sciences Symposium 2012* Bardon QLD.

Trimble 1999, *Trimble Geomatics Office V 1.63 (TGO)*, 1.63, <http://www.trimble.com/products/pdf/tgotechnotes.pdf>.

Trimble 2013, *Trimble Business Centre (TBC)*, <http://www.trimble.com/survey/trimble-business-center.aspx>.

APPENDIX A

Project Specification

University of Southern Queensland

FACULTY OF ENGINEERING AND SURVEYING

ENG4111/4112 Research Project
PROJECT SPECIFIACTION

FOR:	**VITTORIO SUSSANNA**
TOPIC:	AUSGeoid09 PERFORMANCE IN MOUNTAINOUS REGIONS
SUPERVISORS:	Peter Gibbings (USQ) Volker Janssen (LPI)
ENROLEMNT:	ENG4111 Semester 1 2013 ENG4112 Semester 2 2013
PROJECT AIM:	This project will investigate the accuracy of AUSGeoid09 in mountainous regions in NSW. This project will also include a comparison between AUSGeoid09 and its predecessor AUSGeoid98 to evaluate the improvement gained by the new model.
SPONSORSHIP:	Land and Property Information (LPI)
PROGRAMME:	Issue A. 26/02/213

1 Review of literature related to geoid modelling and height datums in general and recent efforts in Australia in particular.
2 Two or more test sites will be selected according to the availability of GNSS static networks approved by Land an Property Information (LPI) that contain AHD71 heights in order to investigate the performance of AUSGeoid09 in mountainous regions.
3 The GNSS static network observations will be analysed and a minimally constrained least squares adjustment will be performed to evaluate data quality.
4 Several least squares adjustments will then be performed using both the AUSGeoid98 and AUSGeoid09 models. Within these adjustments, only ellipsoid heights will be held fixed. Hence, the derived orthometric heights and geoid undulations will not be constrained to AHD71.
5 Ellipsoidal heights derived by AUSPOS online processing provided by Geoscience Australia will be held fixed within the constrained network. These will be selected according to the availability of appropriately accurate heights in the LPI database of AUSPOS solutions.
6 The calculated orthometric heights will be compared with the AHD71 heights (CLASS C, ORDER 3 or better) to ascertain the precision at 95% confidence.
7 Finally, both AUSGeoid09 and AUSGeoid98 geoid-ellipsoid separation (N) will be compared to quantify the expected improvement factor in the connection to AHD71 gained by applying AUSGeoid09.

As time permits:

8 Compare N values derived from adjustments using different methods of geoid interpolation such as Bi-Quadratic, Bi-Linear, Bi-Cubic, Bi-Quartic available within GeoLab options.

APPENDIX B

Snowy Mountains and Mid Hunter Published AHD71 Heights and AUSPOS Solutions Report Summary

LIST OF TABLES

Table B.1: Published AHD71 heights of the 104 checkpoints within the Snowy Mountains network. B-119
Table B.2: Published AHD71 heights of the 82 checkpoints within the Mid Hunter network. B-122
Table B.3: AUSPOS Solutions within the Snowy Mountains network. B-125
Table B.4: AUSPOS Solutions within the Mid Hunter network. B-126

Table B.1: Published AHD71 heights of the 104 checkpoints within the Snowy Mountains network.

Snowy Mountains Checkpoints (Published Heights)							
Checkpoint	**AHD71**	**Class/Order**	**Source**	**Checkpoint**	**AHD71**	**Class/Order**	**Source**
MM10030	1323.649	LCL3	SCIMS	SS1521	808.576	LAL1	SCIMS
MM10110	1121.921	LCL3	SCIMS	SS2857	343.776	LCL3	SCIMS
MM10111	1122.648	LCL3	SCIMS	SS2918	296.122	LCL3	SCIMS
MM10112	1014.206	LCL3	SCIMS	SS5356	277.676	LAL1	SCIMS
MM10113	1028.394	LEL5	SCIMS	SS5660	771.074	LAL1	SCIMS
MM10114	1020.378	LEL5	SCIMS	SS5674	802.875	LCL3	SCIMS
MM10118	848.213	LCL3	SCIMS	SS5675	748.1	LCL3	SCIMS
MM10119	916.484	LCL3	SCIMS	SS5687	724.518	LAL1	SCIMS
MM10120	910.943	LCL3	SCIMS	SS5694	811.311	LAL1	SCIMS
MM10121	430.036	LCL3	SCIMS	SS8394	200.441	LAL1	SCIMS
MM10122	465.745	LCL3	SCIMS	SS8396	203.413	LAL1	SCIMS
MM10123	946.699	LDL4	SCIMS	SS8414	246.893	LAL1	SCIMS
MM10124	875.936	LDL4	SCIMS	SS8415	241.348	LAL1	SCIMS
MM10126	705.13	LDL4	SCIMS	SS8425	321.384	LAL1	SCIMS
MM10129	906.113	LCL3	SCIMS	SS8427	464.585	LAL1	SCIMS
MM10130	1461.358	LDL4	SCIMS	SS8428	427.188	LAL1	SCIMS
MM20000	1476.16	LCL3	SCIMS	SS10113	994.279	LCL3	SCIMS
MM20001	1464.197	LCL3	SCIMS	SS10114	1006.825	LCL3	SCIMS

Checkpoint	AHD71	Class/Order	Source	Checkpoint	AHD71	Class/Order	Source
MM20002	448.293	LCL3	SCIMS	SS10123	1049.382	LCL3	SCIMS
MM20003	1044.065	LCL3	SCIMS	SS10250	950.608	LAL1	SCIMS
PM189	728.999	LAL1	SCIMS	SS23134	757.992	LCL3	SCIMS
PM4539	453.255	LCL3	SCIMS	SS23137	835.478	LCL3	SCIMS
PM4540	334.882	LCL3	SCIMS	SS30254	368.104	LCL3	SCIMS
PM7663	743.166	LCL3	SCIMS	SS34707	1104.265	LCL3	SCIMS
PM7664	773.396	LCL3	SCIMS	SS34712	1120.23	LCL3	SCIMS
PM7665	792.354	LCL3	SCIMS	SS34771	1027.961	LCL3	SCIMS
PM10406	234.88	LAL1	SCIMS	SS36078	306.334	LBL2	SCIMS
PM11739	1080.058	LCL3	SCIMS	SS39974	1093.09	LAL1	SCIMS
PM29061	1024.922	LBL2	SCIMS	SS39976	1028.577	LAL1	SCIMS
PM29063	1027.913	LBL2	SCIMS	SS39982	1157.113	LAL1	SCIMS
PM29355	267.184	LBL2	SCIMS	SS39984	1160.27	LAL1	SCIMS
PM29368	277.548	LAL1	SCIMS	TS56	312.3	LCL3	SCIMS
PM31025	264.041	LAL1	SCIMS	TS563	1717.62	LCL3	SCIMS
PM32467	204.014	LBL2	SCIMS	TS1511	1262.392	LCL3	SCIMS
PM39930	317.517	LBL2	SCIMS	TS1661	891.38	LCL3	SCIMS
PM43850	795.038	LCL3	SCIMS	TS2761-4	2228.266	LCL3	SCIMS
PM43895	948.811	LCL3	SCIMS	TS4470	1219.474	B2	SCIMS
PM43903	634.925	LCL3	SCIMS	TS4471	704.02	LCL3	SCIMS

Checkpoint	AHD71	Class/Order	Source	Checkpoint	AHD71	Class/Order	Source
PM45176	341.501	LDL4	SCIMS	TS4715	829.91	LCL3	SCIMS
PM47428	319.932	LCL3	SCIMS	TS4924-2	556.117	B2	SCIMS
PM47640	957.795	B3	SCIMS	TS5663	831.94	LCL3	SCIMS
PM61939	214.614	LCL3	SCIMS	TS5945	316.5	LCL3	SCIMS
PM71068	671.453	B2	SCIMS	TS5946	240.24	LCL3	SCIMS
PM76482	243.205	B2	SCIMS	TS6144	702.437	A1	SCIMS
PM127070	1738.394	LAL1	SCIMS	TS6734	1327.409	LCL3	SCIMS
PM147955	1402.947	B2	SCIMS	TS7049	887.228	LCL3	SCIMS
PM152621	364.468	LDL4	SCIMS	TS7371	412.097	LCL3	SCIMS
SS1450	777.264	LAL1	SCIMS	TS7372	336.328	LCL3	SCIMS
SS1454	734.035	LAL1	SCIMS	TS12038	185.515	LDL4	SCIMS
SS1486	1079.029	LAL1	SCIMS	PM27	94.146	3	SMES
SS1487	1072.825	LAL1	SCIMS	IS2	95.426	3	SMES
SS1488	1086.965	LAL1	SCIMS	TS7273	5.2	LCL3	SCIMS
SS1490	1009.569	LAL1	SCIMS	PM28485	9.446	LBL2	SCIMS

Table B.2: Published AHD71 heights of the 82 checkpoints within the Mid Hunter network.

Mid Hunter Checkpoints (Published Heights)							
Checkpoint	**AHD71**	**Class/Order**	**Source**	**Checkpoint**	**AHD71**	**Class/Order**	**Source**
GB191	208.611	LAL1	SCIMS	SS22113	105.473	LBL2	SCIMS
PM4942	142.229	LAL1	SCIMS	SS28327	122.845	LCL3	SCIMS
PM6283	603.736	LBL2	SCIMS	SS34105	230.886	B2	SCIMS
PM29397	152.632	LBL2	SCIMS	SS34453	84.602	LCL3	SCIMS
PM33633	375.354	LBL2	SCIMS	SS36069	178.169	LBL2	SCIMS
PM34425	65.127	LBL2	SCIMS	SS39247	770.319	C3	SCIMS
PM34595	189.165	LCL3	SCIMS	SS43232	22.804	B2	SCIMS
PM34603	218.849	LBL2	SCIMS	SS58021	246.641	C3	SCIMS
PM34708	145.559	LCL3	SCIMS	SS89854	745.716	C3	SCIMS
PM47357	200.13	LCL3	SCIMS	SS92149	331.465	D4	SCIMS
PM51512	130.46	LBL2	SCIMS	SS92194	175.521	LCL3	SCIMS
PM51556	112.952	LBL2	SCIMS	SS92196	163.764	LCL3	SCIMS
PM57688	293.666	B2	SCIMS	SS100985	177.572	C3	SCIMS
PM60640	172.834	LBL2	SCIMS	SS128900	107.201	C3	SCIMS
PM60675	279.079	LBL2	SCIMS	TS1098	874.62	C3	SCIMS
PM60690	237.974	LBL2	SCIMS	TS2672-1	983.488	C3	SCIMS
PM71976	421.368	C3	SCIMS	TS2672-2	983.493	C3	SCIMS

Checkpoint	AHD71	Class/Order	Source	Checkpoint	AHD71	Class/Order	Source
PM74988	496.924	C3	SCIMS	TS3297	232.398	LBL2	SCIMS
PM76194	214.375	B2	SCIMS	TS3357	206.33	LCL3	SCIMS
PM79329	269.061	C3	SCIMS	TS5182	146.48	LCL3	SCIMS
PM84025	396.26	B2	SCIMS	TS5318	163.13	LCL3	SCIMS
PM86013	699.623	C3	SCIMS	TS5324	639.663	C3	SCIMS
PM86015	407.561	C3	SCIMS	TS5472	254.58	B3	SCIMS
PM111379	1487.308	C3	SCIMS	TS5518	1259.718	C3	SCIMS
PM120010	320.381	C3	SCIMS	TS5901	1003.959	B2	SCIMS
PM120974	386.801	C3	SCIMS	TS5916	275.37	B2	SCIMS
PM127025	284.187	B2	SCIMS	TS5953	742.183	C3	SCIMS
PM147656	467.122	C3	SCIMS	TS6024	516.827	C3	SCIMS
PM147667	386.697	C3	SCIMS	TS6062	706.217	C3	SCIMS
PM148379	391.036	C3	SCIMS	TS6211	505.922	C3	SCIMS
PM151262	378.352	D4	SCIMS	TS6231	301.432	B2	SCIMS
SS416	260.179	LAL1	SCIMS	TS7097	442.57	LCL3	SCIMS
SS3235	161.554	LAL1	SCIMS	TS7189	413.406	LCL3	SCIMS
SS3239	250.497	LAL1	SCIMS	TS10341	119.771	LBL2	SCIMS
SS3562	280.965	LAL1	SCIMS	TS10464	427.95	C3	SCIMS
SS12261	201.393	LBL2	SCIMS	TS10688	271.739	C3	SCIMS
SS12263	392.717	LBL2	SCIMS	TS10700	163.359	LBL2	SCIMS

Checkpoint	AHD71	Class/Order	Source	Checkpoint	AHD71	Class/Order	Source
SS20752	39.46	LBL2	SCIMS	TS10730	147.374	LBL2	SCIMS
SS20761	104.118	LCL3	SCIMS	TS10802	272.371	B2	SCIMS
SS20789	148.632	LCL3	SCIMS	TS12106	48.367	A1	SCIMS
SS22093	114.452	LBL2	SCIMS	TS12107	270.099	A1	SCIMS

Table B.3: AUSPOS Solutions within the Snowy Mountains network.

Snowy Mountains AUSPOS Solutions								
Mark	**Session Length (hour)**	**Latitude DD.DDD°**	**Longitude DD.DDD°**	**Ellipsoid Height (m)**	**STD (m)**	**RMS (m)**	**Report No**	**Date**
PM28485	12.0	-37.0725231	149.9110826	21.605	±0.004	N/A	3901	13-May-11
PM124297	23.0	-35.4309183	148.5007283	596.236	±0.003	±0.006	101374	06-Jan-04
TS632*	11.3	-36.0610899	146.8179996	280.037	±0.003	N/A	4629	13-Sept-2013
TS7271	4.0	-37.1193984	149.8674573	144.889	±0.006	±0.006	350347	21-Jul-10
TS7371	13.2	-36.2428402	148.1458277	428.043	±0.002	N/A	0974	21-Nov-12
TS6144	22.3	-35.4941497	147.6120569	717.615	±0.004	N/A	4451	20-Dec-12
TS1511	18.3	-36.4381073	148.5862380	1279.658	±0.002	N/A	4224	18-Dec-12
TS6723	5.3	-36.2516544	149.0783637	1095.768	±0.004	N/A	1174	23-Nov-12
TS7273	4.5	-37.0742782	149.9079173	17.361	±0.004	±0.010	350346	21-Jul-21
TS2880	22.0	-35.8648183	147.0668475	680.505	±0.002	N/A	4695	24-Dec-12
TS6884	20.5	-35.8049841	147.7840548	903.840	±0.002	N/A	4931	20-Dec-12
TS6735	16.4	-36.1968247	149.4022999	1254.030	±0.002	N/A	5062	31-Dec-12
TS7370	19.9	-36.4185176	148.6398060	1072.884	±0.002	N/A	5188	02-Jan-13
TS1217	28.4	-35.9590287	147.0292874	325.261	±0.002	±0.005	318366	25-May-07
TS7054	45.5	-36.8057089	149.1584499	905.560	±0.003	±0.006	307118	20-Feb-06
TS6145	6.0	-35.3892311	147.7043420	481.996	±0.002	±0.008	317005	07-Mar-07
TS6831	4.5	-35.2273303	148.1256366	781.035	±0.007	±0.007	199500	05-Jun-09
TS4471	17.5	-35.2870337	148.1593244	721.453	±0.002	±0.004	198936	15-May-09
TS4924-2	5.7	-35.2213113	147.8351179	572.620	±0.008	±0.008	101355	05-Jan-04
TS6734	20.2	-36.1910608	148.8825437	1345.655	±0.002	N/A	5064	31-Dec-12
MM20003	3.5	-36.4174257	148.5827182	1061.377	±0.005	N/A	0875	20-Nov-12

Mark	Session Length (hour)	Latitude DD.DDD°	Longitude DD.DDD°	Ellipsoid Height (m)	STD (m)	RMS (m)	Report No	Date
SS23137	5.0	-35.5093483	148.1443208	853.118	±0.006	±0.007	199496	05-Jan-09
SS39929	5.3	-36.4313675	148.3290476	1858.481	±0.003	N/A	2890	06-Dec-12
PM127070	5.8	-36.3994580	148.4189750	1756.136	±0.003	N/A	0950	21-Nov-12
PM117168	3.4	-35.7682753	147.9981149	725.572	±0.005	N/A	6883	25-Jan-13
SS110734	6.4	-35.9995183	148.7541463	1091.810	±0.005	N/A	7065	29-Jan-13
SS31819	17.5	-35.3463439	147.8872210	739.378	±0.002	±0.004	199499	05-Jan-09
* AUSPOS solution recomputed on 13 Sept 2013 due to missing report and verify LPI database.								

Table B.4: AUSPOS Solutions within the Mid Hunter network.

Mid Hunter AUSPOS Solutions								
Mark	**Session Length (hour)**	**Latitude DD.DDD°**	**Longitude DD.DDD°**	**Ellipsoid Height (m)**	**STD (m)**	**RMS (m)**	**Report No**	**Date**
TS5182	21.4	-32.5214302	151.2955394	173.620	±0.002	N/A	6315	16-Jul-12
TS6026	20.9	-31.8595688	151.4087247	1361.322	±0.002	N/A	8006	31-Jul-12
TS6211	21.2	-32.1510250	149.9771779	533.563	±0.002	N/A	6369	16-Jul-12
TS7097	5.0	-32.7683806	151.0671128	468.991	±0.012	±0.012	338947	15-May-09
TS5318	21.5	-32.4130656	150.6734791	190.379	±0.003	±0.005	306453	12-Jan-06
TS3357	5.8	-32.2248019	150.8780048	234.255	±0.003	±0.006	101549	05-Feb-04
TS5953	23.2	-32.3656986	149.6816067	769.244	±0.002	N/A	5243	03-Jan-13

APPENDIX C

Snowy Mountains and Mid Hunter Ellipsoidal Heights Relative to GRS80 Ellipsoid, Derived From *GeoLab* Constrained LSA and Estimate Accuracy at 95% Confidence Level

LIST OF TABLES

Table C.1: Snowy Mountains ellipsoidal heights relative to GRS80 ellipsoid, derived from *GeoLab* constrained LSA output (SnowyM_C.pdf) showing estimate accuracy at 95% confidence level. C-129

Table C.2: Mid Hunter ellipsoidal heights relative to GRS80 ellipsoid, derived from *GeoLab* constrained LSA output (MidHunter_C.pdf) showing estimate accuracy at 95% confidence level. C-134

Table C.1: Snowy Mountains ellipsoidal heights relative to GRS80 ellipsoid, derived from *GeoLab* constrained LSA output (SnowyM_C.pdf) showing estimate accuracy at 95% confidence level.

Snowy Mountains derived Ellipsoidal Heights								
Checkpoint	**AHD71 Heights (m)**	**GDA94 Latitude (dd.dddd°)**	**GDA94 Longitude (dd.dddd°)**	**GRS80 Ellipsoidal Heights (m)**	**STD (m)**	**Variance (m)**	**STD 95% (x1.96) (m)**	**Variance 95% (x1.96) (m)**
MM10030	1323.649	-35.38537118	148.8050376	1342.862	0.024	0.0006	0.047	0.0011
MM10110	1121.921	-36.04543977	149.0147269	1140.480	0.021	0.0004	0.041	0.0009
MM10111	1122.648	-36.03925601	149.0041445	1141.238	0.021	0.0004	0.041	0.0009
MM10112	1014.206	-35.96722089	148.9836155	1033.046	0.018	0.0003	0.035	0.0006
MM10113	1028.394	-36.06739977	149.5386132	1046.203	0.016	0.0003	0.031	0.0005
MM10114	1020.378	-36.09245338	149.5104742	1038.158	0.016	0.0003	0.031	0.0005
MM10118	848.213	-37.1151317	148.2428507	861.746	0.032	0.0010	0.063	0.0020
MM10119	916.484	-37.08772765	148.2577156	930.181	0.032	0.0010	0.063	0.0020
MM10120	910.943	-37.09206461	148.2663448	924.596	0.032	0.0010	0.063	0.0020
MM10121	430.036	-36.34432041	147.8026118	444.725	0.017	0.0003	0.033	0.0006
MM10122	465.745	-36.40820597	147.833753	480.599	0.017	0.0003	0.033	0.0006
MM10123	946.699	-36.89586779	147.9114989	961.332	0.035	0.0012	0.069	0.0024
MM10124	875.936	-36.89656999	147.8794079	890.479	0.035	0.0012	0.069	0.0024
MM10126	705.130	-36.95331468	147.7728645	719.174	0.038	0.0014	0.074	0.0028
MM10129	906.113	-37.1004486	148.2522564	919.744	0.031	0.0010	0.061	0.0019
MM10130	1461.358	-36.87637459	147.9775897	1476.203	0.036	0.0013	0.071	0.0025
MM20000	1476.160	-36.05489917	148.5330848	1494.872	0.016	0.0003	0.031	0.0005
MM20001	1464.197	-36.06927475	148.5236535	1482.897	0.016	0.0003	0.031	0.0005
MM20002	448.293	-36.39938573	148.1832028	464.540	0.016	0.0003	0.031	0.0005
MM20003	1044.065	-36.41742548	148.5827186	1061.400	0.006	0.0000	0.012	0.0001
PM189	728.999	-35.99588583	149.1362854	747.414	0.017	0.0003	0.033	0.0006

Checkpoint	AHD71 Heights (m)	GDA94 Latitude (dd.dddd°)	GDA94 Longitude (dd.dddd°)	GRS80 Ellipsoidal Heights (m)	STD (m)	Variance (m)	STD 95% (x1.96) (m)	Variance 95% (x1.96) (m)
PM4539	453.255	-35.30457335	148.0260244	470.342	0.015	0.0002	0.029	0.0004
PM4540	334.882	-35.30727129	148.0613215	352.002	0.013	0.0002	0.025	0.0003
PM7663	743.166	-37.03496508	148.9932958	757.607	0.021	0.0004	0.041	0.0009
PM7664	773.396	-37.04798629	148.9257219	787.786	0.022	0.0005	0.043	0.0009
PM7665	792.354	-37.02800777	148.860262	806.856	0.022	0.0005	0.043	0.0009
PM10406	234.880	-35.99512684	146.9761842	247.145	0.012	0.0001	0.024	0.0003
PM11739	1080.058	-36.655385	148.492195	1096.127	0.021	0.0004	0.041	0.0009
PM29061	1024.922	-35.99307567	148.775899	1043.677	0.012	0.0001	0.024	0.0003
PM29063	1027.913	-35.99420258	148.7737596	1046.665	0.012	0.0001	0.024	0.0003
PM29355	267.184	-35.29708338	148.2225521	284.637	0.010	0.0001	0.020	0.0002
PM29368	277.548	-35.31049611	148.231386	295.050	0.011	0.0001	0.022	0.0002
PM31025	264.041	-35.27940502	148.2410163	281.559	0.009	0.0001	0.018	0.0002
PM32467	204.014	-36.01546193	147.0082113	216.361	0.012	0.0001	0.024	0.0003
PM39930	317.517	-35.31526367	148.222647	334.995	0.012	0.0001	0.024	0.0003
PM43850	795.038	-35.52183985	148.1602181	812.709	0.009	0.0001	0.018	0.0002
PM43895	948.811	-35.53251201	148.0998173	966.321	0.011	0.0001	0.022	0.0002
PM43903	634.925	-35.77370305	148.0106703	651.492	0.011	0.0001	0.022	0.0002
PM45176	341.501	-35.59912333	147.5092789	356.014	0.018	0.0003	0.035	0.0006
PM47428	319.932	-35.38798484	147.6651537	335.458	0.013	0.0002	0.025	0.0003
PM47640	957.795	-36.93064814	149.279366	972.595	0.017	0.0003	0.033	0.0006
PM61939	214.614	-35.99904042	146.9951777	226.942	0.010	0.0001	0.020	0.0002
PM71068	671.453	-35.42719896	148.7261838	690.659	0.019	0.0004	0.037	0.0007
PM76482	243.205	-35.14856381	148.2272864	260.955	0.013	0.0002	0.025	0.0003
PM127070	1738.394	-36.39945795	148.418975	1756.144	0.007	0.0000	0.014	0.0001
PM147955	1402.947	-35.45397237	148.7749109	1422.254	0.030	0.0009	0.059	0.0018

Checkpoint	AHD71 Heights (m)	GDA94 Latitude (dd.dddd°)	GDA94 Longitude (dd.dddd°)	GRS80 Ellipsoidal Heights (m)	STD (m)	Variance (m)	STD 95% (x1.96) (m)	Variance 95% (x1.96) (m)
PM152621	364.468	-35.41758889	147.6433414	379.838	0.012	0.0001	0.024	0.0003
SS1450	777.264	-35.92139864	149.1527397	795.896	0.021	0.0004	0.041	0.0009
SS1454	734.035	-35.98515845	149.1362602	752.483	0.017	0.0003	0.033	0.0006
SS1486	1079.029	-36.49777982	149.2798725	1095.935	0.015	0.0002	0.029	0.0004
SS1487	1072.825	-36.50838838	149.2856246	1089.710	0.014	0.0002	0.027	0.0004
SS1488	1086.965	-36.52320825	149.2792624	1103.780	0.013	0.0002	0.025	0.0003
SS1490	1009.569	-36.54985526	149.2797806	1026.269	0.014	0.0002	0.027	0.0004
SS2857	343.776	-35.41254281	147.646334	359.177	0.013	0.0002	0.025	0.0003
SS2918	296.122	-35.30533035	148.2004879	313.513	0.012	0.0001	0.024	0.0003
SS5356	277.676	-35.20987758	148.1691575	295.086	0.012	0.0001	0.024	0.0003
SS5660	771.074	-36.88085628	149.2485073	786.042	0.017	0.0003	0.033	0.0006
SS5674	802.875	-37.01754625	149.0623613	817.375	0.017	0.0003	0.033	0.0006
SS5675	748.100	-37.02131775	149.033329	762.594	0.018	0.0003	0.035	0.0006
SS5687	724.518	-36.90345653	149.2464752	739.368	0.019	0.0004	0.037	0.0007
SS5694	811.311	-36.84220434	149.3759846	826.314	0.019	0.0004	0.037	0.0007
SS8394	200.441	-35.92866389	147.4576533	214.219	0.015	0.0002	0.029	0.0004
SS8396	203.413	-35.94669472	147.5051966	217.320	0.014	0.0002	0.027	0.0004
SS8414	246.893	-35.96182004	147.7971265	261.715	0.017	0.0003	0.033	0.0006
SS8415	241.348	-35.97455051	147.8224193	256.196	0.015	0.0002	0.029	0.0004
SS8425	321.384	-35.9903941	147.9864975	336.869	0.013	0.0002	0.025	0.0003
SS8427	464.585	-35.97891751	148.0226726	480.303	0.014	0.0002	0.027	0.0004
SS8428	427.188	-35.97582559	148.0355199	442.970	0.016	0.0003	0.031	0.0005
SS10113	994.279	-36.48476286	148.563481	1011.379	0.008	0.0001	0.016	0.0001
SS10114	1006.825	-36.4931282	148.5516047	1023.861	0.014	0.0002	0.027	0.0004
SS10123	1049.382	-36.63543277	148.4992305	1065.596	0.020	0.0004	0.039	0.0008

Checkpoint	AHD71 Heights (m)	GDA94 Latitude (dd.dddd°)	GDA94 Longitude (dd.dddd°)	GRS80 Ellipsoidal Heights (m)	STD (m)	Variance (m)	STD 95% (x1.96) (m)	Variance 95% (x1.96) (m)
SS10250	950.608	-36.22966217	149.4525896	968.008	0.012	0.0001	0.024	0.0003
SS23134	757.992	-35.54218133	148.1672697	775.683	0.007	0.0000	0.014	0.0001
SS23137	835.478	-35.50934817	148.1443207	853.109	0.007	0.0000	0.014	0.0001
SS30254	368.104	-35.30511744	148.0705447	385.273	0.012	0.0001	0.024	0.0003
SS34707	1104.265	-36.4426122	148.5014869	1121.774	0.011	0.0001	0.022	0.0002
SS34712	1120.230	-36.4512857	148.4934181	1137.681	0.006	0.0000	0.012	0.0001
SS34771	1027.961	-36.43203098	148.5521511	1045.450	0.006	0.0000	0.012	0.0001
SS36078	306.334	-35.31863914	148.220973	323.798	0.010	0.0001	0.020	0.0002
SS39974	1093.090	-35.99647346	148.7383901	1111.854	0.009	0.0001	0.018	0.0002
SS39976	1028.577	-35.99320756	148.7731998	1047.334	0.012	0.0001	0.024	0.0003
SS39982	1157.113	-36.05929789	148.8540928	1175.764	0.012	0.0001	0.024	0.0003
SS39984	1160.270	-36.08243771	148.8685179	1178.857	0.011	0.0001	0.022	0.0002
TS56	312.300	-36.22049044	148.1242781	328.057	0.011	0.0001	0.022	0.0002
TS563	1717.620	-36.02133495	148.3912086	1736.114	0.017	0.0003	0.033	0.0006
TS1511	1262.392	-36.43810711	148.5862383	1279.654	0.006	0.0000	0.012	0.0001
TS2761-4	2228.266	-36.45583059	148.2634808	2245.446	0.010	0.0001	0.020	0.0002
TS4470	1219.474	-35.23944035	148.5004121	1238.301	0.017	0.0003	0.033	0.0006
TS4471	704.020	-35.28703363	148.1593239	721.450	0.006	0.0000	0.012	0.0001
TS4715	829.910	-35.36028056	148.2165032	847.428	0.007	0.0000	0.014	0.0001
TS4924-2	556.117	-35.22131148	147.8351176	572.621	0.008	0.0001	0.016	0.0001
TS5663	831.940	-35.77764829	149.1655997	850.942	0.029	0.0008	0.057	0.0016
TS5945	316.500	-37.01097193	149.8894403	329.177	0.012	0.0001	0.024	0.0003
TS5946	240.240	-36.91759419	149.8336734	253.507	0.015	0.0002	0.029	0.0004
TS6144	702.437	-35.49414996	147.6120565	717.621	0.008	0.0001	0.016	0.0001
TS6734	1327.409	-36.19106088	148.8825439	1345.661	0.009	0.0001	0.018	0.0002

Checkpoint	AHD71 Heights (m)	GDA94 Latitude (dd.dddd°)	GDA94 Longitude (dd.dddd°)	GRS80 Ellipsoidal Heights (m)	STD (m)	Variance (m)	STD 95% (x1.96) (m)	Variance 95% (x1.96) (m)
TS7049	887.228	-36.96996907	149.0890346	901.923	0.017	0.0003	0.033	0.0006
TS7371	412.097	-36.24283986	148.1458281	428.023	0.009	0.0001	0.018	0.0002
TS7372	336.328	-36.21487169	148.119129	352.060	0.009	0.0001	0.018	0.0002
TS12038	185.515	-36.07754337	146.9155537	197.629	0.011	0.0001	0.022	0.0002
PM27	94.146	-37.56638073	149.1510253	104.694	0.042	0.0018	0.082	0.0035
IS2	95.426	-37.55152353	149.1544199	106.046	0.041	0.0017	0.080	0.0033
TS7273	5.200	-37.07427852	149.9079177	17.355	0.008	0.0001	0.016	0.0001
PM28485	9.446	-37.07252346	149.9110832	21.628	0.008	0.0001	0.016	0.0001
					Mean STD	**Mean Variance**	**Mean STD 95% (x1.96)**	**Mean Variance 95% (x1.96)**
					0.016	**0.0003**	**0.031**	**0.0006**

Table C.2: Mid Hunter ellipsoidal heights relative to GRS80 ellipsoid, derived from *GeoLab* constrained LSA output (MidHunter_C.pdf) showing estimate accuracy at 95% confidence level.

Mid Hunter derived Ellipsoidal Heights with estimate accuracy								
Checkpoint	**AHD71 Heights (m)**	**GDA94 Latitude (dd.dddd°)**	**GDA94 Longitude (dd.dddd°)**	**GRS80 Ellipsoidal Heights (m)**	**STD (m)**	**Variance (m)**	**STD 95% (x1.96) (m)**	**Variance 95% (x1.96) (m)**
GB191	208.611	-32.9223831	150.7218833	235.042	0.016	0.00026	0.0314	0.00050
PM4942	142.229	-32.2824954	150.6486997	169.727	0.009	0.00008	0.0176	0.00016
PM6283	603.736	-32.8077888	149.9759027	630.670	0.019	0.00036	0.0372	0.00071
PM29397	152.632	-32.2918173	150.8691566	180.341	0.009	0.00008	0.0176	0.00016
PM33633	375.354	-32.1111412	150.1228153	403.258	0.011	0.00012	0.0216	0.00024
PM34425	65.127	-32.5105838	151.3737273	92.427	0.011	0.00012	0.0216	0.00024
PM34595	189.165	-32.1729814	150.8878833	217.350	0.009	0.00008	0.0176	0.00016
PM34603	218.849	-32.1673199	150.8967184	247.074	0.009	0.00008	0.0176	0.00016
PM34708	145.559	-32.2605399	150.8842190	173.373	0.008	0.00006	0.0157	0.00013
PM47357	200.13	-32.1148962	150.8719264	228.553	0.009	0.00008	0.0176	0.00016
PM51512	130.46	-32.3441716	150.5773536	157.818	0.009	0.00008	0.0176	0.00016
PM51556	112.952	-32.3703798	150.6910340	140.324	0.008	0.00006	0.0157	0.00013
PM57688	293.666	-31.9545767	151.7192207	323.902	0.016	0.00026	0.0314	0.00050
PM60640	172.834	-32.4045102	150.3500530	199.957	0.010	0.00010	0.0196	0.00020
PM60675	279.079	-32.4266665	150.1334734	306.202	0.010	0.00010	0.0196	0.00020
PM60690	237.974	-32.3542567	150.0972957	265.178	0.011	0.00012	0.0216	0.00024
PM71976	421.368	-31.9210968	151.2361036	451.943	0.011	0.00012	0.0216	0.00024
PM74988	496.924	-32.5151298	149.9838649	524.155	0.014	0.00020	0.0274	0.00038
PM76194	214.375	-32.0578808	150.8800017	243.052	0.010	0.00010	0.0196	0.00020

Checkpoint	AHD71 Heights (m)	GDA94 Latitude (dd.dddd°)	GDA94 Longitude (dd.dddd°)	GRS80 Ellipsoidal Heights (m)	STD (m)	Variance (m)	STD 95% (x1.96) (m)	Variance 95% (x1.96) (m)
PM79329	269.061	-32.4271295	150.0942347	296.249	0.010	0.00010	0.0196	0.00020
PM84025	396.26	-31.9794636	151.6376320	426.677	0.014	0.00020	0.0274	0.00038
PM86013	699.623	-32.7089559	150.0349688	726.770	0.015	0.00023	0.0294	0.00044
PM86015	407.561	-32.3738880	149.9875882	434.803	0.011	0.00012	0.0216	0.00024
PM111379	1487.308	-31.9825817	151.4588956	1518.450	0.012	0.00014	0.0235	0.00028
PM120010	320.381	-32.2290936	151.5176648	349.349	0.013	0.00017	0.0255	0.00033
PM120974	386.801	-32.1688292	149.9355701	414.331	0.012	0.00014	0.0235	0.00028
PM127025	284.187	-32.0617393	151.7281832	313.969	0.017	0.00029	0.0333	0.00057
PM147656	467.122	-32.4062420	149.8715343	494.326	0.013	0.00017	0.0255	0.00033
PM147667	386.697	-32.4066560	149.9593506	413.926	0.011	0.00012	0.0216	0.00024
PM148379	391.036	-32.5922999	150.0881139	418.301	0.013	0.00017	0.0255	0.00033
PM151262	378.352	-32.0371515	150.5226710	406.906	0.013	0.00017	0.0255	0.00033
SS416	260.179	-32.8999698	150.7572842	286.603	0.016	0.00026	0.0314	0.00050
SS3235	161.554	-32.4104422	150.3803209	188.697	0.010	0.00010	0.0196	0.00020
SS3239	250.497	-32.4019587	150.2202034	277.646	0.010	0.00010	0.0196	0.00020
SS3562	280.965	-32.3599754	150.0164563	308.163	0.011	0.00012	0.0216	0.00024
SS12261	201.393	-32.2475966	150.4854775	229.027	0.010	0.00010	0.0196	0.00020
SS12263	392.717	-32.1591561	150.3959906	420.717	0.011	0.00012	0.0216	0.00024
SS20752	39.46	-32.5473893	151.3064160	66.537	0.010	0.00010	0.0196	0.00020
SS20761	104.118	-32.4389109	150.6742563	131.293	0.008	0.00006	0.0157	0.00013
SS20789	148.632	-32.3877442	150.5225258	175.895	0.009	0.00008	0.0176	0.00016
SS22093	114.452	-32.8915039	151.1081239	140.616	0.017	0.00029	0.0333	0.00057
SS22113	105.473	-32.7930996	151.0765639	131.886	0.012	0.00014	0.0235	0.00028
SS28327	122.845	-32.4949150	151.1105543	150.006	0.011	0.00012	0.0216	0.00024
SS34105	230.886	-31.9952017	150.8640682	259.843	0.011	0.00012	0.0216	0.00024

Checkpoint	AHD71 Heights (m)	GDA94 Latitude (dd.dddd°)	GDA94 Longitude (dd.dddd°)	GRS80 Ellipsoidal Heights (m)	STD (m)	Variance (m)	STD 95% (x1.96) (m)	Variance 95% (x1.96) (m)
SS34453	84.602	-32.4556263	150.8539451	111.804	0.010	0.00010	0.0196	0.00020
SS36069	178.169	-32.2818605	150.9405160	206.004	0.009	0.00008	0.0176	0.00016
SS39247	770.319	-32.7630984	150.1862207	797.511	0.016	0.00026	0.0314	0.00050
SS43232	22.804	-32.5665436	151.5953652	50.010	0.014	0.00020	0.0274	0.00038
SS58021	246.641	-32.1973496	151.5493727	275.813	0.014	0.00020	0.0274	0.00038
SS89854	745.716	-32.6389448	150.0331914	772.976	0.014	0.00020	0.0274	0.00038
SS92149	331.465	-32.0702307	150.5113171	359.875	0.013	0.00017	0.0255	0.00033
SS92194	175.521	-32.3108050	150.8844348	203.176	0.009	0.00008	0.0176	0.00016
SS92196	163.764	-32.3035415	150.8804299	191.446	0.009	0.00008	0.0176	0.00016
SS100985	177.572	-32.3557813	151.4711096	205.729	0.012	0.00014	0.0235	0.00028
SS128900	107.201	-32.9853977	151.1289787	133.160	0.021	0.00044	0.0412	0.00086
TS1098	874.62	-32.5330776	149.8765734	901.805	0.018	0.00032	0.0353	0.00064
TS2672-1	983.488	-32.6909723	150.0175711	1010.612	0.017	0.00029	0.0333	0.00057
TS2672-2	983.493	-32.6909819	150.0175082	1010.734	0.016	0.00026	0.0314	0.00050
TS3297	232.398	-32.2733518	150.9063447	260.210	0.008	0.00006	0.0157	0.00013
TS3357	206.33	-32.2248016	150.8780055	234.248	0.008	0.00006	0.0157	0.00013
TS5182	146.48	-32.5214299	151.2955397	173.622	0.009	0.00008	0.0176	0.00016
TS5318	163.13	-32.4130656	150.6734796	190.353	0.008	0.00006	0.0157	0.00013
TS5324	639.663	-32.0646572	150.7628533	668.108	0.010	0.00010	0.0196	0.00020
TS5472	254.58	-32.4461749	150.806416	281.788	0.010	0.00010	0.0196	0.00020
TS5518	1259.718	-32.8259978	150.350891	1286.741	0.021	0.00044	0.0412	0.00086
TS5901	1003.959	-32.1067626	151.7665449	1033.433	0.017	0.00029	0.0333	0.00057
TS5916	275.37	-32.306825	151.6907390	303.799	0.017	0.00029	0.0333	0.00057
TS5953	742.183	-32.3656986	149.6816066	769.255	0.011	0.00012	0.0216	0.00024
TS6024	516.827	-32.2184055	151.5351932	545.856	0.014	0.00020	0.0274	0.00038

Checkpoint	AHD71 Heights (m)	GDA94 Latitude (dd.dddd°)	GDA94 Longitude (dd.dddd°)	GRS80 Ellipsoidal Heights (m)	STD (m)	Variance (m)	STD 95% (x1.96) (m)	Variance 95% (x1.96) (m)
TS6062	706.217	-32.4921392	149.6364786	733.135	0.017	0.00029	0.0333	0.00057
TS6211	505.922	-32.1510250	149.9771775	533.569	0.010	0.00010	0.0196	0.00020
TS6231	301.432	-32.6270527	151.4732331	328.444	0.016	0.00026	0.0314	0.00050
TS7097	442.57	-32.7683800	151.0671133	468.998	0.011	0.00012	0.0216	0.00024
TS7189	413.406	-32.9898904	150.6913796	439.718	0.016	0.00026	0.0314	0.00050
TS10341	119.771	-32.4495066	151.1267957	147.060	0.011	0.00012	0.0216	0.00024
TS10464	427.95	-32.1043290	150.9066093	456.571	0.010	0.00010	0.0196	0.00020
TS10688	271.739	-32.3361686	150.0307587	298.970	0.010	0.00010	0.0196	0.00020
TS10700	163.359	-32.4061355	150.6454533	190.613	0.009	0.00008	0.0176	0.00016
TS10730	147.374	-32.4629270	150.9868156	174.550	0.011	0.00012	0.0216	0.00024
TS10802	272.371	-32.2081543	150.9057229	300.457	0.009	0.00008	0.0176	0.00016
TS12106	48.367	-32.5582399	151.1757474	75.233	0.012	0.00014	0.0235	0.00028
TS12107	270.099	-32.9530468	150.6595151	296.502	0.015	0.00023	0.0294	0.00044

Mean STD	Mean Variance	Mean STD 95% (x1.96)	Mean Variance 95% (x1.96)
0.012	**0.00016**	**0.024**	**0.00031**

APPENDIX D

N Values Derived From AHD71, AUSGeoid09 and AUSGeoid98 and Subsequent Absolute Verification Residuals

LIST OF TABLES

Table D.1: Snowy Mountains AHD71-derived N values and AUSGeoid09-derived N values with bi-linear, bi-quadratic, bi-cubic and bi-quartic interpolation for the 104 checkpoints and subsequent absolute verification residuals D-140
Table D.2: Snowy Mountains AHD71-derived N values and AUSGeoid98-derived N values with bi-linear, bi-quadratic, bi-cubic and bi-quartic interpolation for the 104 checkpoints and subsequent absolute verification residuals. D-145
Table D.3: Mid Hunter AHD71-derived N values and AUSGeoid09-derived N values with bi-linear, bi-quadratic, bi-cubic and bi-quartic interpolation for the 82 checkpoints and subsequent absolute verification residuals. D-150
Table D.4: Mid Hunter AHD71-derived N values and AUSGeoid98-derived N values with bi-linear, bi-quadratic, bi-cubic and bi-quartic interpolation for the 82 checkpoints and subsequent absolute verification residuals. D-154

Table D.1: Snowy Mountains AHD71-derived N values and AUSGeoid09-derived N values with bi-linear, bi-quadratic, bi-cubic and bi-quartic interpolation for the 104 checkpoints and subsequent absolute verification residuals

Snowy Mountains derived N values and absolute residuals using AUSGeoid09									
Checkpoint	**N_{AHD} (m)**	**AUSGeoid09**							
		N Values Bi-Linear (m)	**N Values Bi-quadratic (m)**	**N Values Bi-Cubic (m)**	**N values Bi-Quartic (m)**	**Residuals Bi-Linear (m)**	**Residuals Bi-Quadratic (m)**	**Residuals Bi-Cubic (m)**	**Residuals Bi-Quartic (m)**
MM10030	19.213	19.222	19.225	19.225	19.225	-0.009	-0.012	-0.012	-0.012
MM10110	18.558	18.475	18.476	18.476	18.476	0.083	0.082	0.082	0.082
MM10111	18.590	18.508	18.511	18.510	18.511	0.082	0.079	0.080	0.079
MM10112	18.840	18.748	18.748	18.748	18.748	0.092	0.092	0.092	0.092
MM10113	17.809	17.778	17.779	17.779	17.779	0.031	0.030	0.030	0.030
MM10114	17.780	17.733	17.732	17.733	17.732	0.047	0.048	0.047	0.048
MM10118	13.533	13.354	13.354	13.354	13.354	0.179	0.179	0.179	0.179
MM10119	13.697	13.498	13.499	13.498	13.498	0.199	0.198	0.199	0.199
MM10120	13.653	13.443	13.444	13.444	13.444	0.210	0.209	0.209	0.209
MM10121	14.689	14.570	14.569	14.569	14.569	0.119	0.120	0.120	0.120
MM10122	14.854	14.731	14.731	14.731	14.731	0.123	0.123	0.123	0.123
MM10123	14.633	14.627	14.627	14.626	14.626	0.006	0.006	0.007	0.007
MM10124	14.543	14.529	14.528	14.528	14.528	0.014	0.015	0.015	0.015
MM10126	14.044	14.035	14.034	14.034	14.034	0.009	0.010	0.010	0.010
MM10129	13.631	13.428	13.428	13.428	13.428	0.203	0.203	0.203	0.203
MM10130	14.845	14.894	14.895	14.896	14.896	-0.049	-0.050	-0.051	-0.051
MM20000	18.712	18.723	18.723	18.723	18.723	-0.011	-0.011	-0.011	-0.011
MM20001	18.700	18.696	18.697	18.697	18.697	0.004	0.003	0.003	0.003
MM20002	16.247	16.113	16.112	16.112	16.112	0.134	0.135	0.135	0.135
MM20003	17.335	17.291	17.291	17.291	17.291	0.044	0.044	0.044	0.044

Checkpoint	N_{AHD} (m)	N Values Bi-Linear (m)	N Values Bi-quadratic (m)	N Values Bi-Cubic (m)	N values Bi-Quartic (m)	Residuals Bi-Linear (m)	Residuals Bi-Quadratic (m)	Residuals Bi-Cubic (m)	Residuals Bi-Quartic (m)
PM189	18.415	18.324	18.323	18.324	18.323	0.091	0.092	0.091	0.092
PM4539	17.087	17.049	17.050	17.050	17.050	0.038	0.037	0.037	0.037
PM4540	17.120	17.152	17.151	17.151	17.151	-0.032	-0.031	-0.031	-0.031
PM7663	14.441	14.327	14.327	14.327	14.327	0.114	0.114	0.114	0.114
PM7664	14.390	14.306	14.305	14.306	14.305	0.084	0.085	0.084	0.085
PM7665	14.502	14.402	14.402	14.401	14.402	0.100	0.100	0.101	0.100
PM10406	12.265	12.291	12.291	12.290	12.290	-0.026	-0.026	-0.025	-0.025
PM11739	16.069	15.993	15.995	15.996	15.996	0.076	0.074	0.073	0.073
PM29061	18.755	18.656	18.655	18.655	18.655	0.099	0.100	0.100	0.100
PM29063	18.752	18.656	18.655	18.655	18.655	0.096	0.097	0.097	0.097
PM29355	17.453	17.502	17.501	17.501	17.501	-0.050	-0.049	-0.049	-0.049
PM29368	17.502	17.522	17.521	17.521	17.521	-0.020	-0.019	-0.019	-0.019
PM31025	17.518	17.579	17.577	17.577	17.577	-0.061	-0.059	-0.059	-0.059
PM32467	12.347	12.330	12.329	12.329	12.329	0.017	0.018	0.018	0.018
PM39930	17.478	17.499	17.499	17.498	17.499	-0.021	-0.021	-0.020	-0.021
PM43850	17.671	17.542	17.541	17.542	17.541	0.129	0.130	0.129	0.130
PM43895	17.510	17.412	17.412	17.412	17.412	0.098	0.098	0.098	0.098
PM43903	16.567	16.448	16.448	16.447	16.447	0.119	0.119	0.120	0.120
PM45176	14.513	14.495	14.496	14.495	14.495	0.018	0.017	0.018	0.018
PM47428	15.526	15.437	15.437	15.437	15.437	0.089	0.089	0.089	0.089
PM47640	14.800	14.590	14.592	14.591	14.592	0.210	0.208	0.209	0.208
PM61939	12.328	12.322	12.321	12.322	12.322	0.006	0.007	0.006	0.006
PM71068	19.206	19.193	19.189	19.189	19.189	0.013	0.017	0.017	0.017
PM76482	17.750	17.774	17.772	17.773	17.772	-0.024	-0.022	-0.023	-0.022

Checkpoint	N_{AHD} (m)	N Values Bi-Linear (m)	N Values Bi-quadratic (m)	N Values Bi-Cubic (m)	N values Bi-Quartic (m)	Residuals Bi-Linear (m)	Residuals Bi-Quadratic (m)	Residuals Bi-Cubic (m)	Residuals Bi-Quartic (m)
PM127070	17.750	17.749	17.750	17.750	17.750	0.001	0.000	0.000	0.000
PM147955	19.307	19.284	19.287	19.287	19.288	0.023	0.020	0.020	0.019
PM152621	15.370	15.298	15.298	15.298	15.298	0.072	0.072	0.072	0.072
SS1450	18.632	18.533	18.533	18.533	18.533	0.099	0.099	0.099	0.099
SS1454	18.448	18.358	18.357	18.357	18.357	0.090	0.091	0.091	0.091
SS1486	16.906	16.791	16.792	16.792	16.792	0.115	0.114	0.114	0.114
SS1487	16.884	16.748	16.750	16.750	16.750	0.136	0.134	0.134	0.134
SS1488	16.815	16.690	16.691	16.691	16.691	0.125	0.124	0.124	0.124
SS1490	16.700	16.565	16.566	16.565	16.565	0.135	0.134	0.135	0.135
SS2857	15.401	15.317	15.317	15.317	15.317	0.084	0.084	0.084	0.084
SS2918	17.391	17.439	17.438	17.438	17.438	-0.048	-0.047	-0.047	-0.047
SS5356	17.410	17.442	17.441	17.441	17.441	-0.032	-0.031	-0.031	-0.031
SS5660	14.968	14.833	14.833	14.833	14.833	0.135	0.135	0.135	0.135
SS5674	14.500	14.372	14.372	14.372	14.372	0.128	0.128	0.128	0.128
SS5675	14.494	14.367	14.367	14.367	14.367	0.127	0.127	0.127	0.127
SS5687	14.850	14.732	14.731	14.732	14.731	0.118	0.119	0.118	0.119
SS5694	15.003	14.847	14.846	14.846	14.845	0.156	0.157	0.157	0.158
SS8394	13.778	13.749	13.748	13.746	13.747	0.029	0.030	0.032	0.031
SS8396	13.907	13.871	13.870	13.870	13.870	0.036	0.037	0.037	0.037
SS8414	14.822	14.747	14.744	14.745	14.744	0.075	0.078	0.077	0.078
SS8415	14.848	14.791	14.786	14.788	14.786	0.056	0.061	0.059	0.061
SS8425	15.485	15.379	15.378	15.378	15.378	0.106	0.107	0.107	0.107
SS8427	15.718	15.584	15.584	15.584	15.584	0.134	0.134	0.134	0.134
SS8428	15.782	15.652	15.653	15.652	15.652	0.130	0.129	0.130	0.130

Checkpoint	N_{AHD} (m)	N Values Bi-Linear (m)	N Values Bi-quadratic (m)	N Values Bi-Cubic (m)	N values Bi-Quartic (m)	Residuals Bi-Linear (m)	Residuals Bi-Quadratic (m)	Residuals Bi-Cubic (m)	Residuals Bi-Quartic (m)
SS10113	17.100	17.006	17.005	17.005	17.005	0.094	0.095	0.095	0.095
SS10114	17.036	16.980	16.979	16.979	16.979	0.056	0.057	0.057	0.057
SS10123	16.213	16.151	16.151	16.151	16.151	0.062	0.062	0.062	0.062
SS10250	17.400	17.299	17.298	17.298	17.298	0.101	0.102	0.102	0.102
SS23134	17.691	17.584	17.583	17.583	17.583	0.107	0.108	0.108	0.108
SS23137	17.631	17.508	17.510	17.510	17.510	0.123	0.121	0.121	0.121
SS30254	17.169	17.180	17.180	17.181	17.180	-0.011	-0.011	-0.012	-0.011
SS34707	17.509	17.341	17.339	17.340	17.339	0.168	0.170	0.169	0.170
SS34712	17.451	17.306	17.307	17.306	17.306	0.145	0.144	0.145	0.145
SS34771	17.489	17.295	17.294	17.294	17.294	0.194	0.195	0.195	0.195
SS36078	17.464	17.496	17.495	17.495	17.495	-0.032	-0.031	-0.031	-0.031
SS39974	18.764	18.683	18.682	18.682	18.682	0.081	0.082	0.082	0.082
SS39976	18.757	18.658	18.657	18.657	18.657	0.099	0.100	0.100	0.100
SS39982	18.651	18.530	18.530	18.531	18.531	0.121	0.121	0.120	0.120
SS39984	18.587	18.483	18.483	18.483	18.483	0.104	0.104	0.104	0.104
TS56	15.757	15.702	15.698	15.698	15.698	0.055	0.059	0.059	0.059
TS563	18.494	18.378	18.381	18.382	18.382	0.116	0.113	0.112	0.112
TS1511	17.261	17.198	17.199	17.199	17.200	0.063	0.062	0.062	0.061
TS2761-4	17.180	17.134	17.140	17.140	17.140	0.046	0.040	0.040	0.040
TS4470	18.827	18.841	18.842	18.843	18.843	-0.014	-0.015	-0.016	-0.016
TS4471	17.430	17.367	17.369	17.368	17.369	0.063	0.061	0.062	0.061
TS4715	17.518	17.525	17.528	17.527	17.528	-0.007	-0.010	-0.009	-0.010
TS4924-2	16.504	16.504	16.505	16.505	16.505	0.000	-0.001	-0.001	-0.001
TS5663	19.002	18.889	18.889	18.889	18.889	0.113	0.113	0.113	0.113

Checkpoint	N_{AHD} (m)	N Values Bi-Linear (m)	N Values Bi-quadratic (m)	N Values Bi-Cubic (m)	N values Bi-Quartic (m)	Residuals Bi-Linear (m)	Residuals Bi-Quadratic (m)	Residuals Bi-Cubic (m)	Residuals Bi-Quartic (m)
TS5945	12.677	12.390	12.392	12.393	12.393	0.287	0.285	0.284	0.284
TS5946	13.267	12.987	12.987	12.987	12.987	0.279	0.279	0.279	0.279
TS6144	15.184	15.095	15.097	15.097	15.098	0.089	0.087	0.087	0.086
TS6734	18.252	18.148	18.149	18.149	18.149	0.104	0.103	0.103	0.103
TS7049	14.695	14.554	14.555	14.555	14.555	0.141	0.140	0.140	0.140
TS7371	15.926	15.868	15.865	15.865	15.865	0.058	0.061	0.061	0.061
TS7372	15.732	15.666	15.664	15.664	15.664	0.066	0.068	0.068	0.068
TS12038	12.114	12.064	12.064	12.064	12.064	0.050	0.050	0.050	0.050
PM27	10.548	10.519	10.519	10.519	10.519	0.029	0.029	0.029	0.029
IS2	10.620	10.619	10.618	10.618	10.619	0.001	0.002	0.002	0.001
TS7273	12.155	12.040	12.040	12.039	12.039	0.115	0.115	0.116	0.116
PM28485	12.182	12.031	12.031	12.031	12.031	0.151	0.151	0.151	0.151

Table D.2: Snowy Mountains AHD71-derived N values and AUSGeoid98-derived N values with bi-linear, bi-quadratic, bi-cubic and bi-quartic interpolation for the 104 checkpoints and subsequent absolute verification residuals.

Snowy Mountains derived N values and absolute residuals using AUSGeoid98									
Checkpoint	**N_{AHD} (m)**	**AUSGeoid98**							
		N Values Bi-Linear (m)	**N Values Bi-quadratic (m)**	**N Values Bi-Cubic (m)**	**N values Bi-Quartic (m)**	**Residuals Bi-Linear (m)**	**Residuals Bi-Quadratic (m)**	**Residuals Bi-Cubic (m)**	**Residuals Bi-Quartic (m)**
MM10030	19.213	19.330	19.337	19.335	19.337	-0.117	-0.124	-0.122	-0.124
MM10110	18.558	18.589	18.591	18.591	18.591	-0.031	-0.033	-0.033	-0.033
MM10111	18.590	18.622	18.623	18.623	18.623	-0.032	-0.033	-0.033	-0.033
MM10112	18.840	18.891	18.892	18.894	18.893	-0.051	-0.052	-0.054	-0.053
MM10113	17.809	17.883	17.886	17.885	17.886	-0.074	-0.077	-0.076	-0.077
MM10114	17.780	17.838	17.838	17.839	17.838	-0.058	-0.058	-0.059	-0.058
MM10118	13.533	13.409	13.409	13.409	13.409	0.124	0.124	0.124	0.124
MM10119	13.697	13.559	13.558	13.557	13.558	0.138	0.139	0.140	0.139
MM10120	13.653	13.512	13.509	13.508	13.508	0.141	0.144	0.145	0.145
MM10121	14.689	14.665	14.666	14.666	14.666	0.024	0.023	0.023	0.023
MM10122	14.854	14.822	14.822	14.822	14.823	0.032	0.032	0.032	0.031
MM10123	14.633	14.642	14.637	14.637	14.638	-0.009	-0.004	-0.004	-0.005
MM10124	14.543	14.539	14.535	14.536	14.536	0.004	0.008	0.007	0.007
MM10126	14.044	14.050	14.044	14.044	14.044	-0.006	0.000	0.000	0.000
MM10129	13.631	13.484	13.486	13.485	13.485	0.147	0.145	0.146	0.146
MM10130	14.845	14.880	14.884	14.882	14.883	-0.035	-0.039	-0.037	-0.038
MM20000	18.712	18.729	18.727	18.726	18.727	-0.017	-0.015	-0.014	-0.015
MM20001	18.700	18.696	18.700	18.699	18.700	0.004	0.000	0.001	0.000
MM20002	16.247	16.138	16.163	16.163	16.163	0.109	0.084	0.084	0.084
MM20003	17.335	17.385	17.383	17.382	17.382	-0.050	-0.048	-0.047	-0.047

Checkpoint	N_{AHD} (m)	N Values Bi-Linear (m)	N Values Bi-quadratic (m)	N Values Bi-Cubic (m)	N values Bi-Quartic (m)	Residuals Bi-Linear (m)	Residuals Bi-Quadratic (m)	Residuals Bi-Cubic (m)	Residuals Bi-Quartic (m)
PM189	18.415	18.539	18.539	18.539	18.539	-0.124	-0.124	-0.124	-0.124
PM4539	17.087	17.017	17.022	17.022	17.024	0.070	0.065	0.065	0.063
PM4540	17.120	17.115	17.125	17.124	17.127	0.005	-0.005	-0.004	-0.007
PM7663	14.441	14.439	14.439	14.439	14.439	0.002	0.002	0.002	0.002
PM7664	14.390	14.416	14.417	14.416	14.417	-0.026	-0.027	-0.026	-0.027
PM7665	14.502	14.530	14.519	14.519	14.519	-0.028	-0.017	-0.017	-0.017
PM10406	12.265	12.426	12.430	12.430	12.430	-0.161	-0.165	-0.165	-0.165
PM11739	16.069	16.027	16.021	16.019	16.020	0.042	0.048	0.050	0.049
PM29061	18.755	18.768	18.784	18.783	18.784	-0.013	-0.029	-0.028	-0.029
PM29063	18.752	18.766	18.783	18.782	18.783	-0.014	-0.031	-0.030	-0.031
PM29355	17.453	17.466	17.508	17.506	17.507	-0.014	-0.056	-0.054	-0.055
PM29368	17.502	17.522	17.536	17.535	17.538	-0.020	-0.034	-0.033	-0.036
PM31025	17.518	17.590	17.601	17.597	17.599	-0.072	-0.083	-0.079	-0.081
PM32467	12.347	12.500	12.501	12.501	12.501	-0.153	-0.154	-0.154	-0.154
PM39930	17.478	17.488	17.509	17.508	17.512	-0.010	-0.031	-0.030	-0.034
PM43850	17.671	17.482	17.486	17.486	17.486	0.189	0.185	0.185	0.185
PM43895	17.510	17.332	17.331	17.331	17.331	0.178	0.179	0.179	0.179
PM43903	16.567	16.340	16.345	16.343	16.346	0.227	0.222	0.224	0.221
PM45176	14.513	14.493	14.493	14.493	14.493	0.020	0.020	0.020	0.020
PM47428	15.526	15.454	15.461	15.453	15.459	0.072	0.065	0.073	0.067
PM47640	14.800	14.690	14.693	14.694	14.694	0.110	0.107	0.106	0.106
PM61939	12.328	12.466	12.475	12.475	12.475	-0.138	-0.147	-0.147	-0.147
PM71068	19.206	19.365	19.362	19.362	19.361	-0.159	-0.156	-0.156	-0.155
PM76482	17.750	17.863	17.863	17.862	17.863	-0.113	-0.113	-0.112	-0.113

Checkpoint	N_{AHD} (m)	N Values Bi-Linear (m)	N Values Bi-quadratic (m)	N Values Bi-Cubic (m)	N values Bi-Quartic (m)	Residuals Bi-Linear (m)	Residuals Bi-Quadratic (m)	Residuals Bi-Cubic (m)	Residuals Bi-Quartic (m)
PM127070	17.750	17.698	17.695	17.694	17.694	0.052	0.055	0.056	0.056
PM147955	19.307	19.396	19.403	19.402	19.402	-0.089	-0.096	-0.095	-0.095
PM152621	15.370	15.312	15.314	15.315	15.314	0.058	0.056	0.055	0.056
SS1450	18.632	18.759	18.750	18.750	18.750	-0.127	-0.118	-0.118	-0.118
SS1454	18.448	18.573	18.573	18.573	18.573	-0.125	-0.125	-0.125	-0.125
SS1486	16.906	16.922	16.910	16.910	16.910	-0.016	-0.004	-0.004	-0.004
SS1487	16.884	16.865	16.864	16.864	16.864	0.019	0.020	0.020	0.020
SS1488	16.815	16.818	16.810	16.810	16.810	-0.003	0.005	0.005	0.005
SS1490	16.700	16.697	16.692	16.692	16.692	0.003	0.008	0.008	0.008
SS2857	15.401	15.333	15.335	15.335	15.335	0.068	0.066	0.066	0.066
SS2918	17.391	17.428	17.435	17.434	17.436	-0.037	-0.044	-0.043	-0.045
SS5356	17.410	17.502	17.505	17.505	17.506	-0.092	-0.095	-0.095	-0.096
SS5660	14.968	14.950	14.953	14.953	14.953	0.018	0.015	0.015	0.015
SS5674	14.500	14.482	14.478	14.479	14.478	0.018	0.022	0.021	0.022
SS5675	14.494	14.479	14.475	14.476	14.475	0.015	0.019	0.018	0.019
SS5687	14.850	14.848	14.849	14.849	14.849	0.002	0.001	0.001	0.001
SS5694	15.003	14.973	14.974	14.974	14.974	0.030	0.029	0.029	0.029
SS8394	13.778	13.800	13.801	13.801	13.800	-0.022	-0.023	-0.023	-0.022
SS8396	13.907	13.895	13.904	13.902	13.903	0.012	0.003	0.005	0.004
SS8414	14.822	14.736	14.757	14.756	14.757	0.086	0.065	0.066	0.065
SS8415	14.848	14.802	14.808	14.807	14.808	0.045	0.039	0.040	0.039
SS8425	15.485	15.350	15.358	15.356	15.357	0.135	0.127	0.129	0.128
SS8427	15.718	15.547	15.551	15.549	15.550	0.171	0.167	0.169	0.168
SS8428	15.782	15.617	15.620	15.619	15.619	0.165	0.162	0.163	0.163

Checkpoint	N_{AHD} (m)	N Values Bi-Linear (m)	N Values Bi-quadratic (m)	N Values Bi-Cubic (m)	N values Bi-Quartic (m)	Residuals Bi-Linear (m)	Residuals Bi-Quadratic (m)	Residuals Bi-Cubic (m)	Residuals Bi-Quartic (m)
SS10113	17.100	17.086	17.083	17.083	17.083	0.014	0.017	0.017	0.017
SS10114	17.036	17.060	17.056	17.056	17.056	-0.024	-0.020	-0.020	-0.020
SS10123	16.213	16.179	16.179	16.179	16.179	0.034	0.034	0.034	0.034
SS10250	17.400	17.384	17.418	17.417	17.418	0.016	-0.018	-0.017	-0.018
SS23134	17.691	17.519	17.520	17.520	17.520	0.172	0.171	0.171	0.171
SS23137	17.631	17.440	17.444	17.443	17.443	0.191	0.187	0.188	0.188
SS30254	17.169	17.140	17.146	17.146	17.148	0.029	0.023	0.023	0.021
SS34707	17.509	17.404	17.405	17.404	17.404	0.105	0.104	0.105	0.105
SS34712	17.451	17.370	17.371	17.370	17.370	0.081	0.080	0.081	0.081
SS34771	17.489	17.372	17.365	17.365	17.365	0.117	0.124	0.124	0.124
SS36078	17.464	17.478	17.506	17.505	17.510	-0.014	-0.042	-0.041	-0.046
SS39974	18.764	18.779	18.797	18.797	18.797	-0.015	-0.033	-0.033	-0.033
SS39976	18.757	18.769	18.785	18.784	18.785	-0.012	-0.028	-0.027	-0.028
SS39982	18.651	18.629	18.632	18.633	18.633	0.022	0.019	0.018	0.018
SS39984	18.587	18.579	18.576	18.577	18.576	0.008	0.011	0.010	0.011
TS56	15.757	15.663	15.684	15.678	15.681	0.094	0.073	0.079	0.076
TS563	18.494	18.300	18.302	18.303	18.303	0.194	0.192	0.191	0.191
TS1511	17.261	17.278	17.277	17.276	17.277	-0.017	-0.016	-0.015	-0.016
TS2761-4	17.180	16.989	16.953	16.958	16.956	0.191	0.227	0.222	0.224
TS4470	18.827	18.893	18.890	18.891	18.890	-0.066	-0.063	-0.064	-0.063
TS4471	17.430	17.304	17.333	17.326	17.329	0.126	0.097	0.104	0.101
TS4715	17.518	17.540	17.516	17.520	17.516	-0.022	0.002	-0.002	0.002
TS4924-2	16.504	16.543	16.549	16.548	16.552	-0.039	-0.045	-0.044	-0.048
TS5663	19.002	19.083	19.092	19.091	19.094	-0.081	-0.090	-0.089	-0.092

Checkpoint	N_{AHD} (m)	N Values Bi-Linear (m)	N Values Bi-quadratic (m)	N Values Bi-Cubic (m)	N values Bi-Quartic (m)	Residuals Bi-Linear (m)	Residuals Bi-Quadratic (m)	Residuals Bi-Cubic (m)	Residuals Bi-Quartic (m)
TS5945	12.677	12.484	12.482	12.482	12.481	0.193	0.195	0.195	0.196
TS5946	13.267	13.113	13.110	13.111	13.110	0.153	0.156	0.155	0.156
TS6144	15.184	15.076	15.080	15.081	15.081	0.108	0.104	0.103	0.103
TS6734	18.252	18.242	18.217	18.218	18.215	0.010	0.035	0.034	0.037
TS7049	14.695	14.663	14.662	14.663	14.663	0.032	0.033	0.032	0.032
TS7371	15.926	15.832	15.839	15.838	15.841	0.094	0.087	0.088	0.085
TS7372	15.732	15.642	15.652	15.647	15.649	0.090	0.080	0.085	0.083
TS12038	12.114	12.219	12.221	12.220	12.220	-0.105	-0.107	-0.106	-0.106
PM27	10.548	10.508	10.519	10.519	10.519	0.040	0.029	0.029	0.029
IS2	10.620	10.615	10.620	10.619	10.620	0.005	0.000	0.001	0.000
TS7273	12.155	12.125	12.125	12.125	12.125	0.030	0.030	0.030	0.030
PM28485	12.182	12.119	12.119	12.119	12.119	0.063	0.063	0.063	0.063

Table D.3: Mid Hunter AHD71-derived N values and AUSGeoid09-derived N values with bi-linear, bi-quadratic, bi-cubic and bi-quartic interpolation for the 82 checkpoints and subsequent absolute verification residuals.

Mid Hunter derived N values and absolute residuals using AUSGeoid09									
Checkpoint	**N_{AHD} (m)**	**AUSGeoid09**							
		N Values Bi-Linear (m)	**N Values Bi-quadratic (m)**	**N Values Bi-Cubic (m)**	**N values Bi-Quartic (m)**	**Residuals Bi-Linear (m)**	**Residuals Bi-Quadratic (m)**	**Residuals Bi-Cubic (m)**	**Residuals Bi-Quartic (m)**
GB191	26.431	26.395	26.396	26.395	26.396	0.036	0.035	0.036	0.035
PM4942	27.498	27.524	27.523	27.523	27.523	-0.026	-0.025	-0.025	-0.025
PM6283	26.934	26.973	26.972	26.972	26.972	-0.040	-0.039	-0.039	-0.039
PM29397	27.709	27.675	27.675	27.675	27.675	0.034	0.034	0.034	0.034
PM33633	27.904	27.928	27.927	27.927	27.927	-0.024	-0.023	-0.023	-0.023
PM34425	27.300	27.271	27.269	27.270	27.269	0.029	0.031	0.030	0.031
PM34595	28.185	28.148	28.146	28.147	28.146	0.037	0.039	0.038	0.039
PM34603	28.225	28.192	28.191	28.192	28.192	0.033	0.034	0.033	0.033
PM34708	27.814	27.809	27.809	27.809	27.809	0.005	0.005	0.005	0.005
PM47357	28.423	28.347	28.346	28.346	28.346	0.076	0.077	0.077	0.077
PM51512	27.358	27.320	27.318	27.318	27.318	0.038	0.040	0.040	0.040
PM51556	27.372	27.300	27.299	27.299	27.298	0.072	0.073	0.073	0.074
PM57688	30.236	30.263	30.262	30.261	30.261	-0.027	-0.026	-0.025	-0.025
PM60640	27.123	27.129	27.128	27.127	27.127	-0.006	-0.005	-0.004	-0.004
PM60675	27.123	27.152	27.150	27.152	27.151	-0.029	-0.027	-0.029	-0.028
PM60690	27.204	27.219	27.218	27.218	27.218	-0.015	-0.014	-0.014	-0.014
PM71976	30.575	30.501	30.498	30.498	30.498	0.074	0.077	0.077	0.077
PM74988	27.231	27.208	27.207	27.208	27.208	0.023	0.024	0.023	0.023
PM76194	28.677	28.631	28.629	28.629	28.629	0.046	0.048	0.048	0.048
PM79329	27.188	27.163	27.160	27.161	27.160	0.025	0.028	0.027	0.028

Checkpoint	N_{AHD} (m)	N Values Bi-Linear (m)	N Values Bi-quadratic (m)	N Values Bi-Cubic (m)	N values Bi-Quartic (m)	Residuals Bi-Linear (m)	Residuals Bi-Quadratic (m)	Residuals Bi-Cubic (m)	Residuals Bi-Quartic (m)
PM84025	30.417	30.435	30.432	30.433	30.432	-0.018	-0.015	-0.016	-0.015
PM86013	27.147	27.153	27.153	27.154	27.153	-0.006	-0.006	-0.007	-0.006
PM86015	27.242	27.246	27.248	27.246	27.247	-0.004	-0.006	-0.004	-0.005
PM111379	31.142	31.194	31.198	31.198	31.198	-0.052	-0.056	-0.056	-0.056
PM120010	28.968	28.959	28.958	28.958	28.958	0.009	0.010	0.010	0.010
PM120974	27.530	27.510	27.509	27.509	27.509	0.020	0.021	0.021	0.021
PM127025	29.782	29.824	29.822	29.822	29.821	-0.042	-0.040	-0.040	-0.039
PM147656	27.204	27.245	27.244	27.245	27.244	-0.041	-0.040	-0.041	-0.040
PM147667	27.229	27.243	27.242	27.244	27.243	-0.014	-0.013	-0.015	-0.014
PM148379	27.265	27.200	27.200	27.199	27.199	0.065	0.065	0.066	0.066
PM151262	28.554	28.512	28.512	28.512	28.512	0.042	0.042	0.042	0.042
SS416	26.424	26.407	26.407	26.407	26.408	0.017	0.017	0.017	0.016
SS3235	27.143	27.126	27.124	27.124	27.124	0.017	0.019	0.019	0.019
SS3239	27.149	27.164	27.163	27.163	27.163	-0.015	-0.014	-0.014	-0.014
SS3562	27.198	27.227	27.226	27.226	27.226	-0.029	-0.028	-0.028	-0.028
SS12261	27.634	27.597	27.597	27.597	27.597	0.036	0.036	0.036	0.036
SS12263	28.000	27.941	27.941	27.942	27.942	0.059	0.059	0.058	0.058
SS20752	27.077	27.030	27.029	27.029	27.029	0.047	0.048	0.048	0.048
SS20761	27.175	27.175	27.173	27.173	27.173	0.000	0.002	0.002	0.002
SS20789	27.263	27.219	27.218	27.218	27.218	0.044	0.045	0.045	0.045
SS22093	26.164	26.148	26.146	26.147	26.146	0.016	0.018	0.017	0.018
SS22113	26.413	26.396	26.394	26.394	26.393	0.017	0.019	0.019	0.020
SS28327	27.161	27.101	27.101	27.101	27.101	0.060	0.060	0.060	0.060
SS34105	28.957	28.901	28.900	28.900	28.900	0.056	0.057	0.057	0.057

Checkpoint	N_{AHD} (m)	N Values Bi-Linear (m)	N Values Bi-quadratic (m)	N Values Bi-Cubic (m)	N values Bi-Quartic (m)	Residuals Bi-Linear (m)	Residuals Bi-Quadratic (m)	Residuals Bi-Cubic (m)	Residuals Bi-Quartic (m)
SS34453	27.202	27.186	27.184	27.184	27.184	0.016	0.018	0.018	0.018
SS36069	27.835	27.846	27.845	27.845	27.845	-0.011	-0.010	-0.010	-0.010
SS39247	27.192	27.158	27.157	27.157	27.157	0.034	0.035	0.035	0.035
SS43232	27.206	27.164	27.165	27.164	27.164	0.042	0.041	0.042	0.042
SS58021	29.172	29.175	29.175	29.174	29.174	-0.003	-0.003	-0.002	-0.002
SS89854	27.260	27.199	27.199	27.200	27.200	0.061	0.061	0.060	0.060
SS92149	28.410	28.365	28.364	28.365	28.364	0.045	0.046	0.045	0.046
SS92194	27.655	27.643	27.642	27.642	27.642	0.012	0.013	0.013	0.013
SS92196	27.682	27.659	27.658	27.658	27.658	0.023	0.024	0.024	0.024
SS100985	28.157	28.146	28.145	28.145	28.144	0.011	0.012	0.012	0.013
SS128900	25.959	25.897	25.897	25.896	25.897	0.062	0.062	0.063	0.062
TS1098	27.185	27.189	27.189	27.189	27.189	-0.004	-0.004	-0.004	-0.004
TS2672-1	27.124	27.156	27.156	27.156	27.156	-0.032	-0.032	-0.032	-0.032
TS2672-2	27.241	27.156	27.156	27.156	27.156	0.085	0.085	0.085	0.085
TS3297	27.812	27.808	27.808	27.808	27.808	0.004	0.004	0.004	0.004
TS3357	27.918	27.930	27.929	27.929	27.929	-0.012	-0.011	-0.011	-0.011
TS5182	27.142	27.123	27.122	27.122	27.122	0.019	0.020	0.020	0.020
TS5318	27.223	27.208	27.208	27.207	27.208	0.015	0.015	0.016	0.015
TS5324	28.445	28.494	28.496	28.496	28.496	-0.049	-0.051	-0.051	-0.051
TS5472	27.208	27.204	27.204	27.204	27.204	0.004	0.004	0.004	0.004
TS5518	27.023	27.104	27.110	27.108	27.110	-0.081	-0.087	-0.085	-0.087
TS5901	29.473	29.578	29.582	29.582	29.583	-0.105	-0.109	-0.109	-0.110
TS5916	28.429	28.428	28.427	28.427	28.427	0.001	0.002	0.002	0.002
TS5953	27.072	27.096	27.096	27.096	27.096	-0.024	-0.024	-0.024	-0.024

Checkpoint	N_{AHD} (m)	N Values Bi-Linear (m)	N Values Bi-quadratic (m)	N Values Bi-Cubic (m)	N values Bi-Quartic (m)	Residuals Bi-Linear (m)	Residuals Bi-Quadratic (m)	Residuals Bi-Cubic (m)	Residuals Bi-Quartic (m)
TS6024	29.029	29.033	29.034	29.033	29.034	-0.004	-0.005	-0.004	-0.005
TS6062	26.918	26.921	26.922	26.922	26.922	-0.003	-0.004	-0.004	-0.004
TS6211	27.647	27.591	27.591	27.591	27.592	0.056	0.056	0.056	0.055
TS6231	27.012	26.932	26.932	26.932	26.932	0.080	0.080	0.080	0.080
TS7097	26.428	26.453	26.453	26.453	26.453	-0.025	-0.025	-0.025	-0.025
TS7189	26.312	26.250	26.251	26.251	26.251	0.062	0.061	0.061	0.061
TS10341	27.289	27.290	27.290	27.290	27.290	-0.001	-0.001	-0.001	-0.001
TS10464	28.621	28.487	28.488	28.487	28.488	0.134	0.133	0.134	0.133
TS10688	27.231	27.232	27.231	27.231	27.231	-0.001	0.000	0.000	0.000
TS10700	27.254	27.220	27.217	27.218	27.218	0.034	0.037	0.036	0.036
TS10730	27.176	27.195	27.195	27.195	27.195	-0.019	-0.019	-0.019	-0.019
TS10802	28.086	28.058	28.057	28.057	28.058	0.028	0.029	0.029	0.028
TS12106	26.866	26.885	26.884	26.884	26.884	-0.019	-0.018	-0.018	-0.018
TS12107	26.403	26.412	26.412	26.412	26.412	-0.009	-0.009	-0.009	-0.009

Table D.4: Mid Hunter AHD71-derived N values and AUSGeoid98-derived N values with bi-linear, bi-quadratic, bi-cubic and bi-quartic interpolation for the 82 checkpoints and subsequent absolute verification residuals.

Mid Hunter derived N values and absolute residuals using AUSGeoid98									
Checkpoint	**N_{AHD} (m)**	**AUSGeoid98**							
		N Values Bi-Linear (m)	**N Values Bi-quadratic (m)**	**N Values Bi-Cubic (m)**	**N values Bi-Quartic (m)**	**Residuals Bi-Linear (m)**	**Residuals Bi-Quadratic (m)**	**Residuals Bi-Cubic (m)**	**Residuals Bi-Quartic (m)**
GB191	26.431	26.538	26.555	26.551	26.553	-0.107	-0.124	-0.120	-0.122
PM4942	27.498	27.854	27.858	27.858	27.858	-0.356	-0.360	-0.360	-0.360
PM6283	26.934	27.253	27.255	27.254	27.255	-0.320	-0.322	-0.321	-0.322
PM29397	27.709	27.977	27.984	27.984	27.984	-0.268	-0.275	-0.275	-0.275
PM33633	27.904	28.195	28.196	28.196	28.196	-0.291	-0.292	-0.292	-0.292
PM34425	27.300	27.480	27.483	27.483	27.483	-0.180	-0.183	-0.183	-0.183
PM34595	28.185	28.430	28.428	28.428	28.428	-0.245	-0.243	-0.243	-0.243
PM34603	28.225	28.469	28.468	28.468	28.468	-0.244	-0.243	-0.243	-0.243
PM34708	27.814	28.103	28.105	28.105	28.105	-0.289	-0.291	-0.291	-0.291
PM47357	28.423	28.620	28.622	28.622	28.622	-0.197	-0.199	-0.199	-0.199
PM51512	27.358	27.669	27.672	27.672	27.672	-0.311	-0.314	-0.314	-0.314
PM51556	27.372	27.651	27.652	27.652	27.652	-0.279	-0.280	-0.280	-0.280
PM57688	30.236	30.354	30.362	30.360	30.361	-0.118	-0.126	-0.124	-0.125
PM60640	27.123	27.472	27.472	27.472	27.472	-0.349	-0.349	-0.349	-0.349
PM60675	27.123	27.490	27.481	27.483	27.480	-0.367	-0.358	-0.360	-0.357
PM60690	27.204	27.537	27.543	27.543	27.543	-0.333	-0.339	-0.339	-0.339
PM71976	30.575	30.655	30.666	30.666	30.667	-0.080	-0.091	-0.091	-0.092
PM74988	27.231	27.525	27.520	27.523	27.521	-0.294	-0.289	-0.292	-0.290

Checkpoint	N_{AHD} (m)	N Values Bi-Linear (m)	N Values Bi-quadratic (m)	N Values Bi-Cubic (m)	N values Bi-Quartic (m)	Residuals Bi-Linear (m)	Residuals Bi-Quadratic (m)	Residuals Bi-Cubic (m)	Residuals Bi-Quartic (m)
PM76194	28.677	28.875	28.880	28.880	28.880	-0.198	-0.203	-0.203	-0.203
PM79329	27.188	27.504	27.493	27.494	27.492	-0.316	-0.305	-0.306	-0.304
PM84025	30.417	30.546	30.555	30.554	30.556	-0.129	-0.138	-0.137	-0.139
PM86013	27.147	27.429	27.427	27.427	27.427	-0.282	-0.280	-0.280	-0.280
PM86015	27.242	27.558	27.558	27.559	27.559	-0.316	-0.316	-0.317	-0.317
PM111379	31.142	31.220	31.216	31.216	31.218	-0.078	-0.074	-0.074	-0.076
PM120010	28.968	29.103	29.134	29.133	29.134	-0.135	-0.166	-0.165	-0.166
PM120974	27.530	27.791	27.792	27.791	27.791	-0.261	-0.262	-0.261	-0.261
PM127025	29.782	29.929	29.934	29.935	29.936	-0.147	-0.152	-0.153	-0.154
PM147656	27.204	27.544	27.541	27.542	27.541	-0.340	-0.337	-0.338	-0.337
PM147667	27.229	27.558	27.555	27.556	27.555	-0.329	-0.326	-0.327	-0.326
PM148379	27.265	27.518	27.514	27.515	27.514	-0.253	-0.249	-0.250	-0.249
PM151262	28.554	28.774	28.774	28.775	28.774	-0.220	-0.220	-0.221	-0.220
SS416	26.424	26.626	26.580	26.580	26.580	-0.202	-0.156	-0.156	-0.156
SS3235	27.143	27.469	27.468	27.470	27.468	-0.326	-0.325	-0.327	-0.325
SS3239	27.149	27.491	27.491	27.491	27.491	-0.342	-0.342	-0.342	-0.342
SS3562	27.198	27.545	27.555	27.555	27.555	-0.347	-0.357	-0.357	-0.357
SS12261	27.634	27.910	27.914	27.913	27.913	-0.277	-0.281	-0.280	-0.280
SS12263	28.000	28.239	28.239	28.239	28.239	-0.239	-0.239	-0.239	-0.239
SS20752	27.077	27.261	27.263	27.264	27.263	-0.184	-0.186	-0.187	-0.186
SS20761	27.175	27.505	27.508	27.507	27.507	-0.330	-0.333	-0.332	-0.332
SS20789	27.263	27.557	27.568	27.568	27.569	-0.294	-0.305	-0.305	-0.306
SS22093	26.164	26.306	26.299	26.299	26.298	-0.142	-0.135	-0.135	-0.134
SS22113	26.413	26.589	26.582	26.583	26.582	-0.176	-0.169	-0.170	-0.169

Checkpoint	N_{AHD} (m)	N Values Bi-Linear (m)	N Values Bi-quadratic (m)	N Values Bi-Cubic (m)	N values Bi-Quartic (m)	Residuals Bi-Linear (m)	Residuals Bi-Quadratic (m)	Residuals Bi-Cubic (m)	Residuals Bi-Quartic (m)
SS28327	27.161	27.355	27.360	27.361	27.361	-0.194	-0.199	-0.200	-0.200
SS34105	28.957	29.134	29.142	29.141	29.141	-0.177	-0.185	-0.184	-0.184
SS34453	27.202	27.467	27.488	27.483	27.486	-0.265	-0.286	-0.281	-0.284
SS36069	27.835	28.126	28.127	28.127	28.127	-0.291	-0.292	-0.292	-0.292
SS39247	27.192	27.444	27.422	27.423	27.423	-0.252	-0.230	-0.231	-0.231
SS43232	27.206	27.360	27.369	27.369	27.369	-0.154	-0.163	-0.163	-0.163
SS58021	29.172	29.299	29.340	29.340	29.340	-0.127	-0.168	-0.168	-0.168
SS89854	27.260	27.482	27.482	27.481	27.482	-0.222	-0.222	-0.221	-0.222
SS92149	28.410	28.639	28.639	28.639	28.639	-0.229	-0.229	-0.229	-0.229
SS92194	27.655	27.946	27.945	27.946	27.945	-0.291	-0.290	-0.291	-0.290
SS92196	27.682	27.964	27.963	27.963	27.963	-0.282	-0.281	-0.281	-0.281
SS100985	28.157	28.331	28.340	28.339	28.339	-0.174	-0.183	-0.182	-0.182
SS128900	25.959	26.056	26.053	26.054	26.053	-0.097	-0.094	-0.095	-0.094
TS1098	27.185	27.501	27.473	27.473	27.473	-0.316	-0.288	-0.288	-0.288
TS2672-1	27.124	27.439	27.436	27.436	27.436	-0.315	-0.312	-0.312	-0.312
TS2672-2	27.241	27.439	27.436	27.436	27.436	-0.198	-0.195	-0.195	-0.195
TS3297	27.812	28.095	28.096	28.096	28.096	-0.283	-0.284	-0.284	-0.284
TS3357	27.918	28.219	28.219	28.219	28.219	-0.301	-0.301	-0.301	-0.301
TS5182	27.142	27.353	27.360	27.360	27.360	-0.211	-0.218	-0.218	-0.218
TS5318	27.223	27.565	27.562	27.564	27.561	-0.342	-0.339	-0.341	-0.338
TS5324	28.445	28.726	28.730	28.730	28.730	-0.281	-0.285	-0.285	-0.285
TS5472	27.208	27.494	27.504	27.500	27.501	-0.286	-0.296	-0.292	-0.293
TS5518	27.023	27.258	27.248	27.248	27.248	-0.235	-0.225	-0.225	-0.225
TS5901	29.473	29.644	29.641	29.641	29.641	-0.171	-0.168	-0.168	-0.168

Checkpoint	N_{AHD} (m)	N Values Bi-Linear (m)	N Values Bi-quadratic (m)	N Values Bi-Cubic (m)	N values Bi-Quartic (m)	Residuals Bi-Linear (m)	Residuals Bi-Quadratic (m)	Residuals Bi-Cubic (m)	Residuals Bi-Quartic (m)
TS5916	28.429	28.604	28.607	28.607	28.607	-0.175	-0.178	-0.178	-0.178
TS5953	27.072	27.364	27.369	27.369	27.369	-0.292	-0.297	-0.297	-0.297
TS6024	29.029	29.179	29.196	29.196	29.196	-0.150	-0.167	-0.167	-0.167
TS6062	26.918	27.180	27.199	27.199	27.201	-0.262	-0.281	-0.281	-0.283
TS6211	27.647	27.872	27.874	27.874	27.874	-0.225	-0.227	-0.227	-0.227
TS6231	27.012	27.120	27.123	27.123	27.123	-0.108	-0.111	-0.111	-0.111
TS7097	26.428	26.642	26.641	26.641	26.641	-0.214	-0.213	-0.213	-0.213
TS7189	26.312	26.470	26.445	26.450	26.445	-0.158	-0.133	-0.138	-0.133
TS10341	27.289	27.548	27.555	27.554	27.555	-0.259	-0.266	-0.265	-0.266
TS10464	28.621	28.738	28.738	28.738	28.738	-0.117	-0.117	-0.117	-0.117
TS10688	27.231	27.556	27.557	27.557	27.557	-0.325	-0.326	-0.326	-0.326
TS10700	27.254	27.575	27.575	27.575	27.575	-0.321	-0.321	-0.321	-0.321
TS10730	27.176	27.469	27.480	27.480	27.480	-0.293	-0.304	-0.304	-0.304
TS10802	28.086	28.335	28.334	28.334	28.334	-0.249	-0.248	-0.248	-0.248
TS12106	26.866	27.133	27.139	27.139	27.138	-0.267	-0.273	-0.273	-0.272
TS12107	26.403	26.554	26.578	26.576	26.581	-0.151	-0.175	-0.173	-0.178

APPENDIX E

Descriptive Statistics of Absolute Verification Residuals, Between AHD71-Derived N Values and Geoid-Derived N Values with Bi-Linear, Bi-Quadratic, Bi-Cubic and Bi-Quartic Interpolation as a Function of 100 m Increases in AHD71

LIST OF TABLES

Table E.1: Snowy Mountains descriptive statistics of absolute verification residuals, between AHD71-derived N values and AUSGeoid09-derived N values with bi-linear interpolation as a function of 100 m increases in AHD71. ..... E-161
Table E.2: Snowy Mountains descriptive statistics of absolute verification residuals, between AHD71-derived N values and AUSGeoid09-derived N values with bi-quadratic interpolation as a function of 100 m increases in AHD71. ..... E-162
Table E.3: Snowy Mountains descriptive statistics of absolute verification residuals, between AHD71-derived N values and AUSGeoid09-derived N values with bi-cubic interpolation as a function of 100 m increases in AHD71. ..... E-163
Table E.4: Snowy Mountains descriptive statistics of absolute verification residuals, between AHD71-derived N values and AUSGeoid09-derived N values with bi-quartic interpolation as a function of 100 m increases in AHD71. ..... E-164
Table E.5: Snowy Mountains descriptive statistics of absolute verification residuals, between AHD71-derived N values and AUSGeoid98-derived N values with bi-linear interpolation as a function of 100 m increases in AHD71. ..... E-165
Table E.6: Snowy Mountains descriptive statistics of absolute verification residuals, between AHD71-derived N values and AUSGeoid98-derived N values with bi-quadratic interpolation as a function of 100 m increases in AHD71. ..... E-166
Table E.7: Snowy Mountains descriptive statistics of absolute verification residuals, between AHD71-derived N values and AUSGeoid98-derived N values with bi-cubic interpolation as a function of 100 m increases in AHD71. ..... E-167
Table E.8: Snowy Mountains descriptive statistics of absolute verification residuals, between AHD71-derived N values and AUSGeoid98-derived N values with bi-quartic interpolation as a function of 100 m increases in AHD71. ..... E-168
Table E. 9: Mid Hunter descriptive statistics of absolute verification residuals, between AHD71-derived N values and AUSGeoid09-derived N values with bi-linear interpolation as a function of 100 m increases in AHD71. ..... E-169
Table E.10: Mid Hunter descriptive statistics of absolute verification residuals, between AHD71-derived N values and AUSGeoid09-derived N values with bi-quadratic interpolation as a function of 100 m increases in AHD71. ..... E-170

Table E.11: Mid Hunter descriptive statistics of absolute verification residuals, between AHD71-derived N values and AUSGeoid09-derived N values with bi-cubic interpolation as a function of 100 m increases in AHD71. ..... E-171
Table E. 12: Mid Hunter descriptive statistics of absolute verification residuals, between AHD71-derived N values and AUSGeoid09-derived N values with bi-quartic interpolation as a function of 100 m increases in AHD71. ..... E-172
Table E. 13: Mid Hunter descriptive statistics of absolute verification residuals, between AHD71-derived N values and AUSGeoid98-derived N values with bi-linear interpolation as a function of 100 m increases in AHD71. ..... E-173
Table E. 14: Mid Hunter descriptive statistics of absolute verification residuals, between AHD71-derived N values and AUSGeoid98-derived N values with bi-quadratic interpolation as a function of 100 m increases in AHD71. ..... E-174
Table E. 15: Mid Hunter descriptive statistics of absolute verification residuals, between AHD71-derived N values and AUSGeoid98-derived N values with bi-cubic interpolation as a function of 100 m increases in AHD71. ..... E-175
Table E.16: Mid Hunter descriptive statistics of absolute verification residuals, between AHD71-derived N values and AUSGeoid98-derived N values with bi-quartic interpolation as a function of 100 m increases in AHD71. ..... E-176

AHD71 (m)	Count	Range (m)	Mean (m)	Min (m)	Max (m)	RMS (m)	STD (m)	Outliers
>5	104	0.348	0.076	-0.061	0.287	0.104	0.070	0
>100	100	0.348	0.076	-0.061	0.287	0.103	0.071	0
>200	99	0.348	0.077	-0.061	0.287	0.104	0.071	0
>300	85	0.336	0.086	-0.049	0.287	0.107	0.064	1
>400	73	0.259	0.091	-0.049	0.210	0.108	0.058	0
>500	66	0.259	0.090	-0.049	0.210	0.108	0.060	0
>600	65	0.259	0.091	-0.049	0.210	0.108	0.059	0
>700	63	0.259	0.092	-0.049	0.210	0.109	0.059	0
>800	49	0.259	0.090	-0.049	0.210	0.111	0.065	0
>900	41	0.259	0.087	-0.049	0.210	0.109	0.065	0
>1000	33	0.243	0.075	-0.049	0.194	0.093	0.057	0
>1100	17	0.217	0.057	-0.049	0.168	0.085	0.064	0
>1200	11	0.165	0.025	-0.049	0.116	0.055	0.052	0
>1300	9	0.165	0.025	-0.049	0.116	0.057	0.055	0
>1400	7	0.165	0.018	-0.049	0.116	0.052	0.052	0
>1700	3	0.115	0.054	0.001	0.116	0.072	0.058	0
>2200	1	0.000	0.046	0.046	0.046	0.046	N/A	0

Table E.1: Snowy Mountains descriptive statistics of absolute verification residuals, between AHD71-derived N values and AUSGeoid09-derived N values with bi-linear interpolation as a function of 100 m increases in AHD71.

AHD71 (m)	Count	Range (m)	Mean (m)	Min (m)	Max (m)	RMS (m)	STD (m)	Outliers
>5	104	0.344	0.076	-0.059	0.285	0.103	0.070	0
>100	100	0.344	0.076	-0.059	0.285	0.103	0.071	0
>200	99	0.344	0.077	-0.059	0.285	0.104	0.071	0
>300	85	0.335	0.086	-0.050	0.285	0.107	0.064	1
>400	73	0.259	0.091	-0.050	0.209	0.108	0.058	0
>500	66	0.259	0.089	-0.050	0.209	0.107	0.060	0
>600	65	0.259	0.091	-0.050	0.209	0.108	0.059	0
>700	63	0.259	0.091	-0.050	0.209	0.109	0.060	0
>800	49	0.259	0.090	-0.050	0.209	0.111	0.066	0
>900	41	0.259	0.087	-0.050	0.209	0.108	0.066	0
>1000	33	0.245	0.074	-0.050	0.195	0.093	0.057	0
>1100	17	0.220	0.056	-0.050	0.170	0.084	0.065	0
>1200	11	0.163	0.023	-0.050	0.113	0.054	0.051	0
>1300	9	0.163	0.023	-0.050	0.113	0.056	0.054	0
>1400	7	0.163	0.016	-0.050	0.113	0.050	0.051	0
>1700	3	0.113	0.051	0.000	0.113	0.069	0.057	0
>2200	1	0.000	0.040	0.040	0.040	0.040	N/A	0

Table E.2: Snowy Mountains descriptive statistics of absolute verification residuals, between AHD71-derived N values and AUSGeoid09-derived N values with bi-quadratic interpolation as a function of 100 m increases in AHD71.

AHD71 (m)	Count	Range (m)	Mean (m)	Min (m)	Max (m)	RMS (m)	STD (m)	Outliers
>5	104	0.343	0.076	-0.059	0.284	0.103	0.070	0
>100	100	0.343	0.076	-0.059	0.284	0.103	0.071	0
>200	99	0.343	0.077	-0.059	0.284	0.104	0.071	0
>300	85	0.335	0.086	-0.051	0.284	0.107	0.064	1
>400	73	0.260	0.091	-0.051	0.209	0.108	0.059	0
>500	66	0.260	0.089	-0.051	0.209	0.107	0.060	0
>600	65	0.260	0.091	-0.051	0.209	0.108	0.060	0
>700	63	0.260	0.091	-0.051	0.209	0.109	0.060	0
>800	49	0.260	0.090	-0.051	0.209	0.111	0.066	0
>900	41	0.260	0.087	-0.051	0.209	0.108	0.066	0
>1000	33	0.246	0.074	-0.051	0.195	0.093	0.057	0
>1100	17	0.220	0.056	-0.051	0.169	0.084	0.065	0
>1200	11	0.163	0.023	-0.051	0.112	0.054	0.051	0
>1300	9	0.163	0.023	-0.051	0.112	0.056	0.054	0
>1400	7	0.163	0.016	-0.051	0.112	0.050	0.051	0
>1700	3	0.112	0.051	0.000	0.112	0.069	0.057	0
>2200	1	0.000	0.040	0.040	0.040	0.040	N/A	0

Table E.3: Snowy Mountains descriptive statistics of absolute verification residuals, between AHD71-derived N values and AUSGeoid09-derived N values with bi-cubic interpolation as a function of 100 m increases in AHD71.

AHD71 (m)	Count	Range (m)	Mean (m)	Min (m)	Max (m)	RMS (m)	STD (m)	Outliers
>5	104	0.343	0.076	-0.059	0.284	0.103	0.070	0
>100	100	0.343	0.076	-0.059	0.284	0.103	0.071	0
>200	99	0.343	0.077	-0.059	0.284	0.104	0.071	0
>300	85	0.335	0.086	-0.051	0.284	0.107	0.064	0
>400	73	0.260	0.091	-0.051	0.209	0.108	0.059	0
>500	66	0.260	0.089	-0.051	0.209	0.107	0.060	0
>600	65	0.260	0.091	-0.051	0.209	0.108	0.060	0
>700	63	0.260	0.091	-0.051	0.209	0.109	0.060	0
>800	49	0.260	0.090	-0.051	0.209	0.111	0.066	0
>900	41	0.260	0.087	-0.051	0.209	0.108	0.066	0
>1000	33	0.246	0.074	-0.051	0.195	0.093	0.057	0
>1100	17	0.221	0.056	-0.051	0.170	0.084	0.065	0
>1200	11	0.163	0.022	-0.051	0.112	0.054	0.051	0
>1300	9	0.163	0.022	-0.051	0.112	0.056	0.054	0
>1400	7	0.163	0.016	-0.051	0.112	0.050	0.051	0
>1700	3	0.112	0.051	0.000	0.112	0.069	0.057	0
>2200	1	0.000	0.040	0.040	0.040	0.040	N/A	0

Table E.4: Snowy Mountains descriptive statistics of absolute verification residuals, between AHD71-derived N values and AUSGeoid09-derived N values with bi-quartic interpolation as a function of 100 m increases in AHD71.

AHD71 (m)	Count	Range (m)	Mean (m)	Min (m)	Max (m)	RMS (m)	STD (m)	Outliers
>5	104	0.388	0.022	-0.161	0.227	0.091	0.089	0
>100	100	0.388	0.022	-0.161	0.227	0.091	0.090	0
>200	99	0.388	0.023	-0.161	0.227	0.092	0.090	0
>300	85	0.386	0.033	-0.159	0.227	0.092	0.086	0
>400	73	0.386	0.028	-0.159	0.227	0.093	0.089	0
>500	66	0.386	0.021	-0.159	0.227	0.091	0.089	0
>600	65	0.386	0.022	-0.159	0.227	0.091	0.089	0
>700	63	0.321	0.022	-0.127	0.194	0.086	0.084	0
>800	49	0.311	0.024	-0.117	0.194	0.081	0.078	0
>900	41	0.311	0.022	-0.117	0.194	0.080	0.078	0
>1000	33	0.311	0.005	-0.117	0.194	0.069	0.070	0
>1100	17	0.311	0.015	-0.117	0.194	0.086	0.087	0
>1200	11	0.311	0.010	-0.117	0.194	0.098	0.102	0
>1300	9	0.311	0.021	-0.117	0.194	0.105	0.110	0
>1400	7	0.283	0.043	-0.089	0.194	0.111	0.111	0
>1700	3	0.142	0.146	0.052	0.194	0.160	0.081	0
>2200	1	0.000	0.191	0.191	0.191	0.191	N/A	0

Table E.5: Snowy Mountains descriptive statistics of absolute verification residuals, between AHD71-derived N values and AUSGeoid98-derived N values with bi-linear interpolation as a function of 100 m increases in AHD71.

AHD71 (m)	Count	Range (m)	Mean (m)	Min (m)	Max (m)	RMS (m)	STD (m)	Outliers
>5	104	0.393	0.019	-0.165	0.227	0.091	0.090	0
>100	100	0.393	0.019	-0.165	0.227	0.092	0.091	0
>200	99	0.393	0.020	-0.165	0.227	0.092	0.091	0
>300	85	0.383	0.031	-0.156	0.227	0.091	0.086	0
>400	73	0.383	0.028	-0.156	0.227	0.093	0.089	0
>500	66	0.383	0.021	-0.156	0.227	0.092	0.090	0
>600	65	0.383	0.022	-0.156	0.227	0.092	0.090	0
>700	63	0.352	0.022	-0.125	0.227	0.087	0.085	0
>800	49	0.352	0.024	-0.124	0.227	0.084	0.081	0
>900	41	0.352	0.021	-0.124	0.227	0.083	0.082	0
>1000	33	0.352	0.005	-0.124	0.227	0.074	0.075	0
>1100	17	0.352	0.018	-0.124	0.227	0.092	0.093	0
>1200	11	0.352	0.014	-0.124	0.227	0.106	0.110	0
>1300	9	0.352	0.026	-0.124	0.227	0.115	0.119	0
>1400	7	0.324	0.046	-0.096	0.227	0.121	0.121	0
>1700	3	0.173	0.158	0.055	0.227	0.175	0.091	0
>2200	1	0.000	0.227	0.227	0.227	0.227	N/A	0

Table E.6: Snowy Mountains descriptive statistics of absolute verification residuals, between AHD71-derived N values and AUSGeoid98-derived N values with bi-quadratic interpolation as a function of 100 m increases in AHD71.

AHD71 (m)	Count	Range (m)	Mean (m)	Min (m)	Max (m)	RMS (m)	STD (m)	Outliers
>5	104	0.389	0.020	-0.165	0.224	0.091	0.090	0
>100	100	0.389	0.019	-0.165	0.224	0.092	0.091	0
>200	99	0.389	0.021	-0.165	0.224	0.093	0.091	0
>300	85	0.380	0.031	-0.156	0.224	0.092	0.086	0
>400	73	0.380	0.028	-0.156	0.224	0.093	0.089	0
>500	66	0.380	0.021	-0.156	0.224	0.091	0.090	0
>600	65	0.380	0.022	-0.156	0.224	0.092	0.090	0
>700	63	0.347	0.022	-0.125	0.222	0.087	0.085	0
>800	49	0.345	0.024	-0.122	0.222	0.084	0.081	0
>900	41	0.345	0.021	-0.122	0.222	0.083	0.081	0
>1000	33	0.345	0.005	-0.122	0.222	0.073	0.074	0
>1100	17	0.345	0.018	-0.122	0.222	0.091	0.092	0
>1200	11	0.345	0.014	-0.122	0.222	0.104	0.109	0
>1300	9	0.345	0.026	-0.122	0.222	0.113	0.117	0
>1400	7	0.318	0.046	-0.095	0.222	0.119	0.119	0
>1700	3	0.167	0.156	0.056	0.222	0.172	0.089	0
>2200	1	0.000	0.222	0.222	0.222	0.222	N/A	0

Table E.7: Snowy Mountains descriptive statistics of absolute verification residuals, between AHD71-derived N values and AUSGeoid98-derived N values with bi-cubic interpolation as a function of 100 m increases in AHD71.

AHD71 (m)	Count	Range (m)	Mean (m)	Min (m)	Max (m)	RMS (m)	STD (m)	Outliers
>5	104	0.390	0.019	-0.165	0.224	0.091	0.090	0
>100	100	0.390	0.019	-0.165	0.224	0.092	0.091	0
>200	99	0.390	0.020	-0.165	0.224	0.093	0.091	0
>300	85	0.379	0.031	-0.155	0.224	0.091	0.087	0
>400	73	0.379	0.028	-0.155	0.224	0.093	0.089	0
>500	66	0.379	0.021	-0.155	0.224	0.092	0.090	0
>600	65	0.379	0.022	-0.155	0.224	0.092	0.090	0
>700	63	0.349	0.022	-0.125	0.224	0.087	0.085	0
>800	49	0.349	0.024	-0.124	0.224	0.084	0.081	0
>900	41	0.349	0.021	-0.124	0.224	0.083	0.082	0
>1000	33	0.349	0.005	-0.124	0.224	0.074	0.075	0
>1100	17	0.349	0.018	-0.124	0.224	0.091	0.092	0
>1200	11	0.349	0.014	-0.124	0.224	0.105	0.109	0
>1300	9	0.349	0.026	-0.124	0.224	0.114	0.118	0
>1400	7	0.320	0.046	-0.095	0.224	0.120	0.119	0
>1700	3	0.169	0.157	0.056	0.224	0.173	0.089	0
>2200	1	0.000	0.224	0.224	0.224	0.224	N/A	0

Table E.8: Snowy Mountains descriptive statistics of absolute verification residuals, between AHD71-derived N values and AUSGeoid98-derived N values with bi-quartic interpolation as a function of 100 m increases in AHD71.

AHD71 (m)	Count	Range (m)	Mean (m)	Min (m)	Max (m)	RMS (m)	STD (m)	Outliers
>20	82	0.239	0.013	-0.105	0.134	0.041	0.040	1
>100	77	0.239	0.012	-0.105	0.134	0.042	0.040	0
>200	54	0.239	0.009	-0.105	0.134	0.045	0.045	0
>300	32	0.239	0.010	-0.105	0.134	0.053	0.053	0
>400	22	0.239	0.003	-0.105	0.134	0.057	0.058	0
>500	15	0.190	-0.011	-0.105	0.085	0.052	0.053	0
>600	13	0.190	-0.016	-0.105	0.085	0.054	0.054	0
>700	10	0.190	-0.012	-0.105	0.085	0.058	0.060	0
>800	6	0.190	-0.031	-0.105	0.085	0.069	0.067	0
>900	5	0.190	-0.037	-0.105	0.085	0.075	0.074	0
>1000	3	0.053	-0.079	-0.105	-0.052	0.082	0.026	0
>1200	2	0.029	-0.066	-0.081	-0.052	0.068	0.021	0
>1400	1	0.000	-0.052	-0.052	-0.052	0.052	N/A	0

Table E. 9: Mid Hunter descriptive statistics of absolute verification residuals, between AHD71-derived N values and AUSGeoid09-derived N values with bi-linear interpolation as a function of 100 m increases in AHD71.

AHD71 (m)	Count	Range (m)	Mean (m)	Min (m)	Max (m)	RMS (m)	STD (m)	Outliers
>20	82	0.242	0.014	-0.109	0.133	0.042	0.040	1
>100	77	0.242	0.013	-0.109	0.133	0.043	0.041	0
>200	54	0.242	0.010	-0.109	0.133	0.045	0.046	0
>300	32	0.242	0.010	-0.109	0.133	0.054	0.054	0
>400	22	0.242	0.002	-0.109	0.133	0.058	0.059	0
>500	15	0.194	-0.012	-0.109	0.085	0.054	0.054	0
>600	13	0.194	-0.018	-0.109	0.085	0.056	0.055	0
>700	10	0.194	-0.013	-0.109	0.085	0.060	0.062	0
>800	6	0.194	-0.034	-0.109	0.085	0.072	0.069	0
>900	5	0.194	-0.040	-0.109	0.085	0.078	0.076	0
>1000	3	0.053	-0.084	-0.109	-0.056	0.086	0.027	0
>1200	2	0.031	-0.071	-0.087	-0.056	0.073	0.022	0
>1400	1	0.000	-0.056	-0.056	-0.056	0.056	N/A	0

Table E.10: Mid Hunter descriptive statistics of absolute verification residuals, between AHD71-derived N values and AUSGeoid09-derived N values with bi-quadratic interpolation as a function of 100 m increases in AHD71.

AHD71 (m)	Count	Range (m)	Mean (m)	Min (m)	Max (m)	RMS (m)	STD (m)	Outliers
>20	82	0.243	0.014	-0.109	0.134	0.042	0.040	1
>100	77	0.243	0.013	-0.109	0.134	0.043	0.041	0
>200	54	0.243	0.009	-0.109	0.134	0.045	0.046	0
>300	32	0.243	0.010	-0.109	0.134	0.054	0.054	0
>400	22	0.243	0.002	-0.109	0.134	0.058	0.059	0
>500	15	0.194	-0.012	-0.109	0.085	0.054	0.054	0
>600	13	0.194	-0.018	-0.109	0.085	0.055	0.055	0
>700	10	0.194	-0.013	-0.109	0.085	0.060	0.062	0
>800	6	0.194	-0.033	-0.109	0.085	0.071	0.069	0
>900	5	0.194	-0.039	-0.109	0.085	0.078	0.075	0
>1000	3	0.053	-0.083	-0.109	-0.056	0.086	0.026	0
>1200	2	0.029	-0.070	-0.085	-0.056	0.072	0.021	0
>1400	1	0.000	-0.056	-0.056	-0.056	0.056	N/A	0

Table E.11: Mid Hunter descriptive statistics of absolute verification residuals, between AHD71-derived N values and AUSGeoid09-derived N values with bi-cubic interpolation as a function of 100 m increases in AHD71.

AHD71 (m)	Count	Range (m)	Mean (m)	Min (m)	Max (m)	RMS (m)	STD (m)	Outliers
>20	82	0.243	0.014	-0.110	0.133	0.042	0.040	0
>100	77	0.243	0.013	-0.110	0.133	0.043	0.041	0
>200	54	0.243	0.009	-0.110	0.133	0.045	0.046	0
>300	32	0.243	0.010	-0.110	0.133	0.054	0.054	0
>400	22	0.243	0.002	-0.110	0.133	0.058	0.059	0
>500	15	0.195	-0.012	-0.110	0.085	0.054	0.054	0
>600	13	0.195	-0.018	-0.110	0.085	0.056	0.055	0
>700	10	0.195	-0.014	-0.110	0.085	0.060	0.062	0
>800	6	0.195	-0.034	-0.110	0.085	0.072	0.069	0
>900	5	0.195	-0.040	-0.110	0.085	0.079	0.076	0
>1000	3	0.054	-0.084	-0.110	-0.056	0.087	0.027	0
>1200	2	0.031	-0.071	-0.087	-0.056	0.073	0.022	0
>1400	1	0	-0.0557	-0.0557	-0.0557	0.0557	N/A	0

Table E. 12: Mid Hunter descriptive statistics of absolute verification residuals, between AHD71-derived N values and AUSGeoid09-derived N values with bi-quartic interpolation as a function of 100 m increases in AHD71.

AHD71 (m)	Count	Range (m)	Mean (m)	Min (m)	Max (m)	RMS (m)	STD (m)	Outliers
>20	82	0.290	-0.241	-0.367	-0.078	0.253	0.076	0
>100	77	0.290	-0.243	-0.367	-0.078	0.254	0.077	0
>200	54	0.290	-0.233	-0.367	-0.078	0.246	0.079	0
>300	32	0.262	-0.228	-0.340	-0.078	0.240	0.076	0
>400	22	0.262	-0.233	-0.340	-0.078	0.245	0.079	0
>500	15	0.242	-0.240	-0.320	-0.078	0.249	0.069	0
>600	13	0.242	-0.248	-0.320	-0.078	0.257	0.069	0
>700	10	0.238	-0.234	-0.316	-0.078	0.244	0.073	0
>800	6	0.238	-0.219	-0.316	-0.078	0.234	0.091	0
>900	5	0.238	-0.199	-0.315	-0.078	0.214	0.087	0
>1000	3	0.157	-0.161	-0.235	-0.078	0.173	0.079	0
>1200	2	0.157	-0.156	-0.235	-0.078	0.175	0.111	0
>1400	1	0.000	-0.078	-0.078	-0.078	0.078	N/A	0

Table E. 13: Mid Hunter descriptive statistics of absolute verification residuals, between AHD71-derived N values and AUSGeoid98-derived N values with bi-linear interpolation as a function of 100 m increases in AHD71.

AHD71 (m)	Count	Range (m)	Mean (m)	Min (m)	Max (m)	RMS (m)	STD (m)	Outliers
>20	82	0.286	-0.243	-0.360	-0.074	0.255	0.074	0
>100	77	0.286	-0.244	-0.360	-0.074	0.254	0.075	0
>200	54	0.285	-0.234	-0.358	-0.074	0.247	0.076	0
>300	32	0.263	-0.228	-0.337	-0.074	0.239	0.074	0
>400	22	0.263	-0.230	-0.337	-0.074	0.243	0.078	0
>500	15	0.248	-0.238	-0.322	-0.074	0.247	0.067	0
>600	13	0.248	-0.244	-0.322	-0.074	0.253	0.070	0
>700	10	0.239	-0.229	-0.312	-0.074	0.239	0.072	0
>800	6	0.239	-0.210	-0.312	-0.074	0.224	0.086	0
>900	5	0.239	-0.195	-0.312	-0.074	0.209	0.087	0
>1000	3	0.151	-0.155	-0.225	-0.074	0.167	0.076	0
>1200	2	0.151	-0.149	-0.225	-0.074	0.167	0.107	0
>1400	1	0.000	-0.074	-0.074	-0.074	0.074	N/A	0

Table E. 14: Mid Hunter descriptive statistics of absolute verification residuals, between AHD71-derived N values and AUSGeoid98-derived N values with bi-quadratic interpolation as a function of 100 m increases in AHD71.

AHD71 (m)	Count	Range (m)	Mean (m)	Min (m)	Max (m)	RMS (m)	STD (m)	Outliers
>20	82	0.287	-0.243	-0.360	-0.074	0.255	0.074	0
>100	77	0.287	-0.244	-0.360	-0.074	0.254	0.076	0
>200	54	0.287	-0.234	-0.360	-0.074	0.247	0.076	0
>300	32	0.264	-0.228	-0.338	-0.074	0.240	0.074	0
>400	22	0.264	-0.231	-0.338	-0.074	0.243	0.078	0
>500	15	0.247	-0.238	-0.321	-0.074	0.247	0.067	0
>600	13	0.247	-0.244	-0.321	-0.074	0.253	0.070	0
>700	10	0.239	-0.229	-0.312	-0.074	0.239	0.072	0
>800	6	0.239	-0.210	-0.312	-0.074	0.224	0.086	0
>900	5	0.239	-0.195	-0.312	-0.074	0.209	0.087	0
>1000	3	0.151	-0.155	-0.225	-0.074	0.167	0.076	0
>1200	2	0.151	-0.149	-0.225	-0.074	0.167	0.107	0
>1400	1	0.000	-0.074	-0.074	-0.074	0.074	N/A	0

Table E. 15: Mid Hunter descriptive statistics of absolute verification residuals, between AHD71-derived N values and AUSGeoid98-derived N values with bi-cubic interpolation as a function of 100 m increases in AHD71.

AHD71 (m)	Count	Range (m)	Mean (m)	Min (m)	Max (m)	RMS (m)	STD (m)	Outliers
>20	82	0.284	-0.243	-0.360	-0.076	0.255	0.074	0
>100	77	0.284	-0.244	-0.360	-0.076	0.254	0.075	0
>200	54	0.282	-0.234	-0.357	-0.076	0.247	0.075	0
>300	32	0.261	-0.228	-0.337	-0.076	0.240	0.074	0
>400	22	0.261	-0.231	-0.337	-0.076	0.243	0.078	0
>500	15	0.246	-0.238	-0.322	-0.076	0.247	0.067	0
>600	13	0.246	-0.245	-0.322	-0.076	0.254	0.069	0
>700	10	0.237	-0.230	-0.312	-0.076	0.239	0.072	0
>800	6	0.237	-0.210	-0.312	-0.076	0.224	0.086	0
>900	5	0.237	-0.195	-0.312	-0.076	0.210	0.086	0
>1000	3	0.149	-0.156	-0.225	-0.076	0.168	0.075	0
>1200	2	0.149	-0.150	-0.225	-0.076	0.168	0.105	0
>1400	1	0.000	-0.076	-0.076	-0.076	0.076	N/A	0

Table E.16: Mid Hunter descriptive statistics of absolute verification residuals, between AHD71-derived N values and AUSGeoid98-derived N values with bi-quartic interpolation as a function of 100 m increases in AHD71.

APPENDIX F

Graphical Representation of the Absolute Verification

LIST OF FIGURES

Figure F.1: Snowy Mountains absolute verification residuals, between AHD71-derived N values and geoids-derived (AUSGeoid09 and AUSGeoid98) N values with bi-quadratic interpolation plotted along increasing of longitudes. F-180
Figure F.2: Snowy Mountains absolute verification residuals, between AHD71-derived N values and geoids-derived (AUSGeoid09 and AUSGeoid98) N values with bi-cubic interpolation plotted along increasing of longitudes. F-180
Figure F.3: Snowy Mountains absolute verification residuals, between AHD71-derived N values and geoids-derived (AUSGeoid09 and AUSGeoid98) N values with bi-quartic interpolation plotted along increasing of longitudes. F-181
Figure F.4: Snowy Mountains absolute verification residuals, between AHD71-derived N values and geoids-derived (AUSGeoid09 and AUSGeoid98) N values with bi-quadratic interpolation plotted along increasing of latitudes. F-181
Figure F.5: Snowy Mountains absolute verification residuals, between AHD71-derived N values and geoids-derived (AUSGeoid09 and AUSGeoid98) N values with bi-cubic interpolation plotted along increasing of latitudes. F-182
Figure F.6: Snowy Mountains absolute verification residuals, between AHD71-derived N values and geoids-derived (AUSGeoid09 and AUSGeoid98) N values with bi-quartic interpolation plotted along increasing of latitudes. F-182
Figure F.7: Snowy Mountains absolute verification residuals, between AHD71-derived N values and geoids-derived (AUSGeoid09 and AUSGeoid98) N values with bi-quadratic interpolation plotted along increasing of AHD71. ..... F-183
Figure F.8: Snowy Mountains absolute verification residuals, between AHD71-derived N values and geoids-derived (AUSGeoid09 and AUSGeoid98) N values with bi-cubic interpolation plotted along increasing of AHD71. ..... F-183
Figure F.9: Snowy Mountains absolute verification residuals, between AHD71-derived N values and geoids-derived (AUSGeoid09 and AUSGeoid98) N values with bi-quartic interpolation plotted along increasing of AHD71. ..... F-184
Figure F.10: Mid Hunter absolute verification residuals, between AHD71-derived N values and geoids-derived (AUSGeoid09 and AUSGeoid98) N values with bi-quadratic interpolation plotted along increasing of longitudes. F-184

Figure F.11: Mid Hunter absolute verification residuals, between AHD71-derived N values and geoids-derived (AUSGeoid09 and AUSGeoid98) N values with bi-cubic interpolation plotted along increasing of longitudes. F-185
Figure F.12: Mid Hunter absolute verification residuals, between AHD71-derived N values and geoids-derived (AUSGeoid09 and AUSGeoid98) N values with bi-quartic interpolation plotted along increasing of longitudes. F-185
Figure F.13: Mid Hunter absolute verification residuals, between AHD71-derived N values and geoids-derived (AUSGeoid09 and AUSGeoid98) N values with bi-quadratic interpolation plotted along increasing of latitudes. F-186
Figure F.14: Mid Hunter absolute verification residuals between AHD71-derived N values and geoids-derived (AUSGeoid09 and AUSGeoid98) N values with bi-cubic interpolation plotted along increasing of latitudes. F-186
Figure F.15: Mid Hunter absolute verification residuals, between AHD71-derived N values and geoids-derived (AUSGeoid09 and AUSGeoid98) N values with bi-quartic interpolation plotted along increasing of latitudes. F-187
Figure F.16: Mid Hunter absolute verification residuals, between AHD71-derived N values and geoids-derived (AUSGeoid09 and AUSGeoid98) N values with bi-quadratic interpolation plotted along increasing of AHD71. ..... F-187
Figure F.17: Mid Hunter absolute verification residuals, between AHD71-derived N values and geoids-derived (AUSGeoid09 and AUSGeoid98) N values with bi-cubic interpolation plotted along increasing of AHD71. ..... F-188
Figure F.18: Mid Hunter absolute verification residuals, between AHD71-derived N values and geoids-derived (AUSGeoid09 and AUSGeoid98) N values with bi-quartic interpolation plotted along increasing of AHD71. ..... F-188

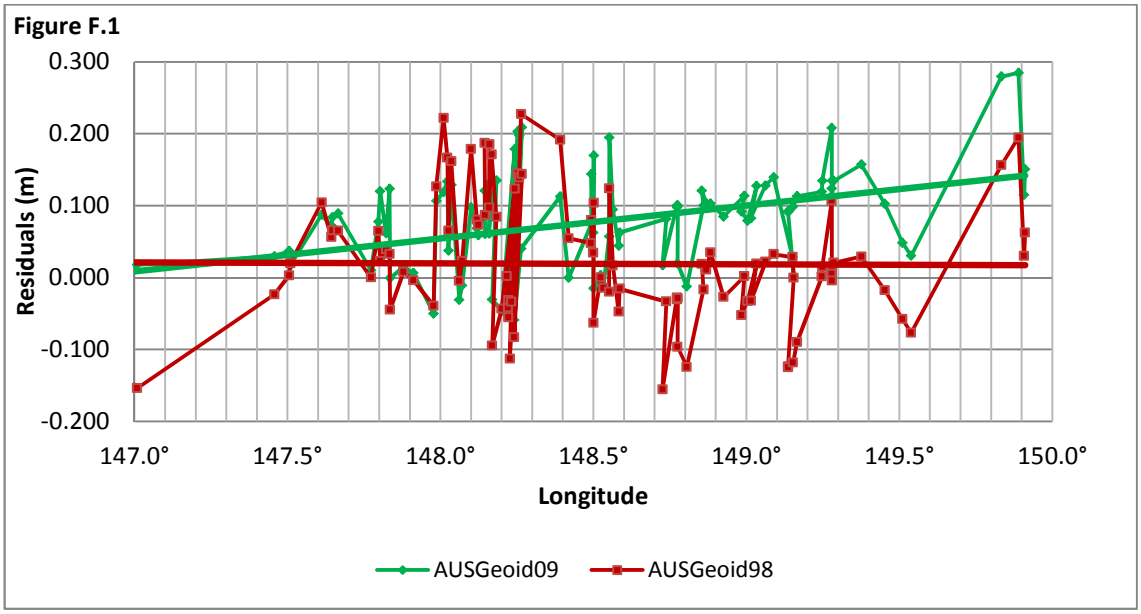

Figure F.1: Snowy Mountains absolute verification residuals, between AHD71-derived N values and geoids-derived (AUSGeoid09 and AUSGeoid98) N values with bi-quadratic interpolation plotted along increasing of longitudes.

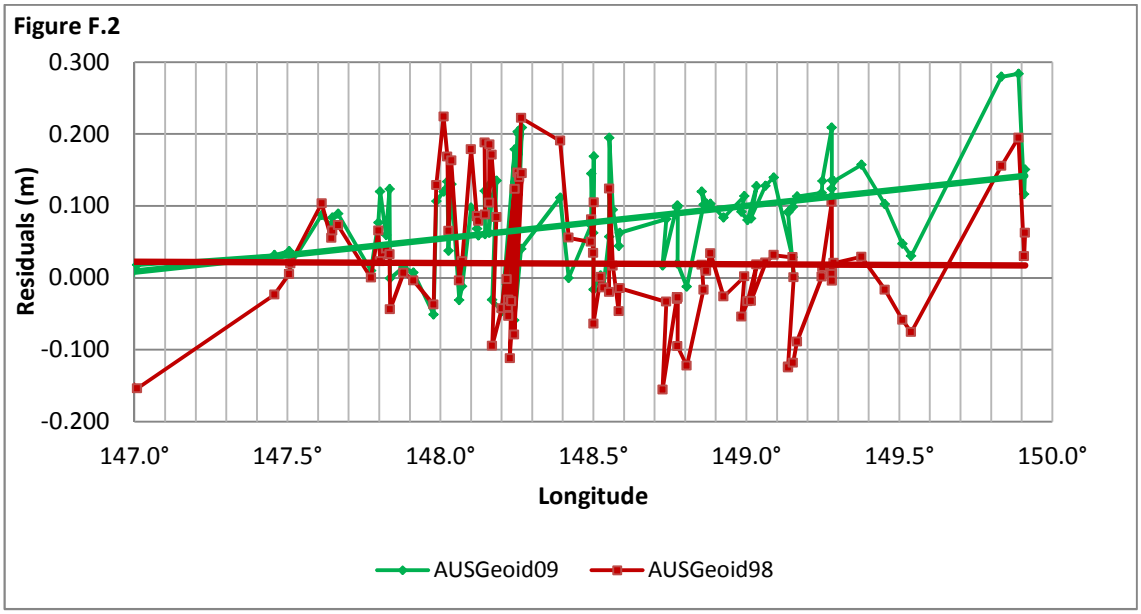

Figure F.2: Snowy Mountains absolute verification residuals, between AHD71-derived N values and geoids-derived (AUSGeoid09 and AUSGeoid98) N values with bi-cubic interpolation plotted along increasing of longitudes.

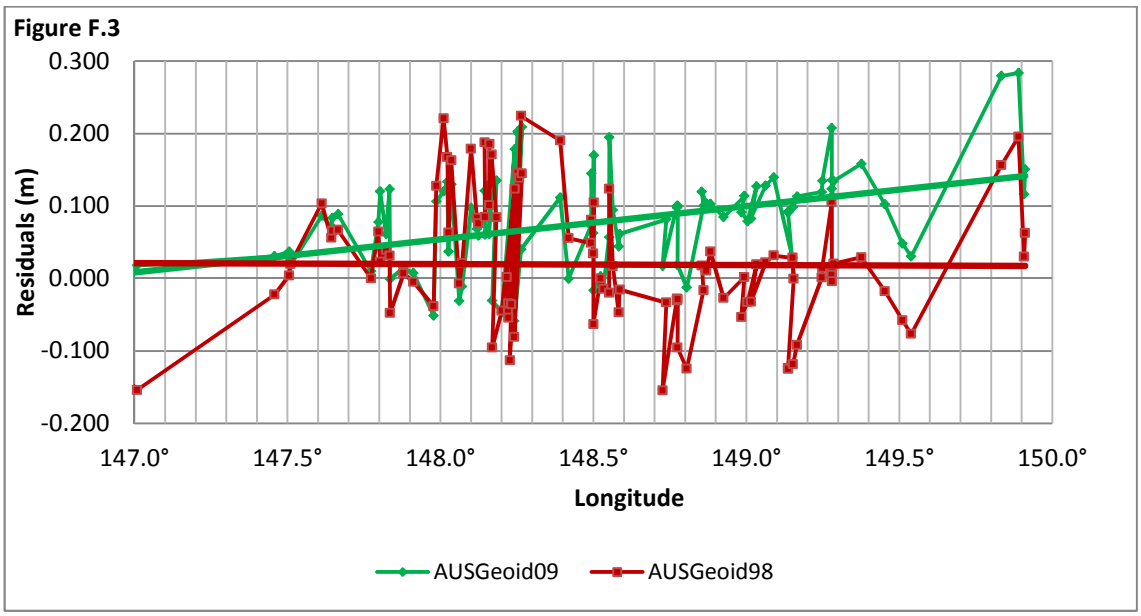

Figure F.3: Snowy Mountains absolute verification residuals, between AHD71-derived N values and geoids-derived (AUSGeoid09 and AUSGeoid98) N values with bi-quartic interpolation plotted along increasing of longitudes.

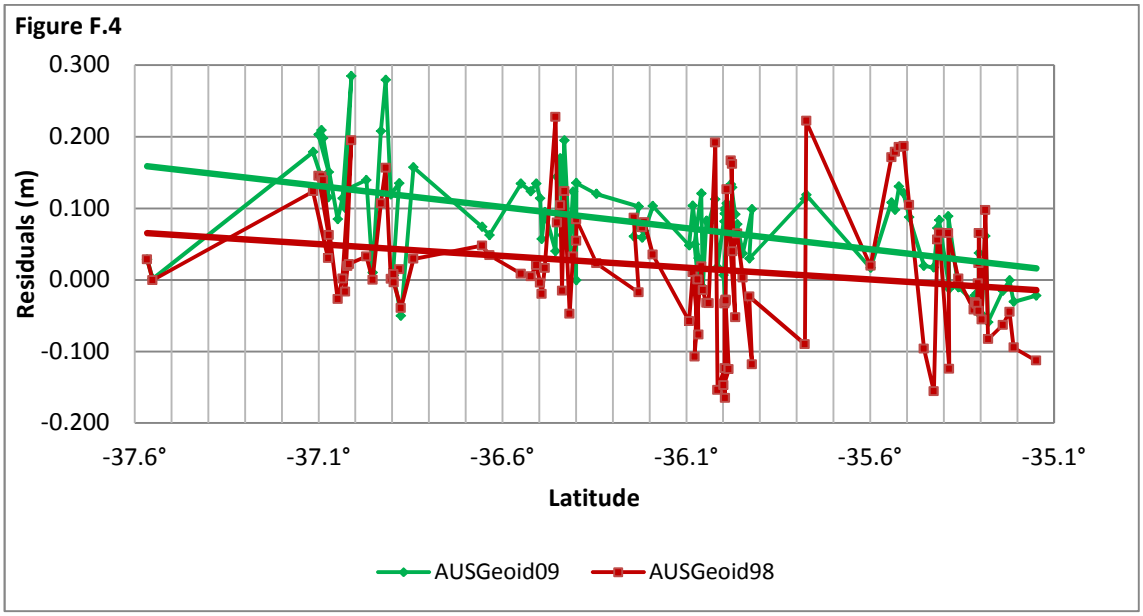

Figure F.4: Snowy Mountains absolute verification residuals, between AHD71-derived N values and geoids-derived (AUSGeoid09 and AUSGeoid98) N values with bi-quadratic interpolation plotted along increasing of latitudes.

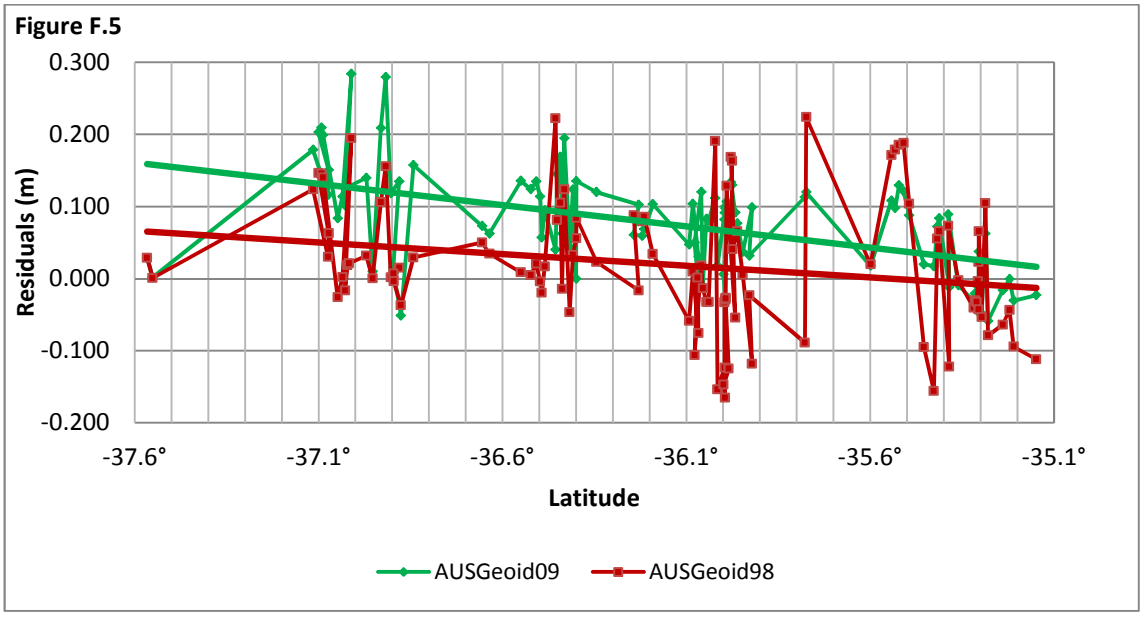

Figure F.5: Snowy Mountains absolute verification residuals, between AHD71-derived N values and geoids-derived (AUSGeoid09 and AUSGeoid98) N values with bi-cubic interpolation plotted along increasing of latitudes.

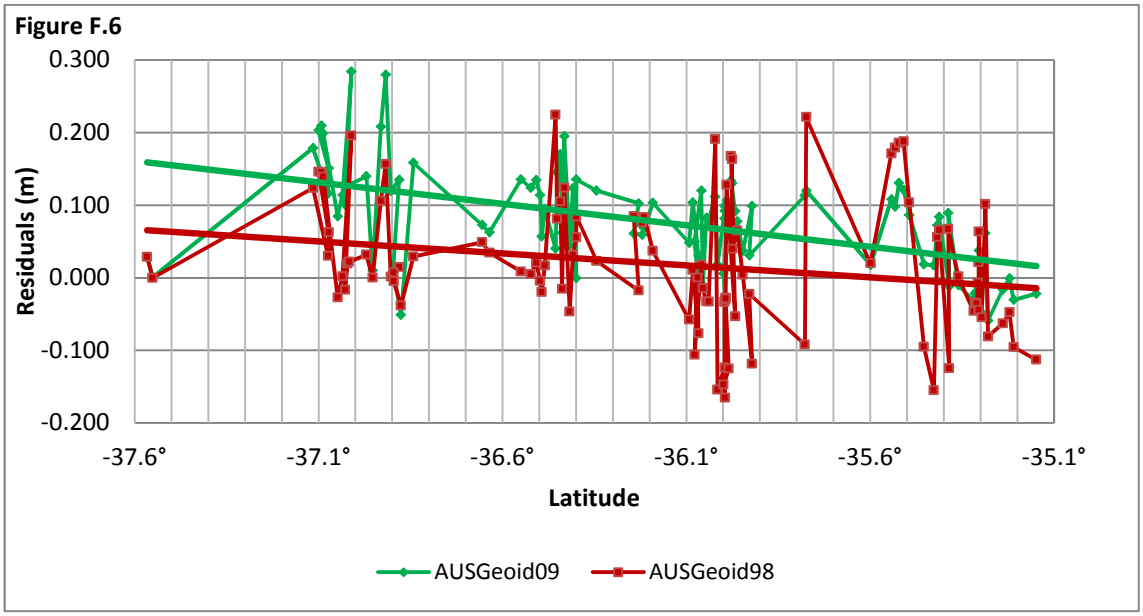

Figure F.6: Snowy Mountains absolute verification residuals, between AHD71-derived N values and geoids-derived (AUSGeoid09 and AUSGeoid98) N values with bi-quartic interpolation plotted along increasing of latitudes.

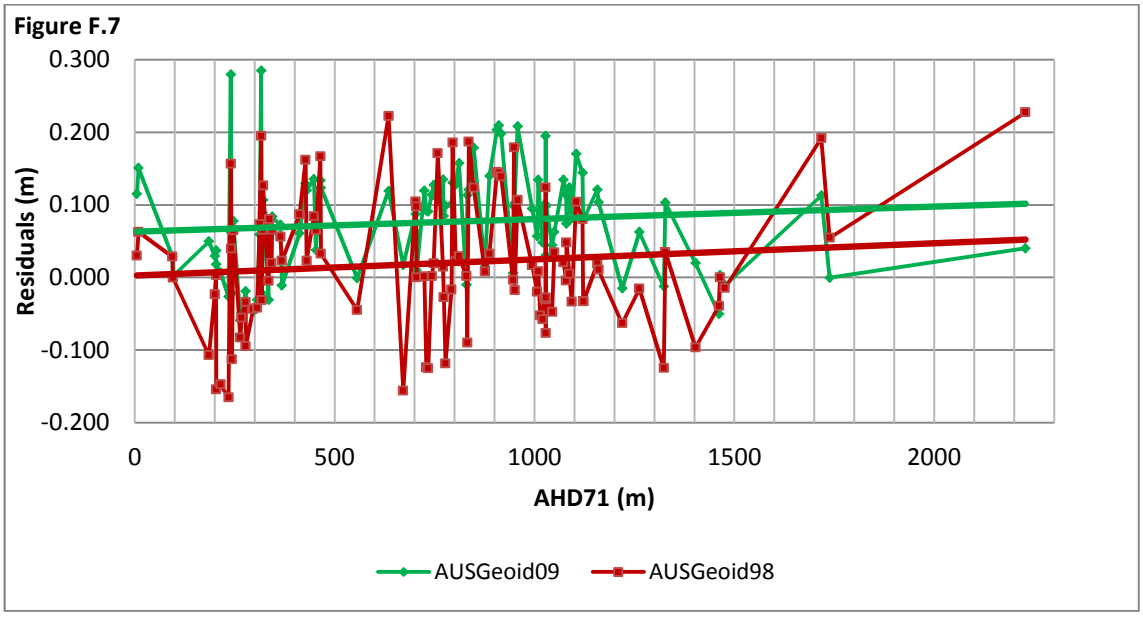

Figure F.7: Snowy Mountains absolute verification residuals, between AHD71-derived N values and geoids-derived (AUSGeoid09 and AUSGeoid98) N values with bi-quadratic interpolation plotted along increasing of AHD71.

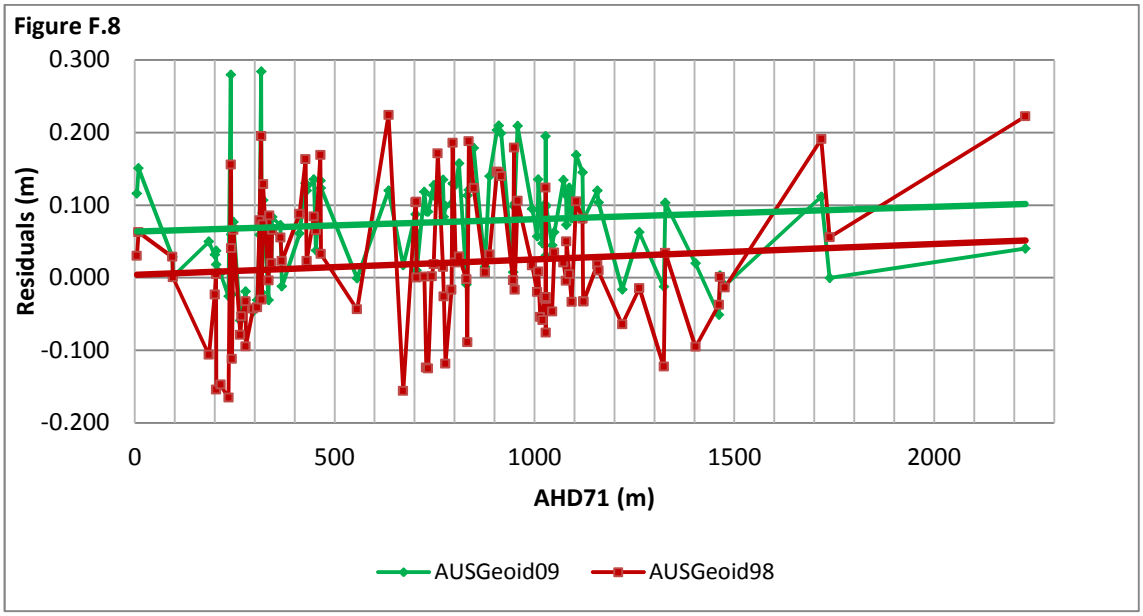

Figure F.8: Snowy Mountains absolute verification residuals, between AHD71-derived N values and geoids-derived (AUSGeoid09 and AUSGeoid98) N values with bi-cubic interpolation plotted along increasing of AHD71.

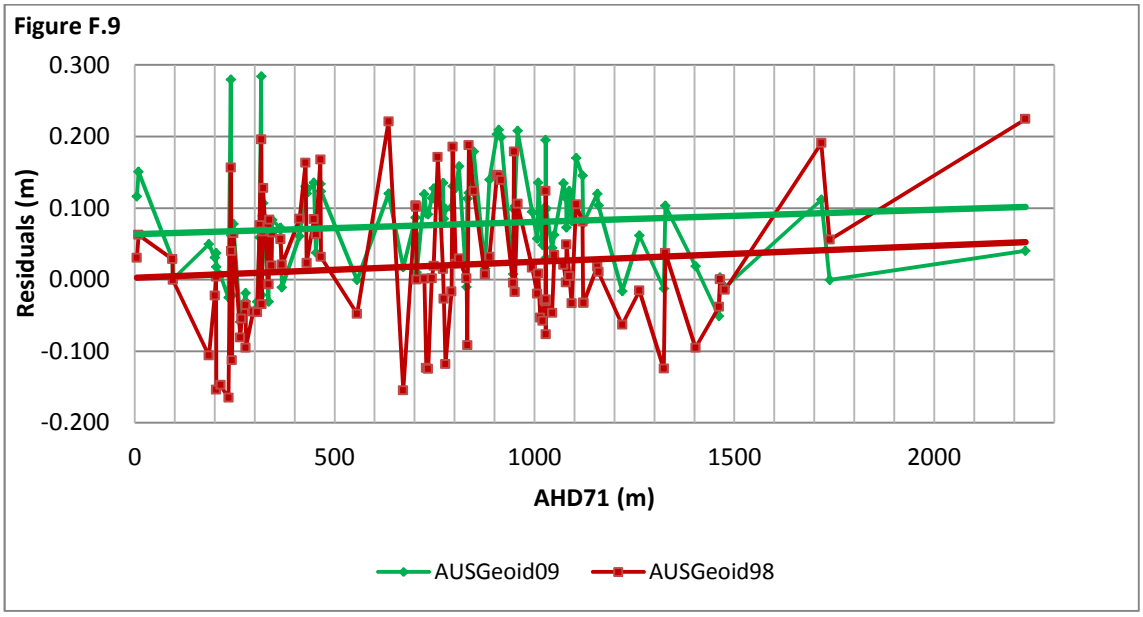

Figure F.9: Snowy Mountains absolute verification residuals, between AHD71-derived N values and geoids-derived (AUSGeoid09 and AUSGeoid98) N values with bi-quartic interpolation plotted along increasing of AHD71.

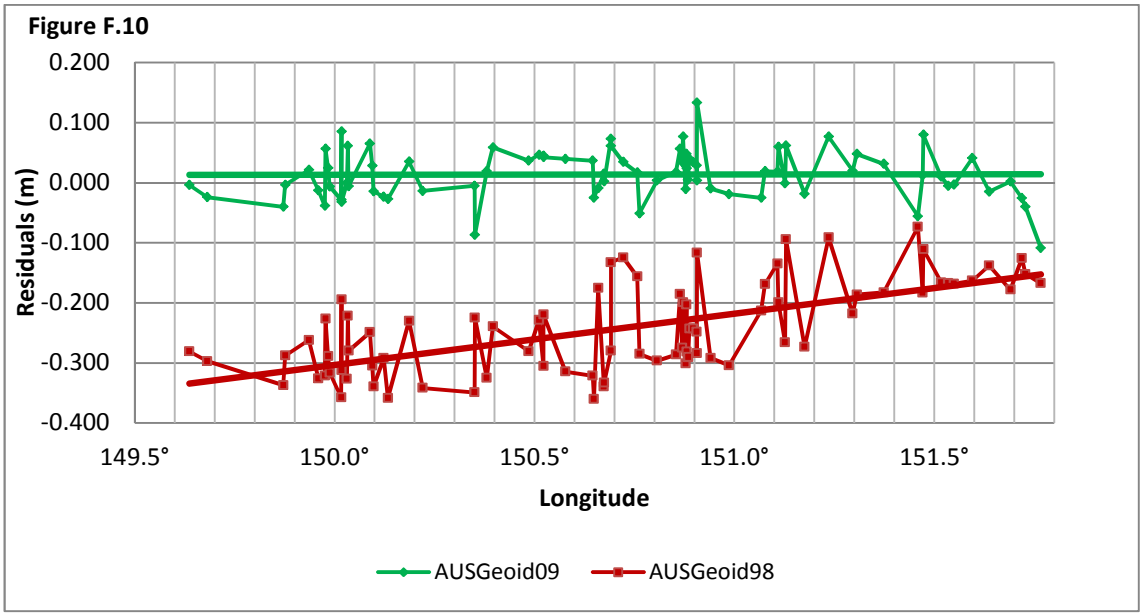

Figure F.10: Mid Hunter absolute verification residuals, between AHD71-derived N values and geoids-derived (AUSGeoid09 and AUSGeoid98) N values with bi-quadratic interpolation plotted along increasing of longitudes.

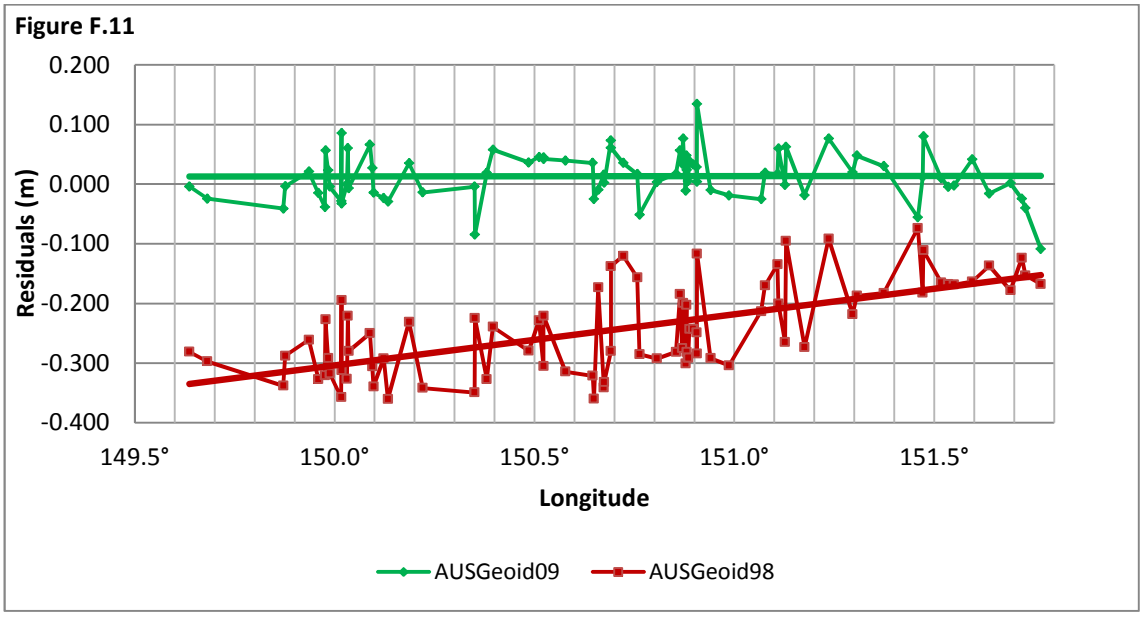

Figure F.11: Mid Hunter absolute verification residuals, between AHD71-derived N values and geoids-derived (AUSGeoid09 and AUSGeoid98) N values with bi-cubic interpolation plotted along increasing of longitudes.

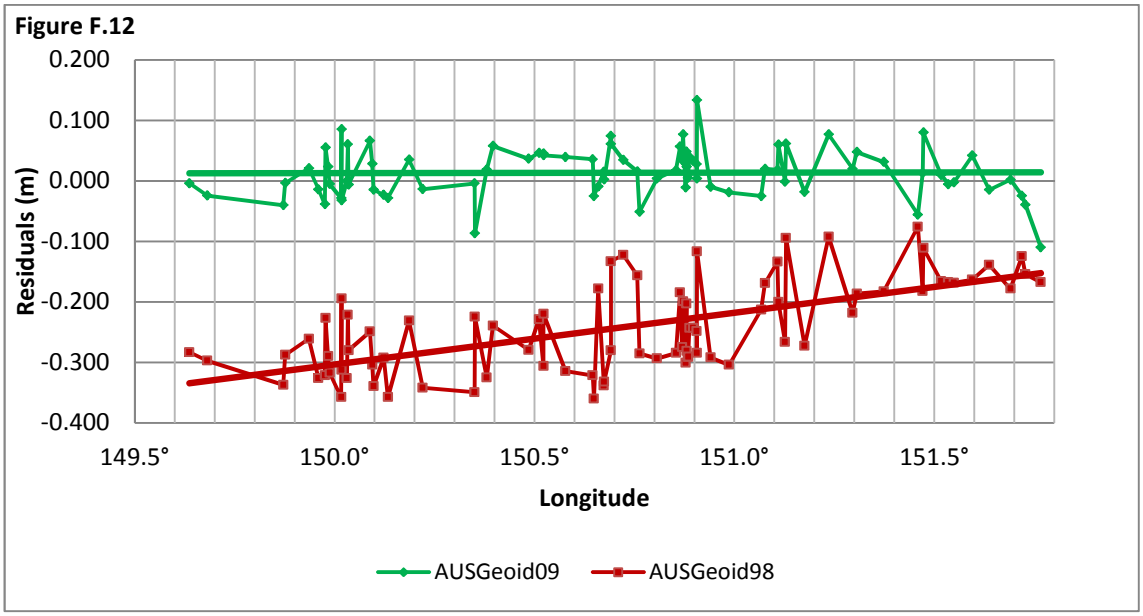

Figure F.12: Mid Hunter absolute verification residuals, between AHD71-derived N values and geoids-derived (AUSGeoid09 and AUSGeoid98) N values with bi-quartic interpolation plotted along increasing of longitudes.

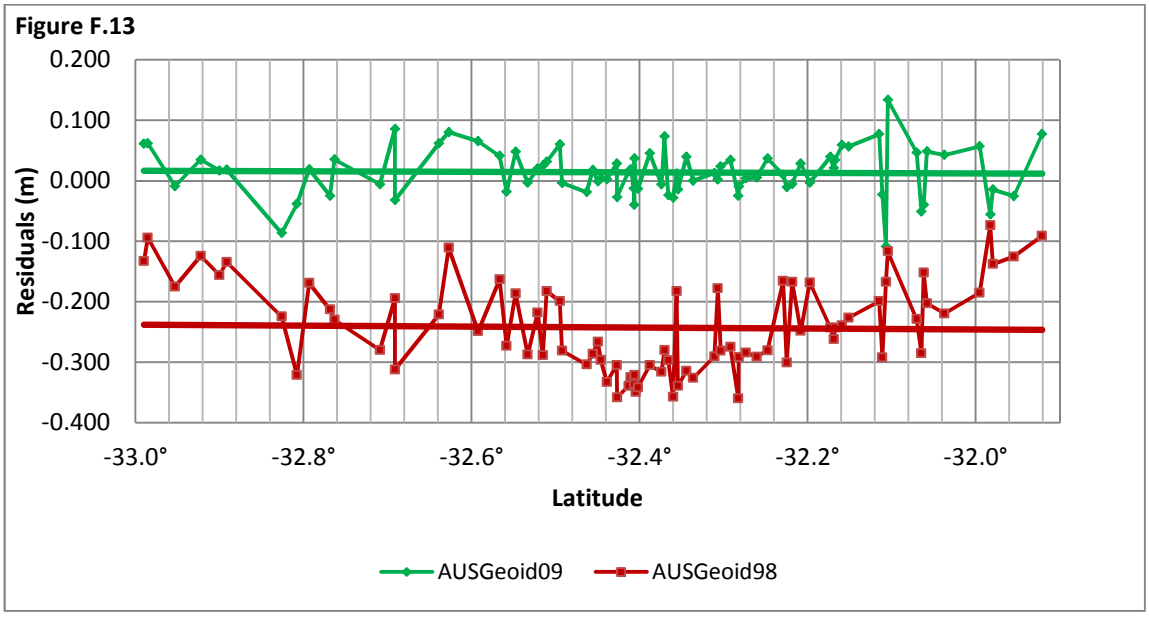

Figure F.13: Mid Hunter absolute verification residuals, between AHD71-derived N values and geoids-derived (AUSGeoid09 and AUSGeoid98) N values with bi-quadratic interpolation plotted along increasing of latitudes.

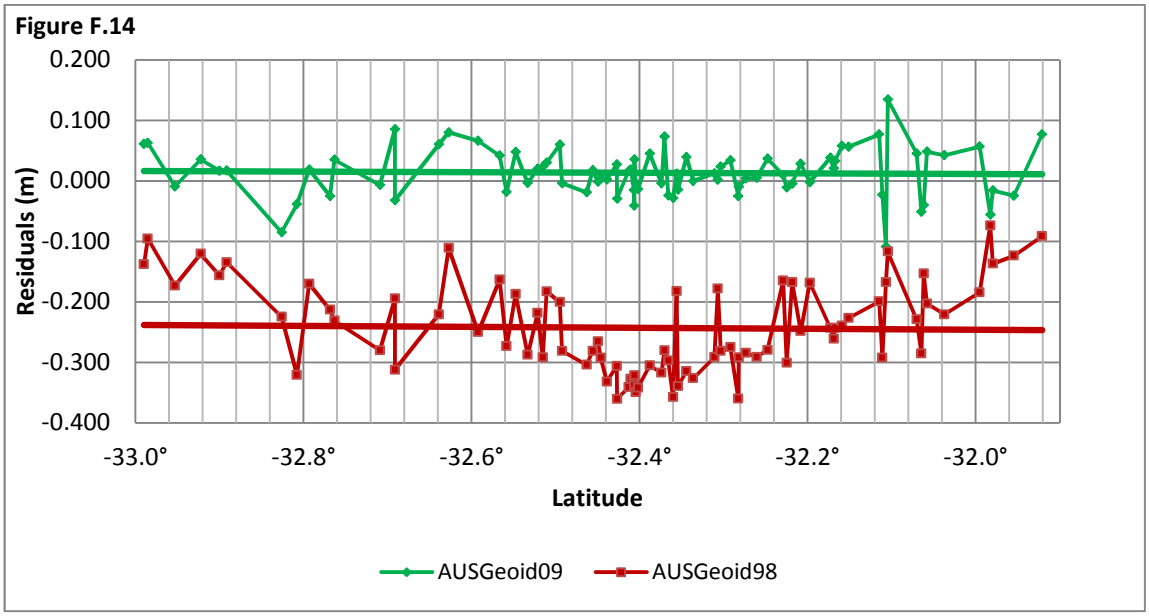

Figure F.14: Mid Hunter absolute verification residuals between AHD71-derived N values and geoids-derived (AUSGeoid09 and AUSGeoid98) N values with bi-cubic interpolation plotted along increasing of latitudes.

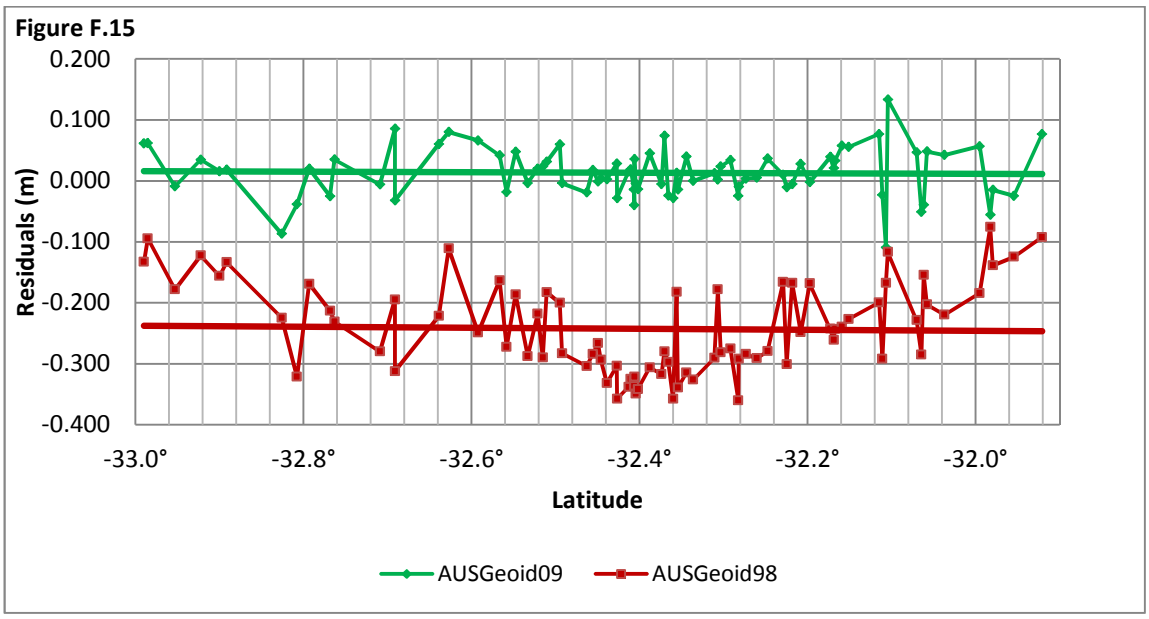

Figure F.15: Mid Hunter absolute verification residuals, between AHD71-derived N values and geoids-derived (AUSGeoid09 and AUSGeoid98) N values with bi-quartic interpolation plotted along increasing of latitudes.

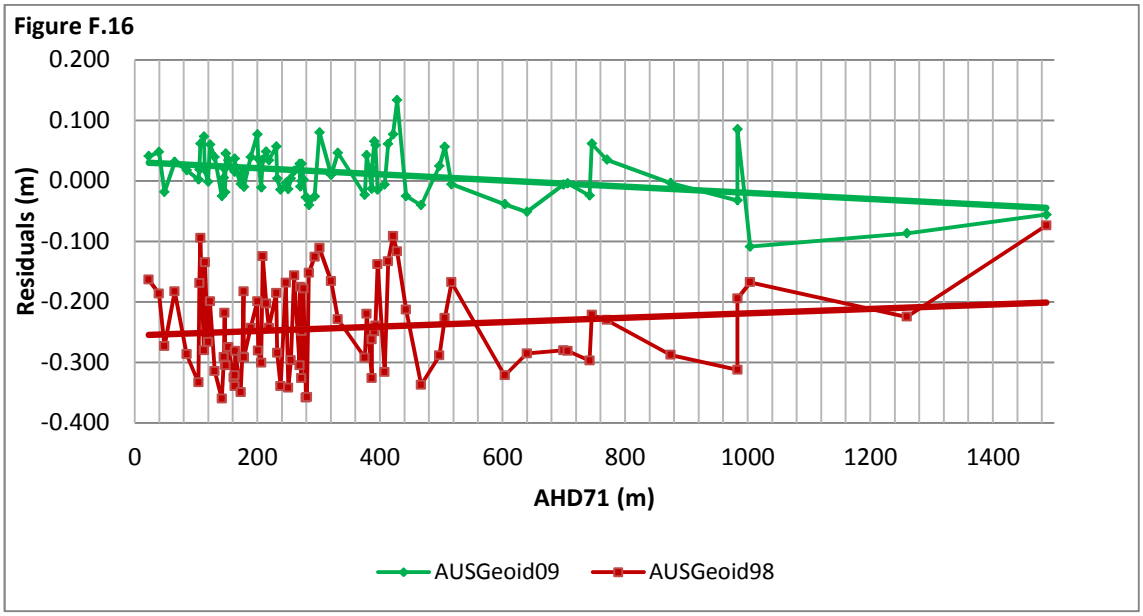

Figure F.16: Mid Hunter absolute verification residuals, between AHD71-derived N values and geoids-derived (AUSGeoid09 and AUSGeoid98) N values with bi-quadratic interpolation plotted along increasing of AHD71.

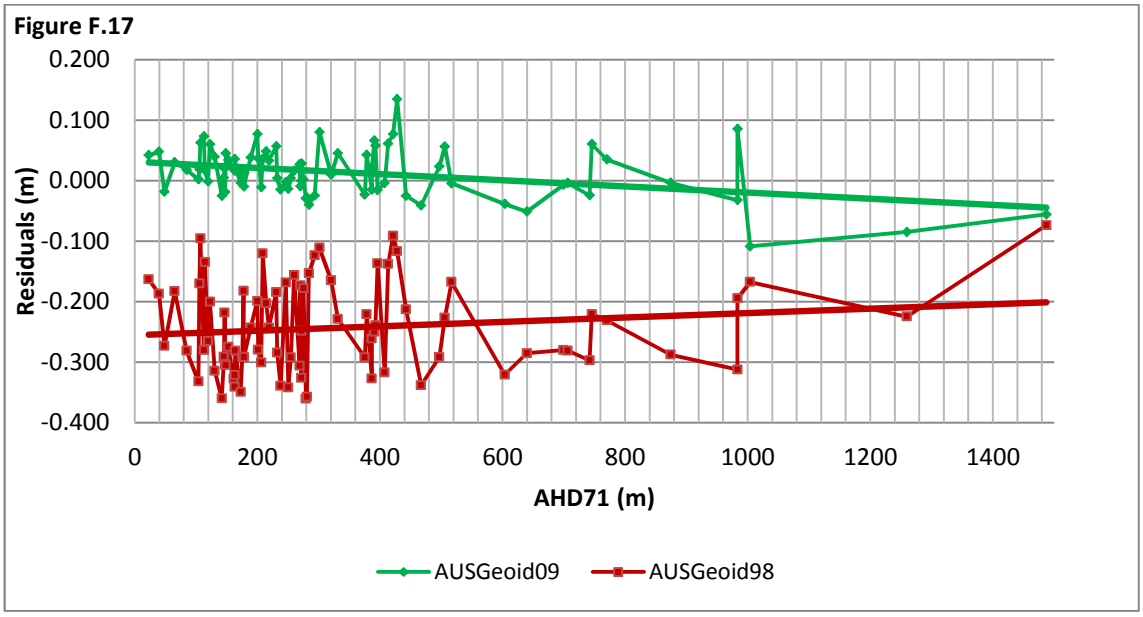

Figure F.17: Mid Hunter absolute verification residuals, between AHD71-derived N values and geoids-derived (AUSGeoid09 and AUSGeoid98) N values with bi-cubic interpolation plotted along increasing of AHD71.

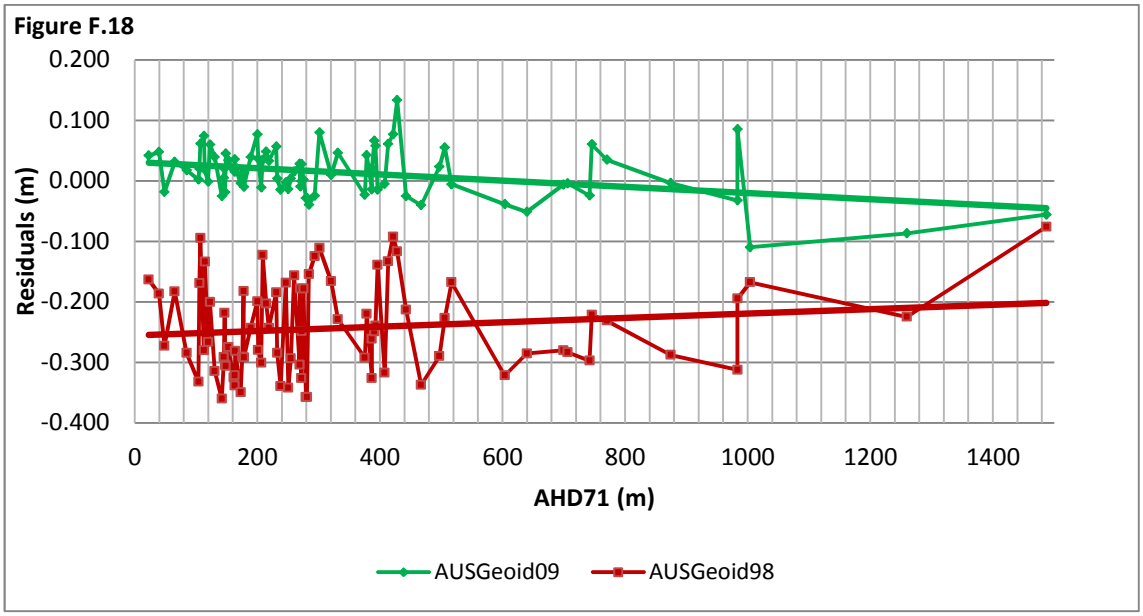

Figure F.18: Mid Hunter absolute verification residuals, between AHD71-derived N values and geoids-derived (AUSGeoid09 and AUSGeoid98) N values with bi-quartic interpolation plotted along increasing of AHD71.

APPENDIX G

Graphical Representation of the Relative Verification

LIST OF FIGURES

Figure G.1: Snowy Mountains relative verification residuals, between AHD71 and AUSGeoid09 (with bi-cubic interpolation) over 66 observed baselines, plotted together with current allowable 3rd order differential levelling miscloses.....G-191
Figure G.2: Snowy Mountains relative verification residuals, between AHD71 and AUSGeoid98 (with bi-cubic interpolation) over 66 observed baselines, plotted together with current allowable 3rd order differential levelling miscloses.....G-191
Figure G.3: Snowy Mountains relative verification residuals, between AHD71 and AUSGeoid09 (with bi-cubic interpolation) over 5,356 possible baselines, plotted together with current allowable 3rd order differential levelling miscloses.....G-192
Figure G.4: Snowy Mountains relative verification residuals, between AHD71 and AUSGeoid98 (with bi-cubic interpolation) over 5,356 possible baselines, plotted together with current allowable 3rd order differential levelling miscloses.....G-192
Figure G.5: Mid Hunter relative verification residuals, between AHD71 and AUSGeoid09 (with bi-cubic interpolation) over 104 observed baselines, plotted together with current allowable 3rd order differential levelling miscloses.....G-193
Figure G.6: Mid Hunter relative verification residuals, between AHD71 and AUSGeoid98 (with bi-cubic interpolation) over 104 observed baselines, plotted together with current allowable 3rd order differential levelling miscloses.....G-193
Figure G.7: Mid Hunter relative verification residuals, between AHD71 and AUSGeoid09 (with bi-cubic interpolation) over 3,320 possible baselines, plotted together with current allowable 3rd order differential levelling miscloses.....G-194
Figure G.8: Mid Hunter relative verification residuals, between AHD71 and AUSGeoid98 (with bi-cubic interpolation) over 3,320 possible baselines, plotted together with current allowable 3rd order differential levelling miscloses.....G-194

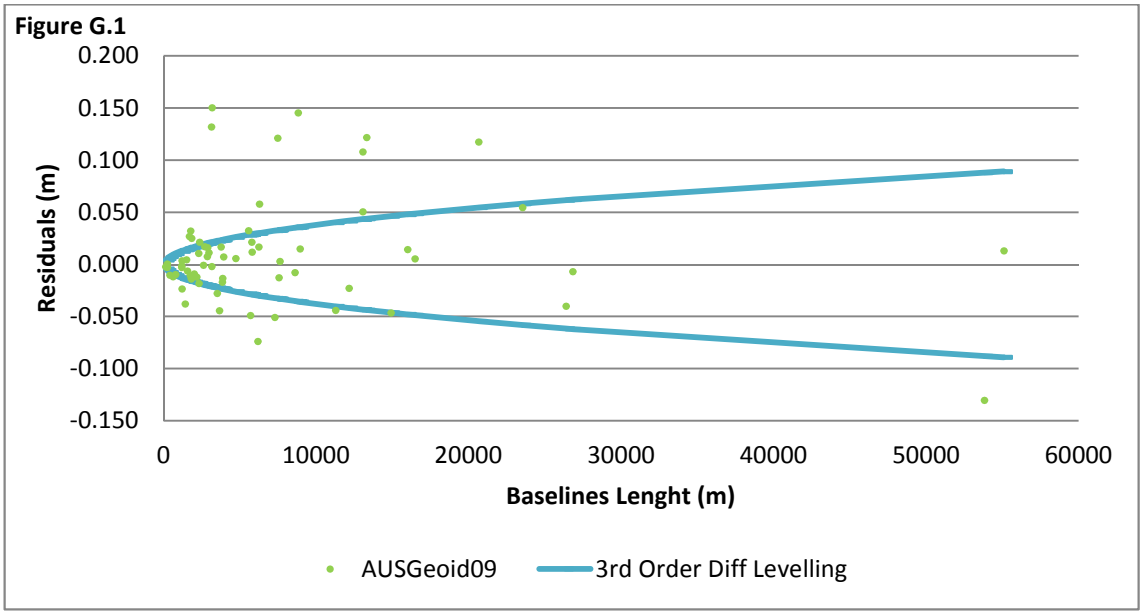

Figure G.1: Snowy Mountains relative verification residuals, between AHD71 and AUSGeoid09 (with bi-cubic interpolation) over 66 observed baselines, plotted together with current allowable 3rd order differential levelling miscloses.

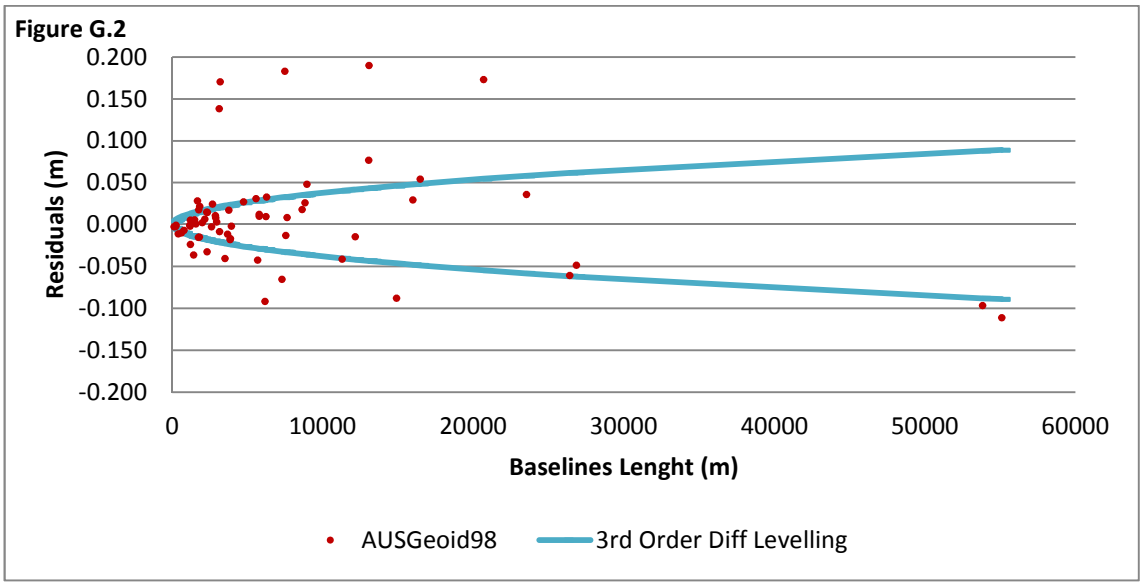

Figure G.2: Snowy Mountains relative verification residuals, between AHD71 and AUSGeoid98 (with bi-cubic interpolation) over 66 observed baselines, plotted together with current allowable 3rd order differential levelling miscloses.

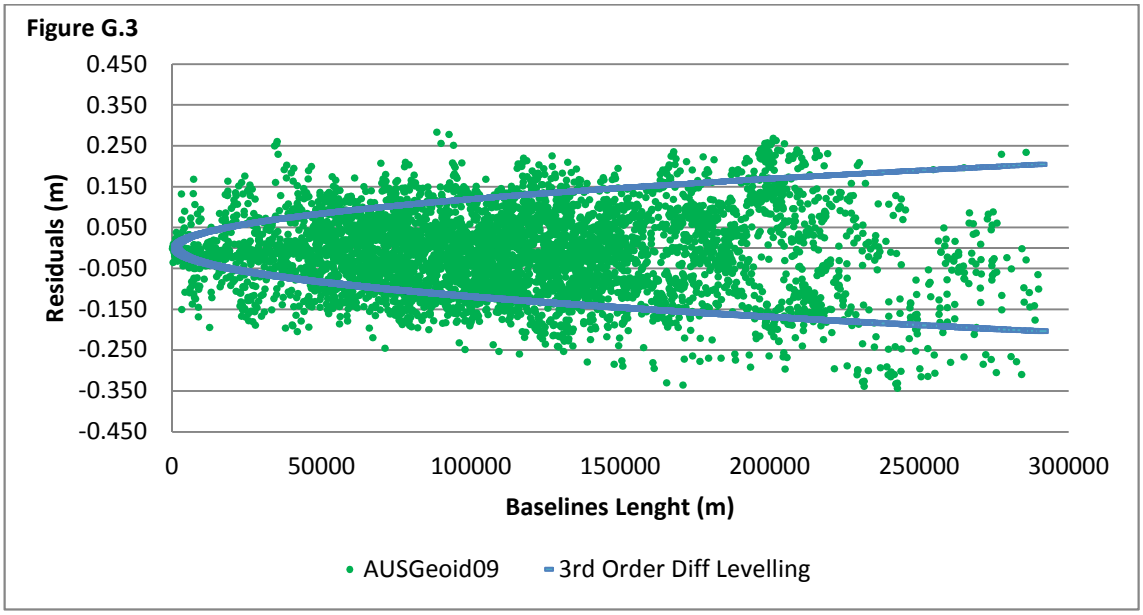

Figure G.3: Snowy Mountains relative verification residuals, between AHD71 and AUSGeoid09 (with bi-cubic interpolation) over 5,356 possible baselines, plotted together with current allowable 3rd order differential levelling miscloses.

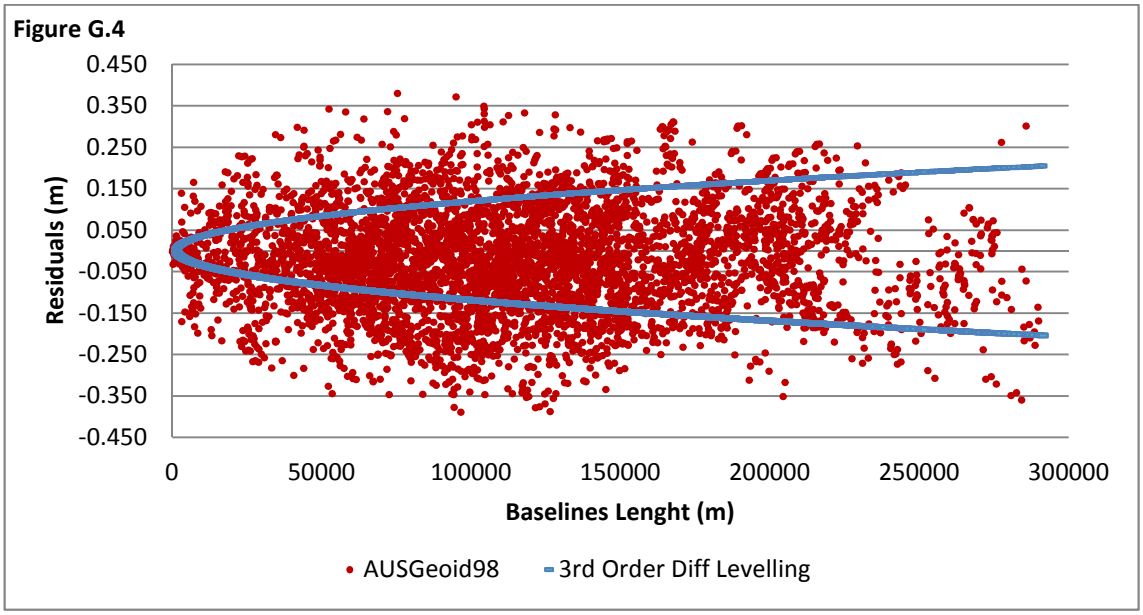

Figure G.4: Snowy Mountains relative verification residuals, between AHD71 and AUSGeoid98 (with bi-cubic interpolation) over 5,356 possible baselines, plotted together with current allowable 3rd order differential levelling miscloses.

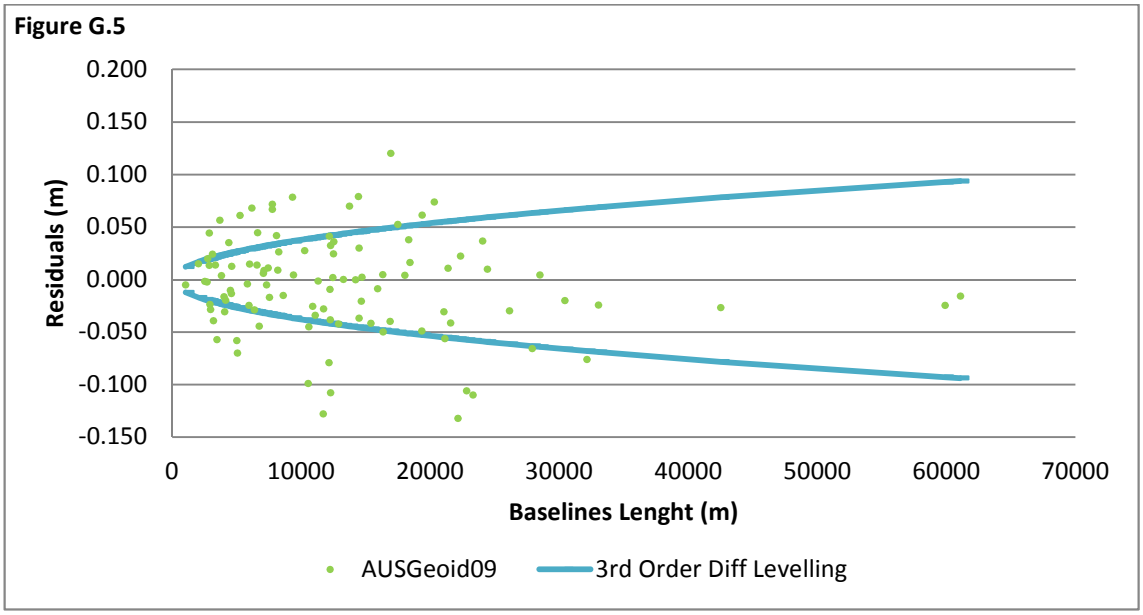

Figure G.5: Mid Hunter relative verification residuals, between AHD71 and AUSGeoid09 (with bi-cubic interpolation) over 104 observed baselines, plotted together with current allowable 3rd order differential levelling miscloses.

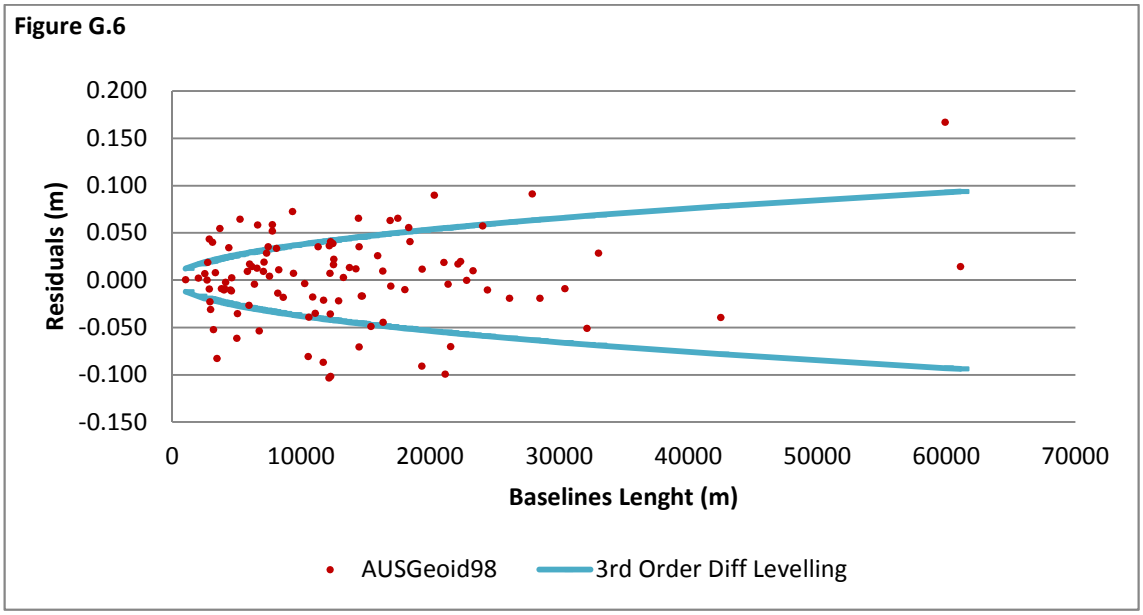

Figure G.6: Mid Hunter relative verification residuals, between AHD71 and AUSGeoid98 (with bi-cubic interpolation) over 104 observed baselines, plotted together with current allowable 3rd order differential levelling miscloses.

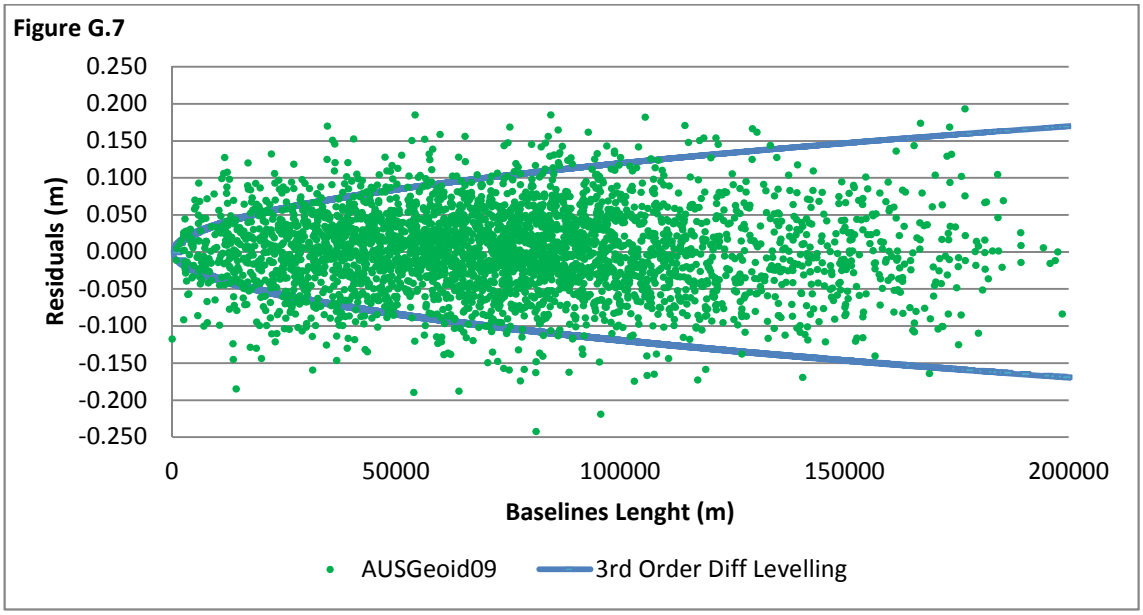

Figure G.7: Mid Hunter relative verification residuals, between AHD71 and AUSGeoid09 (with bi-cubic interpolation) over 3,320 possible baselines, plotted together with current allowable 3rd order differential levelling miscloses.

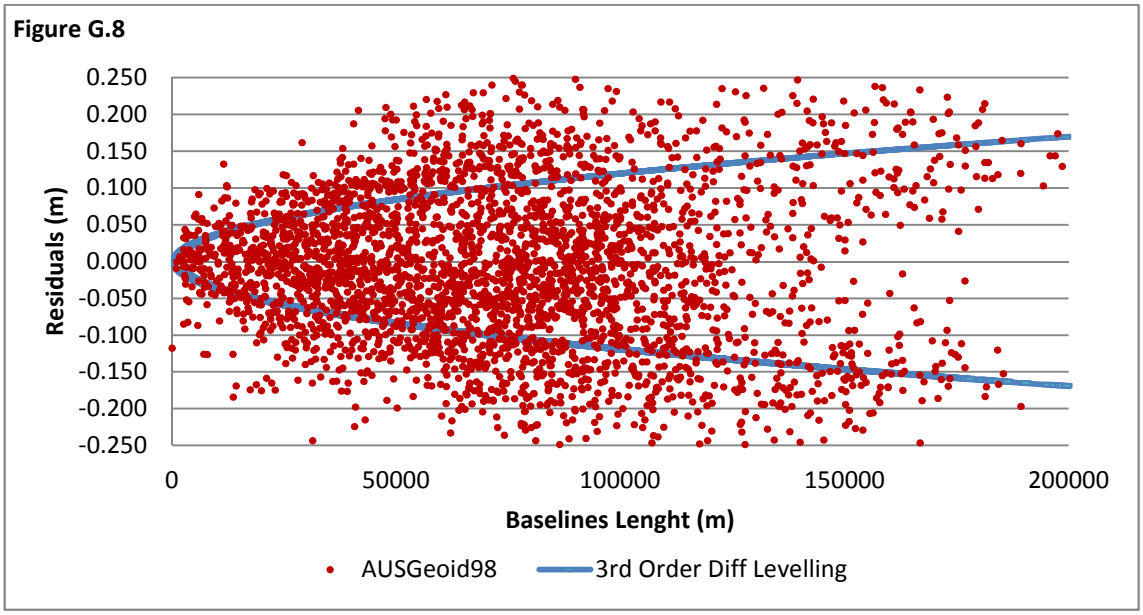

Figure G.8: Mid Hunter relative verification residuals, between AHD71 and AUSGeoid98 (with bi-cubic interpolation) over 3,320 possible baselines, plotted together with current allowable 3rd order differential levelling miscloses.

APPENDIX H

Descriptive Statistics of Relative Verification Residuals as a Function of Rise in Difference in Elevation

LIST OF TABLES

Table H.1: Snowy Mountains descriptive statistics of relative verification residuals, between AHD71 and AUSGeoid09 as a function of 100 m increase of difference in elevation. H-197

Table H.2: Snowy Mountains descriptive statistics of relative verification residuals, between AHD71 and AUSGeoid98 as a function of 100 m increase of difference in elevation. H-198

Table H.3: Mid Hunter descriptive statistics of relative verification residuals, between AHD71 and AUSGeoid09 as a function of 100 m increase of difference in elevation. .H-199

Table H.4: Mid Hunter descriptive statistics of relative verification residuals, between AHD71 and AUSGeoid98 as a function of 100 m increase of difference in elevation. .H-200

ΔAHD (m)	Count (m)	Range (m)	Mean (m)	Min (m)	Max (m)	RMS (m)	STD (m)	Kurtosis	Outliers
>0	5356	0.625	-0.012	-0.343	0.282	0.099	0.099	-0.018	15
>100	4492	0.617	-0.009	-0.335	0.282	0.101	0.100	-0.289	2
>200	3856	0.617	-0.011	-0.335	0.282	0.102	0.101	-0.289	2
>300	3295	0.603	-0.012	-0.335	0.268	0.104	0.103	-0.353	2
>400	2769	0.603	-0.012	-0.335	0.268	0.108	0.107	-0.484	1
>500	2280	0.603	-0.013	-0.335	0.268	0.108	0.107	-0.393	1
>600	1826	0.603	-0.015	-0.335	0.268	0.106	0.105	-0.306	2
>700	1380	0.567	-0.019	-0.335	0.232	0.104	0.102	-0.427	2
>800	925	0.544	-0.023	-0.335	0.209	0.100	0.097	-0.174	2
>900	631	0.528	-0.024	-0.335	0.193	0.093	0.090	0.523	6
>1000	454	0.516	-0.029	-0.335	0.181	0.093	0.089	0.847	4
>1100	314	0.504	-0.029	-0.335	0.169	0.092	0.088	1.109	3
>1200	217	0.500	-0.029	-0.331	0.169	0.095	0.090	0.555	1
>1300	152	0.453	-0.032	-0.284	0.169	0.094	0.089	-0.041	0
>1400	113	0.401	-0.036	-0.284	0.117	0.096	0.090	-0.160	0
>1500	64	0.353	-0.021	-0.243	0.110	0.076	0.073	1.021	1
>1600	47	0.353	-0.020	-0.243	0.110	0.081	0.079	0.930	0
>1700	42	0.338	-0.028	-0.243	0.095	0.083	0.079	0.935	0
>1800	33	0.333	-0.036	-0.243	0.090	0.081	0.074	1.987	0
>1900	25	0.310	-0.047	-0.243	0.066	0.089	0.077	1.585	0
>2000	9	0.149	-0.024	-0.110	0.039	0.049	0.045	0.602	0
>2100	4	0.149	-0.034	-0.110	0.039	0.070	0.071	-4.195	0
>2200	2	0.034	-0.093	-0.110	-0.076	0.095	0.024	N/A	0

Table H.1: Snowy Mountains descriptive statistics of relative verification residuals, between AHD71 and AUSGeoid09 as a function of 100 m increase of difference in elevation.

ΔAHD (m)	Count (m)	Range (m)	Mean (m)	Min (m)	Max (m)	RMS (m)	STD (m)	Kurtosis	Outliers
>0	5356	0.769	-0.024	-0.389	0.380	0.127	0.124	-0.157	3
>100	4492	0.761	-0.023	-0.389	0.371	0.128	0.126	-0.227	1
>200	3856	0.761	-0.026	-0.389	0.371	0.128	0.125	-0.162	1
>300	3295	0.761	-0.029	-0.389	0.371	0.128	0.125	-0.146	1
>400	2769	0.761	-0.029	-0.389	0.371	0.129	0.126	-0.149	1
>500	2280	0.720	-0.029	-0.388	0.333	0.129	0.126	-0.177	0
>600	1826	0.716	-0.032	-0.388	0.329	0.129	0.124	-0.070	0
>700	1380	0.716	-0.039	-0.388	0.329	0.128	0.122	-0.057	2
>800	925	0.716	-0.047	-0.388	0.329	0.132	0.124	-0.246	1
>900	631	0.716	-0.058	-0.388	0.329	0.139	0.127	-0.147	1
>1000	454	0.716	-0.067	-0.388	0.329	0.145	0.129	0.009	1
>1100	314	0.716	-0.072	-0.388	0.329	0.155	0.138	-0.176	0
>1200	217	0.716	-0.076	-0.388	0.329	0.169	0.151	-0.400	0
>1300	152	0.716	-0.091	-0.388	0.329	0.182	0.159	-0.251	0
>1400	113	0.716	-0.106	-0.388	0.329	0.199	0.170	-0.534	0
>1500	64	0.716	-0.087	-0.388	0.329	0.214	0.197	-1.077	0
>1600	47	0.716	-0.082	-0.388	0.329	0.210	0.196	-1.065	0
>1700	42	0.716	-0.109	-0.388	0.329	0.215	0.188	-0.677	0
>1800	33	0.716	-0.125	-0.388	0.329	0.232	0.199	-0.538	0
>1900	25	0.716	-0.136	-0.388	0.329	0.249	0.214	-0.543	0
>2000	9	0.705	-0.013	-0.376	0.329	0.267	0.283	-2.093	0
>2100	4	0.062	0.192	0.160	0.222	0.193	0.025	1.522	0
>2200	2	0.032	0.176	0.160	0.192	0.079	0.023	N/A	0

Table H.2: Snowy Mountains descriptive statistics of relative verification residuals, between AHD71 and AUSGeoid98 as a function of 100 m increase of difference in elevation.

ΔAHD (m)	Count (m)	Range (m)	Mean (m)	Min (m)	Max (m)	RMS (m)	STD (m)	Kurtosis	Outliers
>0	3321	0.437	0.001	-0.243	0.194	0.056	0.057	0.323	14
>100	2315	0.428	0.002	-0.243	0.185	0.061	0.061	0.093	7
>200	1556	0.428	0.004	-0.243	0.185	0.065	0.065	-0.122	2
>300	1061	0.428	0.008	-0.243	0.185	0.069	0.069	-0.256	2
>400	786	0.428	0.013	-0.243	0.185	0.074	0.073	-0.342	2
>500	599	0.428	0.017	-0.243	0.185	0.078	0.076	-0.393	2
>600	428	0.404	0.021	-0.219	0.185	0.084	0.081	-0.770	0
>700	324	0.404	0.022	-0.219	0.185	0.090	0.087	-0.995	0
>800	224	0.404	0.025	-0.219	0.185	0.095	0.092	-1.144	0
>900	135	0.351	0.017	-0.190	0.161	0.094	0.093	-1.427	0
>1000	106	0.351	0.015	-0.190	0.161	0.093	0.092	-1.474	0
>1100	76	0.294	0.001	-0.136	0.158	0.088	0.088	-1.496	0
>1200	52	0.251	-0.018	-0.118	0.133	0.080	0.078	-0.976	0
>1300	27	0.247	-0.036	-0.118	0.129	0.080	0.073	-0.241	0
>1400	5	0.190	-0.045	-0.104	0.086	0.083	0.078	2.771	0

Table H.3: Mid Hunter descriptive statistics of relative verification residuals, between AHD71 and AUSGeoid09 as a function of 100 m increase of difference in elevation.

ΔAHD (m)	Count (m)	Range (m)	Mean (m)	Min (m)	Max (m)	RMS (m)	STD (m)	Kurtosis	Outliers
>0	3321	0.570	-0.009	-0.287	0.284	0.105	0.105	-0.467	0
>100	2315	0.570	-0.012	-0.287	0.284	0.106	0.105	-0.416	0
>200	1556	0.570	-0.010	-0.287	0.284	0.103	0.103	-0.327	0
>300	1061	0.570	-0.005	-0.287	0.284	0.101	0.101	-0.236	0
>400	786	0.570	0.002	-0.287	0.284	0.102	0.102	-0.180	0
>500	599	0.570	0.005	-0.287	0.284	0.106	0.106	-0.194	0
>600	428	0.570	0.007	-0.287	0.284	0.114	0.113	-0.353	0
>700	324	0.570	0.006	-0.287	0.284	0.120	0.120	-0.448	0
>800	224	0.570	0.009	-0.287	0.284	0.129	0.129	-0.585	0
>900	135	0.570	0.028	-0.287	0.284	0.143	0.141	-0.616	0
>1000	106	0.570	0.032	-0.287	0.284	0.154	0.151	-0.789	0
>1100	76	0.570	0.046	-0.287	0.284	0.169	0.163	-0.834	0
>1200	52	0.570	0.059	-0.287	0.284	0.189	0.181	-0.920	0
>1300	27	0.554	0.072	-0.286	0.267	0.199	0.189	-0.767	0
>1400	5	0.317	0.100	-0.109	0.208	0.152	0.128	2.017	0

Table H.4: Mid Hunter descriptive statistics of relative verification residuals, between AHD71 and AUSGeoid98 as a function of 100 m increase of difference in elevation.